Environment, biological clocks and biomineralisation of the shell, in the mussel Mytilus galloprovincialis : the integration of the environment in the shell of bivalves

Victoria Louis

Sorbonne Université

Ecole doctorale des sciences de l'environnement d'Ile de France (ED129)

Laboratoire d'Ecogéochimie des Environnements Benthiques – UMR8222

Laboratoire de Biologie Intégrative des Organismes Marins– UMR7232

Environment, biological clocks and biomineralisation of the shell, in the mussel *Mytilus galloprovincialis*

The integration of the environment in the shell of bivalves

Par **Victoria Louis**

Thèse de doctorat en Science de la Mer

Dirigée par **Franck Lartaud** et **Laurence Besseau**

Présentée et soutenue publiquement le 14 décembre 2022

Devant un jury composé de :

Prof. Segalen, Loïc	Sorbonne Université	Président
Dr. Marin, Frédéric	Université de Bourgogne	Rapporteur
Prof. Verrecchia, Éric	Université de Lausanne	Rapporteur
Dr. Carré, Matthieu	CNRS-SU, Sorbonne Université	Examinateur
Prof. de Rafélis, Marc	Université Paul Sabatier – Toulouse 3	Examinateur
Dr. Mat, Audrey	Université de Vienne	Examinatrice
Dr. Lartaud, Franck	Observatoire de Banyuls/ Mer	Directeur de thèse
Dr. Besseau, Laurence	Observatoire de Banyuls/ Mer	Co-encadrante de thèse

Abstract

Bivalve shells result from a biomineralisation process, which is not constant over time leading to the formation of growth patterns. Shell growth patterns consist in the periodic alternance of increments and growth lines. Their formation is known to be related to environmental and/or physiological conditions, so that shells have been used as biological archives of (paleo)environmental and (paleo)climatic conditions. However, the temporal control of increment formation is still poorly understood. A direct effect of the environmental variability on shell biomineralisation has been firstly proposed, but a possible control by biological clocks is now suggested. In this study both hypotheses were tested in the frame of a multidisciplinary approach joining sclerochronology to chronobiology using the Mediterranean mussel, *Mytilus galloprovincialis* as biological model.

Mussels shell growth patterns were characterised in two Mediterranean coastal lagoons (Canet-Saint-Nazaire and Salses-Leucate), and in one site at sea, in the bay of Banyuls-sur-Mer, over a year of *in situ* experiment. In parallel, environmental variables were measured or retrieved from databases to determine which one might control incrementation in shells. *Mytilus galloprovincialis* shell growth patterns appear variable throughout the year and between the environments studied. Beside daily and tidal incrementation regimes, the production of increments following the mixed semidiurnal tidal regime of the region was observed at certain time of the year. Our results suggest that the incrementation patterns might be controlled by biological clocks together with a periodical variability in increment formation linked to the food availability, thus revealing a possible joint control on the biomineralisation process.

To identify the biological clock(s) of *M. galloprovincialis*, gene expression of potential core genes and related genes of the clock(s) were measured at sea and in aquaria under different manipulated conditions of light and food availability. We showed that the biological clock of *M. galloprovincialis* is probably plastic and that daily and tidal rhythmicity can be endogenous. As growth patterns were formed under constant environmental conditions in aquaria, the hypothesis of a control by biological clocks appears more probable. However, profiles of gene expression observed at sea and in aquaria were different between core biological clock genes and genes related to biomineralisation. As neither the environment nor the biological clock seemed to strictly explain the growth patterns observed, a joint control by both was hypothesised. This control might occur through the valve activity of mussels as valve prolonged closure is believed to be at the origin of growth lines in bivalve shells, due to pH drop in the extrapallial fluid. Valve activity is considered as controlled by biological clocks in oysters and clams.

To test the hypothesis of a joint control through valve activity, shell growth pattern and valve behaviour were measured under different light and food availability conditions for the same individuals. None of the environmental conditions tested seemed to give the rhythm to the biomineralisation process and no significant correlation was observed between the number of increments formed and the valve activity, leading unclear the process by which biological clocks could control biomineralisation. However, this PhD thesis constitutes the basis for further work on the characterisation of the relationship between environmental variations and rhythmic biomineralisation of bivalve shells.

Résumé

La coquille des bivalves se forme par le processus de biominéralisation qui n'est pas constant au cours du temps. Ainsi se forment des patrons de croissance dans la coquille, consistant en une alternance d'incréments et de stries de croissance. Leur formation est connue pour être liée aux conditions environnementales et/ou physiologiques. C'est pourquoi les coquilles de bivalves sont utilisées comme archives biologiques, permettant de reconstruire des (paléo)environnements et des (paléo)climats. Toutefois, les acteurs du contrôle temporel de la formation d'incréments dans la coquille sont encore mal identifiés : certains travaux ont mis en évidence un contrôle direct par les facteurs environnementaux, et d'autres suggèrent l'implication des horloges biologiques. Dans ce travail, les deux hypothèses ont été explorées en utilisant une approche pluridisciplinaire, croisant la sclérochronologie et la chronobiologie, avec la moule de Méditerranée, *Mytilus galloprovincialis,* comme modèle biologique.

Les patrons de croissance des coquilles de moules ont été caractérisés dans deux lagunes méditerranéennes (Canet-Saint-Nazaire et Salses-Leucate) et en mer, dans la baie de Banyuls-sur-Mer, pendant un an. En parallèle, les données environnementales ont été mesurées *in situ* ou obtenues à partir de bases de données, afin de cerner celles susceptibles d'impacter l'incrémentation des coquilles. Les patrons de croissance observés sont variables dans le temps (sur 1 an) et dans l'espace (selon le site étudié). A côté d'une incrémentation journalière (1/jour) ou tidale (2/jour), un régime particulier (lié au régime mixte semi diurne de marée de la région) a été caractérisé dans les coquilles d'individus des trois sites à diverses périodes de l'année. Ces observations suggèrent un contrôle de la biominéralisation des coquilles par des horloges biologiques, imprimant une incrémentation circadienne ou tidale, tandis que la variabilité observée dans la formation d'incréments serait liée à la disponibilité de la nourriture, révélant deux modes distincts du contrôle de la biominéralisation.

Afin d'identifier l(es) horloge(s) biologique(s) de *M. galloprovincialis*, une analyse de l'expression de gènes relatifs à l'horloge biologique a été menée, d'une part sur des échantillons prélevés en mer sur 36 h, et d'autre part sur des moules élevées en aquariums dans des conditions de lumière et de nourrissage contrôlées durant 28h. Nos résultats montrent une horloge plastique chez *M. galloprovincialis*. En aquarium, en conditions constantes de lumière ou de nourrissage, les patrons de croissance observés suggèrent le contrôle d'une horloge biologique. Cependant, aucune corrélation n'a pu être établie entre les profils d'expression des gènes liés à l'horloge et ceux des gènes relatifs à la biominéralisation. Ainsi, ni les fluctuations environnementales, ni l'action des horloges ne peuvent expliquer la formation des patrons de croissance observés de manière exclusive. Un contrôle conjoint est suggéré, médié par l'activité des valves de la coquille de *M. galloprovincialis* dont la fermeture prolongée pourrait être à l'origine de stries de croissance en induisant une diminution du pH dans la cavité extrapalléale. Afin de tester cette l'hypothèse, le comportement valvaire a été enregistré chez des individus élevés en conditions contrôlées (lumière et/ou nourrissage), puis les patrons de croissance des coquilles analysés. Aucune des deux variables environnementales n'a d'impact sur le rythme de biominéralisation, et aucune corrélation n'est établie entre le nombre d'incréments formés et l'activité des valves. Ainsi, le processus par lequel l'horloge biologique pourrait contrôler la biominéralisation reste difficile à préciser. Ce travail constitue néanmoins une base solide pour des études futures sur la caractérisation de la relation entre les variations environnementales et le processus rythmique de formation de la coquille des bivalves.

Acknowledgements

Trois ans c'est long et court à la fois… j'ai l'impression d'être arrivée hier mais, en même temps, les souvenirs de ce moment sont si loin… Trois ans de pur plaisir entre mer, montagnes et sciences, que demander de plus ! A la base on sait que faire un doctorat ce n'est pas facile, mais, au final on apprend tellement ! Pas que scientifiquement mais aussi sur soi-même car une thèse c'est un peu une épreuve. Et cette épreuve fait ressortir le meilleur comme le pire, c'est ce qui permet de se construire. J'ai fait tellement de choses que je n'aurais pas penser faire comme de la couture, du PMT dans l'étang de Canet, me retrouver à 4h du mat avec une lampe frontale sur la tête à ouvrir des moules, voir des bancs de thons et des dauphins au détours d'un échantillonnage, …. En fait je me rends compte que faire un doctorat c'est aussi apprendre à se faire confiance et tout essayer avant de se jeter dans le grand bain.

Mes premières pensées vont évidements à mes encadrants**, Franck Lartaud** et **Laurence Besseau**. Pour commencer, merci de m'avoir fait confiance pour ces 3 ans. Grâce à vous j'ai tellement appris et grandit. J'ai eu de la chance de vous avoir car vous êtes tous les deux des personnes très curieuses scientifiquement et vous vous complétez. Franck, tu as toujours la pêche et voit toujours les choses positivement, je reste toujours impressionnée par ta vivacité d'esprit. Laurence, merci pour ces 3 années à parler sciences mais aussi un peu de tout et de rien sur le coin d'un bureau. Tu arrives toujours à voir le détail qui va faire toute la différence.

Merci **Hector Escriva** et **Katell Guizien** pour votre accueil dans vos unités respectives. Merci **Marc de Rafélis** et **Stéphanie Bertrand** pour avoir accepté de faire partie de mon comité de thèse et de vos critiques constructives année après année. Merci à **Loïc Segalen**, **Frédéric Marin**, **Éric Verrecchia**, **Matthieu Carré**, **Marc de Rafélis** et **Audrey Mat** pour avoir accepté de faire partie de mon jury.

J'ai eu beaucoup d'aide de beaucoup de personnes lors de cette thèse et j'espère oublier personne.

Merci **Erwan Peru** pour ces heures passées en aquario dans le froid à nettoyer de moules. Merci de m'avoir apprise tant de choses en aquariologie et de toujours avoir été là, à veiller sur mes petites protégées pour que leur 4 étoiles ne devienne pas un taudis. En pour le resto gastro merci **Nancy Troulliard** ! Tu as toujours su me fournir du phyto en temps et en heure malgré quelques souches récalcitrantes.

Merci **Éric Martinez** et l'équipage de la Néréis pour m'avoir aidée à marquer mes moules à SOLA. Et merci au duo de plongeurs **Bruno Hesse** et **Jean-Claude Roca**. Jean-Claude, merci pour les quelques heures passées à trier des moules pour qu'elle soit bien calibrée, la technique du petit doigt ça va rester.

Merci **Pascal Roman**, **Valentin Logeux** et **Rémi Pillot** pour m'avoir aidée sur le montage de la v.2 de ma salle d'aquario.

Merci **Charles-Hubert Paulin** pour m'avoir transmis tous ces « tips and tricks » en bio mol.

Merci **Michael Fuentes** pour m'avoir accompagnée au pied levé avant le lock down v.2 pour retrouver mon panier de moule à Canet. Et merci **Stéphane Hourdez** pour me l'avoir retrouvé 4 mois plus tard, c'était inespéré !

En parlant de lagune, merci à **Laurence Fonbonne** et au syndicat mixte RIVAGE pour m'avoir aidée à accéder aux données liées à la lagune de Salses-Leucate. Et puis en mer merci à **Ronan Rivoal** et la

réserve naturelle nationale Cerbère-Banyuls pour la mise en place d'un point d'échantillonnage au Troc.

Merci **Michel Groc** pour l'opportunité de développer l'outil de valvométrie. Un grand merci **Lucas Laveissiere** de l'avoir monté et aussi de toujours avoir répondu à mes appels désespérés quand celui-ci faisait des siennes.

Merci **Laurence Bodiou** (alias Glass Laurence) et le service de la verrerie pour m'avoir permise de me concentrer sur mes manips.

Merci à **Hélène Tabouret**, **Damien Huyghe**, **Pierre Galland**, **Pascal Conan**, **Leila Meistertzheim**, **Gille Vétion**, **Renaud Vuillemin**, **Laurent Zudaire**, **Éric Maria**, **Paul Labatut**, **Christophe Salmeron**, **David Pecqueur**, **Nyree West** et **Yannick Banuls** pour les petits coups de pouces par-ci par-là.

Un grand merci aux étudiants, **Florian Debordes**, **Océane Eychenne** et **Thomas Moura** qui se sont intéressé à mon sujet de thèse au cours de leurs stages.

Un grand merci **Didier Peuzé** pour ton aide dans le micmac de l'administration !

Merci aussi à mes collèges de **l'équipe E2D** qui ont accepté que les moules s'invitent au pays de Némo. Merci **Mélanie**, **Natacha**, **Pauline** et **Vincent** pour votre bonne humeur et tous vos conseils pour le bébé scientifique que j'étais, je crois que je peux dire que j'ai fait ma métamorphose en juvénile à la fin de cette thèse. Merci **Mélanie**, **Natacha**, **Pauline, Camille, Sara, Charlène** pour ces pauses de midi à parler de tout et de rien.

Merci **Agnès et Sébastien**, alias les ascidies, pour leur vent de bonne humeur à l'étage. En plus il y a toujours de la bonne musique dans votre labo. Agnès, c'est toujours un plaisir de te voir émerger dans le bureau avec la banane !

Plus personnellement, merci à toutes les personnes qui ont fait que les PO soient ma nouvelle maison.

D'abord **Lydvina**, merci pour m'avoir emmenée dans ton idée de faire de l'escalade mais aussi pour les heures de rando à pied comme en raquette, les soupers et toutes ces crises de rires.

En parlant de rando, **Mélanie** (encore ^^), tu as été piquée du virus et maintenant on ne peut plus t'arrêter. Merci aussi pour ces supers randos avec des paysages à couper le souffle et aussi pour les peps talks dans les moments de faiblesse.

Merci aussi **Mathilde**, **Adèle** et **Sara** pour ces heures à marcher et papoter dans les superbes montagnes des PO.

Un énorme merci **Marc**, **Pierre**, **Véro**, **Blanche**, **Marie-Carmen**, **Maria**, **Thierry**, **Éric**, **Jean**, **Jeano**, **Fanny, Phillipe,** … pour ces heures passées en bas des voies mais aussi autour d'une bière (après l'effort le réconfort). Passe Muraille a été une seconde maison et le meilleur antidépresseur durant cette thèse.

Pour encore plus d'escalade merci **Corentin**, **Stéphane**, **Serge**, **Vlad**, **Raphael** pour les sorties de temps à autres dans les plus beaux spots des PO.

Et bien sûr merci à tous ceux qui étaient déjà présents avants et sur qui je peux toujours compter malgré la distance.

First, a special thank to Angel and Demons team! **Coco** and **Tim** thanks a lot, it's always so nice to be around you and get your good vibes. **Mario**, you will see, PhD come to an end one day!

Also thanks to the **O&L familly** to still be there by visio of quality or when I'm back to Belgium. It's a pity to be split everywhere and our busy life does not help to keep in touch.

Merci aux Grolesprits, **Anna**, **Fanny**, **Victor**, **Momo**, **Domi**, on ne se voit pas souvent mais c'est toujours comme si on ne ce n'était jamais quitté. Merci, pour ces crises de rires, et tous ces bons moments partagés !

Merci **Wendy**, **Carine**, **Jean-mimi** et **Lara** (alias Little Fox) pour ces super vacances en Manche, votre gentillesse et bonne humeur.

Merci **Papa** et **Maman** de m'avoir fait confiance quand je me suis lancée dans les sciences et de m'avoir permis d'en arriver là. C'est de vous que je tiens ma curiosité et mon envie de tout découvrir depuis petite. **Arnaud**, frérot, merci de toujours avoir le petit mot qui va me faire rire même dans les moments plus difficiles. Merci **Bonne Maman** et **Bon Papa** pour vos encouragements et de me soutenir dans mes projets. Une pensée émue à **Mamy** et **Pépé** qui je suis sûre auraient bien rit sur le fait que je bosse sur les moules que finalement je n'ai jamais aimé avoir dans mon assiette.

Table of contents

List of figures

General introduction

Chapter 1

Chapter 2

General discussion, perspectives and conclusion

Annexes

List of tables

General Introduction

Chapter 1

Chapter 2

General Introduction

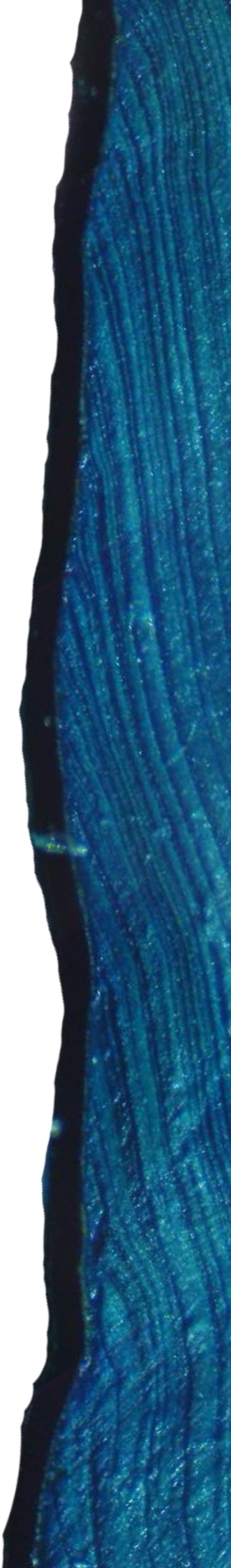

1. Review:

Step in time: Biomineralisation of bivalve's shell

Victoria Louis[1,2], Laurence Besseau[2], Franck Lartaud[1*]

[1] Sorbonne Université, CNRS, Laboratoire d'Ecogéochimie des Environnements Benthiques, LECOB, Banyuls-sur-Mer, France

[2] Sorbonne Université, CNRS, Biologie Intégrative des Organismes Marins, BIOM,Banyuls-sur-Mer, France

*** Corresponding author:** franck.lartaud@obs-banyuls.fr

Keywords: shell biomineralisation; sclerochronology; biological clock; bivalve; environmental archive

Citation:

Louis V, Besseau L and Lartaud F (2022) Step in Time: Biomineralisation of Bivalve's Shell. *Front. Mar. Sci.* 9:906085. doi: 10.3389/fmars.2022.906085

Abstract

Biomineralisation process which is the induction of the precipitation of a mineral by an organism, generates hard tissues such as bones, teeth, otoliths and shells. Biomineralisation rate is not constant over time. This is likely due to variations of environmental and/or physiological conditions, leading to the formation of growth increments or rings. For bivalves, increments are considered as the unit of time recorded in shells. Therefore, shells are used as biological archives of (paleo)environmental and (paleo)climatic conditions. However, the environmental drivers leading to the periodic formation of increments are still poorly understood. Tackling the question of the integration of the environment by the organism is challenging: is there a direct effect of the environmental variability on bivalve shell biomineralisation? Or is biomineralisation controlled by a biological clock? In this review, the different temporal units observed in bivalve shells and the possible regulatory processes are explored and some research trajectories are suggested.

Introduction

One of the main keys of the last 500 Myrs is the flourishment of hard structures produced by organisms. This process called biomineralisation offers large possibilities for evolution of organisms by its use in the support of the general shape of organisms together with an efficient protection of soft tissues (Marin et al., 2007; Murdock, 2020). The production of hard structures by organisms (shell, skeleton) allows better conditions for the preservation of traces of life on the earth, conducing to define this period as the “Phanerozoic times”. Biomineralised structures are now considered as fundamental constituents of the environment, found from the micrometric scale in the skeleton of phytoplankton (the major primary producers) to kilometric scales, visible from the space, such as the Great Barrier Reef formed by corals. The ecological and economic values associated with biomineralisation include the sink of carbon, the shellfish production, the supply of building materials, the formation of habitats (reefs and mounds) by engineer species used as refuges for biodiversity, and their use as archive of (paleo)environmental and (paleo)climatic conditions (Moberg and Folke, 1999; Coen et al., 2007).

Various strategies for mineralisation can be experienced by organisms, through extrinsic biologically-influenced mineralisation (also called organomineralisation) to intrinsic biologically-induced or controlled mineralisation (biomineralisation *s.s.*) (Weiner and Dove, 2003; Dupraz et al.,

2009). In the animal kingdom, biologically-controlled mineralisation is the rule. This process infers enzymatic regulation and active pumping of elements from the external medium, leading to a strong connection between biomineralisation and the metabolism of the organism. Consequently, biomineralisation is not homogeneous nor continuous with time. The growth of shells and skeletons can slow down or even stop, likely related to the dynamics of environmental and physiological conditions. This is notably the case in many mid-latitude species during winter, when the temperature is cold and the food is sparse (Schöne, 2008). Therefore, various growth patterns can be observed depending on the experienced environmental conditions and serve as the basis of sclerochronological analysis.

Sclerochronology is the study of physical and chemical variation in the accretionary tissues of calcified biomaterials, where the increment is the unit of time (Schöne et al., 2003b; Schöne, 2008; Huyghe et al., 2019). By introducing a temporal basis in the study of hard tissues of organisms, this new research field offers a tremendous potential in various disciplinaries such as physiology, ecology, paleoclimatology. The study of growth patterns has long been used as a timescale in calcified tissues (Réaumur, 1709; Pulteney, 1781; von Hessling, 1859). Since growth rate of organisms is largely controlled by environmental drivers, changes in skeleton biomineralisation provide a reliable archive of the environmental variations experienced by organisms (Kennish and Olsson, 1975). This concept is successfully applied for a variety of biomaterials, including shell and skeleton produced by invertebrates such as bivalves and corals, but also in vertebrates (*i.e.*, otoliths of teleost fish and teeth of mammals) (Skinner and Jahren, 2003; Murdock, 2020). The introduction of geochemical approaches allows for a precise quantification of environmental data, as several parameters (temperature, salinity, food, etc) are archived in the form of stable isotopes or minor and trace elements (Epstein et al., 1953; Dodd, 1965). Nowadays, sclerochronology (implying increment counting) and sclerochemistry (when coupled with geochemical proxies) feed various environmental monitoring programs on climate change, pollution events or health status surveys of calcifying species (Schöne, 2013; Schöne and Krause, 2016; Steinhardt et al., 2016). Thanks to technology improvements, we are now able to work from long-term time series (*i.e.*, decennial to centennial) to high-temporal resolution archives (*i.e.*, daily to hourly) (Huyghe et al., 2019; de Winter et al., 2020; Poitevin et al., 2020; Yan et al., 2020). Paradoxically, the inducer of increments formation is still uncertain, and particularly the discrimination between the role of the environment and/or the one of physiological induced changes on growth patterns. Endogenous time-keeping mechanisms, also called biological clocks, have been proposed to regulate periods of growth (Richardson et al., 1979) but the precise role of the environment as a time giver for biomineralisation activity remains to be defined.

The lack of knowledge concerning biomineralisation processes has an impact on the study of the shell growth in a temporal framework and their use as (paleo)environmental archives, which is regularly raised by sclerochronologists (Schöne, 2008; Trofimova et al., 2020). In fact, a gap persists between shell growth increment analysis and the study of biomineralisation processes, as they do not refer to similar timescales. This has led to the separation of scientific communities interested in mineralised tissues on one hand with scientists mostly focused on mechanisms inducing nucleation from calcium carbonate to the formation of the neocrystal, and on the other hand with researchers developing approaches to determine the time frame in which the shell forms in order to use these calcified pieces as biological archives. As new advances in the characterisation of molecular biological clocks and their effect on the physiological activity of bivalves have been made recently, we think that the gap is about to be bridged. In this review, we first report the current knowledge about shell biomineralisation and the formation of bivalve shell increments. Then we explore possible regulatory mechanisms that could involve the environment and/or biological clocks, including temporal and spacial scales poorly investigated yet. Further research directions are finally provided. Many reviews in the field of sclerochronology have been done recently, covering particularly the use of bivalves shells as (paleo)environmental archives (Steinhardt et al., 2016; Butler and Schöne, 2017; Trofimova et al., 2020; Peharda et al., 2021)). This review addresses an additional aspect of the research by linking sclerochronology to chronobiology and enriches the multidisciplinary dimension of sclerochronology.

Shells formation

Hard tissues formed by many organisms can have various functions, such as protection for shells, structuration for bones or equilibrium for otoliths. The process by which hard tissues are formed is biomineralisation, which refers to the active process of precipitation of a mineral by an organism. Organisms produce various minerals, including silica, bioapatite, iron oxides and hydroxides, but the main component produced is calcium carbonate through three polymorphs: calcite, aragonite and, less frequently, vaterite (Skinner and Jahren, 2003). The mineral units are self-assembled within the inter- and intracrystalline organic framework. In bivalve shells, the organic matrix represents on average 0.01 to 5 % of the weight, and is composed of a set of proteins, peptides, free amino acids, lipids, polysaccharides and pigments (Marin et al., 2012). The organic fraction is found under an insoluble hydrophobic phase, which is the main component of the framework for crystal growth, and a soluble acidic phase rich in aspartic acid (Asp), that makes the organic compounds bind calcium ions (Marin et

al., 2007). As such, organic compounds control shell mineralisation, together with the crystal shape and growth (Marin and Luquet, 2004).

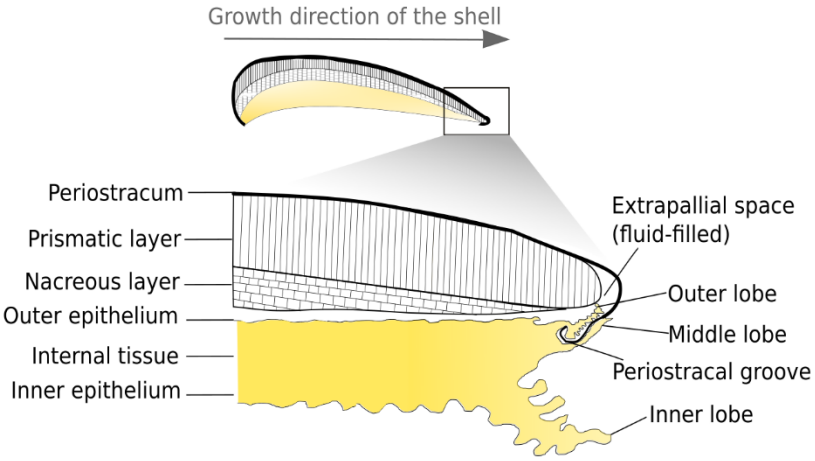

Figure 1: Longitudinal view of *M. galloprovincialis* showing the structural organisation between shell and the underlying mantle. The shell is composed of three layers: the nacreous layer (bottom), the prismatic layer (middle) and the periostracum (upper part). The periostracum seals with the mantle the extrapallial space where mineralisation occurs.

The shell of bivalve is composed of superimposed layers (Figure1). The external layer, called periostracum, is rich in organic compounds. Most bivalves have two subperiostracal layers that can be made of either calcite only, or aragonite only or both. The area of muscle insertion is composed of aragonite. Calcite and aragonite crystals can follow different growth axes, leading to the formation of diverse morphologies and arrangements, called microstructures (Checa, 2018). A wide variety of

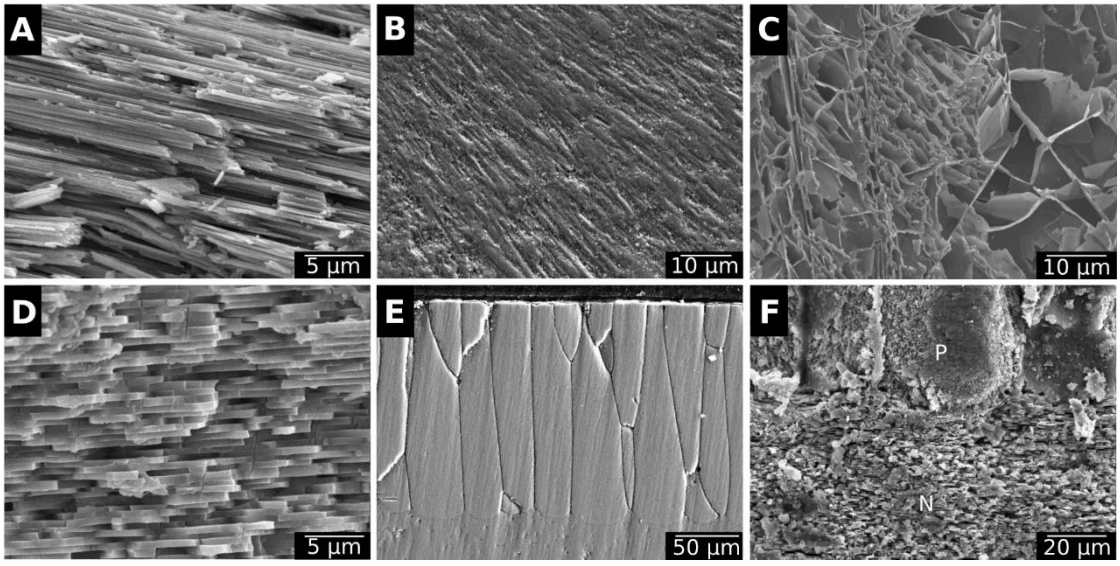

Figure 2: Examples of the various microstructures found in bivalve shells. (A) Crossed foliated calcite in the outer layer of the Antarctic scallop *Adamussium colbecki*. **(B)** Fibro-prismatic calcite from the outer layer of the deep-sea mussel *Bathyomodiolus azoricus*. **(C)** Chalky calcite in the shell of the Japanese oyster *Magallana gigas.* **(D)** Nacre in the inner layer of the deep-sea mussel *B. azoricus*. **(E)** Prismatic aragonite from the outer layer of the freshwater mussel *Anodonta cygnea*. **(F)** Contact between the prismatic (P) and the nacreous (N) layers in the shell of *A. cygnea*.

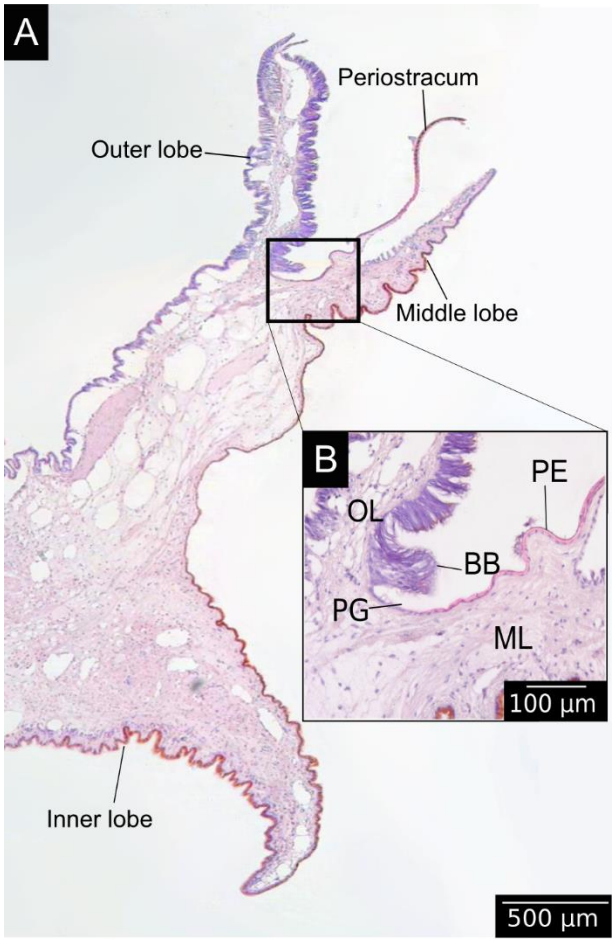

Figure 3: Longitudinal histological section of the mantle edge of *M. galloprovincialis* stained with haematoxylin and eosin. (A) View of a histological section of the periostracum bound to the mantle, in an area divided in three lobes: the outer lobe, the middle lobe and the inner lobe (see the position in the organism in Fig. 1). **(B)** Details of the periostracal groove (PG) located between the outer (OL) and the middle (ML) lobes. The basal bulb (BB) is a group a of cells secreting the periostracum (PE).

microstructures can be found in bivalve shells (Figure 2). For example, Mytilidae have fibrous prismatic calcite in the outer part of the ostracum and aragonite nacreous in the inner part.

Bivalve shells are produced by the mantle, a polarised tissue composed of three layers: the outer epithelium, the internal tissue and the inner epithelium (Figure3A-B). The outer epithelium is also called the calcifying epithelium. The edge of the mantle, where mineralisation occurs, is usually composed of three lobes: the outer, middle and inner lobes having different cell types and therefore different functions (Figure 2 and Figure 3A). The basal bulb, a group of cells located at the base of the outer and middle lobes (Figure 3B), produces the periostracum which covers the outer shell isolating from the external environment a space between the mantle and the shell, called extrapallial space (EPS). The EPS is filled with the extrapallial fluid (EPF), a supersaturated fluid retaining shell components in solution before their incorporation into the matrix (Richardson et al., 1981; Marin et al., 2012). The inorganic part of the EPF is constituted of precursor ions of calcium carbonate and also of others ions such Na^+, K^+, Mg^{2+}, Cl^- and SO_4^2. Bicarbonate and chloride ions concentrations are higher in the EPF than in sea water, the other ions being present in approximatively the same concentration in both fluid (Wilbur and Saleuddin, 1983). Calcium intake by bivalves occurs at different places. Calcium absorption from water takes place in gills and from food in the digestive system. The ions can reach the extrapallial space passively by diffusion through Ca^{2+} channels, actively by Ca^{2+}-ATPase, but also by intercellular spaces (Figure 4) (Carré et al., 2006). Dissolved inorganic carbon (DIC) from seawater is a source of HCO_3^-. Bicarbonate ions are transported to the EPS *via* active transport though HCO_3^-/Cl^- exchangers and Na^+/ HCO_3^- transporters (Coimbra et

al., 1988; Marin et al., 2012; Alves and Oliveira, 2013). The metabolism also releases CO_2, which can be transformed by the carbonic anhydrase (CA) into HCO_3^-. Carbonic anhydrase also generates hydrogen ions, acidifying the EPS. Therefore, an active pumping regulates the pH of the EPF (Marin et al., 2012).

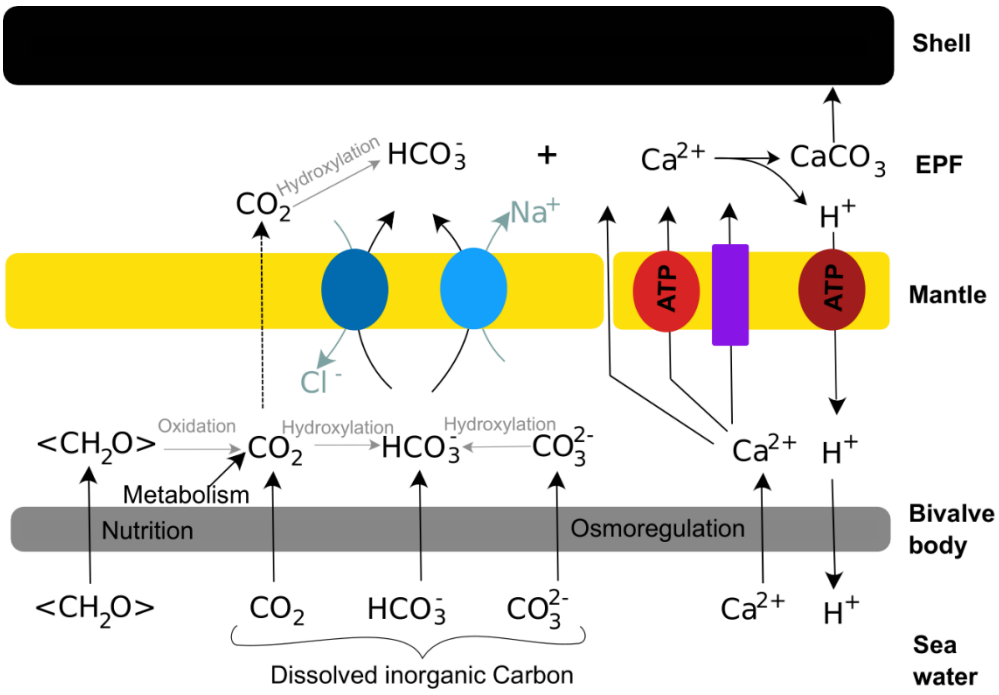

Figure 4: Schematic calcification model of bivalve shells. Calcium reaches the extrapallial fluid (EPF) passively through Ca^{2+} channels (purple rectangle) and cells junctions, and actively throughout Ca-ATPase (light red circle). Bicarbonate ions resulting from dissolved inorganic matter (DIC) and nutrition join the EPF through HCO_3^-/Cl^- exchangers (dark blue circles) and Na^+/ HCO_3^- transporter (light blue circles). Carbon dioxide diffuses through cells to the EPF (dotted arrow). The excess of proton produced by the formation of calcium carbonate is actively pumped out the EPF (dark red circle).

The formation of a calcium carbonate crystal begins with the nucleation, which consists of a highly thermodynamically instable nucleus of $CaCO_3$ regulated by a local supersaturation of organic material. This step is especially favoured by differential expression of polysaccharides and proteins that have different charge density through time (Giuffre et al., 2013). Then, crystal growth and organisation are biologically and physically controlled (Checa, 2018). Two physical control mechanisms are described. The first one is the crystal competition, where the fastest growth axis is outcompeting the others, this type of physical process is observed in case of foliated calcite microstructure and nacre synthesis of bivalves (Checa et al., 2006, 2007). The other physical process is the self-organisation of the organic matrix, acting as a template for crystal growth (Checa, 2018). The precursor of the organic template is a fluid that is self-organised by surface tensions (Checa et al., 2005, 2016). This has been described in the freshwater mussel *Cristaris plicate*, where an organic honeycomb template determines crystal growth direction and size (Tong et al., 2002). The process of self-organisation is

coupled with a biological control by the subcellular recognition of the extracellular matrix *via* its physicochemical properties (Checa et al., 2005; Checa, 2018). This relationship between mantle cells and the extracellular matrix leads to the secretion by the outer epithelium cells of either organic (fluid precursor) or mineral materials. The biological control by the outer epithelium of the mantle is assumed to involve molecular pathways. First studies have found four transcription factors namely *Pf-MSX* (Zhao et al., 2014)*, Pf-AP-1* (Zheng et al., 2015)*, Pf-Rel* (Sun et al., 2015) and *Pf-POU3F4* (Gao et al., 2016), and two receptors called *PfBMPR1B* and *PfBAMBI* (Li et al., 2017) involved in the regulation of the matrix proteins of the pearl oyster *Pinctada fucata*. More recently, bioinformatic tools have been used in order to predict molecular pathways involved in the biomineralisation process. The molecular response to shell damage of the Antarctic clam *Laternula elliptica* has been used to observe the restart of the biomineralisation (Sleight et al., 2020). RNA-seq data analysis underlines two hypothetical pathways: one linked to ions and proteins transport from the outer epithelium to the biomineralisation area, and the other linked to the secretion of organic matrix proteins within the nacreous layer of the shell. This work also points out new potential receptors for which further studies are now required to confirm their putative role in the biomineralisation process.

Shells as biological archives

The molecular pathways involved in the biomineralisation process are constantly activated throughout bivalve life. This means that shell formation should be continuous. However, bivalve shell growth rate is not constant from larval to adult stages (Schöne, 2008). The growth can be described by a Von Bertalanffy growth model, where juvenile specimens have an exponential growth while the growth rate in older individuals slows down and stabilises. At a higher temporal resolution, growth slows down or stops on a regular basis (Lutz and Rhoads, 1977; Karney et al., 2012). This phenomenon is characterised by low carbonate deposition while the organic matrix is still produced, inducing a change in the ratio between mineral and organic material, and the formation of growth lines. Growth lines separate the shell formation into small units of time, so-called growth increments or rings (Figure 5). The growth increment has thus to be distinguished from the shell microstructure, as the later only refers to the crystal shape. Growth lines are discernible very early during the development of bivalves. The first accretion line is visible after 32 hours post fertilisation in *M. galloprovincialis* larvae (Miglioli et al., 2019). This corresponds to a major body organisation change during the planktonic phase, when the larva turns from a ciliated free-swimming planktonic larval form, called trochophore, into a D-

veliger larva, meaning a free-living planktonic larva with a shell. Growth increments are then produced during the entire life of the organism.

It is observed that the shell growth lines mainly result from periodic (*e.g.*, seasonal, daily, tidal) processes, although random growth anomalies can appear (*i.e.*, induced by stressful events such as predation, storm, pollution) (Schöne, 2008). Therefore, growth pattern observable on the shell of an individual primarily reflects the variability in its environment (Figure 5). Considering that shells record the environment surrounding organisms, they can be considered as biological archives.

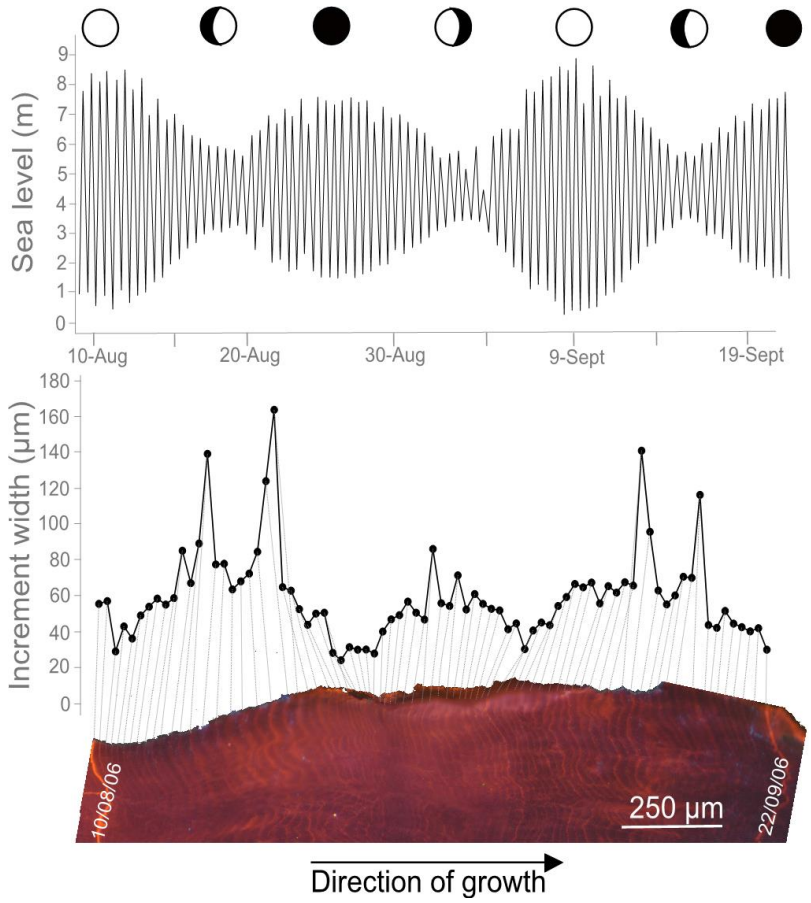

Figure 5: Growth increments in *Magallana gigas* in relation with its environment. Section of the hinge area of *M. gigas* shell showing growth increments and Mn-staining under cathodoluminescence microscopy. The increments are formed tidally and vary in width following the semi-lunar cycle, with higher growth rates during neap tides, likely related to temperature and phytoplankton changes in the surrounding environment (see Huyghe et al., 2019 for further details).

A bibliographical survey based on the keywords “bivalve shell” and “sclerochronology” has gathered 55 bivalve species investigated for their shell growth patterns (Figure 6A). This survey includes species from various types of environments, from freshwater to the deep-sea and from polar to tropical waters. Annual growth lines are the most common observed pattern in the literature (>60%

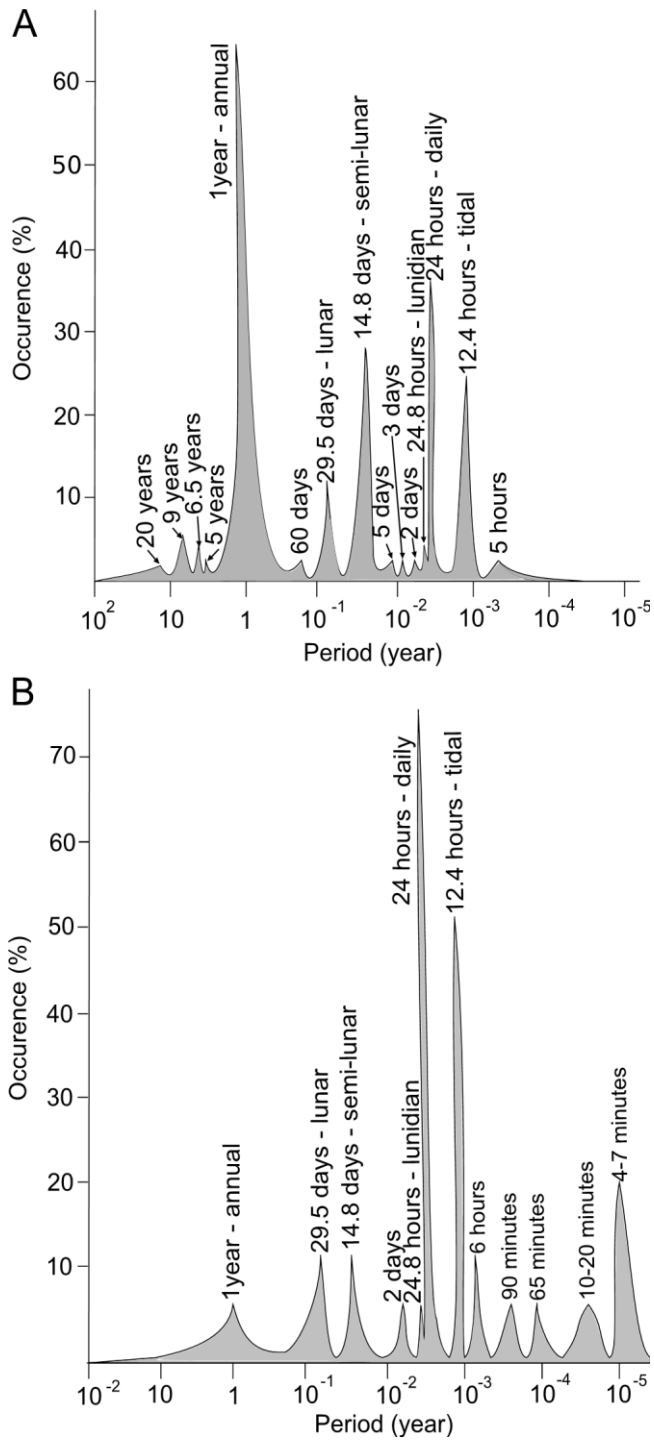

Figure 6: Bibliographic review of periodicities related to the shell growth patterns (A) and biological clocks in bivalves (B). The bibliographic survey for shell increments has been based on the keywords "bivalve shell" and "sclerochronology" and gathers 55 species. The bibliographic review for the biological clocks has been done with the keywords "biological clock bivalve", "circadian clock" and "valvometry", and gathers 17 species. Articles involving ecotoxicological studies are not taken into consideration.

of bivalves), particularly in the shells from mid and high latitude species, and are mainly associated to winter low temperatures that slow down or even stop the growth (Schöne, 2013; Killam and Clapham, 2018) (Table 1). They may also be due to spawning events, assuming that this paramount physiological trait is very energy-consuming, limiting calcification (Jones, 1980). Counting annual growth lines in long-lived species can reveal growth rate changes at lower frequencies, such multi-annual environmental dynamics. The ocean quahog *Arctica islandica* and the pearl freshwater mussel *Margaritifera falcata* exhibit long-term growth periods related to the North Atlantic Oscillation (NAO), which is characterised by colder winters every 5 to 30 years (Schöne et al., 2003a, 2007).

At shorter time-scales, one and two increments per day are classically observed (Schöne et al., 2005). Interestingly, the bibliographic database reveals that in bivalve shells daily growth increments are more commonly observed than semi-daily ones (Figure 6A). While semi-daily increments are closely related to the tidal regime in areas exhibiting two tides per day, daily increments can both correspond to circadian (24h) or circalunidian (24.8h) growth rate changes (Hallmann et al., 2009; Schwartzmann et al., 2011). The growth line count also highlights frequent growth rhythms at periods close to 14.8 and then 29.5 days, that are related to semi-circalunar and circalunar fluctuations

(Figure 6A, Table 1). Less conventional growth cycles are observed (*i.e.,* 60 days, five days, …) but their relationship with environmental cues are poorly described or correspond to local specific conditions. The 60 days pattern observed in the shell of the deep species *Bathymodiolus thermophilus* might reflect current velocity changes in the hydrothermal habitats induced by ridge-crest jets (Nedoncelle et al., 2013, 2015). The five and three days patterns of the mussel *M. galloprovincialis* observed in the Mediterranean lagoon of Salses-Leucate (France) could be due to regular wind events occurring in this area (Andrisoa et al., 2019). The two-day periodicity recorded in the shell of the tropical *Comptopallium radula* could be synchronised with temperature or sea level pressure as both of these parameters display two-day cycles (Thébault et al., 2006).

Although a synchronism with environmental variables appears, the precise origin of growth increments is still discussed in literature. While the integration of environmental variables in shells is a fundamental question for the community of sclerochronologists (Trofimova et al., 2020), two hypotheses have been proposed to explain increment formation: it may be directly controlled by environmental parameters or mediated by biological clocks.

Environmental drivers in shell formation

As illustrated above, tidal rhythms have been identified in the growth patterns of bivalve shells. Lutz and Rhoads (1977) linked this pattern to direct environmental constraints on the physiology of the organisms. At low tide during the emersion period, valves are closed; the metabolism becomes anaerobic, inducing a drop of pH and then an increased calcium ions concentration in the EPF. This has been interpreted as a phase of decalcification; calcium ions integrated into the shell are re-solubilised into the EPF. This hypothesis is sustained by analogous observations made in the EPF of multiple bivalve species such as *Mercenaria mercenaria* and *Crassostrea rhizophorae* (Crenshaw, 1972; Littlewood and Young, 1994). When the quahog *M. mercenaria* closes its valves, the pH decreases and the Ca^{2+} concentration increases within 15 minutes (Crenshaw, 1972). The same observation has been made in the case of the tropical oyster *C. rhizophorae* (Littlewood and Young, 1994). At high tide, valves open and metabolism becomes aerobic again. Subsequently, the biomineralisation activity starts again in an area already containing organic material but that has lost its $CaCO_3$, leading to the formation of a growth line (Lutz and Rhoads, 1977). The increment is formed in a second time during the immersion. This has been observed in different bivalve species such as *Saxidomus gigantea* which is subjected to semi-diurnal or diurnal tides as a function of its location along the West coast of America (Hallmann et

al., 2009). When bivalves are exposed to semi-diurnal tides, a faint additive line assumed as a growth line, appears inside of the increment. Therefore, bivalves exposed to semi-diurnal tidal regimes exhibit shells forming two increments per day, while those that experience daily tides produce one increment per lunar day. Also, the distinctness of the growth line is often linked with the duration of the emersion (Richardson, 1987; Schöne et al., 2003b; Hallmann et al., 2009).

Table 1: Environmental periodic fluctuations and their suggested associated environmental drivers.

Periods		**Suggested associated environmental drivers**
Circannual	~ 365.25 days	- Photoperiod - Temperatures
Circalunar	~ 29.5 days	- Moonlight intensity - Tidal currents - Tidal levels
Semi-circalunar	~ 14.8 days	- Spring and neap tides - Temperatures
Circalunidian	~ 24.8 hours	- Tides
Circadian	~ 24 hours	- Photoperiod - Temperatures
Circatidal	~ 12.4 hours	- Tides - Temperatures

Emersion/immersion cycles are not the only environmental variable reported to initiate increment formation as many bivalve shells from subtidal or freshwater ecosystems also exhibit such tidal growth rhythms (Verrecchia, 2005; Poulain et al., 2011). For example in the deep-sea, tidal increments are observed in the shell of the hydrothermal mussel *B. thermophilus*, living at 2,500 m depth, and interpreted as a result of tidal oscillations in the vent systems (Nedoncelle et al., 2013, 2015). The role of temperature, salinity, dissolved oxygen or nutrient availability is thus regularly mentioned as there is a general consensus in the literature that environmental fluctuations drive the increment width variation (Rodríguez-Tovar, 2014). Other subtidal bivalve species like Pectinids exhibit daily growth increments in their shell, likely related to the day/night alternation. In an experiment conducted to understand the potential environmental drivers of such daily increments, Clark (2005) submitted *Flabellipecten diegensis* to shorter night and day cycles by having an alternation of eight hours of light and eight hours of darkness. After 22 days, specimens had experienced 33 light/dark

cycles and had more or less 30 increments. Changing light exposure is thus suggested as a potential shell production driver.

Biological clocks in bivalves

Interestingly, bivalves from intertidal flats constantly immersed and under stable conditions of temperature, water flow, light and food supply in the laboratory, show semi-daily increment formation. This has been observed for the common cockle *Cerastoderma edule* (Richardson et al., 1980) and the Manilla clam *Ruditapes philippinarum* (Richardson, 1988) and interpreted as possibly resulting from endogenous rhythms in the process of biomineralisation controlled by biological clocks. Since Richardson pioneer studies, biological clocks are now regularly mentioned as a timer for bivalve shell increment formation (Schöne, 2008; Poulain et al., 2011; Warter et al., 2018; Zhao et al., 2020).

Biological timing mechanisms, named biological clocks, are known to orchestrate the biological activities of organisms with the environment, allowing the organisms to anticipate cyclic variations and to increase their fitness (Rosbash, 2009). The clock is made of three major components: i) a central molecular oscillator that keeps track of time, ii) environmental inputs that give the time (also named zeitgebers) and control the central oscillator to ensure the entrainment of the clock and iii) a series of rhythmic outputs corresponding to rhythms of biochemical, physiological or behavioural activities of the organism such as the daily migration throughout the water column by phytoplankton (Figueroa et

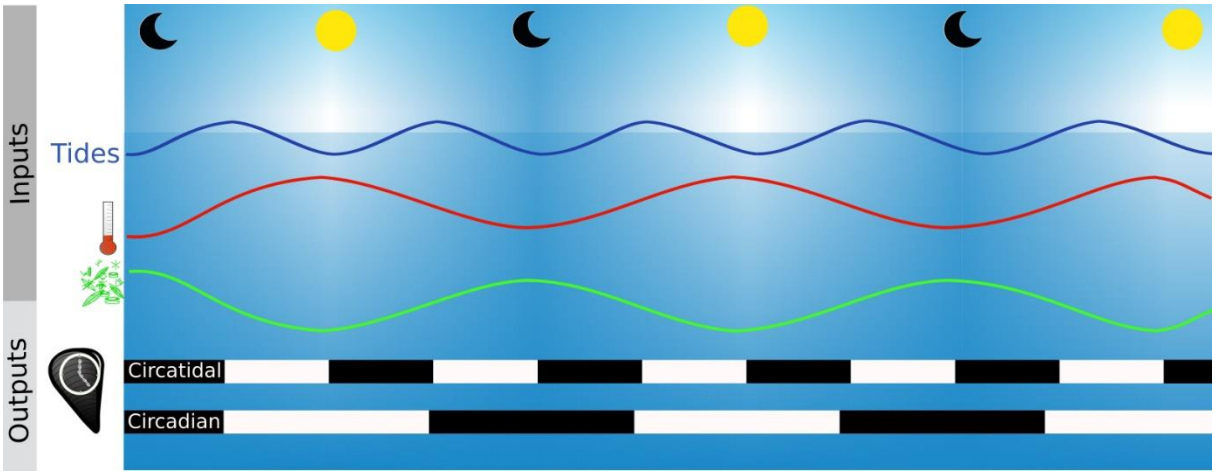

Figure 7: Functioning of biological clocks. Clock inputs are environmental and biotic variations called zeitgebers such as the photoperiod, the thermoperiod (red line), tides (blue line) or phytoplankton migration in the water columns (green lines). The zeitgeber is the synchroniser of the molecular clock of organisms and the outputs are rhythmic periodical processes such as mussel valves opening (black and white bars). Black bars are time when mussels are closed and white bars when they are open.

al., 1998) or the tidal valve gape activity of bivalves (Comeau et al., 2018; Tran et al., 2020) (Figure 7). The clock is synchronised by environmental cues and can be endogeneous, which means that the oscillations persist under constant conditions (Aschoff, 1981).

The biological clock is a time-keeping system highly conserved among organisms and its constituents are described for many species, from cyanobacteria, fungi to mammals among others (Ditty et al., 2003; Tan et al., 2004; Partch et al., 2014). Although its structure can slightly differ, the core is based on one or coupled feedback loops composed of activating and repressing elements. The outputs of this conserved structure are circadian (Dunlap, 1999). Homologous clock genes (*clock* and *bmal* as activators and *cryptochrome 1* and *2*, *period* and *timeless* as repressors) have been described for bivalves, such as the oyster *Magallana gigas* (Perrigault and Tran, 2017), the mussels *M. edulis* (Chapman et al., 2020) and *M. californianus* (Connor and Gracey, 2011), the scallops *Argopecten irradians* (Pairett and Serb, 2013) and *Chlamys islandica* (Perrigault et al., 2020) and even in deep-sea mussels(*i.e.*, *Bathymodiolus azoricus* (Mat et al., 2020)). The main periods associated with biological clocks in bivalves are daily and tidal, but others with lower (several days to a year) or higher frequencies (hours to minutes) have also been reported (Figure 6B).

The photoperiod and the temperature are the main zeitgebers of the circadian biological clock (Dunlap, 1999; Rensing and Ruoff, 2002). Experiments on *M. edulis* have shown that genes of the endogenous clock (*i.e.*, *Clk*, *Cry1*, *ROR/HR3*, *Per* and *Rev-erb/NR1D1*) oscillate with a different amplitude when bivalves are placed in complete darkness (DD - Dark/Dark condition) with a 24 hours temperature cycle of 3.6 ± 0.2 °C compared to those placed in DD and constant temperature (Chapman et al., 2020). It should be noted that the clock system responds to a periodical variation of the temperature and not to the temperature as a calorific energy. Part of the definition of a biological clock is that the system is temperature compensated. This means that the molecular reactions involved in the feedback loop are not slowed down in cooler temperatures or accelerated in warmer temperatures. Otherwise, the benefit of having a biological clock is lost because the given time would be different in function of the temperature.

Various theories have been proposed to explain the circatidal rhythm observed in organisms living in littoral areas, based on either (i) one unimodal circatidal clock, strictly distinct from one unimodal circadian clock (Naylor, 1958), (ii) two unimodal circalunidian clocks coupled in antiphase (Palmer and Williams, 1986) or (iii) one single bimodal oscillator governing both circadian and circatidal patterns (Enright, 1976). Recent work of Tran *et al.* (2020) suggests that oysters are in line with the third hypothesis. Similar studies on other species should be performed to check if this hypothesis is valid for all bivalves.

In chronobiology, the behaviour of an organism is frequently used as an output of biological clocks (Bartness and Albers, 2000). In bivalves shell gaping is a useful tool to study rhythmic behaviour (Perrigault and Tran, 2017; Comeau et al., 2018). Valves gape activity can be measured by valvometry. This technique consists in a Hall sensor and a magnet glued on each valve in order to continuously record the voltage, which is proportionally disrupted by the valve aperture through the decrease of the magnetic field (*i.e.*, magnetic flux density) (Nagai et al., 2006). Analyses conducted in this field revealed a predominantly circatidal valve activity for bivalve species from tidal environments (Tran et al., 2011), while species from subtidal and freshwater habitats exhibit circadian rhythms (García-March et al., 2008; Schwartzmann et al., 2011; Hartmann et al., 2016; Comeau et al., 2018). In aquaria, *M. gigas* submitted to a photoperiodic regime (*i.e.*, 12 hours of light and 12 h in darkness (LD 12:12)), without tidal current, shows a circadian activity of valve aperture (Mat et al., 2012). Free-running conditions, which means the suppression of environmental inputs, is used to test for the endogenous character of the biological clock. Under constant light conditions (*i.e.*, total darkness (DD) or continuous light (LL) over 24 hours), the circadian behaviour of *M. gigas* is kept although a gradual shift appears from a nocturnal to a diurnal activity after two months (Mat et al., 2012). The authors concluded that the circadian clock does exist but is weak in oysters.

A yearlong study on *M. gigas* in the Arcachon Bay, on the Atlantic shoreline in France, described an effect of the sun-earth-moon system on their behaviour (Tran et al., 2011). Constantly immersed, oysters have mainly a tidal shell gaping activity. This tidal activity changes around the synodic month with a longer closure time of the valves during neap tides and an increase with spring tides. Therefore oyster behaviour also follows circalunar oscillations and might be entrained by clocks at such frequencies.

Rhythms of shell biomineralisation: the biological clocks hypothesis

As seen before, environmental rhythmic variations do not exclusively provide explanations regarding the number of increments formed per day, which raises the question of an endogeneous rhythm of biomineralisation. Similar periodicities observed in shell growth patterns and clock genes expression of bivalves (Figure 6A-B) support the prevailing concept that biological clocks are likely to be involved in the control of rhythms of biomineralisation. The existence and nature of the interaction between the two remain to be determined. Although valvometry, a classical output of biological clocks in bivalves, can be used to measure the shell growth rate, direct relationships between valve activity

and growth increment formation are still lacking (Schwartzmann et al., 2011; Andrade et al., 2016). The oyster *M. gigas* exhibits changes in the width of tidal increments according to the moon cycle, showing circalunar (*i.e.*, 29.5 days) and semi-circalunar (*i.e.*, 14.8 days) variations (Huyghe et al., 2019). The tidal activity in valve closure also describes a synodic frequency (Tran et al., 2011). Surprisingly, studies showed that shell growth increments (*i.e.,* growth rate) are wider during neap tides, while valve opening increases at spring tides (Tran et al., 2011; Huyghe et al., 2019). Precautions must be taken when comparing these studies, because oysters have been reared in different habitats; they were continuously immersed in the experiment of Tran et al. (2011) while specimens of Huyghe et al. (2019) were studied in an intertidal habitat with periodic aerial exposures.

At the molecular level, a single bimodal circadian/circatidal clock can entrain valve aperture of oysters at daily or tidal frequencies, following the predominance of the environmental drivers (Mat et al., 2012; Tran et al., 2020). However, such plasticity has not been demonstrated yet nor correlated with daily or tidal incrementation in shells for a single population according to their environment. Oysters constantly bred immersed in the French Mediterranean Thau lagoon, characterised by a reduced tidal regime (<20 cm), exhibit daily growth increments rather than tidal ones as observed in oysters from coastal area of the English Channel (Langlet et al., 2006; Huyghe et al., 2019). Water temperature and phytoplankton vertical migrations, known to be associated with the photoperiod, have been proposed as potential drivers of the daily dynamics of shell growth (Huyghe et al., 2019). Similar observations have been made in mussels. They exhibit tidal growth increments in areas dominated by a strong tidal regime, such as along the coast of the United Kingdom and offshore in the North Sea, independently from their position in the water column (*i.e.*, in intertidal and subtidal conditions) (Richardson, 1989; Richardson et al., 1990). Also, daily growth increments are formed in the French Mediterranean Salses-Leucate lagoon, where tides are strongly reduced (Andrisoa et al., 2019). Altogether, these data suggest that biomineralisation rhythm could vary within the same species and might be controlled by the strongest clock driver present in its environment. This could occur through the activation of genes involved in biomineralisation processes by the biological clocks. For some of genes (*i.e.*, coding for chitinase, nacrein, N16 and MSI60), seasonal and circadian expression rhythms have been described in molluscs (Miyazaki et al., 2008; Banni et al., 2011). Moreover, the mantle transcriptomes of three Pectinids (*i.e.*, *Pecten yessoensis, Pecten magellanicus, Argopecten irradians)* has allowed to identify the expression of genes (*i.e., cry, calmodulin, opsin* and *rhodopsin* among others) with light-mediated functions, tightly linked with biological clocks (Sun et al., 2016). The research area called “shellomics” (*i.e.*, proteomics applied on shells), could help decipher the molecular toolbox for shell construction (Marin, 2020). Omics applied on a temporal basis would help to understand the possible link between biological clocks with the shell growth.

The deep-sea habitat is a promising environment to test the hypothesis of the role of biological clocks on shell biomineralisation and growth rhythms as many environmental drivers are constant or exhibit slight oscillations (*e.g.*, photoperiod, temperature). Mussels living at deep-sea hydrothermal vents produce lunidian and tidal growth increments, as observed for *Bathymodiolus brevior* from the South-West Pacific at 2000 m depth (Schöne and Giere, 2005) and *B. thermophilus* on the East Pacific Rise at 2500 m depth (Nedoncelle et al., 2013, 2015). Measurements of pressure, current velocity and orientation, temperature, pH and sulfide concentration in the deep-sea habitat revealed daily and tidal changes (Nedoncelle et al., 2015), which might result from tidal pumping of vent fluids and mixing with the deep and cold seawater (Crone and Wilcock, 2005; Scheirer et al., 2006). Deep-sea mussels harbour chemosymbionts in their gills that are able to use specific nutrients present in the hydrothermal flume such as sulfide or methane. As a result, the symbionts provide an important source of organic carbon and thus energy fuel for the mussel (Duperron, 2010). This energy supply is used for shell growth when, alternatively, mussels benefit from oxygen of seawater and their symbionts are exposed to electron donors (*i.e.*, H_2S). Growth rates are greater during periods of larger tidal ranges (Nedoncelle et al., 2015). Interestingly, *in situ* behavioural and transcriptomic analysis of biological clock genes of the deep-sea mussel *B. azoricus* from the Mid-Atlantic Ridge, showed that circatidal oscillations are dominant although a circadian response is observed in the laboratory, when mussels are submitted to daily stimuli (*i.e.*, LD photoperiodic condition) (Mat et al., 2020). Based on evidences related to the fractionation of carbon isotopes (*i.e.*, disequilibrium in the relative partitioning of heavier and lighter isotopes between seawater and shells) induced by chemosymbionts activity, the shell $\delta^{13}C$ could be used to track changes in community composition over time, particularly the ratio between methanotrophic and sulfo-oxidising symbionts for bivalve species which host a dual symbiosis, as suggested for *Bathymodiolus* from various hydrothermal vent habitats (Nedoncelle et al., 2014).

The role of symbionts on the physiology of bivalve is an important component for species that host photosynthetic algae in their tissues as phototrophy is the main source of energy for them (Klumpp and Griffiths, 1994). Effects of symbionts on biomineralisation is likely explained by the hypothesis of the light-enhanced calcification (LEC), in which symbionts might increase the energy and the (in)organic components supply throughout photosynthesis (for review see Allemand et al., 2011). The LEC is the current explanation for the higher calcification rate of photosymbiotic species (few cm per year) compared to other non-symbiotic close-related species (Beckvar, 1981; Hawkins and Klumpp, 1995; Allemand et al., 2011). The photoperiod is likely implicated in the shell incrementation rhythm as all symbiotic bivalves show daily growth bands (Pannella and MacClintock, 1968; Schwartzmann et al., 2011; Gannon et al., 2017). The valve activity also exhibits daily patterns, from widely open during the day to provide light to symbionts, to partially or entirely closed at night, as illustrated for the giant

clam *Hippopus hippopus* (Schwartzmann et al., 2011). At molecular scales, multiple studies have been done on *Tridacna squamosa* proteins linked to the biomineralisation process. Light-dependent expression and protein levels are reported in most of them (Ip et al., 2015, 2017, 2018; Boo et al., 2017; Hiong et al., 2017; Cao-Pham et al., 2019; Chew et al., 2019). Rhythmic production pattern under various photoperiodic conditions (*e.g.*, LD, DD, LL) of those proteins has not been studied yet and could indicate if a biological clock is driving their synthesis.

The smallest time units recorded in shells

Daily to tidal units are classically recognised as the basic timeframe of the growth by increment in bivalve shells. But as suggested above (Figure 6A), smaller time units have been described (Yamaguchi et al., 2006; Huyghe et al., 2019). They are reported as the consequence of several growth breaks during the formation of a growth increment, leading to the production of five to ten sub-increments, named micro-increments, per day without recognisable factor controlling their periodicity. Actually, ultradian growth stops are not that infrequent in bivalve shells, as illustrated by Dauphin *et al.* (2003), with amounts of micro growth lines at micrometer scales in the shells of *Pinctada margaritifera* and *Pinna nobilis*. Schöne (2008) has also reported the presence of several ultradian growth micro-increments within daily increments in the shell of *Chione cortezi* and *Anodonta cygnea*. Close similar growth micro-increments were observed in the skeleton of the coral *Pocillopora damicornis* and in mouse teeth (Brahmi et al., 2012; Ono et al., 2019). The mechanisms involved to produce those growth micro-increments remain however unknown.

In the case of bivalves, it is suggested that under stressful conditions (*e.g.*, temperatures above 31°C for *M. galloprovincialis* and *Merceneria merceneria*), the impaired physiological activity may affect shell growth (Ansell, 1968; Anestis et al., 2007a). But it is also assumed that ultradian metronomes must be essential to orchestrate cellular functioning, such as cell division, heart rate and chemical reactions (Lloyd and Murray, 2005). Based on video records, Rodland et al. (2006) measured the behavioural activity of three bivalve species (*A. cygnea*, *A. islandica* and *M. edulis*) and found rhythmic siphon activities on a period of 3 to 7 min and 10 to 20 min, with a duration of valve contraction over 60 to 90 min. These authors suggest that intrinsic mechanisms (*i.e.*, guided by physiological and/or genetic factors), rather than the environment, control such periodicities. The direct link between intrinsic mechanisms and shell microincrements is not established but Rodland *et al.* (2006) hypothesised that hourly rhythms in valve opening could produce microincrements between

1 and 5 µm, similar to those observed by Schöne et al. (2002) inside the lunidian increments of *C. cortezi*. However, micro-increments could also be the result of environmental variations, as illustrated by Yan *et al.* (2020) with the observations of microbands of different fluorescent intensity under confocal microscope in the giant clam *Tridacna* spp. Coupled with geochemical tools (in this case nanoSIMS), the authors revealed hourly changes of Fe/Ca ratios into shells, likely due to vertical mixing of iron in the water column during storm events. Further investigations on these short-term growth units and the search for biological clocks at higher frequencies in bivalves are required. Many studies pointed out ultradian endogenous timekeeping mechanisms in vertebrates that are meeting the temperature compensation and the self-sustained assumptions but no genes involved in the central molecular oscillator has been proposed yet (Ono et al., 2015; Ghenim et al., 2021).

Further research directions

The unit of time in shell, the increment, is well described and often used to infer a time frame to observations made in biomaterials. Unfortunately, the environmental drivers leading to the periodic formation of an increment are still poorly understood. The question is difficult to elucidate as there is probably not only one environmental cue driving the process but rather a combination of several factors among which a hierarchy likely exists. Biological clocks might be involved in increments formation but the regulation between clock and biomineralisation genes, and the production of the resulting growth increment, still need to be deciphered. A gap between the distinct scientific communities working on biomaterials can now be bridged through interdisciplinary researches across molecular biology, ecology and earth sciences. Observations made in this review could be used as some research trajectories.

Thanks to the development of molecular approaches, recent advances have been made to characterise biological clocks and how they affect the physiology of bivalves. A further step has to be taken in order to incorporate the shell response in chronobiological studies. This gap is actually shorter than expected as both chronobiologists and sclerochronologists usually work on similar biological models *(e.g.*, oysters, pectens, mussels). These species are found in a wide spatial repartition and live in different types of habitat (*e.g.*, estuaries, lagoons, coastal marine habitats) which correspond to ideal conditions to study such integrative processes. Both in the field and in aquaria, experiments need to be conducted using different environmental settings, with parameters recorded or controlled, using

combined approaches of gene expressions (*i.e.*, the ones involved in clocks and biomineralisation) together with shell growth patterns analysis.

In addition to classical zeitgebers observed in chronobiology (*i.e.*, photoperiod or temperature), food availability and / or composition could be another important environmental driver of the internal biological clock system, particularly in the control of the shell growth. Valve activity responds to the presence of the energy source of the bivalve (*e.g.*, concentration in chlorophyll *a*) as illustrated for *A. islandica* (Ballesta-Artero et al., 2017). In the absence of food, valves remain closed which could lead to pH decrease in the EPF leading to decalcification. The integration of this environmental cue by a clock is however still unclear. The biological clock is an evolutionary innovation that aims to adjust the rhythm of the organism to its environment in order to optimise its energetic balance. In other terms, it allows the organism to be ready to incorporate nutriments when available, and then use the energy when present. The effect of food availability on endogenous rhythms has been extensively studied on mice and is associated to the peripherical clock system (Escobar et al., 2009). Experiments on suprachiasmatic nucleus ablated rats shown that starved individuals continue to exhibit a circadian food-anticipatory activity (FAA) (Boulos and Terman, 1980; Mistlberger, 2009). The notion of FAA and food-entrainment are different but linked together. The importance of the influence of food as time giver on the FAA is still under discussion (see the review of Mistlberger (2009)). In bivalves, a study on the intertidal filter-feeder clam *Austrovenus stutchburyi* suggests that the FAA is linked to a food-entrained oscillator (Williams and Pilditch, 1997). This possible role of food in shell growth rhythms should be considered in future studies using biological archives for (paleo)environmental reconstructions.

Biomineralisation should be seen as a dynamical process that punctually slows down or even stops. Biomineralisation activity throughout time can be followed directly using the analysis of changes in the composition of the extrapallial fluid (EPF) over time. This technique uses microsensors able to be placed in the extrapallial cavity or by suction of the EPF (Misogianes and Chasteen, 1979; Stemmer et al., 2019). Using this last method, observations of Ca^{2+}, dissolved inorganic carbon (DIC) and pH variations in the fluid suggest that calcification occurs by waves, which is consistent with the observation of increments in the shell (Stemmer et al., 2019). Therefore, this method can be used to visualise directly the effect of an environmental variable on the biomineralisation kinetics.

The inorganic fraction of the shell is not the only one present in the EPF as organic compounds are key components in the biomineralisation process due to their role of backbone for the deposition of inorganic material (Marin and Luquet, 2004). Proteomic approaches can thus be used on EPF samples taken at regular time intervals. A part of organic components of shells are the direct output

of the transcription and translation of genes involved in biomineralisation. Their transcription is not a random process and is the result of molecular pathways reacting to environmental cues. A better understanding of the molecular machinery behind biomineralisation (organic and inorganic compounds) and the reconstitution of the molecular pathways are essential to decipher how the process is activated or repressed (see review Clark, 2020). Molecular characterisation might indicate if there are pathways between the biomineralisation process and the biological clock machinery. Direct response of bivalve behaviour and shell growth to environmental variations can be monitored using a combined approach of valvometry and sclerochronology on the same specimens. This can be done even for short-term experiments as chemical staining such as calcein or manganese have been demonstrated to be rapidly incorporated and visible (< 30 min) during the shell biomineralisation (Langlet et al., 2006; Lartaud et al., 2010; Mahé et al., 2010).

Importantly, the community has to keep in mind that periodicities observed in shells are not necessarily the same during the whole life of a bivalve, which can be at the origin of bias when inferring past and present environments from the study of shell growth patterns. Owen et al. (2002) reported changes of patterns throughout the year in scallops. One daily increment in the juvenile *Pecten maximus* shell is observed during summer and less than one increment per day in winter, when growth rate is slower. Missing increments has been reported for the young oysters *M. gigas* (<one year), forming less than one increment per day instead of bi-daily tidal-influenced growth periodicity for older specimens, while reaching high growth rates during this period (Huyghe et al., 2019). This is in opposition with usual observations. Interestingly, those authors also reported occasional arhythmicity in juveniles part with the formation of up to five increments per day on the youngest part of the shell without any relationship with environmental parameters. As uncommon periodicities are often observed in juveniles, a better understanding of the sensory organs of bivalves and their ontogenesis might give some responses to the integration of environmental drivers throughout the organism life. The larval shell production might be more deeply investigated as this period of life is recognised as particularly sensitive to anthropogenic stressful conditions, such as ocean acidification and global warming (Gobler et al., 2014; Wang et al., 2017).

Conclusion

In conclusion, although widely used to reconstruct past environments and estimate the potential effect of climate change on shellfish production, the dynamic process of bivalves

biomineralisation is still not fully understood and the origins of the periodicities preserved in shells remains unclear. In this review different research axes have been proposed. A better comprehension of the integration of the environment in bivalve shells, driven or not by biological clocks, is crucial in order to refine models notably used to derive growth rate from geochemical profiles in paleoclimatology. Also, the characterisation of ultradian micro-increments observed within the daily or tidal increment, is promising to improve the monitoring of bivalve physiological response to its environment and/or propose a temporal resolution never reached for past environmental studies. Bivalve are known to have a high ecological value as they are recognised as carbon sink and engineering species, forming refuges for biodiversity, their reaction to climate change will have a huge impact on many other species. A better understanding of the relation between the bivalve and its environment will additionally help to forecast the effect of climate changes on those communities.

Additional information

Author contributions

This review is the product of the PhD thesis of VL. following completion of research supervised by FL and LB. VL wrote the original draft. FL and LB edited and revised the manuscript. VL produced the artwork within this article and FL and LB revised it. All authors contributed to the article and approved the submitted version.

Funding

This project has received the financial support from the CNRS through the 80|Prime - MITI interdisciplinary program “TEMPO” and the MITI interdisciplinary program “ARCHIVE”.

Acknowledgments

Authors are grateful to Mélanie Dussenne for checking the spelling.

References

Allemand, D., Tambutté, É., Zoccola, D., and Tambutté, S. (2011). "Coral Calcification, Cells to Reefs," in *Coral reefs: An ecosystem in transition* (Dordrecht: Springer), 119–150. doi:10.1007/978-94-007-0114-4_9.

Alves, M. G., and Oliveira, P. F. (2013). Effects of non-steroidal estrogen diethylstilbestrol on pH and ion transport in the mantle epithelium of a bivalve *Anodonta cygnea*. *Ecotoxicol. Environ. Saf.* 97, 230–235. doi:10.1016/j.ecoenv.2013.07.024.

Andrade, H., Massabuau, J.-C., Cochrane, S., Ciret, P., Tran, D., Sow, M., et al. (2016). High Frequency Non-invasive (HFNI) Bio-Sensors As a Potential Tool for Marine Monitoring and Assessments. *Front. Mar. Sci.* 3, 187. doi:10.3389/FMARS.2016.00187.

Andrisoa, A., Lartaud, F., Rodellas, V., and Neveu, I. (2019). Enhanced Growth Rates of the Mediterranean Mussel in a Coastal Lagoon Driven by Groundwater Inflow. *Front. Mar. Sci.* 6, 753. doi:10.3389/fmars.2019.00753.

Anestis, A., Lazou, A., Pörtner, H. O., and Michaelidis, B. (2007). Behavioral, metabolic, and molecular stress responses of marine bivalve *Mytilus galloprovincialis* during long-term acclimation at increasing ambient temperature. *Am. J. Physiol. - Regul. Integr. Comp. Physiol.* 293, 911–921. doi:10.1152/ajpregu.00124.2007.

Ansell, A. D. (1968). The rate of growth of the hard clam *Mercenaria mercenaria* (L) throughout the geographical range. *ICES J. Mar. Sci.* 31, 364–409. doi:10.1093/icesjms/31.3.364.

Aschoff, J. (1981). "Freerunning and Entrained Circadian Rhythms," in *Biological Rhythms* (Boston, MA.: Springer US), 81–93. doi:10.1007/978-1-4615-6552-9_6.

Ballesta-Artero, I., Witbaard, R., Carroll, M. L., and van der Meer, J. (2017). Environmental factors regulating gaping activity of the bivalve *Arctica islandica* in Northern Norway. *Mar. Biol.* 164, Article 116. doi:10.1007/s00227-017-3144-7.

Banni, M., Negri, A., Mignone, F., Boussetta, H., Viarengo, A., and Dondero, F. (2011). Gene Expression Rhythms in the Mussel *Mytilus galloprovincialis* (Lam.) across an Annual Cycle. *PLoS One* 6, e18904. doi:10.1371/journal.pone.0018904.

Bartness, T. J., and Albers, H. E. (2000). "Activity Patterns and the Biological Clock in Mammals," in *Activity patterns in small mammals* (Springer, Berlin, Heidelberg), 23–47. doi:10.1007/978-3-642-18264-8_3.

Beckvar, N. (1981). Cultivation, spawning, and growth of the giant clams *Tridacna gigas*, *T. derasa*, and *T. squamosa* in Palau, Caroline Islands. *Aquaculture* 24, 21–30. doi:10.1016/0044-8486(81)90040-5.

Boo, M. V., Hiong, K. C., Choo, C. Y. L., Cao-Pham, A. H., Wong, W. P., Chew, S. F., et al. (2017). The inner mantle of the giant clam, *Tridacna squamosa*, expresses a basolateral Na+/K+-ATPase α-subunit, which displays light-dependent gene and protein expression along the shell-facing epithelium. *PLoS One* 12, e0186865. doi:10.1371/journal.pone.0186865.

Boulos, Z., and Terman, M. (1980). Food availability and daily biological rhythms. *Neurosci. Biobehav. Rev.* 4, 119–131. doi:10.1016/0149-7634(80)90010-X.

Brahmi, C., Kopp, C., Domart-Coulon, I., Stolarski, J., and Meibom, A. (2012). Skeletal growth dynamics linked to trace-element composition in the scleractinian coral *Pocillopora damicornis*. *Geochim. Cosmochim. Acta* 99, 146–158. doi:10.1016/j.gca.2012.09.031.

Butler, P. G., and Schöne, B. R. (2017). New research in the methods and applications of sclerochronology. *Palaeogeogr. Palaeoclimatol. Palaeoecol.* 465, 295–299. doi:10.1016/J.PALAEO.2016.11.013.

Cao-Pham, A. H., Hiong, K. C., Boo, M. V., Choo, C. Y. L., Wong, W. P., Chew, S. F., et al. (2019). Calcium absorption in the fluted giant clam, Tridacna squamosa, may involve a homolog of voltage-gated calcium channel subunit α1 (CACNA1) that has an apical localization and displays light-enhanced protein expression in the ctenidium. *J. Comp. Physiol. B Biochem. Syst. Environ. Physiol.* 189, 693–706. doi:10.1007/s00360-019-01238-4.

Carré, M., Bentaleb, I., Bruguier, O., Ordinola, E., Barrett, N. T., and Fontugne, M. (2006). Calcification rate influence on trace element concentrations in aragonitic bivalve shells: Evidences and mechanisms. *Geochim. Cosmochim. Acta* 70, 4906–4920. doi:10.1016/j.gca.2006.07.019.

Chapman, E. C., Bonsor, B. J., Parsons, D. R., and Rotchell, J. M. (2020). Influence of light and temperature cycles on the expression of circadian clock genes in the mussel *Mytilus edulis*. *Mar. Environ. Res.* 159, 104960. doi:10.1016/j.marenvres.2020.104960.

Checa, A. G. (2018). Physical and biological determinants of the fabrication of Molluscan shell microstructures. *Front. Mar. Sci.* 5, 353. doi:10.3389/fmars.2018.00353.

Checa, A. G., Esteban-Delgado, F. J., and Rodríguez-Navarro, A. B. (2007). Crystallographic structure of the foliated calcite of bivalves. *J. Struct. Biol.* 157, 393–402. doi:10.1016/j.jsb.2006.09.005.

Checa, A. G., Macías-Sánchez, E., Harper, E. M., and Cartwright, J. H. E. (2016). Organic membranes determine the pattern of the columnar prismatic layer of mollusc shells. *Proc. R. Soc. B Biol. Sci.* 283, 20160032. doi:10.1098/rspb.2016.0032.

Checa, A. G., Okamoto, T., and Ramírez, J. (2006). Organization pattern of nacre in Pteriidae (Bivalvia: Mollusca) explained by crystal competition. *Proc. R. Soc. B Biol. Sci.* 273, 1329–1337. doi:10.1098/rspb.2005.3460.

Checa, A. G., Rodríguez-Navarro, A. B., and Esteban-Delgado, F. J. (2005). The nature and formation of calcitic columnar prismatic shell layers in pteriomorphian bivalves. *Biomaterials* 26, 6404–6414. doi:10.1016/j.biomaterials.2005.04.016.

Chew, S. F., Koh, C. Z. Y., Hiong, K. C., Choo, C. Y. L., Wong, W. P., Neo, M. L., et al. (2019). Light-enhanced expression of Carbonic Anhydrase 4-like supports shell formation in the fluted giant clam *Tridacna squamosa*. *Gene* 683, 101–112. doi:10.1016/j.gene.2018.10.023.

Clark, G. R. (2005). Daily growth lines in some living Pectens (Mollusca: Bivalvia), and some applications in a fossil relative: Time and tide will tell. *Palaeogeogr. Palaeoclimatol. Palaeoecol.* 228, 26–42. doi:10.1016/j.palaeo.2005.03.044.

Clark, M. S. (2020). Molecular mechanisms of biomineralization in marine invertebrates. *J. Exp. Biol.* 223, jeb206961. doi:10.1242/jeb.206961.

Coen, L. D., Brumbaugh, R. D., Bushek, D., Grizzle, R., Luckenbach, M. W., Posey, M. H., et al. (2007). Ecosystem services related to oyster restoration. *Mar Ecol Prog Ser* 341, 303–307. doi:10.3354/meps341303.

Coimbra, J., Machado, J., Fernandes, P. L., Ferreira, H. G., and Ferreira, K. G. (1988). Electrophysiology of the Mantle of *Anodonta Cygnea*. *J. Exp. Biol.* 140, 65–88. doi:10.1242/JEB.140.1.65.

Comeau, L. A., Babarro, J. M. F., Longa, A., and Padin, X. A. (2018). Valve-gaping behavior of raft-cultivated mussels in the Ría de Arousa, Spain. *Aquac. Reports* 9, 68–73. doi:10.1016/J.AQREP.2017.12.005.

Connor, K. M., and Gracey, A. Y. (2011). Circadian cycles are the dominant transcriptional rhythm in the intertidal mussel *Mytilus californianus*. *Pnas* 108, 16110–16115. doi:10.1073/pnas.1111076108.

Crenshaw, A. (1972). The inorganic composition of molluscan extrapallial Fluid. *Biol. Bull.* 143, 506–512. doi:10.2307/1540180.

Crone, T. J., and Wilcock, W. S. D. (2005). Modeling the effects of tidal loading on mid-ocean ridge hydrothermal systems. *Geochemistry, Geophys. Geosystems* 6, Q07001. doi:10.1029/2004GC000905.

Dauphin, Y., Cuif, J. P., Doucet, J., Salomé, M., Susini, J., and Williams, C. T. (2003). In situ mapping of growth lines in the calcitic prismatic layers of mollusc shells using X-ray absorption near-edge structure (XANES) spectroscopy at the sulphur K-edge. *Mar. Biol.* 142, 299–304. doi:10.1007/s00227-002-0950-2.

de Winter, N. J., Goderis, S., Van Malderen, S. J. M., Sinnesael, M., Vansteenberge, S., Snoeck, C., et al. (2020). Subdaily-Scale Chemical Variability in a *Torreites Sanchezi* Rudist Shell: Implications for Rudist Paleobiology and the Cretaceous Day-Night Cycle. *Paleoceanogr. Paleoclimatology* 35, e2019PA003723. doi:10.1029/2019PA003723.

Ditty, J. L., Williams, S. B., and Golden, S. S. (2003). A Cyanobacterial Circadian Timing Mechanism. *Annu. Rev. Genet.* 37, 513–543. doi:10.1146/annurev.genet.37.110801.142716.

Dodd, J. R. (1965). Environmental control of strontium and magnesium in Mytilus. *Geochim. Cosmochim. Acta* 29, 385–398. doi:10.1016/0016-7037(65)90035-9.

Dunlap, J. C. (1999). Molecular bases for circadian clocks. *Cell* 96, 271–290. doi:10.1016/s0092-8674(00)80566-8.

Duperron, S. (2010). "The Diversity of Deep-Sea Mussels and Their Bacterial Symbioses," in *The vent and seep biota - Aspect from microbes to ecosystems* (Springer, Dordrecht), 137–167. doi:10.1007/978-90-481-9572-5_6.

Dupraz, C., Reid, R. P., Braissant, O., Decho, A. W., Norman, R. S., and Visscher, P. T. (2009). Processes of carbonate precipitation in modern microbial mats. *Earth-Science Rev.* 96, 141–162. doi:10.1016/j.earscirev.2008.10.005.

Enright, J. T. (1976). Plasticity in an isopod's clockworks: Shaking shapes form and affects phase and frequency. *J. Comp. Physiol.* 107, 13–37. doi:10.1007/BF00663916.

Epstein, S., Buchsbaum, R., Lowenstam, H. A., and Urey, H. C. (1953). Revised carbonate-water isotopic temperature scale. *Geol. Soc. Am. Bull.* 64, 1315–1326. doi:10.1130/0016-7606(1953)64[1315:RCITS]2.0.CO;2.

Escobar, C., Cailotto, C., Angeles-Castellanos, M., Delgado, R. S., and Buijs, R. M. (2009). Peripheral oscillators: The driving force for food-anticipatory activity. *Eur. J. Neurosci.* 30, 1665–1675. doi:10.1111/j.1460-9568.2009.06972.x.

Figueroa, F. L., Niell, F. X., Figueiras, F. G., and Villarino, M. L. (1998). Diel migration of phytoplankton and spectral light field in the Ría de Vigo (NW Spain). *Mar. Biol.* 130, 491–499. doi:10.1007/s002270050269.

Gannon, M. E., Pérez-Huerta, A., Aharon, P., and Street, S. C. (2017). A biomineralization study of the Indo-Pacific giant clam *Tridacna gigas*. *Coral Reefs* 36, 503–517. doi:10.1007/s00338-016-1538-5.

Gao, J., Chen, Y., Yang, Y., Liang, J., Xie, J., Liu, J., et al. (2016). The transcription factor Pf-POU3F4 regulates expression of the matrix protein genes *Aspein* and *Prismalin-14* in pearl oyster (*Pinctada fucata*). *FEBS J.* 283, 1962–1978. doi:10.1111/febs.13716.

García-March, J. R., Sanchís Solsona, M. Á., and García-Carrascosa, A. M. (2008). Shell gaping behaviour of *Pinna nobilis* L., 1758: circadian and circalunar rhythms revealed by in situ monitoring. *Mar. Biol.* 153, 689–698. doi:10.1007/s00227-007-0842-6.

Ghenim, L., Allier, C., Obeid, P., Hervé, L., Fortin, J. Y., Balakirev, M., et al. (2021). A new ultradian rhythm in mammalian cell dry mass observed by holography. *Sci. Reports 2021* 11, 1290. doi:10.1038/s41598-020-79661-9.

Giuffre, A. J., Hamm, L. M., Han, N., De Yoreo, J. J., and Dove, P. M. (2013). Polysaccharide chemistry regulates kinetics of calcite nucleation through competition of interfacial energies. *Proc. Natl. Acad. Sci. U. S. A.* 110, 9261–9266. doi:10.1073/pnas.1222162110.

Gobler, C. J., DePasquale, E. L., Griffith, A. W., and Baumann, H. (2014). Hypoxia and Acidification Have Additive and Synergistic Negative Effects on the Growth, Survival, and Metamorphosis of Early Life Stage Bivalves. *PLoS One* 9, e83648. doi:10.1371/JOURNAL.PONE.0083648.

Hallmann, N., Burchell, M., Schöne, B. R., Irvine, G. V., and Maxwell, D. (2009). High-resolution sclerochronological analysis of the bivalve mollusk *Saxidomus gigantea* from Alaska and British Columbia: techniques for revealing environmental archives and archaeological seasonality. *J. Archaeol. Sci.* 36, 2353–2364. doi:10.1016/j.jas.2009.06.018.

Hartmann, J. T., Beggel, S., Auerswald, K., and Geist, J. (2016). Determination of the most suitable adhesive for tagging freshwater mussels and its use in an experimental study of filtration behaviour and biological rhythm. *J. Molluscan Stud.* 82, 415–421. doi:10.1093/mollus/eyw003.

Hawkins, A. J. S., and Klumpp, D. W. (1995). Nutrition of the giant clam *Tridacna gigas* (L.). II. Relative contributions of filter-feeding and the ammonium-nitrogen acquired and recycled by symbiotic alga towards total nitrogen requirements for tissue growth and metabolism. *J. Exp. Mar. Bio. Ecol.* 190, 263–290. doi:10.1016/0022-0981(95)00044-R.

Hiong, K. C., Cao-Pham, A. H., Choo, C. Y. L., Boo, M. V., Wong, W. P., Chew, S. F., et al. (2017). Light-dependent expression of a Na + /H + exchanger 3-like transporter in the ctenidium of the giant clam, *Tridacna squamosa* , can be related to increased H + excretion during light-enhanced calcification. *Physiol. Rep.* 5, e13209. doi:10.14814/phy2.13209.

Huyghe, D., Rafelis, M. De, Ropert, M., Mouchi, V., Emmanuel, L., and Renard, M. (2019). New insights into oyster high - resolution hinge growth patterns. *Mar. Biol.* 166, 48. doi:10.1007/s00227-019-3496-2.

Ip, Y. K., Ching, B., Hiong, K. C., Choo, C. Y. L., Boo, M. V., Wong, W. P., et al. (2015). Light induces changes in activities of Na+/K+-ATPase, H+/K+-ATPase and glutamine synthetase in tissues involved directly or indirectly in light-enhanced calcification in the giant clam, *Tridacna squamosa*. *Front. Physiol.* 6, 68. doi:10.3389/fphys.2015.00068.

Ip, Y. K., Hiong, K. C., Lim, L. J. Y., Choo, C. Y. L., Boo, M. V., Wong, W. P., et al. (2018). Molecular characterization, light-dependent expression, and cellular localization of a host vacuolar-type H+-ATPase (VHA) subunit A in the giant clam, *Tridacna squamosa*, indicate the involvement of the host VHA in the uptake of inorganic carbon and. *Gene* 659, 137–148. doi:10.1016/j.gene.2018.03.054.

Ip, Y. K., Koh, C. Z. Y., Hiong, K. C., Choo, C. Y. L., Boo, M. V., Wong, W. P., et al. (2017). Carbonic anhydrase 2-like in the giant clam, *Tridacna squamosa* : characterization, localization, response

to light, and possible role in the transport of inorganic carbon from the host to its symbionts. *Physiol. Rep.* 5, e13494. doi:10.14814/phy2.13494.

Jones, D. S. (1980). Annual cycle of shell growth increment formation in two continental shelf bivalves and its paleoecologic significance. *Paleobiology* 3, 331–340. doi:10.1017/S0094837300006837.

Karney, G. B., Butler, P. G., Speller, S., Scourse, J. D., Richardson, C. A., Schrder, M., et al. (2012). Characterizing the microstructure of *Arctica islandica* shells using NanoSIMS and EBSD. *Geochemistry, Geophys. Geosystems* 13, Q04002. doi:10.1029/2011GC003961.

Kennish, M. J., and Olsson, R. K. (1975). Effects of thermal discharges on the microstructural growth of *Mercenaria mercenaria*. *Environ. Geol.* 1, 41–64. doi:10.1007/BF02426940.

Killam, D. E., and Clapham, M. E. (2018). Identifying the ticks of bivalve shell clocks: Seasonal growth in relation to temperature and food supply. *Palaios* 33, 228–236. doi:10.2110/palo.2017.072.

Klumpp, D. W., and Griffiths, C. L. (1994). Contributions of phototrophic and heterotrophic nutrition to the metabolic and growth requirements of four species of giant clam (Tridacnidae). *Mar. Ecol. Prog. Ser.* 115, 103–115. doi:10.3354/meps115103.

Langlet, D., Alunno-Bruscia, M., Rafélis, M., Renard, M., Roux, M., Schein, E., et al. (2006). Experimental and natural cathodoluminescence in the shell of *Crassostrea gigas* from Thau lagoon (France): Ecological and environmental implications. *Mar. Ecol. Prog. Ser.* 317, 143–156. doi:10.3354/meps317143.

Lartaud, F., Chauvaud, L., Richard, J., Toulot, A., Bollinger, C., Testut, L., et al. (2010). Experimental growth pattern calibration of Antarctic scallop shells (*Adamussium colbecki*, Smith 1902) to provide a biogenic archive of high-resolution records of environmental and climatic changes. *J. Exp. Mar. Bio. Ecol.* 393, 158–167. doi:10.1016/j.jembe.2010.07.016.

Li, S., Liu, Y., Huang, J., Zhan, A., Xie, L., and Zhang, R. (2017). The receptor genes PfBMPR1B and PfBAMBI are involved in regulating shell biomineralization in the pearl oyster *Pinctada fucata*. *Sci. Rep.* 7, 9219. doi:10.1038/s41598-017-10011-y.

Littlewood, D. T. J., and Young, R. E. (1994). The effect of air-gaping behaviour on extrapallial fluid pH in the tropical oyster *Crassostrea rhizophorae*. *Comp. Biochem. Physiol. -- Part A Physiol.* 107, 1–6. doi:10.1016/0300-9629(94)90264-X.

Lloyd, D., and Murray, D. B. (2005). Ultradian metronome: Timekeeper for orchestration of cellular coherence. *Trends Biochem. Sci.* 30, 373–377. doi:10.1016/j.tibs.2005.05.005.

Lutz, R. A., and Rhoads, D. C. (1977). Anaerobiosis and a Theory of Growth Line Formation. *Science.* 198, 1222–1227. doi:10.1126/science.198.4323.1222.

Mahé, K., Bellamy, E., Lartaud, F., and Rafélis, M. De (2010). Calcein and manganese experiments for marking the shell of the common cockle (*Cerastoderma edule*): tidal rhythm validation of increments formation. *Aquat. Living Resour.* 245, 239–245. doi:https//:doi.org/10.1051/alr/2010025.

Marin, F. (2020). Mollusc shellomes: Past, present and future. *J. Struct. Biol.* 212, 107583. doi:10.1016/j.jsb.2020.107583.

Marin, F., and Luquet, G. (2004). Molluscan shell proteins. *Comptes Rendus - Palevol* 3, 469–492. doi:10.1016/j.crpv.2004.07.009.

Marin, F., Luquet, G., Marie, B., and Medakovic, D. (2007). Molluscan Shell Proteins: Primary Structure, Origin, and Evolution. *Curr. Top. Dev. Biol.* 80, 209–276. doi:10.1016/S0070-2153(07)80006-8.

Marin, F., Roy, N. Le, and Marie, B. (2012). The formation and mineralization of mollusk. *Front. Biosci.* 4, 1099–1125. doi:10.2741/S321.

Mat, A. M., Massabuau, J. C., Ciret, P., and Tran, D. (2012). Evidence for a plastic dual circadian rhythm in the oyster *Crassostrea gigas*. *Chronobiol. Int.* 29, 857–867. doi:10.3109/07420528.2012.699126.

Mat, A. M., Sarrazin, J., Markov, G. V, Apremont, V., Dubreuil, C., Eché, C., et al. (2020). Biological rhythms in the deep-sea hydrothermal mussel *Bathymodiolus azoricus*. *Nat. Commun.* 11, 3454. doi:10.1038/s41467-020-17284-4.

Miglioli, A., Dumollard, R., Balbi, T., Besnardeau, L., and Canesi, L. (2019). Characterization of the main steps in first shell formation in *Mytilus galloprovincialis*: Possible role of tyrosinase. *Proc. R. Soc. B Biol. Sci.* 286, 20192043. doi:10.1098/rspb.2019.2043.

Misogianes, M. J., and Chasteen, N. D. (1979). A chemical and spectral characterization of the extrapallial fluid of *Mytilus edulis*. *Anal. Biochem.* 100, 324–334. doi:10.1016/0003-2697(79)90236-7.

Mistlberger, R. E. (2009). Food-anticipatory circadian rhythms: Concepts and methods. *Eur. J. Neurosci.* 30, 1718–1729. doi:10.1111/j.1460-9568.2009.06965.x.

Miyazaki, Y., Usui, T., Kajikawa, A., Hishiyama, H., Matsuzawa, N., Nishida, T., et al. (2008). Daily oscillation of gene expression associated with nacreous layer formation. *Front. Mater. Sci. China* 2, 162–166. doi:10.1007/s11706-008-0027-3.

Moberg, F., and Folke, C. (1999). Ecological goods and services of coral reef ecosystems. *Ecol. Econ.* 29, 215–233. doi:10.1016/S0921-8009(99)00009-9.

Murdock, D. J. E. (2020). The 'biomineralization toolkit' and the origin of animal skeletons. *Biol. Rev.* 95, 1372–1392. doi:10.1111/brv.12614.

Nagai, K., Honjo, T., Go, J., Yamashita, H., and Seok Jin Oh (2006). Detecting the shellfish killer *Heterocapsa circularisquama* (Dinophyceae) by measuring bivalve valve activity with a Hall element sensor. *Aquaculture* 255, 395–401. doi:10.1016/j.aquaculture.2005.12.018.

Naylor, E. (1958). Tidal and Diurnal Rhythms of Locomotory Activity in *Carcinus Maenas* (L.). *J. Exp. Biol.* 35, 602–610. doi:10.1242/jeb.35.3.602.

Nedoncelle, K., Lartaud, F., de Rafelis, M., Boulila, S., and Le Bris, N. (2013). A new method for high-resolution bivalve growth rate studies in hydrothermal environments. *Mar. Biol.* 160, 1427–1439. doi:10.1007/s00227-013-2195-7.

Nedoncelle, K., Lartaud, F., Pereira, L. C., Yücel, M., Thurnherr, A. M., Mullineaux, L., et al. (2015). Bathymodiolus growth dynamics in relation to environmental fluctuations in vent habitats. *Deep. Res. Part I* 106, 183–193. doi:10.1016/j.dsr.2015.10.003.

Nedoncelle, K., Le Bris, N., de Rafélis, M., Labourdette, N., and Lartaud, F. (2014). Non-equilibrium fractionation of stable carbon isotopes in chemosynthetic mussels. *Chem. Geol.* 387, 35–46. doi:10.1016/J.CHEMGEO.2014.08.002.

Ono, D., Honma, K. I., and Honma, S. (2015). Circadian and ultradian rhythms of clock gene expression in the suprachiasmatic nucleus of freely moving mice. *Sci. Rep.* 5, 12310. doi:10.1038/srep12310.

Ono, R., Koike, N., Inokawa, H., Tsuchiya, Y., Umemura, Y., Yamamoto, T., et al. (2019). Incremental Growth Lines in Mouse Molar Dentin Represent 8-hr Ultradian Rhythm. *Acta Histochem. Cytochem.* 52, 93–99. doi:10.1267/AHC.19017.

Owen, R., Richardson, C. A., and Kennedy, H. (2002). The influence of shell growth rate on striae deposition in the scallop *Pecten maximus*. *J. Mar. Biol. Assoc. United Kingdom* 82, 621–623. doi:10.1017/S0025315402005969.

Pairett, A. N., and Serb, J. M. (2013). De Novo Assembly and Characterization of Two Transcriptomes Reveal Multiple Light-Mediated Functions in the Scallop Eye (Bivalvia: Pectinidae). *PLoS One* 8, e69852. doi:10.1371/JOURNAL.PONE.0069852.

Palmer, J. D., and Williams, B. G. (1986). Comparative studies of tidal rhythms. II. The dual clock control of the locomotor rhythms of two decapod crustaceans. *Mar. Behav. Physiol.* 12, 269–278. doi:10.1080/10236248609378653.

Pannella, G., and MacClintock, C. (1968). Biological and Environmental Rhythms Reflected in Molluscan Shell Growth. *J. Paleontol.* 2, 64–80. doi:10.1017/S0022336000061655.

Partch, C. L., Green, C. B., and Takahashi, J. S. (2014). Molecular architecture of the mammalian circadian clock. *Trends Cell Biol.* 24, 90–99. doi:10.1016/J.TCB.2013.07.002.

Peharda, M., Schöne, B. R., Black, B. A., and Corrège, T. (2021). Advances of sclerochronology research in the last decade. *Paleoceanogr. Paleoclimatol. Paleoecol.* 570, 110371. doi:10.1016/j.palaeo.2021.110371.

Perrigault, M., Andrade, H., Bellec, L., Ballantine, C., Camus, L., and Tran, D. (2020). Rhythms during the polar night: evidence of clock-gene oscillations in the Arctic scallop *Chlamys islandica*. *Proceedings. Biol. Sci.* 287, 20201001. doi:10.1098/rspb.2020.1001.

Perrigault, M., and Tran, D. (2017). Identification of the Molecular Clockwork of the Oyster *Crassostrea gigas*. *PLoS One* 12, e0169790. doi:10.1371/journal.pone.0169790.

Poitevin, P., Chauvaud, L., Pécheyran, C., Lazure, P., Jolivet, A., and Thébault, J. (2020). Does trace element composition of bivalve shells record ultra-high frequency environmental variations? *Mar. Environ. Res.* 158, 104943. doi:10.1016/j.marenvres.2020.104943.

Poulain, C., Lorrain, A., Amice, E., Morize, E., and Paulet, Y. (2011). An environmentally induced tidal periodicity of microgrowth increment formation in subtidal populations of the clam *Ruditapes philippinarum*. *J. Exp. Mar. Bio. Ecol.* 397, 58–64. doi:10.1016/j.jembe.2010.11.001.

Pulteney, R. (1781). *A General View of the Writing of Linnaeus.* London: Payne and White.

Réaumur, R.-A. . (1709). De la formation et de l'accroissement des coquilles des animaux tant terrestres qu'aquatiques, soit de mer, soit de rivière. *Hist. Acad. roy, Sci. Mem. Paris*, 364–400.

Rensing, L., and Ruoff, P. (2002). Temperature effect on entrainment, phase shifting, and amplitude of circadian clocks and its molecular bases. *Chronobiol. Int.* 19, 807–864. doi:10.1081/CBI-120014569.

Richardson, C. A. (1987). Microgrowth patterns in the shell of the Malaysian cockle *Anadara granosa* (L.) and their use in age determination. *J. Exp. Mar. Bio. Ecol.* 111, 77–98. doi:10.1016/0022-0981(87)90021-9.

Richardson, C. A. (1988). Exogenous and endogenous rhythms of band formation in the shell of the clam *Tapes philippinarum* (Adams et Reeve, 1850). *J. Exp. Mar. Bio. Ecol.* 122, 105–126. doi:10.1016/0022-0981(88)90179-7.

Richardson, C. A. (1989). An analysis of the microgrowth bands in the shell of the common mussel *Mytilus edulis*. *J. Mar. Biol. Assoc. United Kingdom* 69, 477–491. doi:10.1017/S0025315400029544.

Richardson, C. A., Crisp, D. J., and Runham, N. W. (1979). Tidally deposited growth bands in the shell of the common cockle, *Cerastoderma edule*. *Malacologia* 18, 277–290.

Richardson, C. A., Crisp, D. J., and Runham, N. W. (1980). An endogenous rhythm in shell deposition in *Cerastoderma edule*. *J. Mar. Biol. Assoc. United Kingdom* 60, 991–1004. doi:10.1017/S0025315400042041.

Richardson, C. A., Runham, N. W., and Crisp, D. J. (1981). A histological and ultrastructural study of the cells of the mantle edge of a marine bivalve, *Cerastoderma edule*. *Tissue Cell* 13, 715–730. doi:10.1016/S0040-8166(81)80008-0.

Richardson, C. A., Seed, R., and Naylor, E. (1990). Use of internal growth bands for measuring individual and population growth rates in *Mytilus edulis* from offshore production platforms. *Mar Ecol Prog Ser* 66, 259–265. doi:10.3354/meps066259.

Rodland, D. L., Schöne, B. R., Helama, S., Nielsen, J. K., and Baier, S. (2006). A clockwork mollusc : Ultradian rhythms in bivalve activity revealed by digital photography. *J. Exp. Biol. Ecol.* 334, 316–323. doi:10.1016/j.jembe.2006.02.012.

Rodríguez-Tovar, F. J. (2014). Orbital climate cycles in the fossil record: From semidiurnal to million-year biotic responses. *Annu. Rev. Earth Planet. Sci.* 42, 69–102. doi:10.1146/annurev-earth-120412-145922.

Rosbash, M. (2009). The implications of multiple circadian clock origins. *PLoS Biol.* 7, e1000062. doi:10.1371/journal.pbio.1000062.

Scheirer, D. S., Shank, T. M., and Fornari, D. J. (2006). Temperature variations at diffuse and focused flow hydrothermal vent sites along the northern East Pacific Rise. *Geochemistry, Geophys. Geosystems* 7, Q03002. doi:10.1029/2005GC001094.

Schöne, B. R. (2008). The curse of physiology — challenges and opportunities in the interpretation of geochemical data from mollusk shells. *Geo-Marine Lett.* 28, 269–285. doi:10.1007/s00367-008-0114-6.

Schöne, B. R. (2013). *Arctica islandica* (Bivalvia): A unique paleoenvironmental archive of the northern North Atlantic Ocean. *Glob. Planet. Change* 111, 199–225. doi:10.1016/j.gloplacha.2013.09.013.

Schöne, B. R., and Giere, O. (2005). Growth increments and stable isotope variation in shells of the deep-sea hydrothermal vent bivalve mollusk *Bathymodiolus brevior* from the North Fiji Basin, Pacific Ocean. *Deep. Res. Part I Oceanogr. Res. Pap.* 52, 1896–1910. doi:10.1016/j.dsr.2005.06.003.

Schöne, B. R., and Krause, R. A. (2016). Retrospective environmental biomonitoring – Mussel Watch expanded. *Glob. Planet. Change* 144, 228–251. doi:10.1016/j.gloplacha.2016.08.002.

Schöne, B. R., Lega, J., Flessa, K. W., Goodwin, D. H., and Dettman, D. L. (2002). Reconstructing daily temperatures from growth rates of the intertidal bivalve mollusk *Chione cortezi* (northern Gulf of California, Mexico). *Palaeogeogr. Palaeoclimatol. Palaeoecol.* 184, 131–146. doi:10.1016/S0031-0182(02)00252-3.

Schöne, B. R., Oschmann, W., Rössler, J., Freyre Castro, A. D., Houk, S. D., Kröncke, I., et al. (2003a). North Atlantic Oscillation dynamics recorded in shells of a long-lived bivalve mollusk. *Geology* 31, 1037–1040. doi:10.1130/G20013.1.

Schöne, B. R., Page, N. A., Rodland, D. L., Fiebig, J., Baier, S., Helama, S. O., et al. (2007). ENSO-coupled precipitation records (1959-2004) based on shells of freshwater bivalve mollusks (*Margaritifera falcata*) from British Columbia. *Int. J. Earth Sci.* 96, 525–540. doi:10.1007/s00531-006-0109-3.

Schöne, B. R., Pfeiffer, M., Pohlmann, T., and Siegismund, F. (2005). A seasonally resolved bottom-water temperature record for the period AD 1866-2002 based on shells of *Arctica islandica* (Mollusca, North Sea). *Int. J. Climatol.* 25, 947–962. doi:10.1002/joc.1174.

Schöne, B. R., Tanabe, K., Dettman, D., and Sato, S. (2003b). Environmental controls on shell growth rates and d 18 O of the shallow-marine bivalve mollusk *Phacosoma japonicum* in Japan. *Mar. Biol.* 142, 473–485. doi:10.1007/s00227-002-0970-y.

Schwartzmann, C., Durrieu, G., Sow, M., Ciret, P., Lazareth, C. E., and Massabuaua, J. C. (2011). In situ giant clam growth rate behavior in relation to temperature: A one-year coupled study of high-frequency noninvasive valvometry and sclerochronology. *Limnol. Oceanogr.* 56, 1940–1951. doi:10.4319/lo.2011.56.5.1940.

Skinner, H. C. ., and Jahren, A. H. (2003). "Biomineralization," in *Trearise on Geochemistry* (Elsevier Ltd.), 117–184. doi:10.1016/B0-08-043751-6/08128-7.

Sleight, V. A., Antczak, P., Falciani, F., Clark, M. S., and Cowen, L. (2020). Computationally predicted gene regulatory networks in molluscan biomineralization identify extracellular matrix production and ion transportation pathways. *Bioinformatics* 36, 1326–1332. doi:10.1093/bioinformatics/btz754.

Steinhardt, J., Butler, P. G., Carroll, M. L., and Hartley, J. (2016). The application of long-lived bivalve sclerochronology in environmental baseline monitoring. *Front. Mar. Sci.* 3, 176. doi:10.3389/fmars.2016.00176.

Stemmer, K., Brey, T., and Gutbrod, M. S. (2019). In situ Measurements of pH, CA2+, and Dic Dynamics within the Extrapallial Fluid of the Ocean Quahog *Arctica islandica*. *J. Shellfish Res.* 38, 71–78. doi:10.2983/035.038.0107.

Sun, J., Xu, G., Wang, Z., Li, Q., Cui, Y., Xie, L., et al. (2015). The effect of NF-κB signalling pathway on expression and regulation of nacrein in Pearl Oyster, *Pinctada fucata*. *PLoS One* 10, e0131711. doi:10.1371/journal.pone.0131711.

Sun, X. J., Zhou, L. Q., Tian, J. T., Liu, Z. H., Wu, B., Dong, Y. H., et al. (2016). Transcriptome survey of phototransduction and clock genes in marine bivalves. *Genet. Mol. Res.* 15, gmr15048726. doi:10.4238/gmr15048726.

Tan, Y., Merrow, M., and Roenneberg, T. (2004). Photoperiodism in *Neurospora Crassa*. *J. Biol. Rhythms* 19, 135–143. doi:10.1177/0748730404263015.

Thébault, J., Chauvaud, L., Clavier, J., Fichez, R., and Morize, E. (2006). Evidence of a 2-day periodicity of striae formation in the tropical scallop *Comptopallium radula* using calcein marking. *Mar. Biol.* 149, 257–267. doi:10.1007/s00227-005-0198-8.

Tong, H., Hu, J., Ma, W., Zhong, G., Yao, S., and Cao, N. (2002). In situ analysis of the organic framework in the prismatic layer of mollusc shell. *Biomaterials* 23, 2593–2598. doi:10.1016/S0142-9612(01)00397-0.

Tran, D., Nadau, A., Durrieu, G., Ciret, P., Parisot, J. P., and Massabuau, J. C. (2011). Field chronobiology of a molluscan bivalve: How the moon and sun cycles interact to drive oyster activity rhythms. *Chronobiol. Int.* 28, 307–317. doi:10.3109/07420528.2011.565897.

Tran, D., Perrigault, M., Ciret, P., and Payton, L. (2020). Bivalve mollusc circadian clock genes can run at tidal frequency. *Proc. R. Soc. B* 287, 20192440. doi:http://dx.doi.org/10.1098/rspb.2019.2440.

Trofimova, T., Alexandroff, S. J., Mette, M. J., Tray, E., Butler, P. G., Campana, S. E., et al. (2020). Fundamental questions and applications of sclerochronology: Community-defined research

priorities. *Estuar. Coast. Shelf Sci.* 245, 106977. doi:10.1016/j.ecss.2020.106977.

Verrecchia, E. P. (2005). "Multiresolution analysis of shell growth increments to detect variations in natural cycles," in *Image Analysis, Sediments and Paleoenvironments* (Dordrecht: Springer), 273–293. doi:10.1007/1-4020-2122-4_14.

von Hessling, T. (1859). *Die Perlmuscheln und ihre Perlen naturwissenschaftlich und geschichtlich; mit Berücksichtigung der Perlengewässer Bayerns*. Leipzig: Engelmann.

Wang, X., Wang, M., Jia, Z., Song, X., Wang, L., and Song, L. (2017). A shell-formation related carbonic anhydrase in *Crassostrea gigas* modulates intracellular calcium against CO2 exposure: Implication for impacts of ocean acidification on mollusk calcification. *Aquat. Toxicol.* 189, 216–228. doi:10.1016/J.AQUATOX.2017.06.009.

Warter, V., Erez, J., and Müller, W. (2018). Environmental and physiological controls on daily trace element incorporation in *Tridacna crocea* from combined laboratory culturing and ultra-high resolution LA-ICP-MS analysis. *Palaeogeogr. Palaeoclimatol. Palaeoecol.* 496, 32–47. doi:10.1016/j.palaeo.2017.12.038.

Weiner, S., and Dove, P. M. (2003). "An overview of biomineralization processes and the problem of the vital effect," in *Biomineralization*, eds. P. M. Dove, J. J. De Yoreo, and S. Weiner (Washington: The mineralogical society of America), 1–24.

Wilbur, K. M., and Saleuddin, A. S. M. (1983). "Shell Formation," in *The Mollusca: Physiology Part. 1* (New York: Academic Press Inc.), 235–287. doi:10.1016/b978-0-12-751404-8.50014-1.

Williams, B. G., and Pilditch, C. A. (1997). The entrainment of persistent tidal rhythmicity in a filter-feeding bivalve using cycles of food availability. *J. Biol. Rhythms* 12, 173–81. doi:10.1177/074873049701200208.

Yamaguchi, K., Seto, K., Takayasu, K., and Aizaki, M. (2006). Shell Layers and Structures in the Brackish Water Bivalve, *Corbicula japonica*. *Quat. Res.* 45, 317–331. doi:10.4116/jaqua.45.317.

Yan, H., Liu, C., An, Z., Yang, W., Yang, Y., Huang, P., et al. (2020). Extreme weather events recorded by daily to hourly resolution biogeochemical proxies of marine giant clam shells. *Proc. Natl. Acad. Sci. U. S. A.* 117, 7038–7043. doi:10.1073/pnas.1916784117.

Zhao, L., Shirai, K., Tanaka, K., Milano, S., Higuchi, T., Murakami-Sugihara, N., et al. (2020). A review of transgenerational effects of ocean acidification on marine bivalves and their implications for sclerochronology. *Estuar. Coast. Shelf Sci.* 235, 106620. doi:10.1016/j.ecss.2020.106620.

Zhao, M., He, M., Huang, X., and Wang, Q. (2014). A homeodomain transcription factor gene, PfMSX, activates expression of Pif gene in the pearl oyster *Pinctada fucata*. *PLoS One* 9, e103830. doi:10.1371/journal.pone.0103830.

Zheng, X., Cheng, M., Xiang, L., Liang, J., Xie, L., and Zhang, R. (2015). The AP-1 transcription factor homolog Pf-AP-1 activates transcription of multiple biomineral proteins and potentially participates in *Pinctada fucata* biomineralization. *Sci. Rep.* 5, 14408. doi:10.1038/srep14408.

2. *Mytilus galloprovincialis* as model for this work

Bivalves are a class of molluscs characterised by a shell composed of two valves. It regroups notably mussels, oysters, clams and scallops. Bivalves are present in many aquatic ecosystems from fresh to marine waters, from coastal areas to the deep sea, and from polar to tropical habitats (Gosling, 2004). They are recognised for their high economical, ecological and socio-cultural values (Figure 8) (Smaal et al., 2018). This group represents 14 % of the total marine production in the world, which corresponds to 15 millions of tons per year on average and generates about 23 billion US$ income (Wijsman et al., 2018). Among this, 89% are produced in aquaculture but mostly using seed fished or collected in natural stocks (Figure 8A, B). Ecologically, bivalves are recognised for multiple ecosystem services such as water clarification or nutrients and carbon cycles regulation (Cranford, 2018; Filgueira et al., 2018b; Jansen et al., 2018). They are also ecosystem-engineers as some bivalves such as oysters and mussels are constituting beds and reefs recognised as hotspot of biodiversity and also as natural structures of protection against coastal erosion and submersion events (Figure 8C, D) (Craeymeersch and Jansen, 2018; Ysebaert et al., 2018). Socio-cultural values are more subjective characteristics but as important as the economic and ecological ones. They are related to community activities, past and

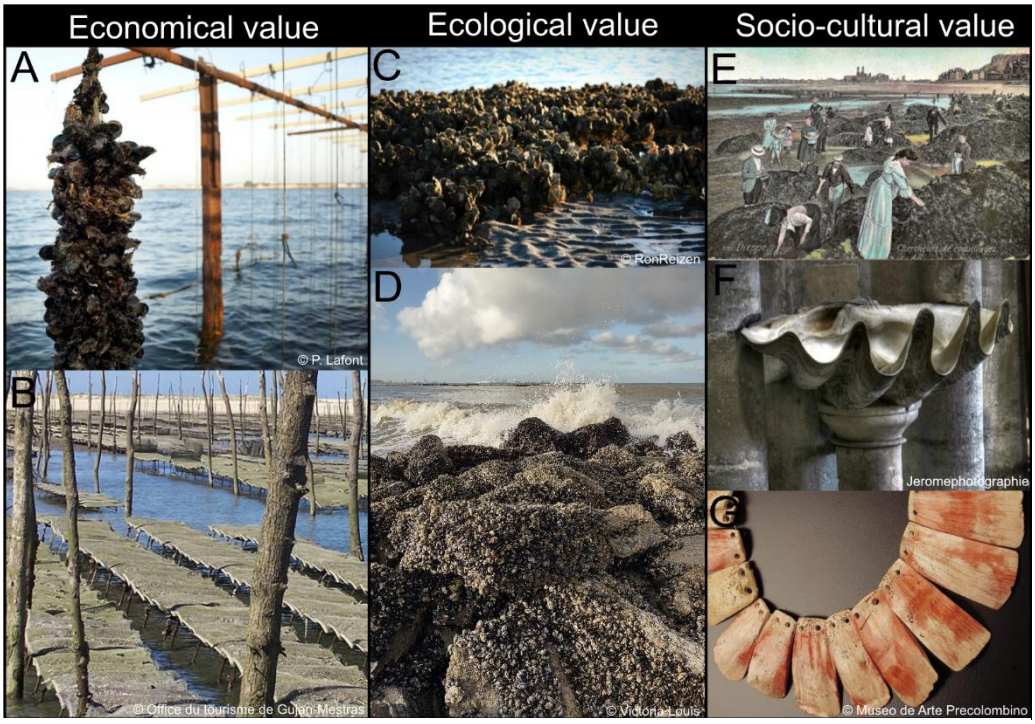

Figure 8: Economical, ecological and socio-cultural values of bivalves. A) Mussel farming of *Mytilus galloprovincialis* in the Mediterranean lagoon of Thau (France). B) Oyster farming of *Magallana gigas* in Arcachon Bay (France). C) Oyster reef composed of *Magallana gigas* in Holland. D) *Mytilus edulis* bed on break-water (Belgium). E) Post card "Chercheur de coquillage" at Dieppe (France). Font made of a valve of *Tridacna gigas* in the abbey of Fécamp (France). E) Pre-columbian neckless made of *Argopecten purpuratus* (Peru).

present artistic work, or scientific applications such as the reconstruction of past human-environment interactions (Figure 8E, F, G) (Smaal and Strand, 2018). Although widely used, knowledge about bivalves is mainly focused on few species and on specific aspects mostly linked to aquaculture and ecotoxicology. Multiple gaps still remain in the scientific knowledge, like molecular biology as DNA extraction can be challenging mainly due to the richness of their tissues in proteins and polysaccharides (Adema, 2021). Therefore, some fundamental processes such as shell biomineralisation are still not fully described at the genomic level (Clark, 2020).

The Mytilidae family is one of the best studied family among the bivalve class (Gosling, 2004). *Mytilus* species are widely distributed on the geographical point of view. The family notably includes the subfamilies of Mytilinae and of Bathymodiolinae, which are most commonly called deep-sea mussels. In research, mytilids are mainly used in ecotoxicological studies and environmental quality assessment, including programs such as “Mussel Watch” in USA (Goldberg, 1975) or “ROCCH-National chemical contamination network” in France (Claisse et al., 1992; Besse et al., 2012). The Mytilidae species inhabiting in the Mediterranean Sea is *Mytilus galloprovincialis*. With the recent globalisation and the development of the shipping industry, its geographical distribution is extended to the East Atlantic coast, Japan Sea (Wilkins et al., 1983; McDonald et al., 1990), South Africa (Branch and Steffani, 2004), from California to Canada (McDonald and Koehn, 1988; Heath et al., 1995), Hawaii (Apte et al., 2000), Mexico (Ramírez and Cáceres-Martínez, 1999) and south-east Australia (McDonald et al., 1991). This invasive success is due to its reproduction features and its large ecological tolerance. Pan-genome analysis revealed that *M. galloprovincialis* genome is composed of a core set of genes (45 000) and an huge amount of “dispensable” genes (20 000) that could participate to the high invasive and high resilience capacities of the species (Gerdol et al., 2020). *Mytilus galloprovincialis* can be found in lagoon at a salinity comprised between 10 to over 40 and support temperatures from 5 to 30 °C (Andrisoa et al., 2019). However, these values constitute physiological tolerance limits for *M. galloprovincialis* mussels, as demonstrated by a low metabolic capacity for a salinity reaching 35 (Freitas et al., 2017) and with an increase of mortality above a temperature of 28°C (Anestis et al., 2007b). Finally, this species inhabits intertidal and subtidal environments, fixed to hard substrate by a material made of a complex of adhesive proteins, the byssus (Gosling, 2004). Intertidal environments have been shown to be more energy-demanding than subtidal environments on this species (Sarà et al., 2011).

As most organisms, the energy in mussels is allocated to three main activities which are growth, reproduction and somatic maintenance in a ratio that depends on their habitat (Monaco and McQuaid, 2018). As gametogenesis is an energy consuming process, it reduces the growth of mussels (Okaniwa et al., 2010). The main environmental factors influencing the energy allocation are the water

temperature, which is also the body temperature of the mussel as bivalves are ectotherms, and the food availability. Indeed, food availability was pointed out as the predominant environmental factor driving gametogenesis and shell growth of bivalves (Ceccherelli and Rossi, 1984; Cáceres-Martínez and Figueras, 1998; Purroy et al., 2018). *Mytilus galloprovincialis* is mainly feeding on phytoplankton, as well as organic and dissolved matter (Babarro et al., 2003; Filgueira et al., 2018a).

Mussels are characterised by a flexible reproduction strategy, as spawning can occur at different periods in function of environmental conditions and in function of inter-annual climatic variations as well (Seed, 1976; Gosling, 2004). The gametogenesis of *M. galloprovincialis* inhabiting the Ria of Vigo (Atlantic Ocean) occurs from late autumn to early winter (Cáceres-Martínez and Figueras, 1998). Late winter, gametogenesis was completed and some minor spawn events were observed. A massive spawning event took place in spring, followed by a fast gametogenesis and a minor spawning event in summer. In autumn mussels accumulates reserves. In Mediterranean Sea, nearby the Ebro delta, shifted timing was observed with ripe mussels from September to January and a massive spawn in winter (Galimany et al., 2005). A second minor spawning event was observed in April and summer is a resting stage. Multi-sites observation made in the Gulf of La Spezia (Ligurian Sea, Italy) showed slight shift in the timing of gametogenesis and spawning events between studied sites (Balbi et al., 2017). Fecundation occurs in the water column, fertilised eggs give rise to free ciliated larvae (trochophore) after 24 hours (Bayne, 1976; Gosling, 2004). Secretion of the shell begins at the trochophore stage of development (Bayne, 1976; Miglioli et al., 2019). D-veliger stage reached after 48 hours of development, is fully covered by the shell. D-veliger has a velum to swim and feed. Planktonic stage stops when reaching ~300 µm shell length, three to five weeks post fecundation depending on water temperature, salinity and food availability (Bayne, 1976; Gosling, 2004). Mussels settlement is occurring in two steps; 1) settlement to filamentous substrate and growth up to ~2 mm and 2) final recruitment onto adult mussel bed (Seed, 1976).

The growth of bivalves is known to be influenced by both endogenous and exogeneous factors (Bayne, 2004). Two mains phenotypes are described within a population, fast and slow growing individuals. This difference in growth rate has been described for many bivalve species such as clams, oysters and mussels (Bayne, 2004; Tamayo et al., 2011; Prieto et al., 2018). Fast growing individuals are characterised by an increased feeding rate, larger gills-surface area and a reduced metabolic cost whereas slow growers require more energy for maintenance and growth (Bayne, 2004; Tamayo et al., 2011). Recently, differences at the gene expression level showed a transcription upregulation of genes related to response to stimulus, growth and cell activity in fast growing specimens (Tamayo et al., 2015). In addition, bivalves show a great flexibility of feeding and growth response to the food

availability in their environment at short (minute to hour) and long term (day to month) (Bayne, 2004). Nevertheless, the response to food levels is similar in function of the physiological profile. When food is present in quantity, both fast and slow growing individuals will increase their standard metabolisms by enhancing their absorption rate (Tamayo et al., 2015; Prieto et al., 2018). But higher food concentration increases the growth of slow growing individuals only slightly, causing their growth to stop when food become sparse (Tamayo et al., 2011). Both molecular and physiological studies on *M. galloprovincialis* showed that the difference in growth rate between individuals is predominantly derived from endogenous factors rather than exogenous factors (*e.g.,* food levels) (Prieto et al., 2018, 2019). Therefore, when studying the shell growth of bivalves, a high inter-individual variability is to be expected.

In the precedent section, variations in the time imbedded within growth increments of shells was reported. In function of their environment, some species showed either tidal or daily increments. This variation of incrementation periodicity was observed in *M. galloprovincialis*. Studies made in Japan described tidal incrementation in Tokyo Bay and further north, at Otsuchi Bay (Tanaka et al., 2019; Zhao et al., 2019). In both environments, mussels lived in the intertidal zone and exposed to semi-diurnal tidal regime. Patterns observed were clearly related to tides as increments width showed variation linked to tidal coefficient. In environments where tides are limited or almost inexistent, as in the Salses-Leucate lagoon from the Mediterranean Sea, only one increment per day is formed (Andrisoa et al., 2019). In this case, multiple environmental variables (*i.e.,* photoperiod, temperature, salinity, water depth and wind speed) follow the same periodicity. Then it is difficult to define which of them drives the biomineralisation process. This led to the question of the possible implication of internal biological clocks in the growth incrementation.

The biological clock of *M. galloprovincialis* has not been identified yet. This work has been previously done for other Mytilidae (*i.e*., *Mytilus edulis*, *Mytilus californianus* and *Bathymodiolus azoricus*) and identified the canonical clock genes based on homologies of sequence with vertebrates and non-vertebrate genes (Connor and Gracey, 2011; Chapman et al., 2017, 2020; Mat et al., 2020). The canonical core genes are *Clock*, *Bmal*, *Period*, *Timeless*, *Timeout*, *ROR/HR3*, *Rev-erb*, *Cry1* and *Cry2* (Dunlap, 1999; Perrigault and Tran, 2017). The first identification of potential core clock genes was done on a transcriptome made on *Mytilus califonianus* (Connor and Gracey, 2011) based on mussels reared under photoperiodic conditions (L:D 12:12) and simulated semidiurnal tides. *Clock* and *Bmal* exhibit no expression rhythmicity whereas *Cry1* and *ROR/HR3* have a circadian expression (Table 2). Research made on *Mytilus edulis* showed that the core genes composing the biological clock had variation of their expression over time under photoperiodic light regime (L:D) and under constant

darkness (D:D) (Chapman et al., 2020). Also, a third condition was tested in order to characterise the implication of temperature oscillation on biological clock. To achieve it, mussels were subjected to total darkness and thermocycles over 24 hours (D:D TC). Significant oscillations were found in L:D and in D:D for five of the eight genes tested (*i.e.*, *Clock*, *Cry1*, *ROR/HR3*, *Period* and *Rev-erb*), indicating endogenous control (Table 2). Sometimes, a second pic was observed under LD (*Cry1* and *Rev-erb*) and DD (*Cry1*, *Clock* and *ROR/HR3*) suggesting tidal oscillations. Thermocycles impacted *Rev-erb* that lost its variation of expression. Although variations observed looked daily or tidal depending on the gene and the condition, none statistical test was done to quantify the rhythm. *Bathymodiolus azoricus* is inhabiting deep-sea hydrothermal vents, therefore they are living in total darkness. Most genes studied did not show rhythmic expression, only *Period* and *Timeless* showed circatidal expression *in situ* (Mat et al., 2020) (Table 2). In the lab, under L:D cycle condition, only *Period* conserved its rhythmicity of expression. Those results were partially attributed to the low expression of clock genes and a high interindividual variability. All previous molecular chronobiological studies made on Mytilidae seems to get contrasting results and no clear patterns were observed.

Table 2: Expression of biological clock genes in Mytilidae. Circatidal (CT) expressions are in light blue whereas dark blue colour is circadian (CD) expression. In white is non-significant (ns) rhythmicity. When not assessed in the study, genes are coloured in grey. Photoperiodic conditions are the alternance of light and dark phases (L:D) or constant dark (D:D). TC are thermocycles.

	Mytilus californianus (Connor and Gracey, 2011)	*Mytilus edulis* (Chapman et al., 2020)			*Bathymodiolus azoricus* (Mat et al., 2020)	
	L:D 12:12-Tides	L:D 10:14	D:D	D:D TC	In situ (D:D)	L:D 12:12
Clock	ns	CD	CT	CD	ns	ns
Bmal	ns	ns	CD	ns	ns	ns
Period		CD	CD	CD	CT	CT
Timeless					CT	ns
Timeout		CD	CT	CD	ns	ns
RORb	CD	CD	CT	CD		
Rev-erb		CT	CD	ns		
Cry1	CD	CT	CT	CD	ns	ns
Cry 2					ns	ns

Biological clocks orchestrate multiple physiological functions of an organisms (Dunlap, 1999). In the case of bivalves, the valve activity is considered as an output of biological clocks (Tran et al., 2011; Perrigault and Tran, 2017). Valvometry is the measurement of the valve aperture. Different technics were developed and the most commonly used consist in a captor and a magnet glued on each valve of an individual using the Hall effect (Figure 9).

Figure 9: Valvometry device on a mussel. On the left a hall captor was glued and on the right magnets. Difference of potential is variating in function of the valve movements.

The Hall effect is the production of a difference of potential when an electric current flows through a conductor in a magnetic field. The variation of the difference of potential is measured and transformed in valve openness (Tran et al., 2003; Nagai et al., 2006). Regarding *M. galloprovincialis*, rhythmic valves activity has been previously observed in different habitats. A study was achieved in the Black Sea where tides are also almost inexistent (*i.e*., tidal range = 1.1 cm in Crimean Peninsula) (Medvedev, 2018). *In situ*, mussels showed circadian behaviour, being globally open at night and closed during the day (Trusevich et al., 2021). Another study took place in the Venice Lagoon where there is a stronger microtidal regime than in Crimea, with tidal range comprised between 50 cm at neap tides and 100 cm at spring tides (Cucco and Umgiesser, 2006). In this region, researchers observed a switch from bimodal (circadian and circatidal) activity in summer to circatidal in winter (Bertolini et al., 2021). The variability in valve activity was reported as strictly linked to the local tidal regime of the lagoon. The last study took place in the Ría de Arousa, on the North Atlantic coast of Spain. This region is characterised by semidiurnal tides having up to three meters of tidal range (Comeau et al., 2018). Mussels showed circadian patterns following the photoperiodic regime as in Crimea, but their behaviour was not synchronised. Only one individual on eight, living deeper in the water column exhibited circatidal behaviour. In aquaria under natural water and illumination, mussels showed also circadian behaviour following the photoperiodic regime (Gnyubkin, 2010). Those data suggested that *M. galloprovincialis* behaviour is probably driven by both the photoperiod and the tides but the literature data is not sufficient enough to discriminate which is the predominant factor. It would be interesting to test mussel's behaviour under free-running conditions, which means under constant environmental conditions, in order to test the endogenous nature of their rhythmic behaviour.

Previous studies on key aspects for this research such as growth, genomic and behaviour of *M. galloprovincialis* provided a basis to work on less studied targeted fields such as biological clocks and

biomineralisation. Its relationship with its environment is well described for basic biological processes such as reproduction and growth. This species is found in several environments within the area studied in this work, constituting a good choice to understand the interaction between the mussel periodical growth pattern formation and environmental periodic variations. Therefore, *M. galloprovincialis* has been chosen as the biological model for this study.

3. Thesis aims

This thesis aims to understand how environmental signals, mostly temporal ones, are integrated into the shell of a bivalve throughout its growth, so that it becomes a biological archive. Based on an exhaustive reading of the literature on the subject (Louis et al., 2022), two major hypotheses emerged which have been tested in this work; i) biomineralisation is an autonomous physiological process which is directly controlled by the variations of the environment or ii) during shell growth, biomineralisation is a rhythmic process which is under the control of biological clocks (Figure 10).

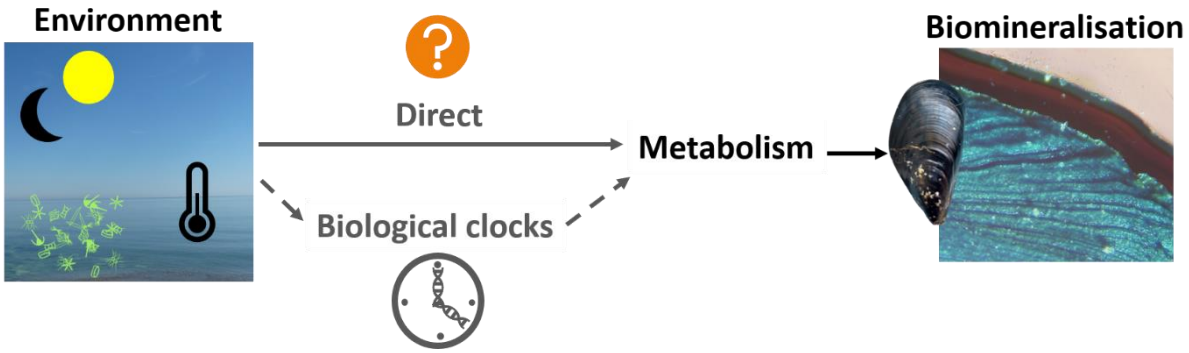

Figure 10: Main biological question of this thesis. "Is there a direct control of the environment on the biomineralisation or is the integration of the environment mediated by biological clocks?"

To address the main question of this work, its components had to be characterised. In this work we:

1. Characterised shell growth pattern of *Mytilus galloprovincialis* in different Mediterranean environments.
2. Identified the molecular actors of the biological clock oscillator of *Mytilus galloprovincialis* and characterised one presumed output (*i.e.*, valve activity).
3. Characterised *M. galloprovincialis* response to the photoperiod and the food availability.

To respond to these questions, a multidisciplinary approach has been used by combining two scientific disciplinaries; (1) sclerochronology which is the analysis of growth patterns in biomineralised tissues and (2) chronobiology which is the study of timing process in an organism. Based on chemical mark and recapture techniques, the sclerochronological analysis of the shells will reveal the internal growth patterns for specimens bred one year *in situ* (*i.e.*, at sea and in coastal lagoons). Same approach

was developed in aquaria. In chronobiology, the expression of selected genes (*i.e.*, genes involved in biological clocks and in the biomineralisation process) was followed *in situ* at daily scale and in aquaria to test different zeitgebers (*i.e.*, photoperiod and food availability). In addition, the valve activity, a classical output of biological clocks on bivalves, was measured through valvometry for aquaria experiments.

Chapter 1: Shell growth patterns of *Mytilus galloprovincialis* in Mediterranean environments

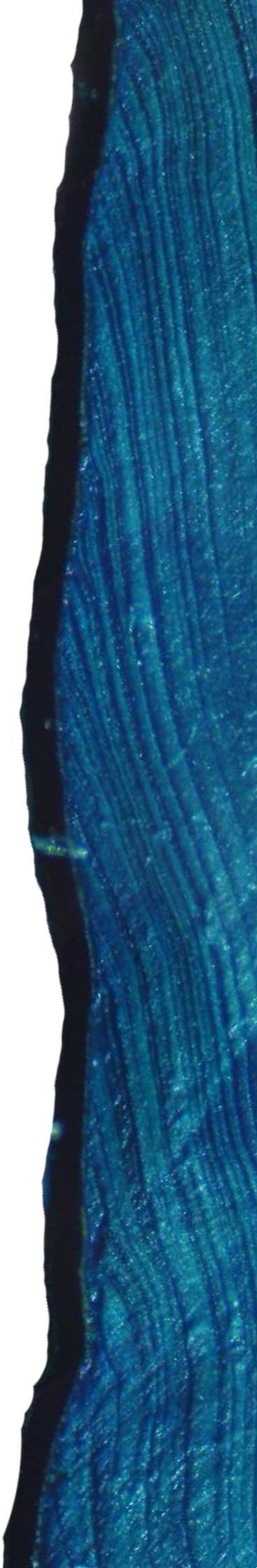

Preamble

This chapter is focussed on the study of growth patterns in the shell of *M. galloprovincialis* in three Mediterranean environments. In a first research article, an *in situ* experiment on mussel shells from two coastal lagunas (*i.e*., laguna of Salses-Leucate and laguna of Canet-Saint-Nazaire) and a sampling point situated at sea (*i.e*., Bay of Banyuls-sur-Mer) was conducted. In this part of the project, the growth patterns in shells were characterised over a year (June 2020 – June 2021) using a method of mark-recapture. In parallel, the environmental conditions were measured in each studied area (*i.e*., water temperature) or retrieved from databases (*i.e*., tide, wind force and direction, salinity, pH, O_2 and chlorophyll *a*), and compared to shell growth patterns identified to determine the role of the environmental variability on the dynamic of mineralisation of mussels. In the last section of the chapter we raised some limits in the use of the typical methods to reveal shell growth patterns (*i.e.*, Mutvei etching on shell sections), linked to the quality of growth increment revelation in some parts of the shells. Therefore, other technics for sclerochronological analysis were tested to improve the readability of shell growth patterns for further studies.

1: Article n°1:

A possible joint role of the environment and potential biological clock(s) in shell growth patterns formation of the Mediterranean mussel, *Mytilus galloprovincialis*.

Victoria Louis[1,2], Florian Desbordes[1], Laurence Besseau[2*], Franck Lartaud[1*]

[1] Sorbonne Université, CNRS, Laboratoire d'Ecogéochimie des Environnements Benthiques, LECOB, F-66650, Banyuls-sur-Mer, France

[2] Sorbonne Université, CNRS, Biologie Intégrative des Organismes Marins, BIOM, F-66650, Banyuls-sur-Mer, France

*Co-last authors

Key words: Mediterranean environments, sclerochronology, mixed semidiurnal tidal regime

Abstract

The accretionary tissues of bivalves are used to reconstruct (paleo)climates and (paleo)environments. But the formation processes of growth increments, the unit of time in shells, is still under discussion, particularly regarding the role of environmental parameters as forcing factor implied in the incrementation patterns. This study investigates the shell growth patterns of *Mytilus galloprovincialis* in three Mediterranean environments, two coastal lagunas and the open sea, an area submitted to small tidal variations. The sclerochronological analysis based on one-year breeding and monthly calcein staining reveals shell growth patterns highly variable in function of the environment but also between individuals of a same habitat. Moreover, the number of increments formed per day, the incrementation regime, variated throughout the year within an environment. When food was sparse, incrementation periodicity shifted from following the tidal regime of the studied region to circadian or circatidal periodicities indicating a possible control by biological clock(s). Supernumerary increments might vary in function of chlorophyll *a* concentration probably due to valve aperture variations above a certain threshold. This study revealed a possible joint control of the biomineralisation process.

Introduction

Shells of bivalves are biological archives used to reconstruct (paleo)climatic and (paleo)environmental variations, including seasonal to infra-seasonal scales, notably based on the analysis of their growth patterns (Schöne et al., 2005b; de Winter et al., 2020). Shell growth patterns consist in the alternation of calcified growth increments and lines, corresponding to slowdown of the growth or growth breaks. The sclerochronological analysis reveals that these increments can be formed following different periodicities (*i.e.*, annual, lunar, semi-lunar, lunidian, daily, tidal and below) but the drivers of the process of shell incrementation are not well identified and still subject to discussion (see review in Louis et al., 2022). The environmental variability seems to be an important component for the regularity of the increment formation. Tides are commonly considered to be at the origin of shell increments periodicity (Lutz and Rhoads, 1977). This is sustained by observations of different growth patterns related to the type of tidal regime. For the butter clam *Saxidomus gigantea,* individuals living in semidiurnal tidal region (*i.e.*, two cycles of high / low water per 24 hour period) classically form two increments per day, whereas individuals inhabiting in diurnal tidal region (*i.e.*, one cycle of high / low water per 24 hour period) exhibit only one increment formed per day (Hallmann et

al., 2009). However, others variables can drive the biomineralisation process. For example, the pectinid *Decatopecten radula* is forming one increment every two days in the Indo-West Pacific Ocean, likely related to the wind regime in this region (Thébault et al., 2006). In addition, disruptions between shell growth lines formation and variations of the environment can be observed, both in the field and in aquaria studies. The implication of biological clock(s) as timer of the biomineralisation process was thus suggested (Richardson, 1987, 1988; Schöne, 2008; Louis et al., 2022).

Number of sclerochronological studies concentrate on the shell growth response in environments submitted to macrotidal regime (Schöne et al., 2003; Huyghe et al., 2019), with distinct responses depending on species. Pectinids appear to form daily increments (Chauvaud et al., 1998) while mussels and oysters are known to form two increments per day in relation with their surrounding semidiurnal tidal environment (Huyghe et al., 2019; Tanaka et al., 2019). Mytilids from the deep-sea also exhibit the formation of tidal increments related to tidal variations of hydrothermal vent systems (Nedoncelle et al., 2013, 2015). Surprisingly, the oyster *Magallana gigas* and the mussel *Mytilus galloprovincialis* from the Mediterranean Sea, an area where tidal ranges are small to almost inexistent, are suggested to form daily increments (Langlet et al., 2006; Andrisoa et al., 2019a). However, these results come from very limited studies and in restricted environments, the Mediterranean coastal lagunas. Sclerochronological studies on bivalves from open areas of the Mediterranean Sea are sparse and mainly dedicated to the analysis of the annual growth patterns (Peharda et al., 2016; Bargione et al., 2020). We therefore lack knowledge about the role of the environmental conditions in the formation of shell growth increments in such environments.

The *Mytilus* genus is known for its high physiological plasticity and behavioural flexibility regarding environments (Bayne, 2004). *Mytilus galloprovincialis* is widely distributed and is present in different environments such as estuaries, coastal lagunas, intertidal coastal areas or subtidal open sea (Seed and Suchanek, 1992; Branch and Steffani, 2004; Gosling, 2004). As most organisms, mussels energy is allocated to three main physiological activities: growth, reproduction and somatic maintenance (Monaco and McQuaid, 2018). The energy allocation to either of the three activities depends on the environment of the organisms. The main influencing environmental factors are water temperature as bivalves are ectotherms, and food availability (Ceccherelli and Rossi, 1984; Cáceres-Martínez and Figueras, 1998). The last was pointed out as the predominant environmental factor driving the gametogenesis and the shell growth of bivalves (Purroy et al., 2018).

In order to decipher the impact of the environmental variables on shell growth patterns of mussels and better understand the control of the biomineralisation process, this study focused on *M. galloprovincialis* from different types of Mediterranean environments. To achieve this goal, mussels

were reared in two Mediterranean coastal lagunas (*i.e.*, Salses-Leucate and Canet-Saint-Nazaire) as well as at sea, in the Gulf of Lion, from June 2020 to June 2021. The condition index, the growth and the number of increments formed per day were measured each month and environmental variables were recorded or retrieved from databases in each studied location.

Material and methods

Study sites and organisms

Two Mediterranean coastal lagunas and one site at sea from the Southern part of the French Mediterranean coast were selected for this study (Figure 11). These Mediterranean coastal lagunas are inland shallow water bodies formed 15 kyr BP ago during the Flandrian transgression, separated from the sea by a sandy barrier interrupted by small inlets, currently corresponding to artificial openings ensuring a permanent connection with the Mediterranean seawater (Arnaud and Raimbault, 1969; Pérez-Ruzafa et al., 2019). Salses-Leucate (SL) laguna is connected to the sea by three inlets and has a continuous supply of freshwater throughout two main groundwater discharges (Hervé and Bruslé, 1980; Bec et al., 2011). This laguna has an average depth of two meters, a surface of 54 km² and is oligotrophic (Souchu et al., 2010). The laguna of Canet-Saint-Nazaire (CSN) is smaller (6 km²) and shallower (0.35 m on average) (Hervé and Bruslé, 1981; Bec et al., 2011). It has only one sea water inlet and is supplied in freshwater by three small rivers that are partially obstructed or dry, part of the year. This laguna is considered as hypertrophic but the water quality is poor because of low water circulation inducing an increase of concentrations in nitrogen and phosphate compounds (Derolez et al., 2021; Fiandrino et al., 2021). Moreover, the accumulation of organic matters and sediments can cause low oxygen concentration (< 5 $mg.L^{-1}$) when warm weather. Lagunas are known to be very dynamic environments that respond to climatic conditions faster than the open sea (Pérez-Ruzafa et al., 2019). The sea site chosen for this study was the bay of Banyuls-sur-Mer, where mussels have been seen growing between 1 and 15 m depth on the flank of the SOLA buoy, an autonomous station from the Oceanological Observatory of Banyuls-sur-Mer located in half a nautical mile from the coast. This area is monitored in the framework of the SOMLIT and ILICO national programs. The region has a particular wind regime characterised by violent and cold wind orientated West to North-West called Tramontane and South-East humid wind called Marin (Météo-France, 2020).

In situ *experimental design*

In SL and CSN lagunas, respectively 134 mussels (50.1±6.6 mm) and 68 mussels (45.4±3.9 mm) were placed in a cylindrical cage from June 2020 to June 2021. At SL laguna, mussels collected from the seawater inlet of Port Leucate were installed in a weighted cage which was placed ~40 cm below the water surface at Port Fitou, on the same area used in Andrisoa et al., 2019a (Figure 11A). At CSN laguna the weighted cage was filled with mussels collected on site and immerged ~30 cm below the water surface. The cage was located on the eastern side of the laguna, nearby the Village des Pêcheurs (Figure 11B). At sea, 54 mussels collected on site were put in a cage and fixed to the SOLA buoy 3 meters deep in June 2020 (Figure 11C). This cage was lost during a storm in December 2020. A second one, containing 75 mussels (44.3±8.8 mm), was installed from December 2020 to June 2021.

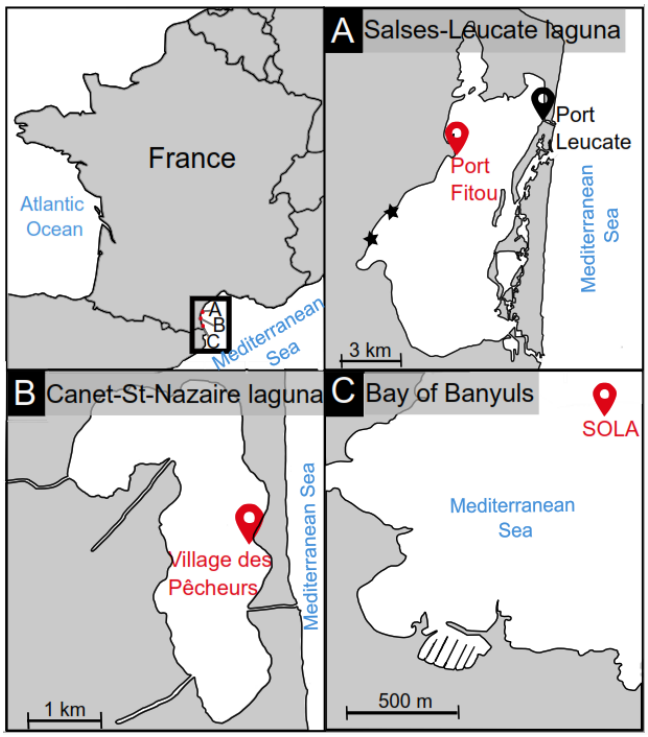

Figure 11: Locations of the 3 studied sites along the southern French Mediterranean coast. A) The Salses-Leucate laguna has three main sea water inlets on the eastern side and two mains groundwater discharges on the western side (black stars). Mussels were collected nearby the sea water inlet of Port Leucate (black sign) and transferred to the study site (red sign) located at Port Fitou. B) The Canet-St-Nazaire laguna has one main sea water inlet and is supplied in freshwater by three small rivers. Mussels were collected and redeployed at the study point, Village des Pêcheurs (red sign). C) In the bay of Banyuls-sur-Mer mussels were collected and redeployed on the oceanographic buoy of SOLA (red sign) located half a nautical mile from the coast.

Once a month, mussels were dyed using a calcein solution at a concentration of 150 mg/L during one hour. Calcein is a fluorochrome that is incorporated into the calcium-carbonate structure (Moran and Marko, 2005). In order to calculate their condition index (CI), eight mussels were sampled

in SL laguna and at sea, and six at CSN laguna as the number of mussels first deployed was lower. At CSN laguna, a gap in the calcein dye session occurred from October 2020 to January 2021 (*i.e.*, during 4 months) due to the turbidity and a higher sea level that prevented the recovery of the cage.

Water temperatures were measured every 30 minutes by a sensor device placed into the cage at each location. Wind speed and orientation data were retrieved from the station "Perpignan" of the French meteorological service (Météo France), with a sampling rate of 3 hours. At sea, data of salinity, chlorophyll *a* concentration, oxygen and pH were extracted from the SOMLIT database (https://www.somlit.fr/) for SOLA buoy (Cocquempot et al., 2019). Measurements at sea were taken every week. For lagunas, environmental data were provided by the Pôle-relais lagunes méditerranéennes and the FILMED network with a sampling rate of one per month at SL (*i.e.*, salinity, pH and water level) and every two weeks measurements at CSN (*i.e.*, salinity, pH and oxygen). The tidal regime in the region is mixed semidiurnal with a small tidal range of 30 cm, which causes a shift from semidiurnal to diurnal tidal regime in case of small tidal coefficient (Figure 12).

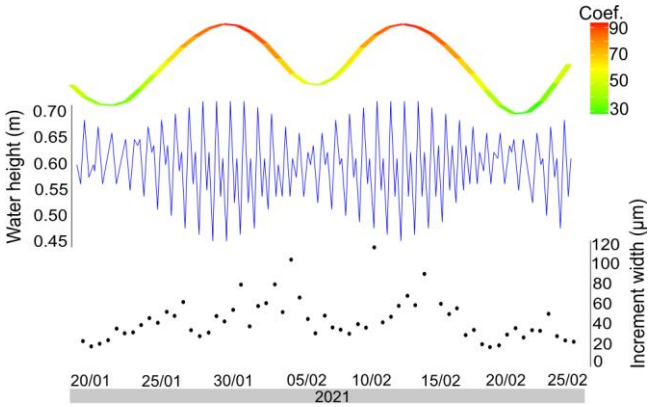

Figure 12: Increment width variations of the mussel SOLA0605 in relation with the tidal regime in the bay of Banyuls-sur-Mer in February 2021. The tidal coefficient (*i.e.*, green to red gradient) is following circalunar oscillations due to the rotation of the moon around the earth and the earth around the sun. As the tidal range is small in the bay of Banyuls, when the tidal coefficient is small, the tidal regime switched from semidiurnal to diurnal (blue line). Therefore, the region has a mixed semidiurnal tidal regime characterised by unequal tides occurring every 12.4 hours. The (semi)-circalunar oscillation observed in tidal range are observed in mussel increment width variation (black dots).

Shell preparation

After a year, all remaining mussels were sampled. At the laboratory, soft tissues were removed from shells and gonadal state was visually checked (*i.e.*, empty *vs* full, male *vs* female). Both tissues were separately dried in an oven at 65°C during 24 hours and weighted. The ratio between the tissue dry weight and the shell dry weight was calculated in order to get the CI of the organism (Davenport and Chen, 1987; Andrisoa et al., 2019a).

Shells were cut from the umbo to the posterior margin on the maximum growth axis and fixed on a microscope slide (Figure 13A). Slides of 0.5 mm thickness were cut using a Buehler Isomet low-speed saw (Buehler, Lake Bluff, IL, USA). Cut shells were grinded at P120 -P240 -P600 and P1200 and polished using Al_2O_3 powder consecutively of 3, 1 and 0.3 µm (Nedoncelle et al., 2013). Calcein marks were visualised using an epifluorescent microscope (Olympus BX61, Olympus Corporation, Tokyo, Japan) by exciting the fluorochrome with a blue light at 495 nm (Figure 13B). The calcein wave length reemission is at 515 nm (green).

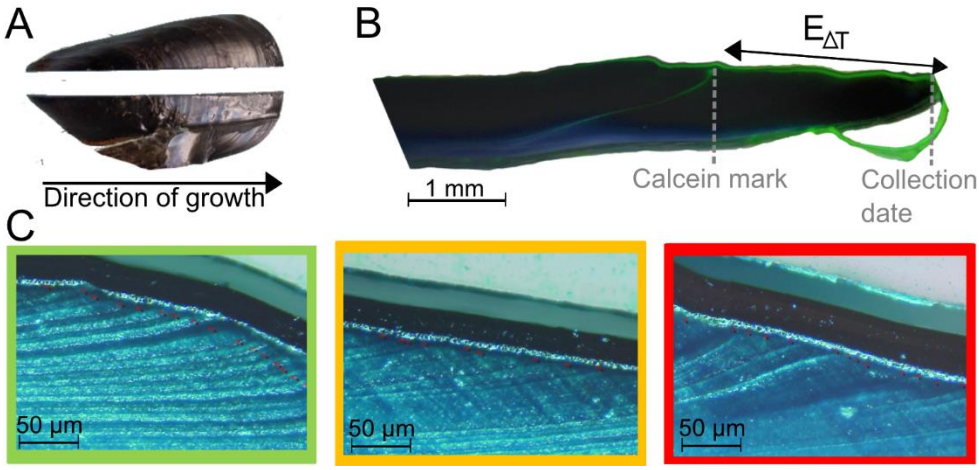

Figure 13: Shell preparation for growth patterns analysis. A) Mussels were cut from the umbo to the posterior margin along the maximum growth axis. B) Calcein mark revealed by fluorescent microscopy. The growth of the shell over a known period ($E_{\Delta T}$) was measured between the calcein mark in green and the posterior margin of the shell. The periostracum surrounding the shell exhibited some autofluorescence. C) Growth patterns were revealed using a Mutvei treatment. The lecture of the growth patterns was rated in three categories according to their readability. Green category pools clear growth patterns, orange category pools partially readable growth patterns and red category pools not readable growth patterns.

Increments were revealed using the Mutvei's solution which produces a filigreed three-dimensional relief of organic resistant (growth lines) and calcified depressions (growth increments). It is composed of 500 mL of 1 % acetic acid, 500 ml of 25 % glutaraldehyde, and 5 g alcian blue powder. Slides were put in the solution for one hour at temperatures comprised between 37 and 40°C (Schöne et al., 2005a). Treated shell sections were visualised using a camera (SONY DF W X700, Sony corporation, Tokyo, Japan) mounted on a microscope (Leitz DIAPLAN, Leitz, Germany) and reflected light. The software Visilog 6.2 Noesis was used to take pictures.

Growth pattern characterisation

Pictures were assembled and processed using the softwares Gimp and ImageJ. The distance between the calcein monthly marks was measured along the external side of the shell in order to

quantify the growth per month. Also, the number of increments were counted between calcein marks. The readability of the increments was rated. Arbitral rating between green, orange and red was attributed to each increment of each mussel, the colour green being clear incrementations and the red unreadable sections (Figure 13C). Rates were transformed in percentage. Then, a coefficient of certitude was calculated per month and mussel:

$$(2 \times \text{number of green} + 1 \times \text{number of orange} + 0 \times \text{number of red}) / 200 \quad (1)$$

The coefficient was comprised between 1 and 0. It was compared with monthly averaged environmental and biological data per studied area using Pearson correlation as implemented in R (v.4.1.2) (R Core Team, 2020).

The width of the increments was measured in order to assess periodicities embedded in shells. As reading growth patterns is difficult, some increments might be missed, leading to occasional aberrant increment widths. In order to decrease their influence on growth rate periodicity assessment, data were smoothed using the Lowess smoothing (*i.e.*, locally scatterplot smoothing) as it is known to remove outliers (Cleveland, 1979). This was done using the package "gplot" (Warnes et al., 2020) on R. Data quality was assessed in R using an autocorrelation function (ACF) to check the absence of randomness and *via* partial autocorrelation function (PACF) (Gouthiere et al., 2005b, 2005a). Periodicities were first evaluated using a Lomb-Scargle periodogram using the package "lomb" in R (Ruf, 2022). Peaks having a p-value < 0.05 were validated using a cosine model implemented with the packages "cosinor" and "card" in R (Sachs, 2014; Shah, 2020). Cosine model was constructed for the frequency having the highest normalised power as described in (Nelson et al., 1979; Bingham et al., 1982):

$$Y(t) = A.\cos(2\pi t/\tau + \phi) + M + \varepsilon(t) \quad (2)$$

Where Y(t) is the increment width at the time t, A is the amplitude, τ is the period, ϕ is the acrophase, M is the mesor and ε(t) is the relative error at the time t. The model was statistically validated *via* a goodness-of-fit test and the normality and homogeneity of the variance of the residuals. (Gouthiere et al., 2005a; Cornelissen, 2014). Rhythm was evaluated *via* an error ellipse test and the percentage of rhythm was assessed (Bingham et al., 1982; Cornelissen, 2014). In order to test imbricated rhythmicity, the analysis was redone without the smoothing step by re-injecting the residuals. The same development was applicated without the smoothing step on the data of temperatures and wind speed.

von Bertalanffy growth curve reconstruction

Mussels shell growth was modelled using the von Bertalanffy equation (von Bertalanffy, 1938):

$$E_{t+\Delta t} = E_{\infty} (1 - \exp^{[-K(t - t_0)]}) \quad (3)$$

where $E_{t+\Delta t}$ is the total shell length (cm) measured along the maximum growth axis on the external side of the shell, E∞ is the asymptotic theorical shell length (cm), K is the growth coefficient ($year^{-1}$) and t_0 is a time constant evaluated from the minimum size of the mussel at its settlement (E_0). E_0 and t_0 were assumed to be equal to zero in the calculation (Ramón et al., 2007; Andrisoa et al., 2019a). $E_{\Delta t}$ was measured for each mussel from the first calcein mark to the posterior edge of the shell. The parameters K and E∞ were calculated using the linear regression between E_t and $E_{t+\Delta t}$ to define the Ford-Walford slope *a* and the *y*-intercept *b* (Walford, 1946; Hart and Chute, 2009):

$$E_t = E_{t+\Delta t} - E_{\Delta t} \quad (4)$$

$$E_{t+\Delta t} = a * E_t + b \quad (5)$$

$$K = - \ln(a) / \Delta t \quad (6)$$

$$E\infty = b/(1-a) \quad (7)$$

Statistical analysis

Outliers were searched and removed for each environmental and biological data using a Grubbs test (Package "outlier" on R (Komsta, 2011)). The monthly mean of each environmental and biological variable was computed per location. PCA regrouping environmental and biological data by study sites were done in R using the package "FactoMineR" (Lê et al., 2008). To discard parts of growth pattern observed that were not readable and to increase the power of statistical test, the arbitrary value of 0.7 of confidence was chosen as a threshold. By removing months of shells with a confidence inferior to 0.7, the percentage of explained variance of PCA axis increased without changing the correlations observed.

Normality and homogeneity of the variance of the data were assessed using a Shapiro-Wilk and Leven's tests ("Car" package on R (Fox and Weisberg, 2019)). When both conditions ($\alpha \geq 0.05$) were respected, one-way ANOVA was used to assess the difference in CI and growth rate within the same location between months and also between locations at the annual level. If conditions were not respected, Kruskal-Wallis rank sum test was used based on the package "dunn.test" in R (Dinno, 2017).

T-test was applied on the number of increments counted per mussels of one location in order to test if tidal (*i.e.*, two per day), daily (*i.e.*, one per day) or mixed semidiurnal tidal regime (*i.e.*,

depending on the local tidal regime) increments were formed at the monthly scale based on high confidence level measurements (*i.e.*, confidence level >0.7) (Mirzaei and Shau-Hwai, 2016). The observed number of increments formed by the population was compared to the expected number of increments in the different tidal conditions.

Simple linear regressions were made in order to define the number of increments formed in function of shell growth. Outliers were removed using a Grubbs test in R. Normality of the data was assessed using a Shapiro-Wilk test and if it was not fulfilled a logarithmic correction was applied. This was done on all datapoints in each location but also per regime of incrementation (*i.e.*, tidal, daily and following mixed semidiurnal tidal regime).

Results

Condition index

The ratio between soft and hard tissues was used to calculate the condition index (CI) of mussels. As data were lacking for the site at sea between June 2020 to December 2020 (see Methods), only the average CI from January 2021 to June 2021 could be compared between sites. The CI was similar for mussels from the CSN laguna (mean CI = 16.0±5.1) and for those at sea (mean CI = 14.5±2.9) (ANOVA, n = 182, $p>0.05$), with a higher variability in the laguna than at sea. At SL laguna, the CI of mussels was significantly lower and less variable than in the two others locations (mean CI = 9.4±1.7) (ANOVA, $p<0.05$). In the three locations studied, no significant differences were observed between males and females (ANOVA, n = 61 (SL), n = 45 (CSN), n = 60 (sea), $p>0.05$). Significant difference was observed between mussels having full and empty gonads at SL laguna (χ^2, n = 130, $p<0.001$) but not in the two other study sites (ANOVA, n = 67 (CSN), n = 65 (sea), $p>0.05$).

In details, the CI of mussels from SL laguna described a significant seasonal trend with higher values in December-January (mean CI = 13.5±2.5; χ^2, n = 130, $p<0.05$) and lower values in May-June (mean CI = 6.3±1.5) (Figure 14A). Although data were lacking in autumn (see Methods), a seasonal trend was also clearly visible for mussels from CSN laguna (χ^2, n = 67, $p<0.05$), but differed from specimens of SL laguna with higher values in summer (*i.e.*, July to September, mean CI = 24.3±4.3) and lower values in winter (*i.e.*, January to March, mean CI = 10.5±2.2). At sea, the CI was significantly lower in January and February (mean CI = 12.3±1.8; χ^2, n = 65, $p<0.05$) than in May and June (mean CI = 17.8±3.1). Interestingly, the CI significantly increased in March (mean CI = 17.5±2.9) which was similar to summer month before a drop in April (mean CI = 10.3±0.9).

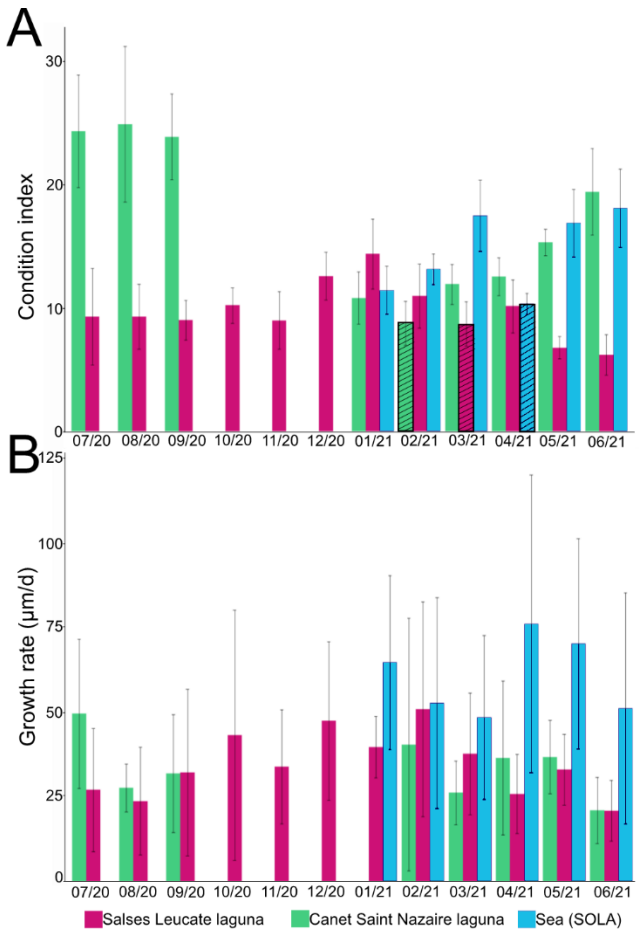

Figure 14: Condition index and growth rate of *Mytilus galloprovincialis* in Mediterranean lagunas and at sea. A) The ratio between dry soft tissues and dry hard tissues was calculated to get the condition index of the mussel. Probable spawning events based on visual observation of the gonads and the drop of the condition index are stripped. Due to loss of cages, data are missing at Canet-Saint-Nazaire from October to December 2020. At sea, data were measured after December 2020. B) Averaged monthly growth rate of mussels was calculated and data were missing for the same reason than for the condition index.

Growth curve

In June 2021 the remaining mussels were sampled at each studied location. For the site at sea, 27 mussels were recovered and for SL and CSN lagunas, 26 and 17 mussels respectively. The mortality in SL laguna was higher than in the two other sampling locations (*i.e.*, 15% of mortality vs 4%). The calcein dyes were not successful for all the individuals. Shells presenting missing calcein marks, which limits the establishment of a precise chronological scale, were removed from the set. Finally, 16 shells from the site at sea, 13 for SL laguna and 12 for CSN laguna were used in this study.

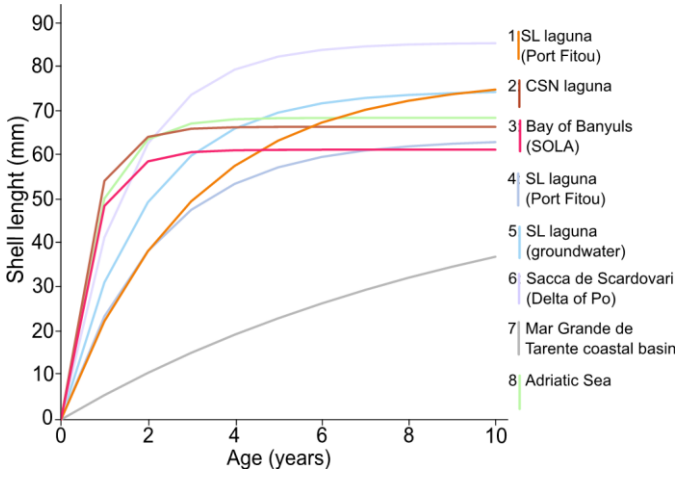

Figure 15: von Bertalanffy growth models of *Mytilus galloprovincialis* in Mediterranean environments. 1) Salses-Leucate laguna - Port Fitou (K= 0.34, E∞= 77.8). 2) Canet-Saint-Nazaire laguna, Village des pêcheurs (K= 1.69, E∞= 66.7). 3) Bay of Banyuls, SOLA (K= 1.57, E∞= 61.5). 4) Salses-Leucate laguna - Port Fitou (K= 0.46, E∞= 63.9) (Andrisoa et al., 2019a). 5) Salses-Leucate – Groundwater-influenced site (K= 0.54, E∞= 75) (Andrisoa et al., 2019a). 6) Sacca de Scardovari, delta of Po river (K= 0.66, E∞= 85.9) (Ceccherelli and Rossi, 1984). 7) Mar Grande de Tarente coastal basin (K= 0.1, E∞= 58.7) (Posa and Tursi, 1991). 8) Adriatic Sea (K= 1.32, E∞= 68.8) (Peharda et al., 2007).

Based on calcein staining, the total growth length of mussel population could be measured through mussel shells from each studied location over a year, and von Bertalanffy growth curves estimated (Figure 15). In SL laguna and at sea, the first calcein mark was not found for respectively three and six mussels, therefore they were not used in the growth curve estimation. At SL laguna (n = 10) mussels had a slower growth and reach their maximal size (77.8 mm) after seven years. At CSN laguna (n = 12) and at sea (n = 10) growth curves were similar, mussels reached their maximal size after a steep exponential phase within their two first years. The maximal length was slightly bigger for shells from the CSN laguna (66.7 mm) than the ones at sea (61.5 mm), but both were lower compared to the maximum length expected in SL laguna.

Shell growth rate

The mean growth rate of mussel shells was 34.7±21.5 µm.d^{-1} at SL laguna, 32.0±19.4 µm.d^{-1} at CSN laguna and 60.4±32.9 µm.d^{-1} at sea, in the Bay of Banyuls-sur-Mer (Figure 14B). As some periods were missing (*i.e.*, lack of staining during the autumn at CSN laguna, loose of the mussel cage in December 2020 at sea), comparison of growth rates between sites could only be achieved on the period from January to June 2021. During this period, the mean growth rate was similar in the two lagunas (SL = 32.5±10.3 µm.d^{-1} and CSN = 32.1±7.5 µm.d^{-1}) (ANOVA, n = 31, $p>0.05$) and significantly higher at sea (mean growth rate: 59.6±10.7 µm.d^{-1}) (ANOVA, n = 31 , $p<0.001$). Also, at annual level, no significant difference was observed when comparing growth rates of males and females (χ^2, n = 14, $p>0.05$).

Shell growth rates were then averaged per month, based on the monthly staining. For each site, there were no significant differences in shell growth rates between months (χ^2, n = 94 (SL), n = 67 (CSN), n = 65 (sea), $p>0.05$) (Figure 14B).

Growth increments

The readability of the increments was assessed *via* a classification into three categories in order to get a confidence level per month for each mussel shell (see Methods). The overall mean confidence level was 0.66±0.06 for mussel shells living at sea, 0.71±0.07 for shells from CSN laguna and 0.73±0.1 for shells from SL laguna (Table 3). Mean confidence levels were similar between the studied areas and months (χ^2, n = 153, $p>0.05$). This was also the case between male and females (χ^2, n = 14, $p>0.05$).

The number of increments formed per day was estimated from the analysis of 8 shells at SL laguna, 8 shells at CSN laguna and 11 shells at sea (Table 3), and reported on Figures 16 and 17 for samples SL0601, CSN0602 and SOLA0624, for SL, CSN and sea environment respectively. Shells for which too many increments were missing and retro-dating too uncertain were removed. The number

Table 3: Mean number of increments formed per day and confidence levels of the readability of shell increments in the three studied environments. Confidence level of readability of the increment was rated on three categories and reported as a coefficient, 0 being unreadable and 1 being a perfect reading. In grey are the raw data and in black is the mean increments observed when measurements below 0.7 of confidence level were removed.

	SL		CSN		SOLA (at sea)	
	Mean number of increments	Readability	Mean number of increments	Readability	Mean number of increments	Readability
07/20	1.3±0.4 1.3±0.4	0.94	2.0±0.5 2.3±0.3	0.71		
08/20	1.3±0.4 1.2±0.4	0.94	1.8±0.4 1.8±0.4	0.81		
09/20	1.2±0.4 1.3±0.4	0.85	1.4±0.3 1.5±0.3	0.60		
10/20	1.3±0.4 1.5±0.4	0.81	1.1±0.3 1.2±0.4	0.78		
11/20	1.2±0.4 1.4±0.4	0.69				
12/20	1.5±0.4 1.6±0.5	0.63			1.7±0.5 1.4±0.1	0.55
01/21	1.5±0.4 1.7±0.2	0.67				
02/21	1.6±0.3 1.6±0.5	0.62	1.5±0.4 1.4±0.4	0.62	1.6±0.5 1.5±0.3	0.66
03/21	1.8±0.5 1.7±0.6	0.66	1.6±0.7 1.5±0.6	0.79	1.7±0.5 1.7±0.5	0.76
04/21	1.4±0.6 1.3±0.4	0.69	1.9±0.4 1.7±0.4	0.67	2.4±0.8 2.5±1.0	0.67
05/21	1.7±0.4 1.4±0.1	0.65	1.9±0.5 1.9±0.4	0.60	2.1±0.4 2.1±0.4	0.72
06/21	1.3±0.3 1.3±0.3	0.62	1.4±0.4 1.5±0.4	0.71	2.0±0.6 2.1±0.5	0.60

of increments formed per day in SL laguna was variable through the studied period and two groups appeared. The first was constituted of summer months where the number of increments formed per day was close to one (mean number of increment.d^{-1} = 1.2 to 1.3 in summer 2020 and 2021) (Table 3). The confidence level was the highest in July and August 2020 (confidence level = 0.94 to 0.85) and tended to decrease through the year, to be at 0.62 in June 2021. In winter and spring, the number of increments formed per day was comprised between 1.5 and 1.8 from December 2020 to March 2021 and the confidence level was stable at that time (mean confidence level = 0.65±0.02). In the CSN laguna, the pattern was opposite with almost two increments formed per day in spring and summer (mean number of increment.d^{-1} = 1.9±0.1) but not in June 2021, where 1.4 increments were formed per day (confidence level = 0.71). In winter, the confidence level was high (confidence level = 0.78) and 1.1 increment was formed per day. In September, February and March, the number of increments formed was similar in both lagunas. At sea, the number of increments formed was a bit higher than in

both lagunas from April 2021 to June 2021 (mean number of increment.d^{-1} = 2.2±0.6). In winter, the confidence level was low (confidence level = 0.55), which was impacting the number of increments formed corrected (*i.e.*, removal of samples with a confidence level below 0.7) that passed from 1.7 to 1.4 increment.d^{-1}.

Table 4: Differences between expected and observed number of increments formed per day in Salses-Leucate and Canet-Saint-Nazaire lagunas and at sea. Only measurements having a confidence level > 0.7 were used in this test. In bold numbers were the most probable incrementation pattern formed, closer the value was to zero, more the mean observed number of increments was close to the expected value. Daily: 1 increment per day; Tidal: 2 increments per day; Mixed: following the mixed semidiurnal tidal regime of the region.

	Salses-Leucate laguna			Canet-Saint Nazaire laguna			SOLA (at sea)		
	Daily	Tidal	Mixed	Daily	Tidal	Mixed	Daily	Tidal	Mixed
07/20	**1.83**	-5.17*	-3.61*	11.72*	**2.50**	3.87			
08/20	**1.20**	-5.61*	-4.81*	4.47*	-1.25	**-0.54**			
09/20	**1.66**	-6.32*	-4.26*	5.01*	-4.12*	**-2.30**			
10/20	**2.29**	-6.46*	-4.27*						
11/20	4.63	-5.62	**-1.98**	**1.35**	-4.97*	-3.01			
12/20	3.98	-2.45	**-0.31**				6.44*	-4.89*	**-0.31**
01/21	8.56*	-3.96*	**1.60**						
02/21	3.89	-2.59	**-1.30**	2.81	-3.81	**-2.48**	5.25*	-5.06*	**-1.91**
03/21	3.33	-1.74	**-0.48**	2.08	-1.80	**-0.80**	4.83*	-1.77	**-1.19**
04/21	**1.84**	-5.37*	-4.28*	4.20	-1.70	**-0.80**	4.69*	**1.23**	2.00
05/21	9.99*	-13.81*	**-9.56***	5.07*	-0.78	**0.26**	8.64*	**1.42**	2.71
06/21	**2.79**	-7.95*	-6.16*	2.54	-3.11	**-2.17**	5.75*	**0.47**	1.24

The observed number of increments in shells was compared to the expected number of increments if the increment formation was either daily, tidal or following mixed semidiurnal tidal regime. The results of t-tests were presented in Table 4. T-tests showed that in shells from SL laguna, one increment was formed per day from July 2020 to October 2020, in April 2021 and in June 2021. Between November 2020 and March 2021, the number of increments formed per day followed a model driven by the mixed semidiurnal regime as occurring in the region. As previously observed, at the laguna of CSN, the pattern was opposite to SL with one increment formed per day from October 2020 to January 2021. The rest of the year except July 2020, the number of increments formed per day followed the mixed semidiurnal tidal regime of the region. At sea, the number of increments formed was related to the tidal regime of the region (*i.e.*, a mixed semidiurnal regime) from December 2020 to March 2021 and switched to follow semidiurnal tidal regime in April 2021.

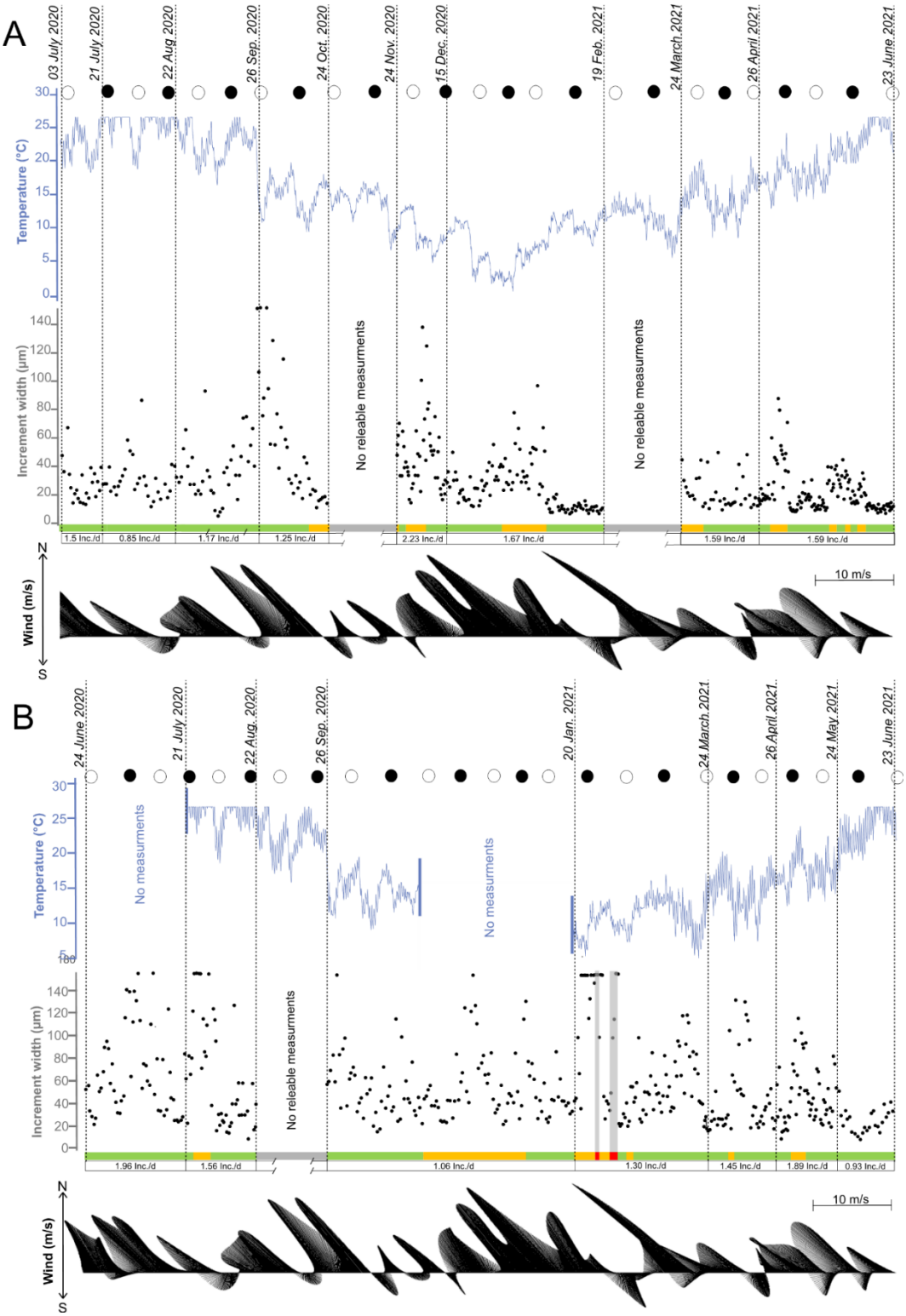

Figure 16: Increment width variation of the mussel SL0601 raised in the Salses-Leucate laguna (A) and of the mussel CSN0602 raised in the Canet-Saint-Nazaire laguna (B) in relation with environmental variations. Dates of visualised calcein marks are delimiting number of increments formed per day within the period. Green, yellow and red bands indicate the confidence level on the increment lecture. When red bands, grey shadow was displayed as data points were not reliable. Recorded temperatures are the blue line. Moon cycle is pictured by black and white circles (*i.e.*, empty and full moon). Wind direction and force are in black. In both locations, an increase of the increment width was observed after strong Tramontane wind blow (NW), probably due to an enrichment of the water due to resuspension of sediments (Andrisoa et al., 2019b; Rodellas et al., 2020). At the same time, the water temperature tended to drop.

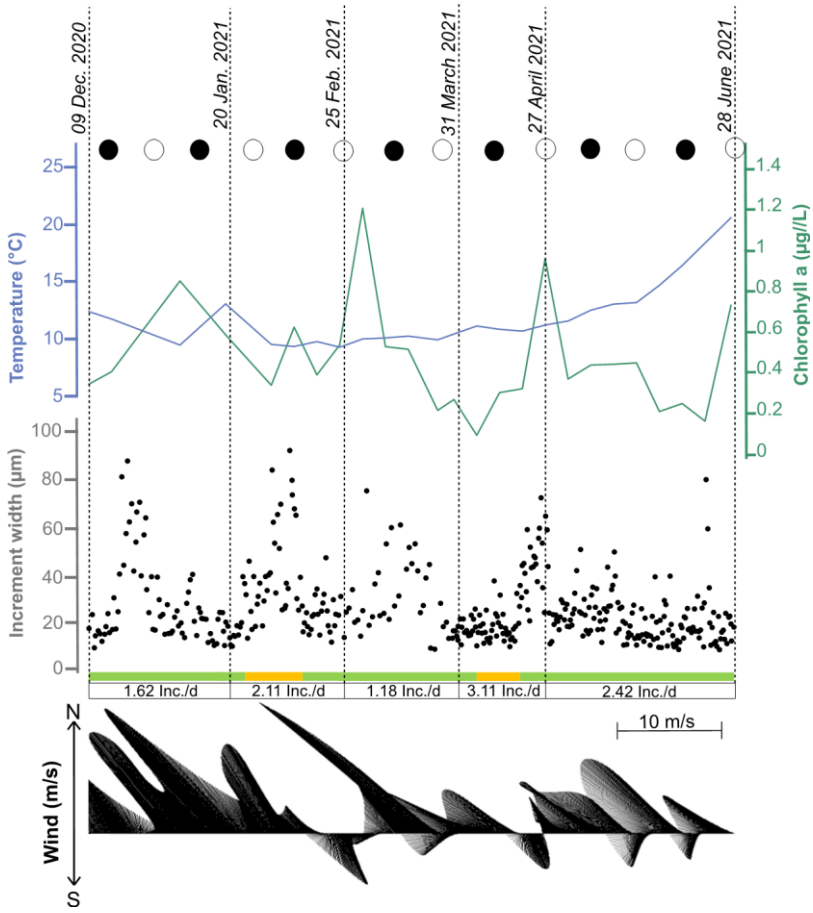

Figure 17: Increment width variation of the mussel SOLA0624 raised in the Bay of Banyuls in relation with environmental variations. Dates of visualised calcein marks are delimiting number of increments formed per day within the period. Green and yellow bands indicate the confidence level on the increment lecture. Recorded temperatures are the blue line and the chlorophyll *a* is the green line. Moon cycle is pictured by black and white circles (*i.e.*, empty and full moon). Wind direction and force are in black. The increment width increased with the increase of chlorophyll *a*.

The number of increments formed was compared to the shell growth using a simple linear regression (Supplementary Figure S1). Taking all the measurements, the coefficient of determination was medium in all locations (SL, n = 37, R^2 = 0.51, p<0.001; CSN, n = 28, R^2 = 0.47, p<0.001; sea, n = 31, R^2 = 0.36, p<0.001). When separating the incrementation regimes observed, the growth rate explained well the incrementation under mixed semidiurnal tidal regime at SL laguna (n = 15, R^2 = 0.84, p<0.001) whereas when taking daily incrementation pattern the regression was not significant (n = 13, R^2 = 0.02, p>0.05). The strong relationship observed in SL laguna when incrementation followed the mixed semidiurnal tidal regime was not observed both in CSN laguna (n = 23, R^2 = 0.38, p<0.001) and at sea (n = 15, R^2 = 0.16, p>0.05). Also, regression could not be built under daily regime in CSN laguna due to the low number of measurements available (n = 4). At sea, the correlation of the tidal incrementation pattern observed with growth rate was higher than while following mixed semidiurnal tidal regime (n = 17, R^2 = 0.39, p<0.003).

Next, the increment width variability was studied in order to get insight into putative lower frequency periodicities present in shells. Increment widths measured showed a huge variability within each shell, without clear seasonal trend (Figures 16, 17, Supplementary Table S1). The variability in growth increment width was analysed under a Lomb-Scargle spectral analysis. In SL laguna, 5 shells on

the 8 used showed a periodical pattern comprised between 39 and 48 increments. This pattern was also found in 7/8 shells from CSN laguna (frequencies comprised between 38 and 50) and only 4/11 at sea (frequencies comprised between 38 and 50). Frequencies comprised between 16 and 32 increments were also observed in 4/8 shells in SL, 6/8 shells in CSN and 6/11 shells at sea. At sea, the majority of individuals studied (9/11) exhibited a cyclic pattern of 55 to 77 increments. In both lagunas, frequencies between 70 and 93 increments were observed (5/8 in SL and 4/8 in CSN).

Frequencies observed in shell increment width variation could be converted in days by inferring the time needed to produce one increment in each environment. At sea, this time was more stable through the year and was of 1.76 increment formed on average per day as it was assumed that the regional tidal regime was followed (*i.e.*, 355 tidal cycles on 202 days of experiment). Applied on the 38 to 53 increments patterns, it resulted in patterns distributed between 32 to 21.5 days. Looking to growth rate variation in relation to the tidal regime and coefficient, the circalunar periodicity was clearly visible (Figure 12). In lagunas the approximation of periodicities would be greater as the unit of time was less constant over the studied period, in SL on average 1.75 increment were formed in a day (*i.e*, 623 tidal cycles on 356 days of experiment) and in CSN 1.76 increment per day (*i.e.*, 639 tidal cycles on 364 days of experiment). Applied on patterns of ~45 increments observed, it showed periodicity around 26 days. Also, semi-circalunar periodicities (around 14 days) were observed in the three locations which were the 18 to 24 increments patterns in SL, the 16 to 32 patterns at CSN and the 17 to 26 at sea.

Comparison of mussel CI and shell patterns with the environmental parameters

Values of the environmental variables measured were averaged at monthly scale in order to be compared and described in the three environments studied (Supplementary Table S2, S3 and S4). In all environments, temperatures showed seasonal variations. In both lagunas, temperature oscillated from 23 to 26 °C on average in summer and 6 to 8 °C in winter. At sea, variations were less important between summer and winter, with respectively a water temperature comprised between 20 to 22°C and 12 to 15 °C. No such seasonality was observed for salinity and it was lower and more variable in both lagunas (mean salinity SL = 33.7±1.9 and CSN = 32.4±3.5) than at sea, where the salinity was almost stable (mean salinity = 37.6±0.4). The pH was relatively stable through the year in CSN laguna and at sea (mean pH = 8.2±0.1 and 8.0±0.1 respectively), whereas more variable and higher in SL laguna (mean pH = 8.3±0.2). In SL laguna and at sea, the chlorophyll *a* concentration was variable but no cyclicity was observed (mean Chl *a*: 0.8±0.2 µg.L^{-1} at SL and 0.7±0.4 µg.L^{-1} at sea). In SL laguna, the mean Chlorophyll *a* level was lower from August to October 2020 (mean Chl *a* = 0.54±0.1 µg.L^{-1}) and

higher in January 2021 (mean Chl *a* = 1.1) (Supplementary Table S2). At sea, chlorophyll *a* levels were low in summer (mean Chl *a* = 0.17±0.1 µg.L^{-1}) and increased in November (mean Chl *a* = 1.63 µg.L^{-1}) (Supplementary Table S4). The oxygen concentration exhibited a seasonal variation in CSN laguna, being higher in winter (around 10 ml.L^{-1}) and lower in summer (around 8 ml.L^{-1}). On the contrary, the oxygen level was more stable and lower at sea (mean yearly O_2 concentration at sea = 5.6±0.4 ml.L^{-1}).

Then, the monthly average of shell growth rates, condition indexes and number of increments formed per day were compared to the environmental parameters. To assess common variations through the year, PCAs were performed per localisation. At SL laguna, the first dimension of the environmental cues on the PCA was primarily explained by temperature and chlorophyll *a* concentration, regrouping summer months on the left and winter ones on the right (Figure 18A). The second axis showed the instability of the water body due to gales that happened mostly during winter. Interestingly the water level at Port Fitou was negatively related to the wind speed (Pearson's correlation = -39 %, n = 12). The response of mussels to this variability in their habitat showed that the growth rate and the condition index covariates (68%). They were negatively related to the temperature (-48 % and -74 % for the growth rate and the CI respectively) and to a lesser extent to the pH (-54% and -34% for the growth rate and the CI respectively). Only the CI was positively correlated to chlorophyll *a* level (34%). The number of increments formed was correlated to chlorophyll *a* level (50%) and it was also negatively related to the temperature (-48%). In the other laguna, located at CSN, the first dimension of the PCA was related to the water temperature, O_2 concentration and the pH, regrouping winter months on the left and summer ones on the right (Figure 18B). The second dimension was tightly linked to the salinity and the wind speed. Contrary to SL laguna, the CI appeared positively related to the temperature (Pearson's correlation = 97%, n = 8). In this laguna, the number of increments formed in mussel shells covaried with the shell growth rates and the CI (63% and 70% respectively). The number of increments was also related to the wind speed (42 %) and inversely to the salinity (-53%) and the pH (-28%). In the last location studied, at sea, first dimension of the PCA regrouped the temperatures and the chlorophyll *a* concentration (Figure 18C). The second axis was related to more stable environmental data (*i.e.*, salinity, pH and wind speed). The condition index was positively related to temperatures (Pearson's correlation = 53%, n = 6) and inversely to chlorophyll *a* level (-30%). The growth was significantly correlated with the salinity (84%) and related to the pH (46%). The number of increments formed was followed similar monthly variation with the growth (53%) as at CSN laguna but not with the CI (1%). Contrary to CSN laguna, at sea the number of increments was inversely related to the wind speed (-44%), the chlorophyll *a* level (-52%) and correlated with the salinity (84%) and the pH (45%).

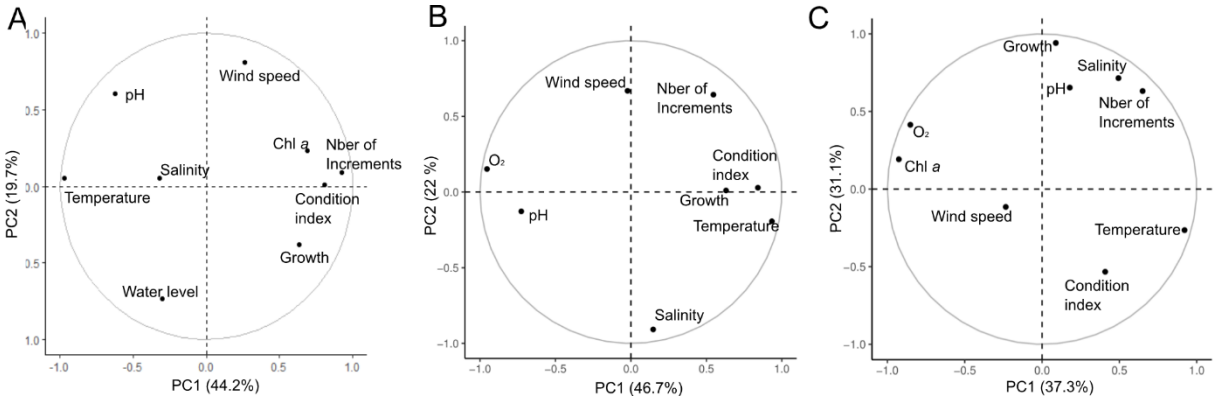

Figure 18: Principal component analysis describing environmental parameters and the biological changes of mussels (*i.e.*, CI, shell growth rate and number of increments) at monthly scale in the lagunas of A) Salses-Leucate and of B) Canet-Saint-Nazaire and C) at sea.

Based on the parameters measured infra-daily (*i.e.*, for wind speed and direction, and the temperature), the response of shell growth through increment width could be studied at a higher frequency than the monthly averages. The Tramontane wind blow events (orientated NW), were often followed by strong drops in temperature, such as during the event of the 26th of September 2020, with a decrease of 12 °C in less than 24 hours in both lagunas (Figure 16). These events over prolonged periods were frequently associated to an increase in the width of increments with a small lag in both lagunas. Particularly in SL laguna, strong Marin wind events (oriented SE) reduced the increment width. At sea, none relationship with temperatures or wind events were observed (Figure 17). However, an increase in the increment width was observed when the concentration in chlorophyll *a* increased.

The FFT analysis of the environmental variables were done to be compared to periodicities at lower frequencies found in shells. Analysis revealed a periodicity of 22 and 16 days for the wind speed in the Perpignan area, covering the three sites. A 101 days cycle was also observed for this parameter. The temperatures showed a circalunar periodicity in both lagunas (25 and 28 days in SL and CSN lagunas, respectively) combined with a 9-days cycle and daily oscillations. Additionally, a 44 days period was also observed in SL laguna and a 55 days period in CSN laguna. At sea, temperatures observed only a circalunar periodicity (28 days) and a 9-days periodicity.

Discussion and Conclusion

In this study, we have several evidences that *Mytilus galloprovincialis* from the Mediterranean Sea might form growth increments with a periodicity related to a mixed semidiurnal tidal regime of the region, although the shells are exposed to low tidal range (~30 cm at sea). This uncommon periodicity

might be due to a joint control of the biomineralisation process by both directly the environment and biological clock(s).

A previous study on *M. galloprovincialis* shells from SL laguna, in the same area chosen for our study, reported daily incrementation in shells. There were likely induced by the important daily variability of the environmental parameters, including temperature, salinity, water depth and wind speed (Andrisoa et al., 2019a). Our results are not conflicting with this study as in this site as, at certain periods of the year, shells rather exhibited daily growth increments. This change in the increment rhythm formation is still unclear but likely suggests that growth of bivalve shells reflects the complexity of their habitat. In intertidal habitats submitted to semidiurnal tides, *M. galloprovincialis* forms two increments per day as described by Tanaka et al. (2019) for shells from the Bay of Tokyo. It was proposed that the incrementation pattern was directly linked to tides, following the theory of growth line formation at low tides. It would be due to a pH decrease during aerial exposure, when valves are closed (Lutz and Rhoads, 1977). Similar tidal growth lines were described in the shell of *Mytilus edulis*, a close related species, from tidal emergence areas of the Wadden Sea (Buschbaum and Saier, 2001) and in the north of Wales (Richardson, 1989). In environments submitted to another type of tidal regime, shell growth appears directly related to its rhythmicity, in the studied locations a mixed semidiurnal regime.

However, another hypothesis could explain the uncommon growth rhythm observed in Mediterranean mussels. In our study, in addition to uncommon periodicities, a large variability within individuals were observed in the shell incrementation. Similarly to what has been observed in this study, the shell incrementation in *M. edulis* from continuously submerged sites in tidal environments lost the tidal periodicity and a huge variability in the number of increments formed within the shell was observed (Richardson, 1989; Richardson et al., 1990). As observed in *M. galloprovincialis* at sea, *M. edulis* produced less than one to two increments per day and animals showed widely different growth rates although growing in the same environmental conditions. These observations suggested that rhythm might reflect an interplay between innate signals and exogenous constrains as previously proposed by Richardson et al. (1980; 1988), based on laboratory experiments on *Cerastoderma edule* and *Ruditapes philippinarium*. Such innate growth response of subtidal shells was associated with a significant correlation between the number of growth bands and the rate of shell deposition (Richardson, 1988, 1989). In the 3 sites studied, we observed that monthly averaged shells growth rates and the number of increments followed similar trends. Nevertheless, while looking at the regression analysis of the number of increments formed in function to the growth, the coefficient of determination (*i.e.,* the R-squared) indicated that the growth rate cannot explain the number of increments formed in all locations all along the year. Interestingly, while looking to periods of

incrementation following mixed semidiurnal tidal regime, the regression analysis showed a good correlation between the growth and the number of increments formed in SL laguna. On the contrary, periods of daily incrementation had non-significant linear relation. This might be related to the joint controlled biomineralisation (*i.e*., external and endogenous factors), as suggested for other bivalves by Richardson et al. (1980) and Richardson (1988). In these studies, difference appeared among growth lines, between strong growth lines likely driven by tides and weak bands that should be related to the influence of growth rate. In this study, growth lines looked very different but no distinction between weak and strong bands could be made. Moreover, when looking only the period of incrementation following mixed semidiurnal tidal regime, the relationship between growth and incrementation was not as strong in shells from CSN laguna compared to the ones from SL laguna and non-significant for shells at sea. As the growth rate cannot explain uncommon incrementation found in all locations, it is suggested that another interplay might be involved to explain the switch in incrementation periodicity observed.

PCA suggests that the number of increments was linked to the level of chlorophyll *a* and inversely correlated to temperatures at SL laguna. In the CSN laguna, the number of increments formed per day increased with Tramontane wind blow events (>10 $m.s^{-1}$) and was inversely linked to the salinity and the pH. Unfortunately, no chlorophyll *a* measurement was available at this laguna. However, as lagunas are shallow, wind events are known to resuspend the sediment in the water column (Rodellas et al., 2020). By enriching the water this phenomenon promotes the development of primary producers (Rodellas et al., 2018; Andrisoa et al., 2019b). Comparison of increment width with the wind blow, we notice the growth rate increased after a prolonged Tramontane wind events in both lagunas. Therefore, the increase in shell growth rate was likely due to increase in food availability after a wind event, as already observed by Andrisoa (2019a) in SL laguna. Then, wind increase can be associated to a short-term increase in food availability and considered as an indicator of the food levels in lagunas.

Taking this into consideration, shifts between daily and incrementation following mixed semidiurnal tidal regime in lagunas seems to be tightly linked to the food availability. The main difference between the two lagunas was their trophic levels, with a very high concentration of chlorophyll *a* and suspended matter in CSN compared to SL (Souchu et al., 2010; Bec et al., 2011). The nutrient status of mussels can be approached via their CI (*i.e.*, the ratio between the dry flesh weight and the dry shell weight) (Orban et al., 2002). As the CI of mussels from SL laguna (9.4±1.7) was lower than the CI of mussels from the hypertrophic laguna of CSN (of 16.0±5.1), therefore in the SL laguna, food availability might be a limiting factor for the shell growth. Then, increments might be missing due to growth stops or being too close from each other impairing their readability. It is supported by the

confidence level of the readability of growth patterns established, which was lower when chlorophyll *a* level was low (*i.e.*, Chl *a* <0.55 µg.L^{-1} from August 2020 to October 2020). This concentration in chlorophyll *a* of 0.5 µg.L^{-1} is known as a threshold at which the filtration activity (*i.e.,* valve gape and siphon area) of *M. galloprovincialis* decreases until the complete closure of the valves (Maire et al., 2007). Impact of low chlorophyll *a* concentration was also reported to decrease the clearance rate when lower than 2.08 µg.L^{-1} in presence of pulverised sediment (Filgueira et al., 2009). Another indicator that the food availability is likely impacting the increment formation is that at SL laguna two peaks of phytoplankton occurred during the studied period, one in spring (around March) and one in autumn (around November) (Fiandrino et al., 2021), and at these periods mussels formed increments following the mixed semidiurnal tidal regime of the region. At CSN laguna, the concentration in chlorophyll *a* is reported to be regularly above 10 µg.L^{-1}, which is very high regarding to other Mediterranean ecosystems (Derolez et al., 2021). Therefore, mussels living in CSN laguna probably had none to low constraints regarding the food availability. However, from October to January the presence of detrimental conditions of turbidity at this period might be at the origin of the lower number of increments formed. During this period, the cage was lost due to low visibility conditions and then found from behind the rock on which it was deployed, partly recovered by mud. The shift of incrementation in shells during autumn might be linked to the clogging of the gills system by amount of suspended matter (Peterson, 1985). Therefore, in Mediterranean lagunas, when food availability conditions are favourable, mussels formed increments according to the tidal regime of the area (here a mixed semidiurnal tidal regime). Otherwise, they tend to form one increment per day, putatively related to an endogenous clock.

As observed in the lagunas, the increment width in mussel shells at sea increased when the level of chlorophyll *a* increases in the water column. Interestingly, the shell growth rate was 2 times larger than the ones measured in lagunas, probably linked to the energy demands that is higher in highly variable environments such as lagunas compared to the more buffered conditions at sea (Pérez-Ruzafa et al., 2019). In addition, the relationship between the number of increments formed in marine shells and their environmental conditions was different that the one observed from laguna areas, with a negative relationship with the level of chlorophyll *a* and the wind force, whereas the number of increments covariate with the salinity, the pH and the temperature variations. This difference of constraints was also reflected in the incrementation patterns at sea, as contrarily with what was observed in lagunas, the number of increments formed per day shifted to tidal pattern (*i.e*, 2 per day). Otherwise, they were following the mixed semidiurnal of the region. The origin of the switch between the two incrementation regimes was less clear at sea. However, it has been shown that a potential biological clock might switch its periodicity between circatidal and bimodal (*i.e*., circadian and

circatidal) at sea (Bertolini et al., 2021). It is possible that the clock was bimodal with a stronger circadian entrainment, generating daily incrementation from December to March and switch to circatidal from April to June, generating circatidal increments. Supernumerary increments could occur when chlorophyll *a* level is above the threshold, leading to patterns following the mixed semidiurnal tidal regime of the region in winter and in spring leading to a bit more than two increments formed per day.

Our results likely suggest that the biomineralisation process is under a joint control of biological clock(s) and the environment, and more precisely the feeding conditions. Biological clocks are molecular feedback loops that are set and reset by environmental factors, and orchestrate many physiological and behavioural activities (Dunlap, 1999). Currently, it is not clear if one or two molecular clockworks generates circadian and circatidal rhythmicity in marine environments (Goto and Takekata, 2015; Häfker et al., 2023). Interestingly, under food availability stress, one or two increments were formed in according to the environment surrounding mussels. Previous studies have shown that in function of its environment, the biological clock of the oyster *M. gigas* can switch between circatidal and circadian frequencies (Mat et al., 2012, 2014; Tran et al., 2020). This could be also the case for the putative biological clock of mussels too as lagunas have a different environmental dynamic than the open sea, while the drivers of the biological clock are still not well described in the case of subtidal species. As biological clocks are known to drive the valve aperture of bivalves, the putative interplay between the biomineralisation process and the clock might not be direct (Tran et al., 2020).

In intertidal environments, growth lines are produced during the emersion phase due to a decrease in pH in the extrapallial fluid as valves closed (Lutz and Rhoads, 1977). Valve aperture rhythms driven by biological clocks in phase with tides might lead to one or two prolonged closure time a day, producing one or two growth lines, depending respectively the diurnal and semidiurnal tidal regimes (Figure 19A, B). Tidal incrementation in relation to semidiurnal tidal regime was observed in the butter clam *Saxidomus gigantea* (Hallmann et al., 2009). Growth lines were weaker and increment wider when clams emerged during a shorter duration in neap tides, showing that tides generate incrementation patterns in shells of intertidal bivalves. Similar observations were achieved on *M. galloprovincialis* in the bay of Tokyo (Tanaka et al., 2019). This could explain the circalunar and semi-circalunar periodicities of increment width observed in the shells from all studied locations as circalunar valve behaviour have been described in bivalves (Payton and Tran, 2019).

Based on our observations, we can propose an additional model for shells from subtidal environment associated to Mediterranean laguna systems, where tidal range is low and environmental constraints on biological clock(s) marked by daily periodicities (*e.g.*, temperature, photoperiod…).

Thus, the biological clock should adopt a daily rhythm for Mediterranean mussels, while the environmental limits (*e.g.*, food availability, turbidity, …) will produce supernumerary increments leading to growth patterns following the mixed semidiurnal tidal regime of the region (Figure 19C). Therefore, cycles in concentration in chlorophyll *a* at daily levels, likely influenced by the local hydrology, could be at the origin of growth lines in shells. This could also be at the origin of the high variability in increments observed as mussels were grouped into cages, and due to intraspecific competition mussels located in the centre did not have the same access to food than the one from the periphery (Cubillo et al., 2012; Karayücel et al., 2015). Therefore, aside the control of biological clocks, environmental forcing factors could be at the origin of intermediate shell growth patterns observed.

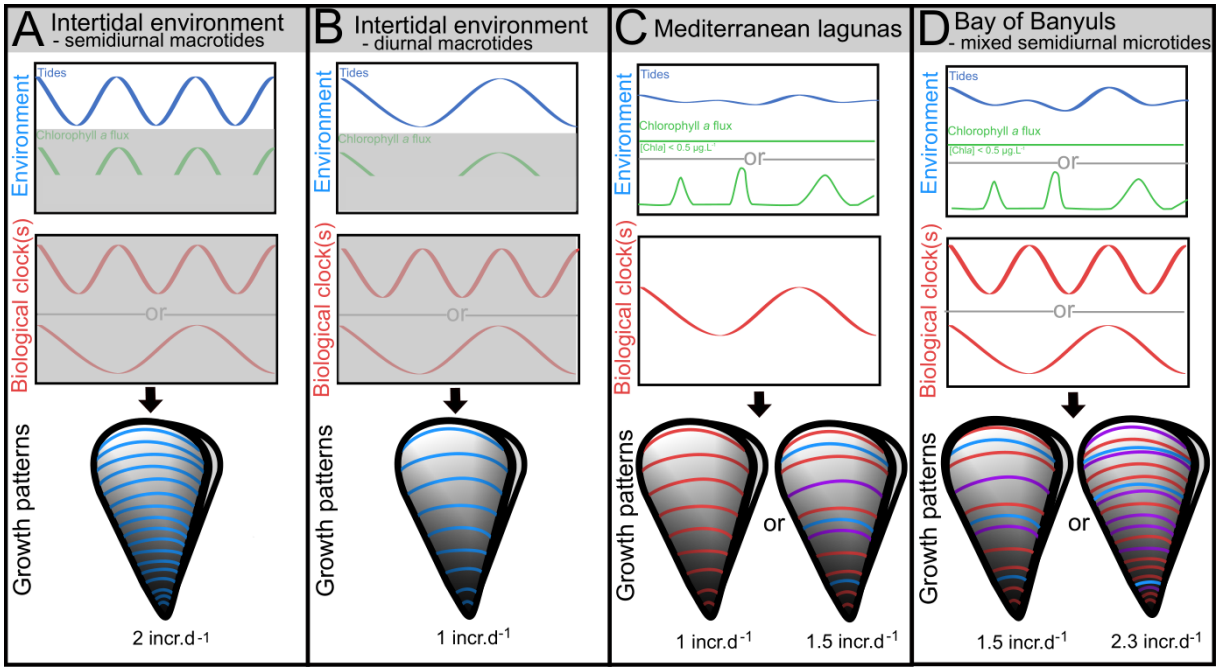

Figure 19: Simplification of the joint control of the growth line formation in function of the environment. Environmental forcing factors represented are tides (blue) and chlorophyll *a* flux (green). Chlorophyll *a* flux is a measurement of the food availability taking the chlorophyll concentration and the current velocity (Comeau et al., 2018). Shell growth lines can be controlled by putative biological clock(s) (red), by the environment (light blue) or both (purple). A) and B) Under intertidal environment the growth line is formed when the mussel is outside the water. The alternation of emersion and immersion is predominant on chlorophyll *a* flux and biological clock control. C) In Mediterranean lagunas tides are really reduced and biological clock periodicity is supposed to be daily. When the chlorophyll flux is null, one increment per day is formed, controlled by the biological clock. Food availability is variable in time and not all the time synchronized with the biological clock, leading to all kind of increments and uncommon growth patterns. D) In the bay of Banyuls, there is a mixed semidiurnal microtidal regime (*i.e.*, tidal range = 30 cm) and the food availability not synchronized with the biological clock, leading to uncommon periodicities in growth patterns as seen in this study.

In the Mediterranean Sea, where tides are limited, shell growth patterns oscillate between ~1.5 increments formed per day to 2 or more increments per day (Figure 19D). The potential biological clock seems to switch from tidal to bimodal periodicities, as observed at the valve activity level in Venice laguna in winter where the tidal range is comprised between 50 and 100m (Bertolini et al., 2021). The origin of the switch between the two periodicities is still unclear but seemed to be mediated

by tides. In the bay of Banyuls where tides are stronger than in both lagunas, switch could be also possible from circadian to circatidal endogenous rhythms generating daily or tidal increments. Environmental constrains such the food availability can lead to supernumerary increments (Figure 19D).

To test if intermediate shell growth patterns are directly related to tidal regime via the chlorophyll *a* concentration, measurements of the dynamic of chlorophyll *a* concentration in relation with tides in the bay of Banyuls should be taken in order to discriminate if this incrementation regime is related to the semidiurnal tidal regime of the region or not.

In conclusion, when studying environments based on shells pattern in subtidal species inhabiting region of small tidal range and limiting access to feeding conditions, precaution should be taken as the increment formation rate varies through time and space, according to several endogenous and exogenous forcing factors. This seems to be tightly linked to chlorophyll *a* flux as it might break the innate biomineralisation pattern inherited from potential biological clock(s) rhythm of valves aperture when food is available. This might lead to an increase of the number of valves opening/closure cycles and thus the formation of growth lines. More studies are thus needed to better understand the interplay between biomineralisation, biological clock(s) and food availably.

Additional information

Acknowledgments

We acknowledge the “conservatoire du littoral” of Perpignan to let us do experiments in both lagunas and the community from “Le domaine de Pedros” facilitated access to Fitou (Salses-Leucate laguna). We are grateful to Laurence Fonbonne (Rivage Leucate), the Pôle-relais lagunes méditerranéennes and the FILMED network for sharing environmental data on lagunas and to the SOMLIT network for data at sea. We are thankful to captain Eric Martinez and crew from the Néreis II as well as the divers, Jean-Claude Roca and Bruno Hesse (Sea Service from Banyuls Oceanographical Observatory) for the experiment at sea. We are also thankful to the “Réserve of Cerbère-Banyuls” for facilitating the work at sea. We are greatful to Erwan Peru for sharing temperatures beacons. We acknowledge the facilities of Biology platform of imaging (BioPIC). We are very grateful to Stephane Hourdez who found back the cage of Canet-Saint-Nazaire. We would like to thank Vincent Laudet for its review on the draft.

Funding

This project has received the financial support from the CNRS through the 80|Prime - MITI interdisciplinary program “TEMPO” and the MITI interdisciplinary program “ARCHIVE”

References

Andrisoa A, Lartaud F, Rodellas V, Neveu I. 2019a. Enhanced Growth Rates of the Mediterranean Mussel in a Coastal Lagoon Driven by Groundwater Inflow. *Front. Mar. Sci.* 6:753

Andrisoa A, Stieglitz TC, Rodellas V, Raimbault P. 2019b. Primary production in coastal lagoons supported by groundwater discharge and porewater fluxes inferred from nitrogen and carbon isotope signatures. *Mar. Chem.* 210:48–60

Arnaud P, Raimbault R. 1969. The Salses-Leucate pond. Its principal physicochemical characteristics and their variations (in 1955- 1956 and from 1960- 1968). *Rev. Trav. Inst. Pech. Marit.* 33(4):335–443

Bargione G, Vasapollo C, Donato F, Virgili M, Petetta A, Lucchetti A. 2020. Age and Growth of Striped Venus Clam *Chamelea gallina* (Linnaeus, 1758) in the Mid-Western Adriatic Sea: A Comparison of Three Laboratory Techniques. *Front. Mar. Sci.* 7:582703

Bayne BL. 2004. Phenotypic Flexibility and Physiological Tradeoffs in the Feeding and Growth of Marine Bivalve Molluscs. *Integr. Comp. Biol.* 44(6):425–32

Bec B, Collos Y, Souchu P, Vaquer A, Lautier J, et al. 2011. Distribution of picophytoplankton and nanophytoplankton along an anthropogenic eutrophication gradient in French Mediterranean coastal lagoons. *Aquat. Microb. Ecol.* 63(1):29–45

Bertolini C, Rubinetti S, Umgiesser G, Witbaard R, Bouma TJ, et al. 2021. How to cope in heterogeneous coastal environments: Spatio-temporally endogenous circadian rhythm of valve gaping by mussels. *Sci. Total Environ.* 768:145085

Bingham C, Arbogast B, Guillaume GC, Lee JK, Halberg F. 1982. Inferential statistical methods for estimating and comparing cosinor parameters. *Chronobiologia*. 9(4):397–439

Branch GM, Steffani CN. 2004. Can we predict the effects of alien species? A case-history of the invasion of South Africa by *Mytilus galloprovincialis* (Lamarck). *J. Exp. Mar. Bio. Ecol.* 300(1–2):189–215

Buschbaum C, Saier B. 2001. Growth of the mussel *Mytilus edulis* L. in the Wadden Sea affected by tidal emergence and barnacle epibionts. *J. Sea Res.* 45(1):27–36

Cáceres-Martínez J, Figueras A. 1998. Distribution and abundance of mussel (*Mytilus galloprovincialis* Lmk) larvae and post-larvae in the Ria de Vigo (NW Spain). *J. Exp. Mar. Bio. Ecol.* 229(2):277–87

Ceccherelli V, Rossi R. 1984. Settlement, growth and production of the mussel *Mytilus galloprovincialis*. *Mar. Ecol. Prog. Ser.* 16:173–84

Chauvaud L, Thouzeau G, Paulet YM. 1998. Effects of environmental factors on the daily growth rate of *Pecten maximus* juveniles in the Bay of Brest (France). *J. Exp. Mar. Bio. Ecol.* 227(1):83–111

Cleveland WS. 1979. Robust locally weighted regression and smoothing scatterplots. *J. Am. Stat. Assoc.* 74(368):829–36

Cocquempot L, Delacourt C, Paillet J, Riou P, Aucan J, et al. 2019. Coastal ocean and nearshore observation: A French case study. *Front. Mar. Sci.* 6(JUN):324

Comeau LA, Babarro JMF, Longa A, Padin XA. 2018. Valve-gaping behavior of raft-cultivated mussels in the Ría de Arousa, Spain. *Aquac. Reports*. 9:68–73

Cornelissen G. 2014. Cosinor-based rhythmometry. *Theor. Biol. Med. Model.* 11(1):1–24

Cubillo AM, Peteiro LG, Fernández-Reiriz MJ, Labarta U. 2012. Influence of stocking density on growth

of mussels (*Mytilus galloprovincialis*) in suspended culture. *Aquaculture*. 342–343:103–11

Davenport J, Chen X. 1987. A comparison of methods for the assessment of condition in the mussel (*Mytilus edulis* L.). *J. Molluscan Stud.* 53(3):293–97

de Winter NJ, Goderis S, Van Malderen SJM, Sinnesael M, Vansteenberge S, et al. 2020. Subdaily-Scale Chemical Variability in a *Torreites Sanchezi* Rudist Shell: Implications for Rudist Paleobiology and the Cretaceous Day-Night Cycle. *Paleoceanogr. Paleoclimatology*. 35(2):1–21

Derolez V, Bec B, Cimiterra N, Foucault E, Messiaen G, et al. 2021. OBSLAG 2020 - volet eutrophisation.Lagunes méditerranéennes (période 2015-2020). Etat DCE de la colonne d'eau et du phytoplancton, tendance et variabilité des indicateurs

Dinno A. 2017. dunn.test: Dunn's Test of Multiple Comparisons Using Rank Sums

Dunlap JC. 1999. Molecular bases for circadian clocks. *Cell*. 96(2):271–90

Fiandrino A, Serais O, Caillard E, Munaron D, Cimiterra N. 2021. Bulletin de la Surveillance de la Qualité du Milieu Marin Littoral 2020. Région Occitanie - Départements des Pyrénées Orientales, de l'Aude, de l'Hérault, du Gard. Languedoc-Roussillon

Filgueira R, Fernández-Reiriz MJ, Labarta U. 2009. Tasa de aclaramiento del mejillón *Mytilus galloprovincialis*. I. Respuesta a intervalos extremos de clorofila. *Ciencias Mar.* 35(4):405–17

Fox J, Weisberg S. 2019. *An R Companion to Applied Regression*. Thousand Oaks (CA): Sage. Third ed.

Gosling E. 2004. *Bivalve Molluscs: Biology, Ecology and Culture*. Oxford and Malden (Massachusetts)

Goto SG, Takekata H. 2015. Circatidal rhythm and the veiled clockwork. *Curr. Opin. Insect Sci.* 7:92–97

Gouthiere L, Claustrat B, Brun J, Mauvieux B. 2005a. Éléments méthodologiques complémentaires dans l'analyse des rythmes: Recherche de périodes, modélisation. Exemples de la Mélatonine plasmatique et de courbes de températures. *Pathol. Biol.* 53(5):285–89

Gouthiere L, Mauvieux B, Davenne D, Waterhouse & J. 2005b. Complementary methodology in the analysis of rhythmic data, using examples from a complex situation, the rhythmicity of temperature in night shift workers. *Biol. Rhythm Res.* 36(3):177–93

Häfker NS, Andreatta G, Manzotti A, Falciatore A, Raible F, Tessmar-raible K. 2023. Rhythms and Clocks in Marine Organisms. *Ann. Rev. Mar. Sci.* 15:13.1–13.30

Hallmann N, Burchell M, Schöne BR, Irvine G V., Maxwell D. 2009. High-resolution sclerochronological analysis of the bivalve mollusk *Saxidomus gigantea* from Alaska and British Columbia: techniques for revealing environmental archives and archaeological seasonality. *J. Archaeol. Sci.* 36(10):2353–64

Hart DR, Chute AS. 2009. Estimating von Bertalanffy growth parameters from growth increment data using a linear mixed-effects model, with an application to the sea scallop *Placopecten magellanicus* . *ICES J. Mar. Sci.* 66(10):2165–75

Hervé P, Bruslé J. 1980. L'étang de Salses-Leucate, écologie générale et ichtyofaune. *Vie Milieu*. 30:275–83

Hervé P, Bruslé J. 1981. L'étang de Canet-Saint-Nazaire (P.O.). Écologie générale et Ichthyofaune. *Vie Milieu*. 31(1):17–25

Huyghe D, Rafelis M De, Ropert M, Mouchi V, Emmanuel L, Renard M. 2019. New insights into oyster high - resolution hinge growth patterns. *Mar. Biol.* 166:48

Karayücel S, Çelik MY, Karayücel I, Öztürk R, Eyüboğlu B. 2015. Effects of stocking density on survival, growth and biochemical composition of cultured mussels (*Mytilus galloprovincialis*, Lamarck 1819) from an offshore submerged longline system. *Aquac. Res.* 46(6):1369–83

Komsta L. 2011. outliers: Tests for Outliers

Langlet D, Alunno-Bruscia M, Rafélis M, Renard M, Roux M, et al. 2006. Experimental and natural cathodoluminescence in the shell of *Crassostrea gigas* from Thau lagoon (France): Ecological and environmental implications. *Mar. Ecol. Prog. Ser.* 317:143–56

Lê S, Josse J, Husson F. 2008. FactoMineR: An R Package for Multivariate Analysis. *J. Stat. Softw.* 25(1):1–18

Louis V, Besseau L, Lartaud F. 2022. Step in Time : Biomineralisation of Bivalve's Shell. *Front. Mar. Sci.* 9:906085

Lutz RA, Rhoads DC. 1977. Anaerobiosis and a Theory of Growth Line Formation. *Science (80-.).* 198(4323):1222–27

Maire O, Amouroux JM, Duchêne JC, Grémare A. 2007. Relationship between filtration activity and food availability in the Mediterranean mussel *Mytilus galloprovincialis*. *Mar. Biol.* 152(6):1293–1307

Mat AM, Charles J, Ciret P, Tran D. 2014. Looking for the clock mechanism responsible for circatidal behavior in the oyster *Crassostrea gigas*. *Mar. Biol.* 161:89–99

Mat AM, Massabuau JC, Ciret P, Tran D. 2012. Evidence for a plastic dual circadian rhythm in the oyster *Crassostrea gigas*. *Chronobiol. Int.* 29(7):857–67

Météo-France. 2020. *Les vents régionaux*. https://meteofrance.com/comprendre-la-meteo/le-vent/les-vents-regionaux

Mirzaei MR, Shau-Hwai AT. 2016. Assessing cockle shells (*Anadara granosa*) for reconstruction subdaily environmental parameters: Implication for paleoclimate studies. *Hist. Biol.* 28(7):896–906

Monaco CJ, McQuaid CD. 2018. Applicability of Dynamic Energy Budget (DEB) models across steep environmental gradients. *Sci. Rep.* 8(1):16384

Moran AL, Marko PB. 2005. A simple technique for physical marking of larvae of marine bivalves. *J. Shellfish Res.* 24(2):567–71

Nedoncelle K, Lartaud F, de Rafelis M, Boulila S, Le Bris N. 2013. A new method for high-resolution bivalve growth rate studies in hydrothermal environments. *Mar. Biol.* 160(6):1427–39

Nedoncelle K, Lartaud F, Pereira LC, Yücel M, Thurnherr AM, et al. 2015. Bathymodiolus growth dynamics in relation to environmental fluctuations in vent habitats. *Deep. Res. Part I*. 106:183–93

Nelson W, Tong YL, Lee JK, Halberg F. 1979. Methods for cosinor-rhythmometry. *Chronobiologia*. 6(4):305–23

Orban E, Di Lena G, Nevigato T, Casini I, Marzetti A, Caproni R. 2002. Seasonal changes in meat content, condition index and chemical composition of mussels (*Mytilus galloprovincialis*) cultured in two different Italian sites. *Food Chem.* 77:57–65

Payton L, Tran D. 2019. Moonlight cycles synchronize oyster behavior. *Biol. Lett.* 15: 20180299

Peharda M, Black BA, Purroy A, Mihanović H. 2016. The bivalve *Glycymeris pilosa* as a multidecadal

environmental archive for the Adriatic and Mediterranean Seas. *Mar. Environ. Res.* 119:79–87

Peharda M, Župan I, Bavčević L, Frankić A, Klanjšček T. 2007. Growth and condition index of mussel *Mytilus galloprovincialis* in experimental integrated aquaculture. *Aquac. Res.* 38(16):1714–20

Pérez-Ruzafa A, Pérez-Ruzafa IM, Newton A, Marcos C. 2019. Chapter 15: Coastal Lagoons: Environmental Variability, Ecosystem Complexity, and Goods and Services Uniformity. In *Coasts and Estuaries: The Future*, eds. E Wolanski, JW Day, M Elliot, R Ramachandran, pp. 253–76. Elsevier

Peterson CH. 1985. Patterns of Lagoonal Bivalve Mortality After Heavy Sedimentation and Their Paleoecological Significance. *Paleobiology*. 11(2):139–53

Posa D, Tursi A. 1991. Growth Models of *Mytilus galloprovincialis* Lamarck on the mar grande and on the mar Piccolo of Taranto (Southern Italy). *Stat. Appl*. 3:135–43

Purroy A, Milano S, Schöne BR, Thébault J, Peharda M. 2018. Drivers of shell growth of the bivalve, *Callista chione* (L. 1758) – Combined environmental and biological factors. *Mar. Environ. Res.* 134:138–49

R Core Team. 2020. R: A Language and Environment for Statistical Computing

Ramón M, Fernández M, Galimany E. 2007. Development of mussel (*Mytilus galloprovincialis*) seed from two different origins in a semi-enclosed Mediterranean Bay (N.E. Spain). *Aquaculture*. 264(1–4):148–59

Richardson CA. 1987. Tidal bands in the shell of the clam *Tapes philippinarum* (Adams & Reeve, 1850). *Proc. R. Soc. Lond. B.* 230(1260):367–87

Richardson CA. 1988. Exogenous and endogenous rhythms of band formation in the shell of the clam *Tapes philippinarum* (Adams et Reeve, 1850). *J. Exp. Mar. Bio. Ecol.* 122(2):105–26

Richardson CA. 1989. An analysis of the microgrowth bands in the shell of the common mussel *Mytilus edulis*. *J. Mar. Biol. Assoc. United Kingdom*. 69(2):477–91

Richardson CA, Crisp DJ, Runham NW. 1980. An endogenous rhythm in shell deposition in *Cerastoderma edule*. *J. Mar. Biol. Assoc. United Kingdom*. 60(4):991–1004

Rodellas V, Cook PG, McCallum J, Andrisoa A, Meulé S, Stieglitz TC. 2020. Temporal variations in porewater fluxes to a coastal lagoon driven by wind waves and changes in lagoon water depths. *J. Hydrol.* 581:124363

Rodellas V, Stieglitz TC, Andrisoa A, Cook PG, Raimbault P, et al. 2018. Groundwater-driven nutrient inputs to coastal lagoons: The relevance of lagoon water recirculation as a conveyor of dissolved nutrients. *Sci. Total Environ.* 642:764–80

Ruf T. 2022. lomb: Lomb-Scargle Periodogram

Sachs M. 2014. cosinor: Tools for estimating and predicting the cosinor model

Schöne BR. 2008. The curse of physiology — challenges and opportunities in the interpretation of geochemical data from mollusk shells. *Geo-Marine Lett.* 28:269–85

Schöne BR, Dunca E, Fiebig J, Pfeiffer M. 2005a. Mutvei ' s solution : An ideal agent for resolving microgrowth structures of biogenic carbonates. *Palaeogeogr. Palaeoclimatol. Palaeoecol.* 228:149–66

Schöne BR, Pfeiffer M, Pohlmann T, Siegismund F. 2005b. A seasonally resolved bottom-water temperature record for the period AD 1866-2002 based on shells of *Arctica islandica* (Mollusca,

North Sea). *Int. J. Climatol.* 25(7):947–62

Schöne BR, Tanabe K, Dettman D, Sato S. 2003. Environmental controls on shell growth rates and d 18 O of the shallow-marine bivalve mollusk *Phacosoma japonicum* in Japan. *Mar. Biol.* 142:473–85

Seed R, Suchanek TH. 1992. Population and community ecology of Mytilus. In *The Mussel Mytilus: Ecology, Physiology, Genetics and Culture*, ed. E Gosling, pp. 87–169. Elsevier ed.

Shah AS. 2020. card: Cardiovascular and Autonomic Research Design

Souchu P, Bee B, Smith VH, Laugier T, Fiandrino A, et al. 2010. Patterns in nutrient limitation and chlorophyll a along an anthropogenic eutrophication gradient in French Mediterranean coastal lagoons. *Can. J. Fish. Aquat. Sci.* 67(4):743–53

Tanaka K, Okaniwa N, Miyaji T, Murakami-Sugihara N, Zhao L, et al. 2019. Microscale magnesium distribution in shell of the Mediterranean mussel *Mytilus galloprovincialis*: An example of multiple factors controlling Mg/Ca in biogenic calcite. *Chem. Geol.* 511:521–32

Thébault J, Chauvaud L, Clavier J, Fichez R, Morize E. 2006. Evidence of a 2-day periodicity of striae formation in the tropical scallop *Comptopallium radula* using calcein marking. *Mar. Biol.* 149(2):257–67

Tran D, Perrigault M, Ciret P, Payton L. 2020. Bivalve mollusc circadian clock genes can run at tidal frequency. *Proc. R. Soc. B*. 287:20192440

von Bertalanffy L. 1938. A quantitative theory of organic growth. *Hum. Biol.* 10(2):181–213

Walford LA. 1946. A new graphic method of describing the growth of animals. *Biol. Bull.* 90(2):141–47

Warnes GR, Bolker B, Bonebakker L, Gentleman , Robert Huber W, Liaw A, et al. 2020. gplots: Various R Programming Tools for Plotting Data

Supplementary Data - A possible joint role of the environment and potential biological clock(s) in shell growth patterns formation of the Mediterranean mussel, *Mytilus galloprovincialis*.

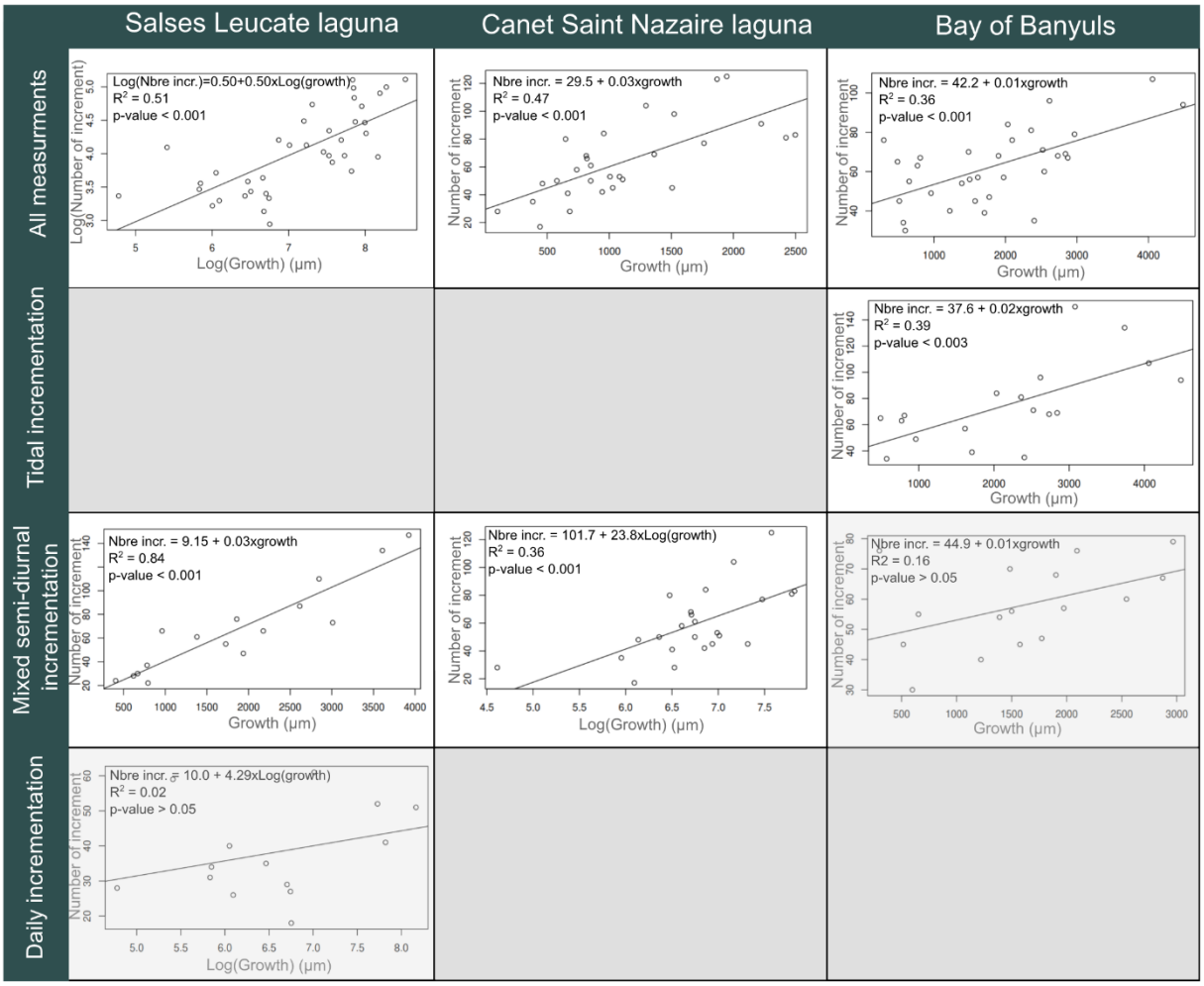

Figure S1: Number of increments formed depending on the growth. All values were first used to reconstruct linear regression in the three studied locations. Then, subsets were made based on the periodicity of incrementation observed (*i.e.*, tidal, daily or following mixed semidiurnal tidal regime of the region). Non-significant regressions are shaded in grey.

Table S1: Significant frequencies observed in increment width variations in shells of mussels.

	>100]	[90->99]	[80->89]	[70->79]	[60->69]	[50->59]	[40->49]	[30->39]	[20->29]	[10->19]
SL0601				76			41		27	
SL0602	112			70			43	33	24	
SL0603	155	93					46			12
SL0612			86					39		
SL0618					60				23	
SL0620			89							
SL0623	139					56			20	
SL0626	125				63		48		21	18
CSN0601	107						41		23	
CSN0602						58	46	31		16
CSN0606								39-32		
CSN0609			81				47	38		
CSN0610	117				65		49			
CSN0611	138	92		79					20	
CSN0614		91				50		32		
CSN0617				79		50	42		28	16
SOLA0602	154									17-15
SOLA0603	193			77						
SOLA0605	109				66					17
SOLA0606	120			76						18
SOLA0607	171		85			57			21	
SOLA0608	168					56			26	
SOLA0609	138		83			52		38		
SOLA0618			82		66		47-41			
SOLA0622						55				
SOLA0623	185				62		46	37		19
SOLA0624	150			75		50	41			

Table S2: Salses-Leucate laguna environmental variables averaged per month. Wind data were retrieved from the station "Perpignan" at the French meteorological service (Météo France). The other environmental variables were provided by the Pôle-relais lagunes méditerranéennes and the FILMED network.

Month	T (°C)	Salinity	Wind Speed (m/s)	pH	Water levels (m)	Chl *a* (µg/L)
07/20	23.67	31.63	4.72	8.64	3	0.70
08/20	24.32	32.9	4.05	8.54	0	0.55
09/20	20.70	36.38	4.51	8.22	4	0.53
10/20	14.71	37.16	4.32	8.21	4	0.55
11/20	13.13	31.1	3.34	7.95	3	0.90
12/20	7.81	32.75	4.40	8.21	2	0.75
01/21	5.56	32.05	5.14	8.2	-1	1.1
02/21	10.98	34.17	3.88	8.05	5	0.9
03/21	11.46	34.68	4.74	8.14	-1	0.9
04/21	14.50	30.32	4.11	8.39	4	1.0
05/21	18.08	36.99	4.42	8.48	-2	0.9
06/21	23.56	34.73	4.42	8.39	6	0.7

Table S3: **Canet-Saint-Nazaire laguna environmental variables averaged per month**. Wind data were retrieved from the station "Perpignan" at the French meteorological service (Météo France). The other environmental variables were provided by the Pôle-relais lagunes méditerranéennes and the FILMED network.

Month	T (°C)	Salinity	Wind speed (m/s)	pH	O_2 (ml/L)
07/20	25.87	24.91	4.72	8.04	6.83
08/20	24.24	35.54	4.05	8.24	8.01
09/20	20.17	36.37	4.51	8.13	7.85
10/20	14.58	35.37	4.32	8.21	9.23
11/20	12.63	32.71	3.34	8.32	10.10
12/20	7.78	29.21	4.40	8.19	10.56
01/21	6.53	27.39	5.14	8.31	11.62
02/21	11.12	30.95	3.88	8.15	9.67
03/21	12.04	28.78	4.74	8.26	9.47
04/21	14.31	34.84	4.11	8.33	9.75
05/21	18.05	33.96	4.42	8.24	8.83
06/21	23.76	38.97	4.42	8.11	7.69

Table S4: Environmental variables averaged per month at sea. Wind data were retrieved from the station "Perpignan" at the French meteorological service (Météo France). Others data were extracted from the SOMLIT database.

Month	T (°C)	Salinity	Chl *a* (µg/L)	Wind speed (m/s)	O_2 (ml/L)	pH
07/20	21.57	37.74	0.18	4.72	5.19	8.04
08/20	22.22	38.02	0.16	4.05	4.99	8.03
09/20	19.55	37.94	0.32	4.51	5.14	7.98
10/20	16.73	38.05	0.69	4.32	5.37	7.92
11/20	15.80	37.52	1.63	3.34	5.60	7.97
12/20	14.74	37.83	0.79	4.40	5.49	7.95
01/21	13.60	37.64	1.04	5.14	5.91	7.93
02/21	11.81	36.56	0.85	3.88	5.91	7.91
03/21	12.47	36.67	1.1	4.74	6.19	8.12
04/21	13.30	37.88	0.81	4.11	6.06	8.14
05/21	14.91	37.85	0.85	4.42	5.82	8.19
06/21	20.02	37.44	0.42	4.43	5.33	7.99

2. Review of additional technics for the sclerochronological analysis of *Mytilus galloprovincialis* shells

Foreword

Among technics used to observe growth patterns in calcified tissues, both on the outer and the inner part of shells, Mutvei etching (Schöne et al., 2005) is classically used on sections of mussel shells (Andrisoa et al., 2019; Tanaka et al., 2019; Vriesman et al., 2022). However, this technic showed some limits as demonstrated in the chapter 1.1, in which we illustrated that shell growth patterns were not always readable on large portions of *M. galloprovincialis* shells. Moreover, ultradian units of time called micro-increments were described in shells of several bivalves (Yamaguchi et al., 2006; Huyghe et al., 2019; Louis et al., 2022) and not seen here for *M. galloprovincialis*. The mechanisms involved in their production remain unclear. It could be linked to intrinsic mechanisms (*i.e.*, guided by physiological and/or genetic factors) or directly by the environment (Rodland et al., 2006; Yan et al., 2020). In this part of the work, we aimed at improving the readability of growth patterns in the shell of *M. galloprovincialis* and increasing the temporal resolution of the observations, to detect the presence or not of those micro-increments. To achieved it, three techniques previously used on other species were tested, the cathodoluminescence (CL), the Laser Scanning Confocal Microscope (LSCM) and semithin sections observed with transmitted light microscope.

In the oyster *M. gigas*, cathodoluminescence is a reliable technique to observe daily and tidal increments (Langlet et al., 2006; Barbin et al., 2008; Barbin, 2013; Huyghe et al., 2019). The CL phenomenon results from the interactions between a light-emitting center (chemical element or impurity) and the atomic environment inside the crystal lattice during excitation by an electron gun (Machel et al., 1991; Barbin and Schvoerer, 1997). In calcite, CL emission (~620 nm) is mainly due to the presence of Mn^{2+} trapped into the lattice during mineral growth (El Ali et al., 1993; de Rafélis et al., 2000). Enrichment of the water in Mn^{2+} produces more luminous mark that can be used as calibrator in time (Lartaud et al., 2010). But to our knowledge mussel shells were never observed under CL microscopy.

Autofluorescence in shells can be detected directly on shell sections with an epifluorescent microscope, using the conditions for calcein observation (*i.e.*, emission in blue light at 495 nm and observation in green at 515 nm) (Mahé et al., 2010). But classically for bivalve shells, the autofluorescence is weak avoiding a direct lecture of such growth increments. Good results were

obtained using LSCM on the shell of *Tridacna* ssp. (Yan et al., 2020). Using this technique, autofluorescence is observed more accurately leading to the identification of growth lines of which the brightness could be related to extreme weather events such tropical cyclones.

Semithin sections made on decalcified shells of *M. edulis* revealed also shell growth patterns, however due to decalcification time (*e.g.*, seven days), this technique is sparse in the literature (Richardson, 1989). Recently, semithin sections were used on multiple bivalves species in order to describe the form and the function of the mantle edge in Protobranchia (Salas et al., 2022). Shell growth patterns are observable due to transparency differences between growth lines and increments.

Materials and methods

Shell preparation

Mussels were collected in the Bay of Banyuls (SOLA buoy) and at the Salses-Leucate laguna. Thin sections of 0.5 mm of shells were prepared and mounted on microscopic slides as described in the chapter 1.1. They were used for LSCM and cathodoluminescence analysis.

Cathodoluminescence

One shell section from SOLA was imaged using CL imaging, following the protocol applied on the oyster *M. gigas* (Lartaud et al., 2010; Huyghe et al., 2020). Slides were observed with a cold cathode (Cathodyne-OPEA, 15–20 kV and 200–400 µA mm−2 under a pressure of 0.05 Torr) to reveal the natural luminescence variability in the shells. A Nikon D5000 (1400 ASA) camera (Nikon, Tokyo, Japan) was used for luminescence image acquisition.

LSCM analysis

Three mussel shells were imaged, one from SOLA and two from Salses-Leucate laguna. Images of 40x magnification (z-stack) were produced on a Leica SP8 Laser Scanning Confocal Microscope (LSCM) (Leica Microsystems, Wetzlar, Germany). Laser excitation at a wavelength from 488 to 502 nm triggered auto-fluorescence of the fluorescent organic material incorporated in the calcite lattice with emission detection at 500 to 550 nm, following the protocol of Yan et al. (2020). Images were processed using the software Image J (Rasband, 2020) and compared with the growth patterns observed using Mutvei etching and reflected light.

Semithin section

A piece (3 mm x 2mm) of the posterior edge of the shell was sampled and embedded in Epon® resin. Prior to embedding, shell was dehydrated in a graded ethanol series (50, 70, 95, 100 %) for 5 min and finally a mixed solution of ethanol 100% and propylene oxide (50:50, 10 min) followed a pure solution of propylene oxide (10 min). The embedding was achieved using successive dilutions of propylene oxide in Epon® (3/4, 1/2, 1/4). Shell pieces were embedded in pure Epon® for 40 min in a vacuum. The piece of shell was placed in a mold for 3 hours prior to a polymerisation of 48h at 60°C. Semithin sections (1 µm) were obtained with a diamond blade on a Leica Ultracut R microtome (Leica Microsystems, Wetzlar, Germany). Sections were visualised under an AxioPlan 2 (Zeiss, Oberkochen, Germany) imaging microscope equipped with a camera ProgRes® CF^{cool} (Jenoptik, Jena, Germany). Slides were also observed using an epifluorescent microscope (Olympus BX61, Olympus Corporation, Tokyo, Japan) by exciting the fluorochrome with a blue light at 495 nm, and collecting the calcein emitted signal at 515 nm (green).

Results

Cathodoluminescence

The periostracum showed a bit of luminescence in red (Figure 20A-B). The main part of the shell did not display clear luminescence (dark blue in the outer layer and dark green in the inner layer) (Figure 20A). Some fine lines were slightly discernible in the outer shell layer, closer to the periostracum, but no clear increment (Figure 20A). None increment was observed in the aragonite inner shell layer, both along the shell and in the hinge (Figure 20B). Micro-increments could not be observed.

LSCM analysis

Growth patterns were visible in mussels using an excitation at 502 nm instead of 488 nm (*i.e.*, wavelength used in Yan et al. (2020)). None increment was detectable on the shell coming from SOLA. At Salses-Leucate laguna, increments were observable on both shells, but less marked than samples treated with Mutvei etching. On shell Leu92, 26 increments were counted on LSCM image (Figure 21A) rather than 42 on Mutvei etched slide (Figure 21B). The confocal imaging on the shell Leu97 showed 14 increments (Figure 21C) whereas 33 increments were counted on the Mutvei etched slide (Figure

21D). On both images taken using LSCM, faint perpendicular lines to growth lines were observed. No micro-increment was observed both under LSCM and Mutvei etching.

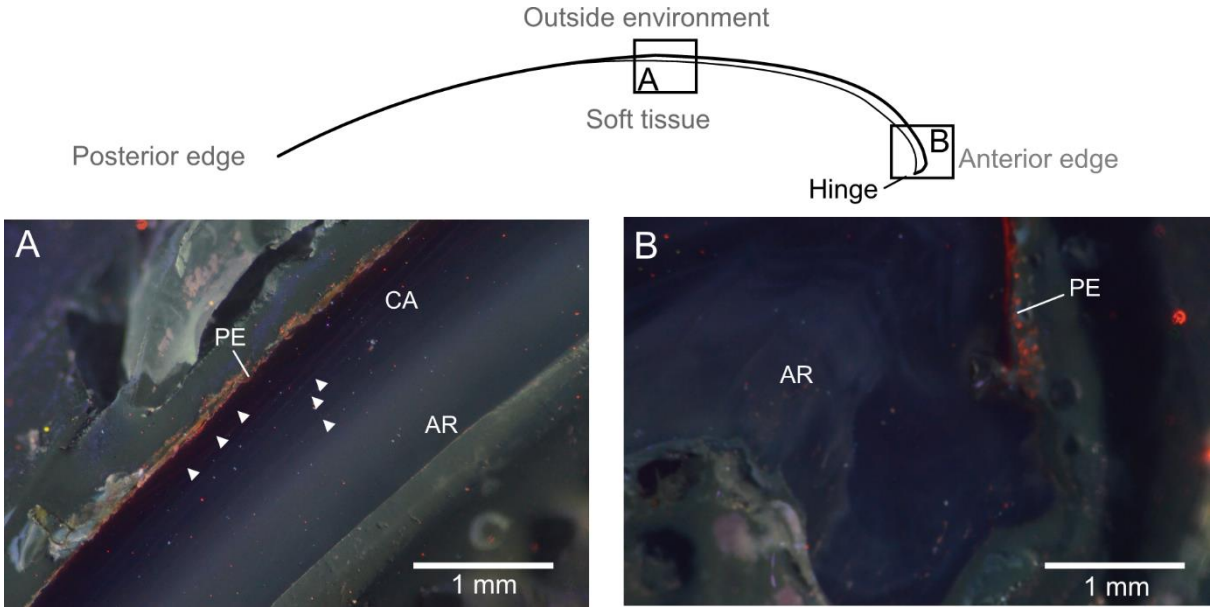

Figure 20: Shell section of *Mytilus galloprovincialis* observed using cathodoluminescence microscopy. A) Faints red lines were observed in the outer calcite layer (CA) of *M. galloprovincialis* (white arrows). The periostracum (PE) showed red luminescence. B) Hinge section of the shell made of aragonite (AR), luminescence was observed only in the periostracum.

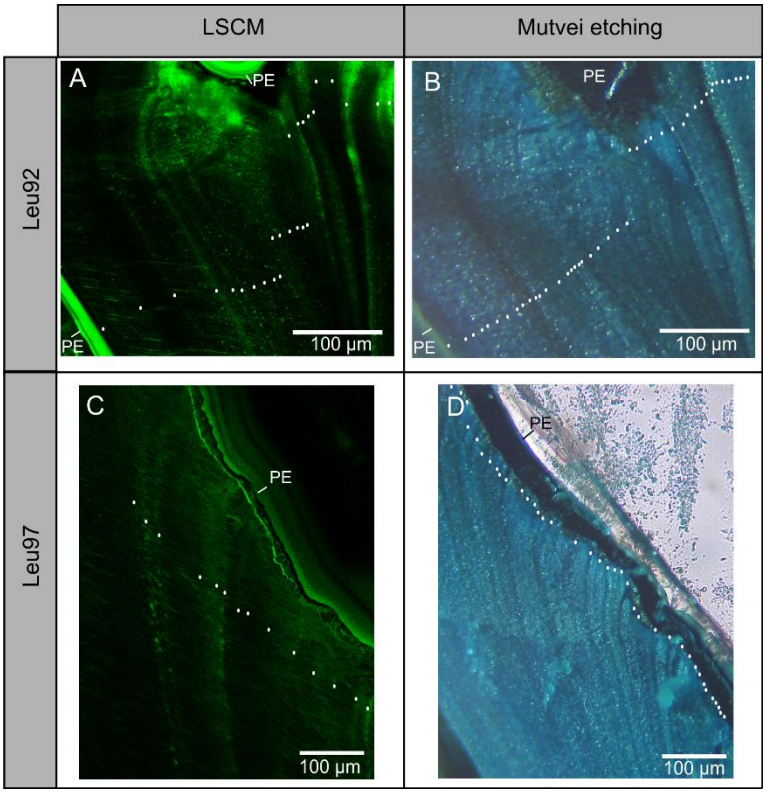

Figure 21: Comparison of LSCM imaging and Mutvei etched sections observed under reflected light on *Mytilus galloprovincialis* shell section. White dots are the growth lines A) Section of the mussels Leu92 observed under LSCM microscope. B) Mutvei etched sections of the mussels Leu92 observed under reflected light. C) Section of the mussels Leu97 observed under LSCM microscope. B) Mutvei etched sections of the mussels Leu97 observed under reflected light.PE: periostracum

Semithin section

The periostracum was successfully cut whereas the rest of the shell could not be cut. Therefore, increments and micro-increments could not be observed. Observation of the periostracum under transmitted light showed two layers. The above layer, also called periostracal lamina (PL), was coloured in pink (Figure 22A) and the bottom layer, or fibrous matrix (FM), displayed alveolate white tissues. The fluorescence microscopy revealed that the periostracum autofluorescence is mostly related to the bottom layer (Figure 22B).

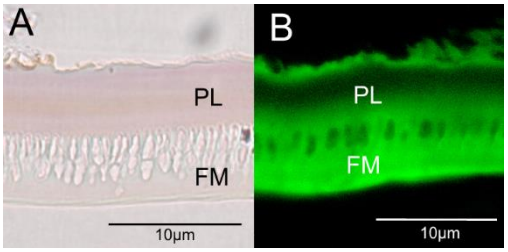

Figure 22: Semithin section of the periostracum of *Mytilus galloprovincialis*. A) Under photonic microscope the periostracum showed two layers, the pink external is the periostracal lamina (PL) and bellow it is the fibrous matrix (FM). B) Under epifluorescent microscope, only the fibrous matrix showed autofluorescence.

Discussion

In chapter 1.1, it has been showed that the readability of patterns can be difficult reducing the number of shells suitable for sclerochronological analysis. Different methods were tested to improve the readability of the increments in *M. galloprovincialis* shells, increasing by the way the dataset. Another aim of improving the lecture of the growth patterns of shell was to detect and analyse micro-increments.

The LSCM imaging showed contrasted results. Growth patterns were visible in shells from Salses-Leucate laguna whereas none was observed in the shell from the bay of Banyuls. However, only one sample was tested in the last location. Additionally, the number of increments counted with this technic was lower than the number of increments visible using Mutvei etching of the shell. We conclude that the quality of revelation of lines with LSCM imaging was lower compared to the Mutvei treatment. Therefore, LSCM is less suitable than the Mutvei method to observe shell growth patterns in *M. galloprovincialis*. The LSCM technic was first used on the shell of *Tridacna* ssp., revealing daily growth bands clearly identified in the aragonite structure (Yan et al., 2020). Those authors also showed a coupling between light intensity of growth patterns and the elemental ratio (*i.e.*, Sr/Ca and Fe/Ca), measured via NanoSIMS analysis. Peaks of fluorescence intensity was related to weather extreme events such as tropical cyclones, marine phytoplankton bloom events and cold surges. Although the control of the integration of Sr^{2+} ions in shells is still under discussion, the Sr/Ca ratio is often related

to sea surface temperature and/or influence of the shell growth rate and the metabolic rate (Otter et al., 2019). The Fe/Ca ratio has been related to changes in redox conditions, linked to phytoplankton bloom (Bruland et al., 2001; Gao et al., 2009; de Winter and Claeys, 2017). The environments studied in this work (*i.e.*, Mediterranean Sea and laguna) might be more buffered than subtropical waters, reducing the readability of shell growth patterns. Also, the difference in pattern readability between species could be linked to the microstructure of the shell. *Tridacna* has a shell made of crossed-lamellar aragonite (Lin et al., 2006) whereas *M. galloprovincialis* outer layer is fibro-prismatic calcite (Checa et al., 2014). The perpendicular lines to growth increments observed might be the microstructure that overlap.

Using cathodoluminescence (CL), pure calcite should have a weak dark-blue luminescence and the presence of Mn^{2+} in the calcite lattice would be yellow to orange-red brighter luminescence (Barbin, 2000). The CL images showed dull blue luminescence in the outer calcite layer with some rare fine lines, nearby the periostracum, difficult to reveal. In aragonite material, emission should be in green to yellow due to the crystallographic environment (Barbin, 2000). The bottom aragonite layer turns to be dull green compared to the outer calcite layer, but no increment can be seen. Surprisingly, the hinge region did not show luminescence, or rather a dark blue luminescence as in the outer calcite areas. The luminescence is known to be principally due to the presence of Mn^{2+} that substituted Ca^{2+} ions (Barbin, 2000). The amount of Mn^{2+} incorporated in shells is primarily related to the metabolic activity and then to the environment of the bivalve (*i.e.*, water chemistry, temperature and depth). Therefore, the incorporation of manganese ion in shells is probably different in function of the species and/or the type of environment. In the oyster *M. gigas* this technic is widely used and well suited for growth patterns analysis for both Atlantic and Mediterranean specimens (Langlet et al., 2006; Lartaud et al., 2010; Huyghe et al., 2019). In the Atlantic mussel *M. edulis*, variations in the Mn/Ca ratio were observed but could not be related to shell growth rate or incrementation (Freitas et al., 2009). In Mediterranean mussels the CL did not show clear growth patterns, therefore Mutvei etching remains the more appropriate method.

Semithin sections successfully showed the composition of the periostracum, divided into two layers (Paillard and Maes, 1995). The most external, called periostracal lamina, was slightly colored and might be richer in pigments. Below it, the white alveolate layer observed is the fibrous matrix. But as this technique totally disintegrated the calcified parts while cutting, we recommend to avoid using it for shell growth pattern analysis. A preparatory light decalcification step in EDTA is probably necessary to observe growth patterns in shells using this technic. This was previously done by Richardson (1989) to observed growth patterns in *M. edulis*, growth lines which are richer in organic material appeared darker than the increments.

In conclusion, among the three additional technics tested on *M. galloprovincialis* shells in order to improve the readability of shell patterns, none gave successful results and, in our hands, Mutvei etching remained the best method. Subsequently, micro-increments were never observed. Other technics could be tested such the laser-ablation inductively-coupled-plasma mass spectrometry (LA-ICPMS), which allowed spatial geochemical analysis on thin cut of shells (Warter and Müller, 2017). Two others technics, profilometry and microtomography are currently tested within the framework of the MITI interdisciplinary program “ARCHIVE” project (see Annex 1).

Chapter 2: Biomineralisation of *Mytilus galloprovincialis* shell and biological clocks

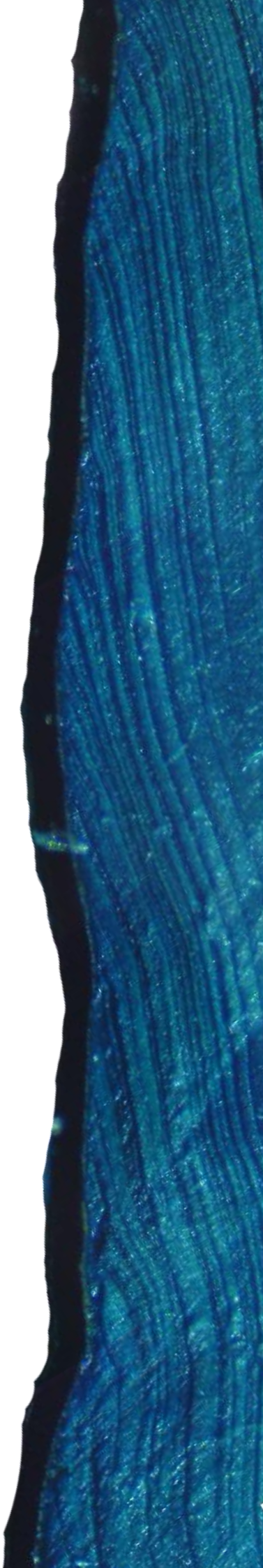

Preamble

Chapter 2 is focused on the identification of the biological clock and on its possible output, the mussel's behaviour. Hypothesis related to the periodic formation of increment in *M. galloprovincialis* shell were further investigated.

First, genetic biomarkers used in this study were chosen and their sequences retrieved by blasting known sequences of close-related species on sequence reads archives of *M. galloprovincialis*. Targeted genes were core genes of the canonical biological clock, genes known to be related to biological clocks and genes related to the biomineralisation process. Gene expressions was then characterised in the mantle of mussels using *in situ* hybridisation. In a second research article, gene expression of this set of genes was followed over time using NanoString technology. Measurements of gene expressions were taken at sea and in controlled environment *via* in aquaria experiments, where the role of photoperiod and food availability as zeitgeber of biological clocks and/or biomineralisation was tested. Finally, shell growth patterns and behaviour were recorded under crossed targeted environmental conditions. As the NanoString technology is rarely used in chronobiological study in molluscs, we compared it to the qPCR method which is commonly used to validate this choice for further studies.

1. Identification of *Mytilus galloprovincialis* biomarkers involved in biomineralisation and biological clocks

Foreword

One aim of this PhD work was to analyse the spatio-temporal gene expression variations of specific genes in order to explore the hypothesis of a control of the biomineralisation process by biological clocks. Genes expression variability was assessed i) temporally, through successive mussel tissues samplings (every 4 hours over 32 h) and ii) spatially, through *in situ* hybridisation (ISH) of transcripts in the mantle tissue. Twenty-four genes were targeted: *i.e.*, 9 genes related to potential biological clocks, 10 others associated to biomineralisation and 5 housekeeping genes. No genomic data was available at the beginning of this study and most targeted mRNA sequences were not available for the species *M. galloprovincialis*. Therefore, the mRNA sequences selected either for the potential biological clocks or for biomineralisation related genes were based on close-related species known sequences and read archives retrieved of *M. galloprovincialis* from NCBI. Targeted genes were all confirmed using the later annotated genome of *M. galloprovincialis* (Gerdol et al., 2020).

Materials and methods

To build the targeted mRNA sequences for *M. galloprovincialis*, a basic alignment search tool (BLASTn on Genbank) was used on sequence read archives (accession number SRX1240182) of the targeted species using known sequences of close-related species available on Genbank. Contigs obtained were aligned and collapsed into one sequence using the software BioLign v.2.0.9 (Hall, 2001). The validity of the sequence was assessed by a BLAST on nucleotide and transcript sequences databases in GenBank. Finally, maximum likelihood trees (Nei and Kumar, 2000) were made based on amino acid sequences using the JTT model (Jones et al., 1992) with a gamma distribution as implemented in the software Mega X (Kumar et al., 2018). The statistical robustness of relationships was assessed using bootstrap method with 1000 replicates.

In 2020, a partially annotated assembled genome of *M. galloprovincialis* was released (CGA_900618805.1, Gerdol et al., 2020) and sequences were blasted on it (*i.e.*, blastx) for cross-validation. When the translated contig was matching with a hypothetical protein in the genome, a

research of conserved domains on pfam database was done using the NCBI Conserved Domain Search Service (Yang et al., 2020).

Results and discussion

Potential core biological clock genes

The biological clock is a conserved molecular mechanism that has been described in prokaryotes and eukaryotes (Dunlap, 1999). It is composed of simple or coupled transcription and translation feedback loops (TTFL) although genes composing the TTFL slightly varies. Molecular biological clock has been first characterised in *Drosophila melanogaster* with the isolation and functional description of the PER protein (Reddy et al., 1984; Hardin, 1994; Zeng et al., 1994) (Figure 23A). Later the clock

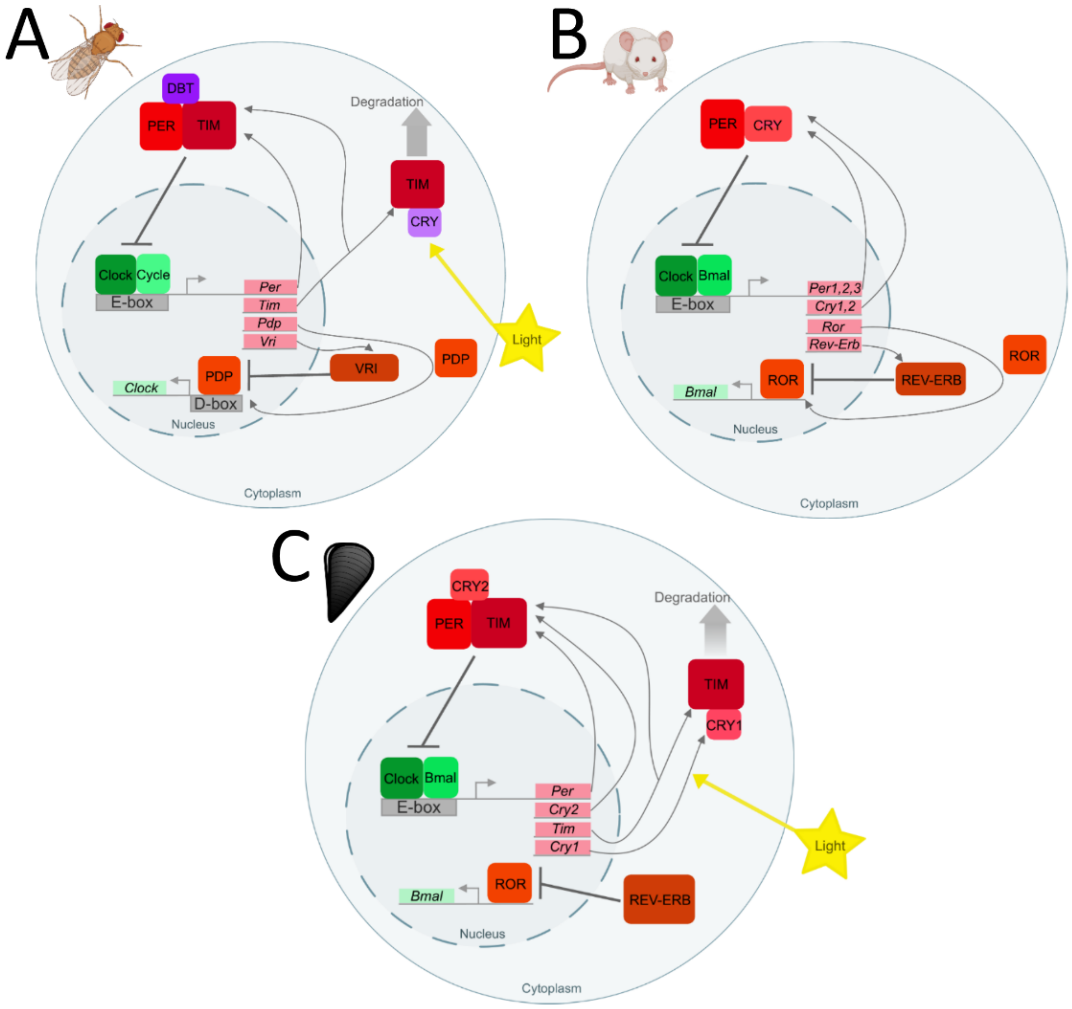

Figure 23: Schematic representation of molecular clocks in different species. A) Simplified molecular clockwork in *Drosophila melanogaster*. B) Simplified in molecular clockwork in mammals C) Hypothetical molecular clockwork in oyster *Magallana gigas*. Adapted from A) Zordan and Sandrelli (2015), B) Emery and Reppert (2004), C)Perrigault and Tran (2017).

gene *Timeless* (*Tim*) has been identified in the same species and TIM protein has been showed to heterodimerizes with PER (Gekakis et al., 1995; Myers et al., 1995). Proteins CLOCK and CYCLE were later identified and described as forming a heterodimer that binds to an E-box activating the transcription of *Per* and *Tim* in drosophila (Hao et al., 1997; Darlington et al., 1998). The dimer PER:TIM has been shown to inhibit the binding of CLOCK:CYCLE on the E-Box, repressing their own transcription and ensuring that the cycle last 24 hours. DOUBLETIME (DBT) is a regulator of the PER phosphorylation and accumulation (Price et al., 1998). CRYPTOCHROME (CRY) has been shown to be the primary circadian photoreceptor (Emery et al., 1998). CRY binds to TIM leading to its degradation and have a role of entrainment of the clock by the light (Busza and Emery, 2004). A coupled feedback loop composed of VRILLE and PDP regulate the transcription of *Clock* (Cyran et al., 2003; Glossop et al., 2003). In mammals the orthologs CLOCK and BMAL were described as the activator of the transcription

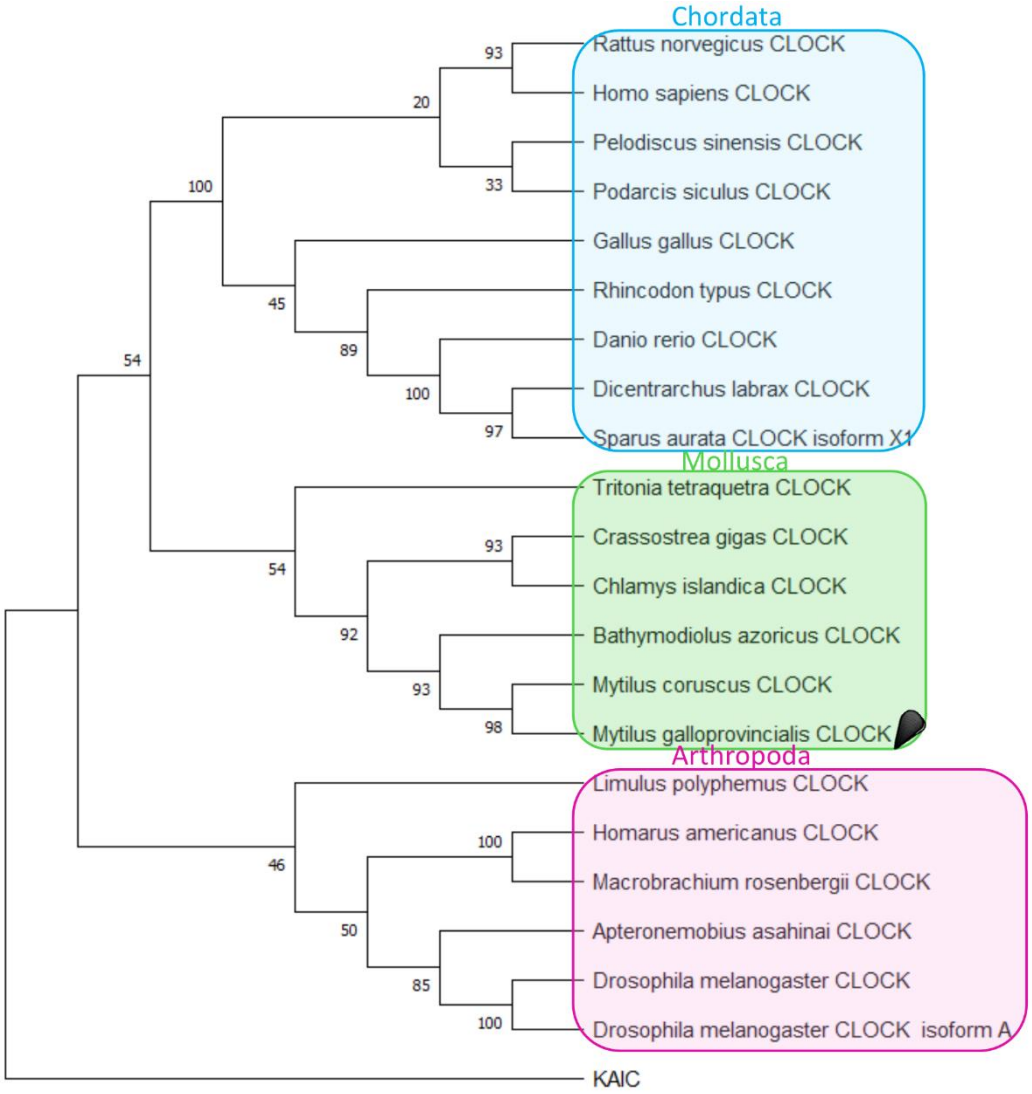

Figure 24: Phylogenetic tree based on CLOCK sequences. The tree was generated using the maximum likelihood method and the JTT matrix-based model and the gamma distribution. Percentage of bootstraps were based on 1 000 replicates.

of three *Periods* (*Per1*, *Per2* and *Per3*) and two *Cryptochromes* (*Cry1* and *Cry2*) (reviewed in Hardin and Panda, 2013) (Figure 23B). Mammals CRY has the function of drosophila TIM in the TTFL. The coupled feedback loop is composed of the nuclear hormone receptor ROR and REV-ERB that regulate the transcription of *Bmal*.

Potential core molecular actors of the biological clock have been already identified in multiples bivalves such as oyster (Perrigault and Tran, 2017), clam (Perrigault et al., 2020), blue mussel (Chapman et al., 2017, 2020) and deep-sea mussel (Mat et al., 2020). Based on gene expression, Perrigault and Tran (2017) proposed an hypothetical molecular clockwork in the oyster *M. gigas*. Similarly to drosophila, a trimer is formed constituted in case of oysters of PER:TIM:CRY2 (Figure 23C). CRY1 is here regulating the degradation of the dimer or trimer through its interaction with TIM and has a role in the entrainment of the clock by the light (Chaves et al., 2011; Mat et al., 2016). However functional analyses are required to characterise the biological clock in bivalves.

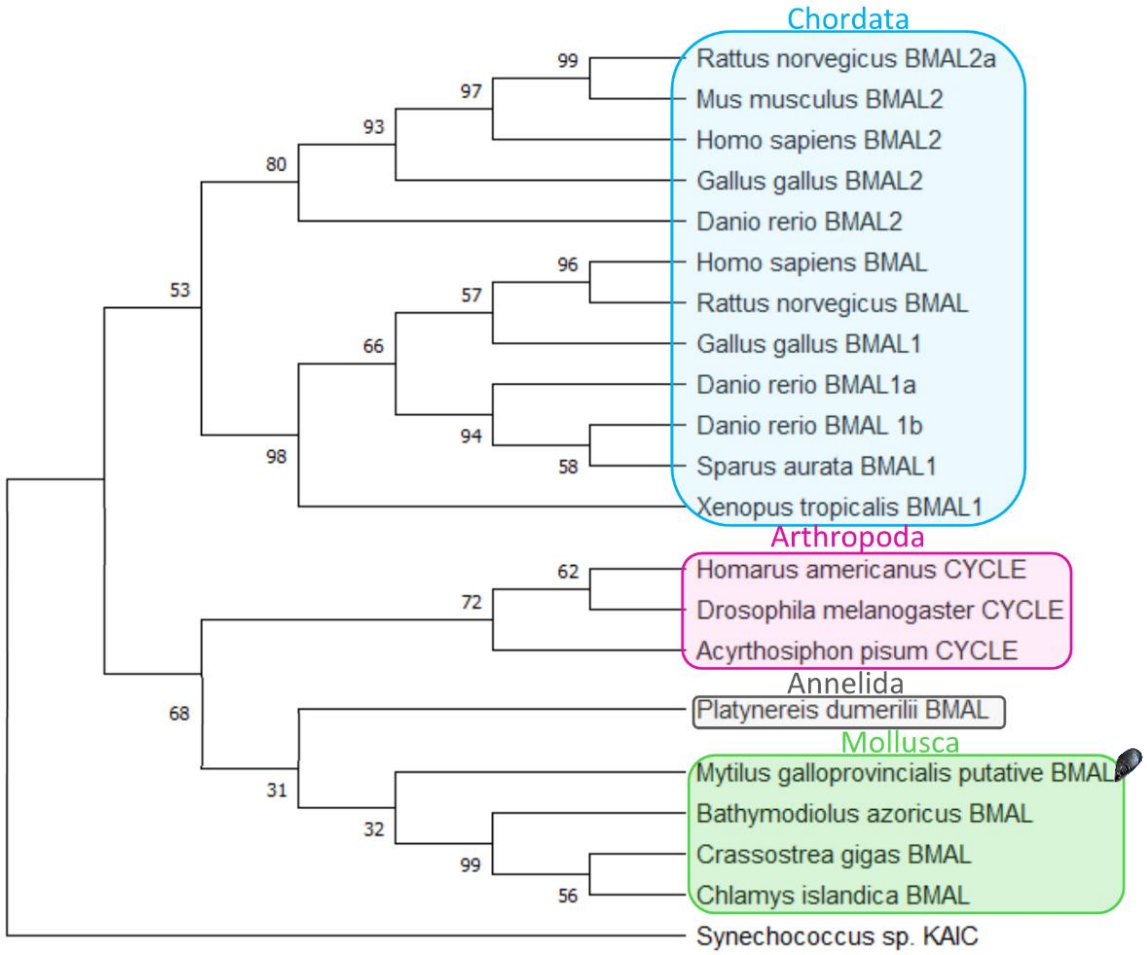

Figure 25: Phylogenetic tree based on BMAL sequences. The tree was generated using the maximum likelihood method and the JTT matrix-based model and the gamma distribution. Percentage of bootstraps were based on 1 000 replicates.

Most potential genes of the core set of the biological clock were already identified for *Mytilus edulis* (Chapman et al., 2017, 2020). Looking to positive elements, *Clock* (*i.e.*, *Circadian locomotor output cycles kaput*) gene mRNA sequence built was 409 bp long and matched at 99% with *M. edulis* sequence (KJ671527.1). The translated amino acid sequence had 87% identity with the annotated CLOCK protein (VDI68759.1) on *M. galloprovincialis* genome. Phylogenetic tree showed that the amino acid sequence was similar with identified sequences in close-related bivalves (Figure 24). For *Bmal* (*i.e.*, *Aryl hydrocarbon receptor nuclear translocator-like*), the 252 bp sequence built matched at 99% with *M. edulis* sequence (KJ671529.1) and blastx on the annotated genome showed a match with a hypothetical predicted protein (VDI55294.1) at 86%. Conserved domain search on pfam database showed bHLH-Pas (basic helix-loop-helix-Per-ARNT-Sim) domain, which is necessary to bind an E-box and activate the transcription of repressive factors of the feedback loop constituting the biological clock (Dunlap, 1999). The generated tree based on amino-acid sequences clustered the sequence with close-related species (*i.e.*, *B. azoricus, M. gigas* and *C. islandica*) (Figure 25).

Among negative elements, a 679 bp contig corresponding to *period* mRNA sequence was retrieved from reads alignment, that possess 96% homology with *M. edulis* sequence (MH836580.1) The translated sequence was aligned on the later annotated genome and showed 99% homology with *Period* (VDI70018.1 and VDI70019.1). Phylogeny tree grouped the sequence with Mytilidae PERIOD sequences (Figure 26). *Cryptochrome* 1 (*cry*1) contig retrieved was 296 bp long and matched with *M. edulis* at 99% (KJ671528.1). The translated amino acid sequence matched at 99% with the annotated Cryptochrome protein (VDH90443.1). *Cryptochrome 2* (*cry2*) had no sequence described for the *Mytilus* complex, therefore *M. gigas* sequence (KX371074.1) was used to assemble contigs from the sequence read archive. A 643 bp sequence was retrieved and was similar at 75% with the *cry2* sequence of the madeira cockroach, *Rhyparobia maderae*. The translated amino acids sequence matched at 99% with the Cryptochrome protein (VDI01404.1) annotated in *M. galloprovincialis* genome. Phylogeny tree grouped the sequence with close-related bivalves CRY2 (Figure 27). *Timeout* assembled mRNA sequence was 851 bp and had 99% homology with *timeout-like* of *M. edulis* (KX576716.1). The amino acid sequence matched with two annotated sequence of the *M. galloprovincialis* genome, the protein Aubergine (VDI77989.1) with 98% of identity and a coverage of 73%, and the protein Timeless (VDI83092.1) with 99% of identity over 65% of the sequence. The first protein, Aubergine, has a role in the development of the germline (Rui et al., 2020). By searching the conserved domain of the sequence, two appeared, the PIWI domain of eukaryote which is related to the germline development and Timeless protein. The match on Timeless annotated protein had only

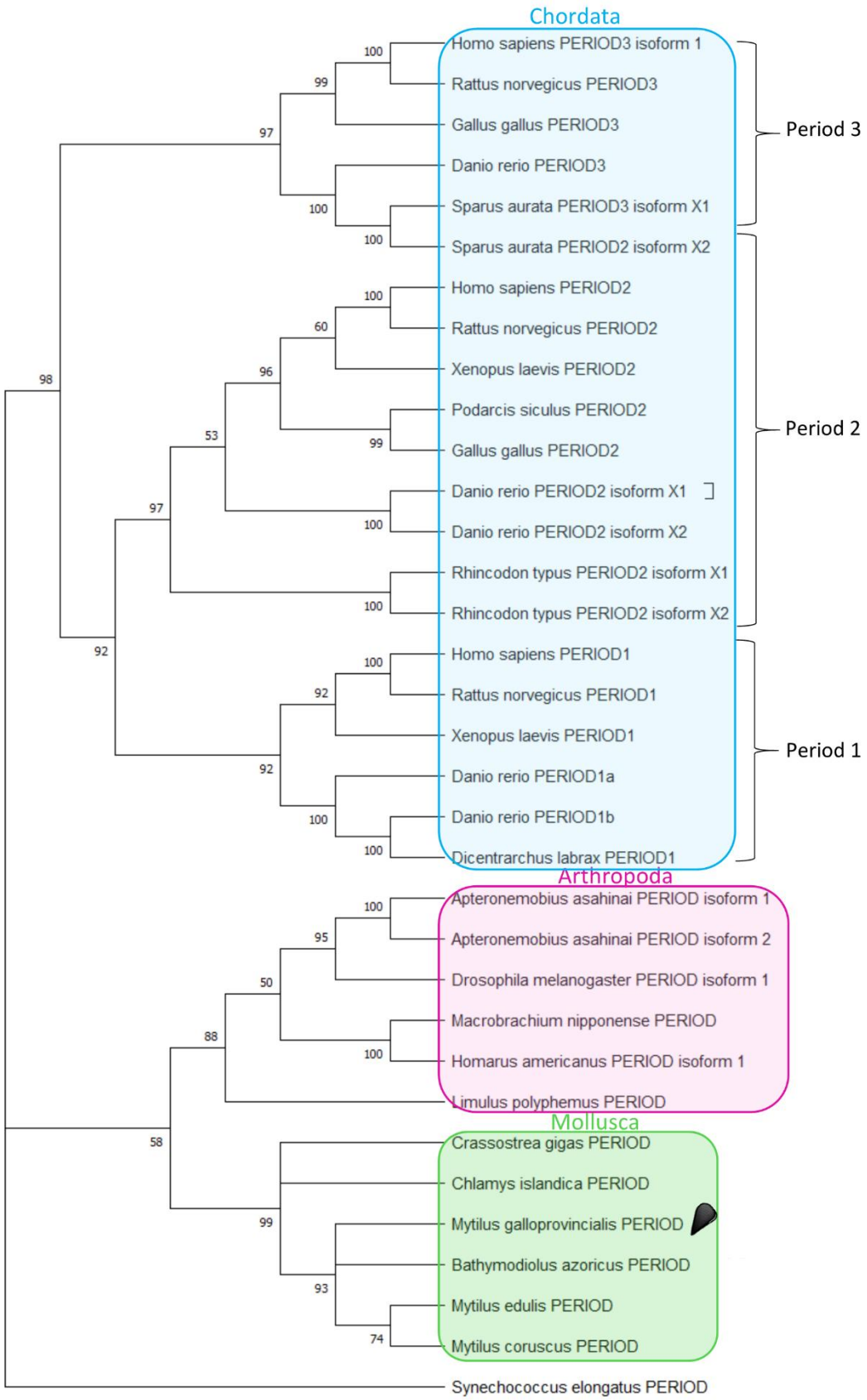

Figure 26: Phylogenetic tree based on PERIOD sequences. The tree was generated using the maximum likelihood method and the JTT matrix-based model and the gamma distribution. Percentage of bootstraps were based on 1 000 replicates.

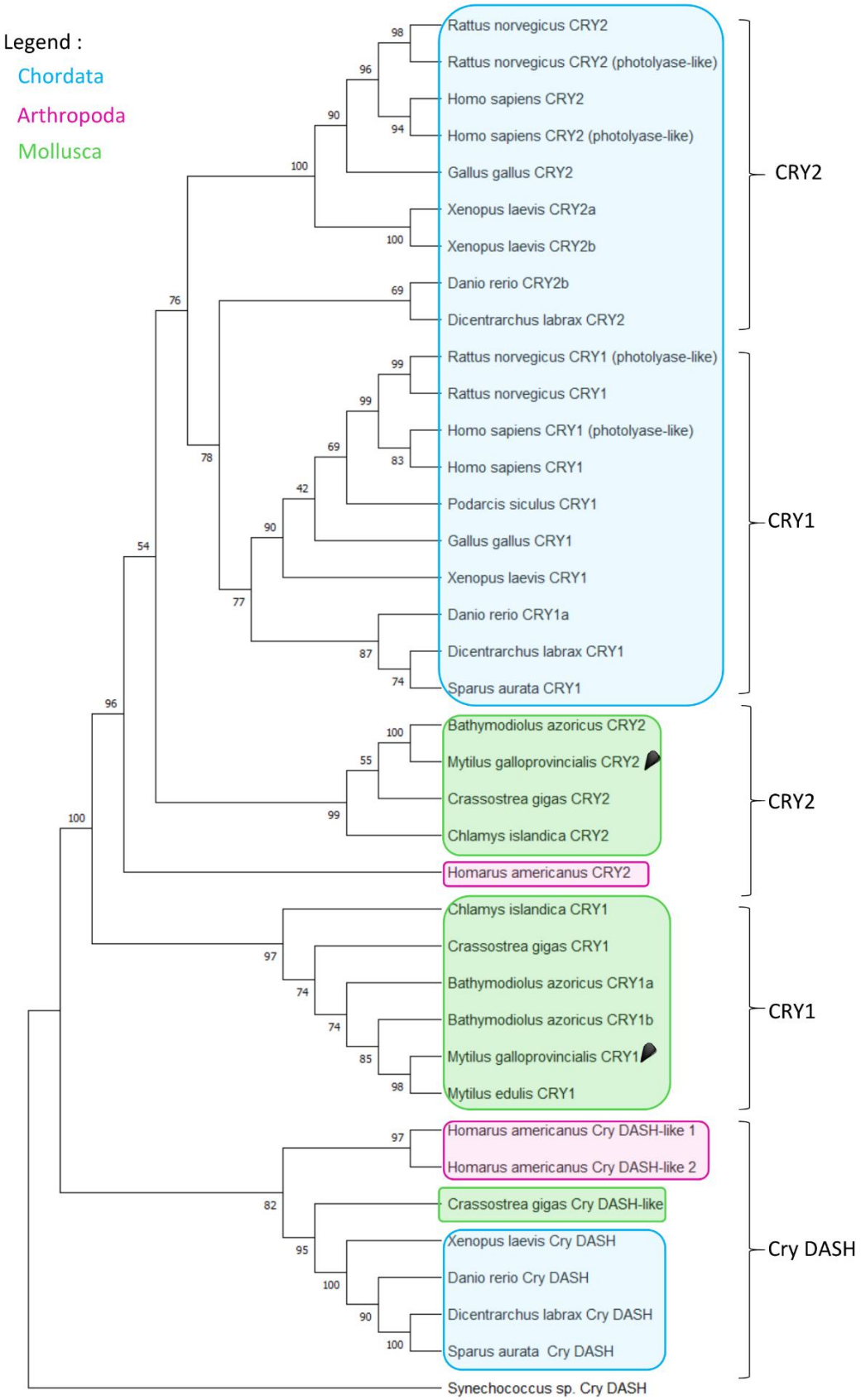

Figure 27: Phylogenetic tree based on CRYPTOCHROMES sequences. The tree was generated using the maximum likelihood method and the JTT matrix-based model and the gamma distribution. Percentage of bootstraps were based on 1 000 replicates.

the timeless domain. In insect, it has been suggested that *Timeless* resulted from a gene duplication of *Timeout* (Rubin et al., 2006). In *B. azoricus*, one *Timeless* and two *Timeout* sequences that might be isoforms were identified (Mat et al., 2020). The sequences used in this study matched at 89% with the second isoform of timeout of *B. azoricus*. Phylogenetic tree based on amino-acid sequences grouped the built sequence with TIMEOUT sequences of Mytilidae (Figure 28).

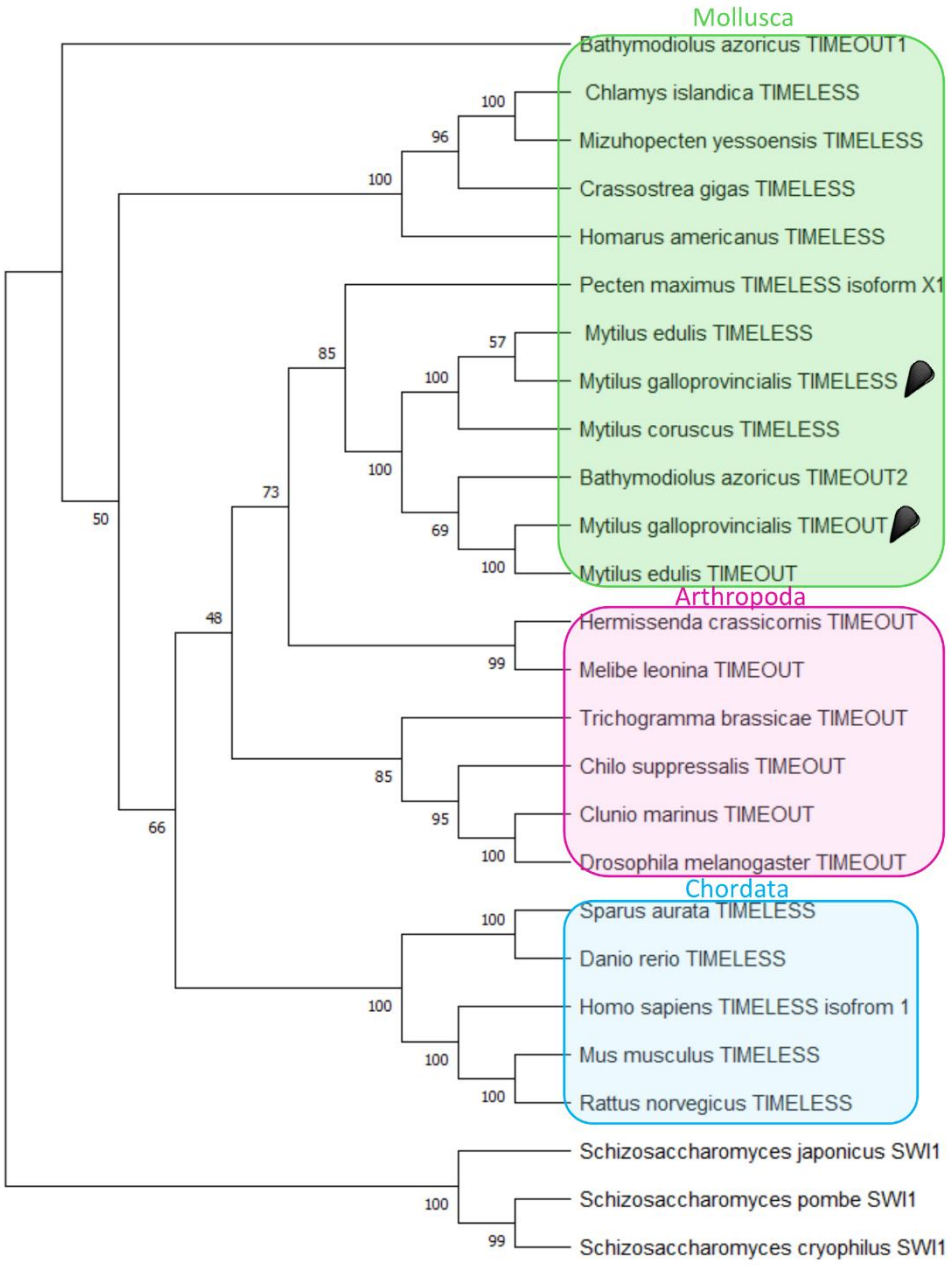

Figure 28: Phylogenetic tree based on TIMEOUT and TIMELESS sequences. The tree was generated using the maximum likelihood method and the JTT matrix-based model and the gamma distribution. Percentage of bootstraps were based on 1 000 replicates.

Rorb (*i.e.*, *RAR-related orphan receptor B*) has been recognised to be involved in time keeping mechanisms (Jetten et al., 2001). It has been proved that its alteration disrupts the expression of *Clock*, *Cycle* (*i.e.*, the arthropod ortholog of *Bmal*) and *Tim* in firebrats, *Thermobia domestica* (Kamae et al.,

2014). Rhythmic expression of *Rorb* has been previously observed in Mytilids (Connor and Gracey, 2011; Chapman et al., 2020) and has been suggested as likely transcription promotor of *Bmal* in oyster and be regulated by REV-ERB (Figure 23) (Perrigault and Tran, 2017). No *Rev-erb* sequence was built for *M. galloprovincialis* in this study. *Rorb* sequences built in *M. galloprovincialis was* 469 bp long and matched at 99% with *M. edulis rorb/hr3-like* mRNA but only on 36% of the sequence. Therefore, a blast was done on TSA of *M. galloprovincialis*, and the sequence was identical to a mRNA sequence (GGUW01039936.1), validating the contig. The amino-acid sequence matched with a nuclear receptor from the Subfamily 1 group F member 4 of *M. galloprovincialis* (VDI83019.1). Among the conserved domain of this protein there was the DNA binding domain of Retinoid-related orphan receptor.

Biological clocks related genes

Rhodopsin is a photoreceptor known to have a role in the circadian entrainment of biological clocks notably in the fruit fly, *Drosophila melanogaster* (Senthilan et al., 2019). Rhythmic expression of *Rhodopsin* has been observed in the mantle of the Arctic scallop *C. islandica* (Perrigault et al., 2020). For *rhodopsin*, *M. edulis* mRNA sequence was not published yet and the sequence was built from *rhodopsin* sequence of *Argonauta nodosa* (AY545166.1). A 108 bp contig was constructed but none similar sequence was found in GenBank nucleotide database. To validate it, a blast has been done on transcript sequence archives (TSA) of *M. galloprovincialis* and the sequence matched at 99% over 62% of a sequence (GHIK01098750.1). As a blast of the last sequence on database matched for *rhodopsin* of many molluscs, it was assumed that our sequence was coding for Rhodopsin. Later comparison with the annotated genome validated the sequence with 99% of homology with an annotated *r-Opsin* (VDI13980.1).

In vertebrates Arylalkylamine-N-acetyltransferase, AANAT, is an enzyme involved in the rhythmic production of melatonin which secretion and release are rhythmically controlled by biological clocks (Klein, 2007). Recently, similar observation has been made in labial palps of the razor clam, *Sinonovacula constricta* (Zhu et al., 2022). *Aanat* mRNA sequence was based on *M. edulis* sequence, the 380 bp matched at 99% with *M. edulis* (KX576715.1). Amino acid sequence aligned with a hypothetical protein at 95% but only on 15% of the sequence (VDH95523). Nevertheless, our sequence presented a N-Acyltransferase superfamily conserved domain in which N-acetyltransferase domains are a member. This confirmed that the built sequence is coding for an AANAT.

The last gene targeted was the *HSP70* that is supposed to play a role in the folding and chaperoning shell matrix proteins (Sleight et al., 2020). In bivalve the Hsp70 expression varies in relation with the temperatures (Toyohara et al., 2005; Anestis et al., 2010). The *hsp70* sequence

(GenBank accession number AB180908.1, Toyohara et al., 2005) was already described for *M. galloprovincialis*.

Cell-autonomous 12 hours clock gene

In the recent years, another cell-autonomous 12 hours clock regulation of gene expression was described in mammals (Zhu et al., 2018). XBP1s was suggested as regulator and proved to be independent from the canonical biological clock in mice (Pan et al., 2020). This gene was already described in molluscs as part of the signalling pathway IRE1-XBP1 and known to play a role on a large spectrum of biological process (Huang et al., 2018). X-*box binding protein 1* (*Xbp1*) sequence retrieved was 526 bp long and based on the sequence of *M. edulis* (DQ201827.1). It matched at 97% with the sequence of *M. edulis*. The translated sequence matched at 93% on the annotated sequence XBP1 in *M. galloprovincialis* genome (VDI08907.1).

Biomineralisation related genes

Genes involved at different levels of the biomineralisation process were targeted. Shells are made of mineral and organic contents (Skinner and Jahren, 2003). Two genes related to the mineral formation were targeted; *Plasma membrane calcium ATPase* and *Carbonic anhydrase*. Plasma membrane calcium ATPase is known to transport calcium ions, increasing the calcium ions concentration in the extrapallial fluid (EPF) (Hüning et al., 2013). Carbonic anhydrase is an enzyme forming HCO_3^- from CO_2 and H_2O. The HCO_3^- binds with calcium ions to form the mineral part of the shell, the calcium carbonate. Sequence coding for *carbonic anhydrase II* was already available on NCBI (KT818923.1). Concerning *plasma membrane calcium-transporting ATPase* (*ca2⁺ATPase*) mRNA sequence, reads of *M. galloprovincialis* were collapsed into a contig based on the gastropod *Haliotis rufescens* sequence (XM_048397027.1). The final contig of 247 bp matched at 78% over 74% of the sequence of the gastropod. To validate this sequence, a blast has been done on transcribed-RNA sequences (TSA) of *M. galloprovincialis*. The contig built was identical to a sequence (GHIK01179846.1), validating the contig. The translated sequence matched at 100% over 92% of Ca^{2+} transporting ATPase in the annotated genome of *M. galloprovincialis* (VDI68446.1). However, both proteins have also other functions not directly related to the biomineralisation process and proteins specific to the process were targeted (Le Roy et al., 2014; Pavičić-Hamer et al., 2015).

The organic matrix in shells is composed of several proteins that are recognised to control the shell mineralisation (Marin and Luquet, 2004; Feng et al., 2017). Three of them were implicated in the chitin metabolism which is one major polysaccharide constituting the building frame for nacre tablet

formation (Addadi et al., 2006; Engel, 2017). Chitin synthase is involved in the chitin synthesis and Chitinase for the chitin remodelling (Engel, 2017). Tyrosinase has a chitin binding domain and is recognised to correct the chitin remodelling (Miglioli et al., 2019). C*hitin synthase* (EF535882.1) was already described in NCBI for *M. galloprovincialis*. Again, some targeted genes sequences were described for other Mytilids, facilitating the construction of *M. galloprovincialis* sequences. *Chitinase* contig was constructed from *M. edulis* sequence (MG827131) and was 201 bp long. The nucleotide sequence matched at 100 % with *chitinase-like protein-1* mRNA of *Mytilus chilensis*, validating the contig. The amino-acid sequence was the same than the later-annotated on the genome of *M. galloprovincialis* (VDI28372.1). *Tyrosinase* mRNA sequence has been assembled using the *tyrosinase-like* sequence of *Mytilus coruscus* (KP57802.1) and was 877 bp long. The blast on Genbank nucleotide sequence did not find similar sequence although research on translated sequence matched at 100% over the 69 first amino-acids of the Tyrosinase-like protein of *M. galloprovincialis* (OPL33388.1) from the base pair number 2 to 208 on the nucleotides sequence. Moreover, looking to the reads alignment the coverage between them was insufficient in many places after 280 bp on the contig. Therefore, the contig was trimmed to be 206 bp long.

Two potential inhibitors of the formation of the mineral process were targeted. *Perlwapin* was first the tablets of nacre in the abalone *Haliotis laevigata* (Treccani et al., 2006). It is formed of a succession of WAP (Whey Acidic Protein) domain sequences that may inhibit the growth of nacre. In *M. galloprovincialis*, the PERLWAPIN has been identified (Marie et al., 2011). The WAP domains were conserved but their function in calcium carbonate deposition is unknown. The mRNA sequence of *perlwapin* was already available on NCBI (FL494664.1, Venier et al., 2009). NACREIN has been first identified in the nacreous layer of *Pinctada fucata* and later in the prismatic layer as well (Miyamoto et al., 1996; Miyashita, 2002). The protein is composed of two domains, one acting as a carbonic anhydrase and another that might inhibit the calcium carbonate precipitation (Miyamoto et al., 2005). Daily oscillation of gene expression has been observed in the mantle of *P. fucata* (Miyazaki et al., 2008). A Nacrein-like protein has been identified in the shell of *Mytilus galloprovincialis* and *nacrein* sequence is available in databases (KP670943.1, Gao et al., 2015).

Among other functions, BMP2 is known to regulate the biomineralisation (Miyashita et al., 2008; Zhao et al., 2016). *Bmp2* contig of 176 bp was obtained based on sequence of the clam *Sinonovacula constricta* (MH822126.1). Nucleotide sequence did not match with any sequence on GenBank whereas it was identical to an mRNA sequence in TSA of *M. galloprovincialis* (GHIK01116414.1). The translated amino acid sequence had 100% of identity with *BMP2/4* annotated gene in *M. galloprovincialis* genome (VDI49543.1 and VDI49544.1).

Housekeeping genes

For the housekeeping genes, five were required for the gene expression analysis by NanoString. *α-tubulin* (HM537081.1), *actin* (AF157491.1) and *ef1α* (AB162021.1) mRNA sequences were previously described in *M. galloprovincialis*. The commonly used *18s* and *28s* were not suitable as their expressions were too high in comparison with the targeted genes. Therefore, *Rpl7* and *Hprt1* genes were used. *Rpl7* contig was assembled from *M. gigas rpl7* sequence (AJ557884). It matched with a TSA sequence of *M. galloprovincialis* (GAEN01008711.1), validating the contig. Later analysis on the genome assembly showed a 99% of identity with the annotated protein RPL7e (VDI30485.1). The same was done for *hprt1* based on the known sequence of *M. edulis* (KJ808673.1). The cross-validation on annotated *M. galloprovincialis* genome showed a 100% identity with HPRT sequence (VDI66978.1).

2. Expression of targeted genes in the posterior edge of the mantle: spatial variability

Foreword

Bivalve shells are formed through a biologically induced biomineralisation process (Weiner and Dove, 2003). Shells are made of calcium carbonate and organic compounds. Organic compounds are known to control the shell mineralisation, forming a building frame and controlling the crystal shape and growth (Marin and Luquet, 2004). The mantle is considered to be the organ of the formation of the shell, secreting the organic compounds that are released into the extrapallial fluid located between the mantle and the shell. It should be noted that the hypothesis of the control of biomineralisation by biological clocks has already been proposed (Richardson et al., 1980; Schöne, 2008; Louis et al., 2022). Considered as a structurally and functionally heterogeneous tissue (Bjärnmark et al., 2016), the mantle is a polarised tissue composed of three layers: the outer epithelium also called the calcifying epithelium, the internal tissue and the inner epithelium (Wilbur and Saleuddin, 1983). In this study, histological description and *in situ* hybridisation (ISH) were achieved on the targeted tissue in order to explore spatial variation of gene expression related to the biomineralisation process and expression of putative core biological clock genes.

Materials and methods

Tissue collection and fixation

Mussels*, M. galloprovincialis*, were sampled in the bay of Banyuls-sur-Mer at 10:00 a.m. and sacrificed at noon. The posterior edge of the mantle of mussels were sampled and fixed in 4% paraformaldehyde (PFA) in phosphate buffer saline (PBS) at 4°C. Tissues were dehydrated in a graded ethanol series (70, 95, 100%), dipped 3 min in toluene and then in Paraplast® (Merck, Darmstadt, Germany) (at 60°C); after 15 h of impregnation, they were embedded in a new bath of Paraplast®. Eight micrometers thick sections (using a MicroM HM 340^{E} microtome, Thermo Fisher Scientific, Waltham, MA, USA) were layered on glass slides (coated with a 2% solution of 3−aminopropyl-triethoxy-silane). Prior to histological colorations and ISH, sections were successively deparaffinised in toluene, rehydrated (through descending ethanol series) and placed in PBS.

Histology

Tissues were contrasted according to haematoxylin/eosin procedure. Slides were first incubated in Harris haematoxylin solution (30 sec) (Harris, 1900), rinsed with tap water, incubated in 0.5% and 5% eosin bathes, and finally rinsed with tap water. Sections were dehydrated in a graded ethanol series and finally mounted in Entellan™ (Merck, Darmstadt, Germany). Sections were visualised using a AxioPlan 2 Imaging microscope (Zeiss, Oberkochen, Germany) equipped with a ProgRes® CF^{cool} (Jenoptik, Jena, Germany).

In situ *hybridisation*

Five genes were targeted, two related to the putative biological clock; *Period* and *Clock* and three genes linked to the biomineralisation process: *Carbonic anhydrase*, *Chitinase* and *Bone morphogenic protein-2* (*Bmp2*) (Table 5). Primers sequences were designed based on sequences retrieved on NCBI or reconstructed based on close-related species. Sequences were subcloned into a pGEX4T1 expression plasmid (Novagen; EMD Chemicals Inc, PA, USA) containing a GST (glutathione *S*-transferase) tag. Anti-sense (AS) and sense (S) riboprobes were produced with the commercial kit (Roche-Diagnostics DIG labelling kit, Merck, Darmstadt, Germany) according to the manufacturer recommendations.

Table 5: Targeted genes characteristics used in ISH on the posterior edge of the mantle of *M. galloprovincialis*.

Gene	Primers	Amplicon length	T° of hybridisation
Period	F : 5´-TGTTGTGTCCACCTTTCCCT-3´ R : 5´-CAAGGTGGGTCTGAGTGTCT-3´	535 bp	65°C
Clock	F : 5´-CGGCAGTACAGGCAAAGAC-3´ R : 5´-AGGTTTCCTCCCCTTTCTGC-3´	708 bp	65°C
Carbonic anhydrase	F : 5´-CGGAGACAAAGGGACC-3´ R : 5´-CGAGGCAATGAACACAGGAA-3´	706 bp	65°C
Chitinase	F : 5´-TTGTCGTATCCCACCCACT -3´ R : 5´-AGGAATTTGAAAATGAGGCTCA-3´	528 bp	65°C
Bmp2	F : 5´-ACCGACATCCACAACCTTCT-3´ R : 5´-CCTTGACATTCACCCAGCAG-3´	733 bp	65°C

The ISH was performed on proteinase K treated sections using the digoxigenin (DIG) labelled antisense and sense probes, as described elsewhere (Besseau et al., 2006). Briefly, sections were hybridised overnight at 65°C in a hybridisation buffer with the probes (1µg/mL). The sections were then incubated overnight in a solution (1/5000) of the anti-DIG antibody conjugated to alkaline phosphatase (Roche, Merck, Darmstadt, Germany). Alkaline phosphatase (AP) activity was revealed by the presence of a purple precipitate, after incubation with the AP substrate (Roche, Merck, Darmstadt,

Germany). Sections were observed using a AxioPlan 2 Imaging microscope equipped with a ProgRes® CF^{cool} camera.

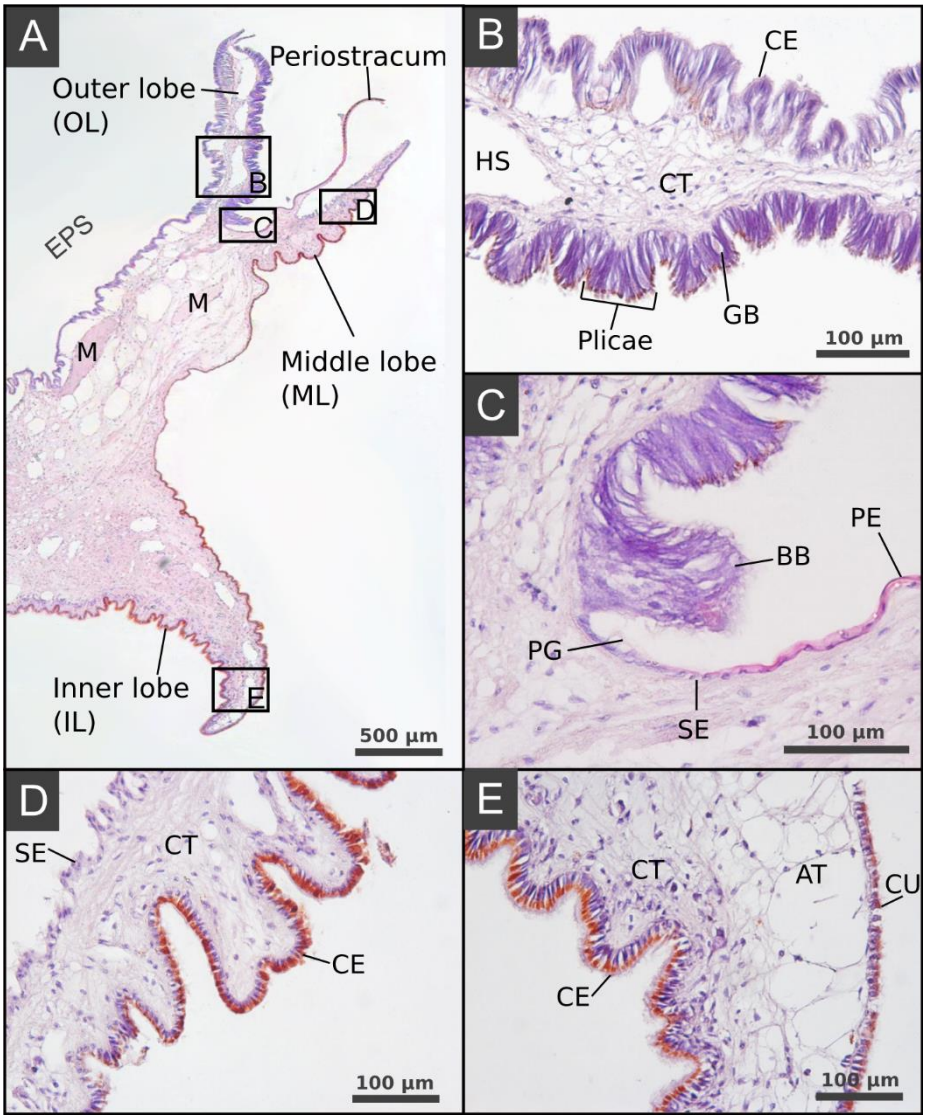

Figure 29: Longitudinal histological sections of the posterior edge of the mantle of *Mytilus galloprovincialis* stained with haematoxylin and eosin. A) The posterior edge is composed of three lobes, the inner lobe (IL), the middle lobe (ML) and the outer lobe (OL). Between the outer and the middle lobes, the periostracum is sealing the extrapallial space (EPS) from the external environment. B) The outer lobe is composed of columnar epithelium (CE) with microvilli or cilia. Goblet cells (GB) could be observed within the plicae. C) The periostracal groove (PG) is located between the OL and the ML, the last plicae is the basal bulb (BB) which is specialised in the secretion of the periostracum (PE). D) The middle lobe has different epithelium; the outer side has squamous epithelium (SE) whereas the inside has columnar epithelium. E) Edge of the inner lobe. CT, connective tissue; AT, adipose tissue; HS, haemolymph sinus; M, muscle fibres.

Results

Histology

The posterior edge of the mantle was composed of the connective tissue within which there were muscle fibres, adipose tissues and haemolymph sinus (Figure 29A). The edge of the mantle was composed of three lobes that exhibit different cell structure. The outer lobe was composed of a columnar epithelium with microvilli or cilia. Goblet cells could be observed within the plicae (Figure 29B). The middle lobe had squamous epithelium at its outer side and columnar epithelium inside (Figure 29D). The periostracal groove was located between the outer and middle lobes. In this groove was located the basal bulb (Figure 29C). The inner lobe was composed of cubic and columnar epithelium (Figure 29E).

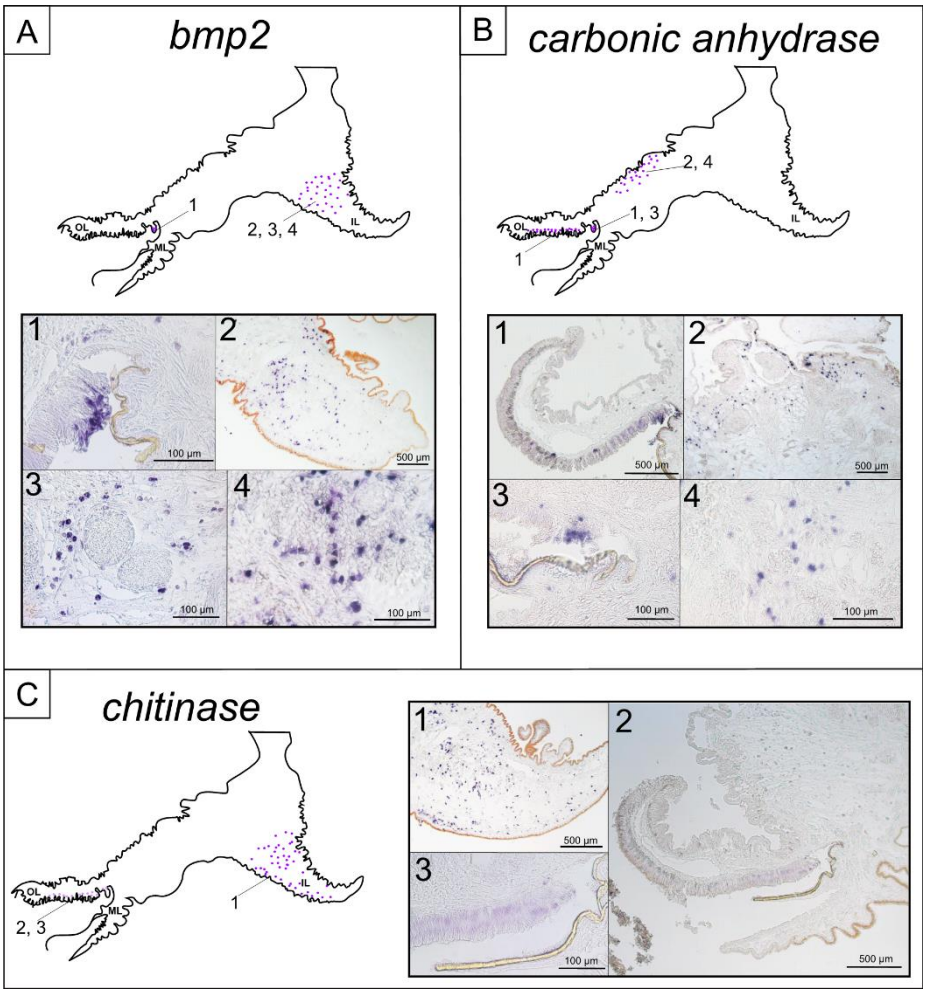

Figure 30: Biomineralisation related gene expression in the posterior edge of the mantle of *Mytilus galloprovincialis* revealed by *in situ* hybridisation. A) Expression of *Bmp2* in the basal bulb (1) and in the connective tissue of the inner lobe (2, 3, 4). B) Expression of *Carbonic anhydrase* in the basal bulb (1, 3) and the inner part of the outer lobe (1). The gene was also expressed along the calcifying epithelium of the mantle (2, 4). C) Expression of *Chitinase* in the connective tissue of the inner lobe (1) and low expression in the inner part of the outer lobe (2, 3).

In situ *hybridisation*

On our histological sections, no signal was detected with the sense probes considered as negative control (Supplementary data, Figure S2) excepted for the clock sense probe. The three biomineralisation related genes were not all expressed in the same area of the mantle at noon (Figure 30). *Bmp2* transcripts were present at the edge of the basal bulb and in the connective tissue of the inner lobe (IL) (Figure 30A). Expression of *Carbonic anhydrase* (*CA*) was also detected in the basal bulb as well and along the inner part of the outer lobe (OL) and the calcifying epithelium (Figure 30B). *Chitinase* gene was expressed in the connective tissue of the IL and a discrete signal was observed in the inner part of the OL (Figure 30C). *Clock* mRNA were broadly detected in the edge of the mantle (*i.e.*, in the outer lobe and the basal bulb, in the connective tissue of the inner lobe and of the calcifying epithelium) (Figure 31A). In contrast, *period* transcripts were found only in the inner part of the OL, the basal bulb and in the epithelium along the ML (Figure 31B).

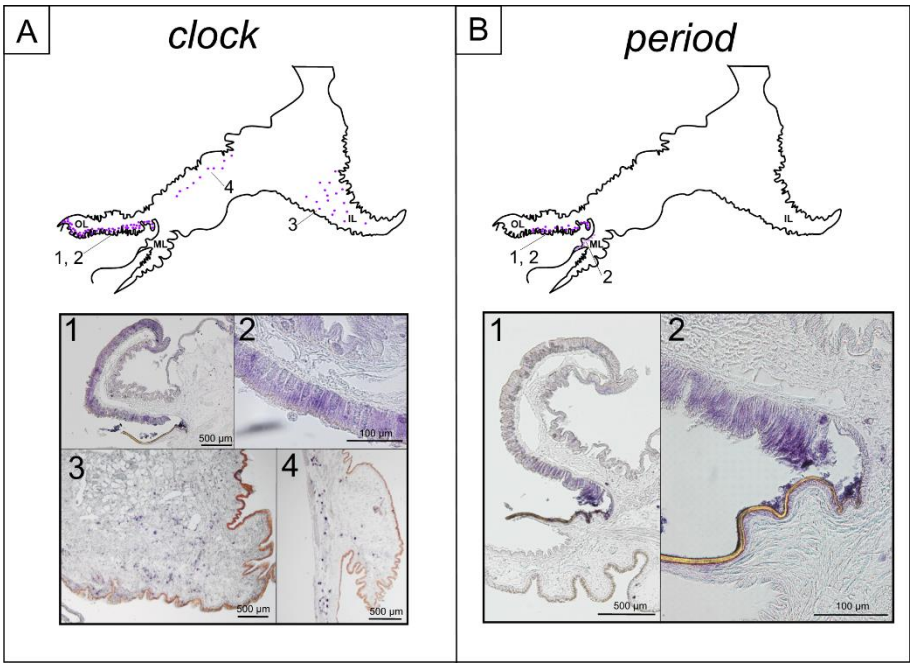

Figure 31: Putative core biological clock gene expression in the posterior edge of the mantle of *Mytilus galloprovincialis* revealed by *in situ* hybridisation. A) *Clock* is expressed in the outer lobe and the basal bulb (1,2) and in the connective tissue of the inner lobe and of the calcifying epithelium (3,4). *Period* is highly expressed in the basal bulb and to a smaller extend in the inner part of the outer epithelium (1,2). The gene was also expressed along the outer epithelium of the middle lobe (2).

Discussion

The posterior edge of the mantle is composed of three lobes which exhibit different cell structures and functions. The outer lobe is known for being involved in the shell secretion, the middle lobe has a sensory function and the muscular inner lobe controls the water flow in the mantle cavity (Gosling, 2004). The basal bulb is constituted by a group of cells known to secrete the periostracum which constitutes the external layer of the shell (Richardson et al., 1981).

The genes *Bmp2*, *Carbonic anhydrase* and *Chitinase* are involved at different steps of the biomineralisation pathway. BMP2 is known to promote biomineralisation (Miyashita et al., 2008; Zhao et al., 2016). Carbonic anhydrase is an enzyme forming HCO_3^- from CO_2 and H_2O and *Chitinase* is encoding an enzyme remodelling the chitin, a major organic compound of the shell (Engel, 2017). Transcripts of all three genes were detected in the basal bulb and the OL, known for secreting the prismatic layer (Nudelman et al., 2007). However, *carbonic anhydrase* mRNA were the only transcripts observed in the calcifying epithelium, a tissue area related to the nacre formation. The presence of *chitinase* mRNA in the IL has been already mentioned in *M. gigas* and *Magallana honkongensis* (Okada et al., 2013; Liao et al., 2021). In both species, the expression was observable in the epithelium of the IL whereas in *M. galloprovincialis* it was present along the epithelium and in the connective tissue. The IL is the first tissue in contact with the water entering in the mantle cavity (Gosling, 2004). Therefore, it was hypothesised that its presence in the IL epithelium was related to its role in immunity by hydrolysation of chitin-coated microorganisms (Okada et al., 2013). However, the presence of *bmp2* and *chitinase* transcripts within the IL could be related to haemolymph sinuses present within the mantle tissue (Eggermont et al., 2020). It has been shown that haemocytes H2 and H3 (which are looking as irregularly shaped granulocytes) expressed several genes related to shell organic compounds (Mount et al., 2004; Ivanina et al., 2017). The haemolymph is often described as playing an important role in the biomineralisation process as both mineral and organic compounds of the shell were found in it (Song et al., 2019).

In several species such the drosophila and the mouse, the gene *Clock* is coding for an active element of the biological clock, while the gene *Period* constitutes one of the repressive elements (Dunlap, 1999). *Clock* transcripts were observed in all cell structures where biomineralisation related genes were observed. The gene *Period* was expressed in the inner part of the OL and the basal bulb as most of the biomineralisation gene but it was the only gene expressed in the epithelium along the ML. The overlap of putative core biological clock and biomineralisation related expressions is thus encouraging the hypothesis of a control of clocks on the biomineralisation process.

Supplementary data - Expression of targeted genes in the posterior edge of the mantle: spatial variability

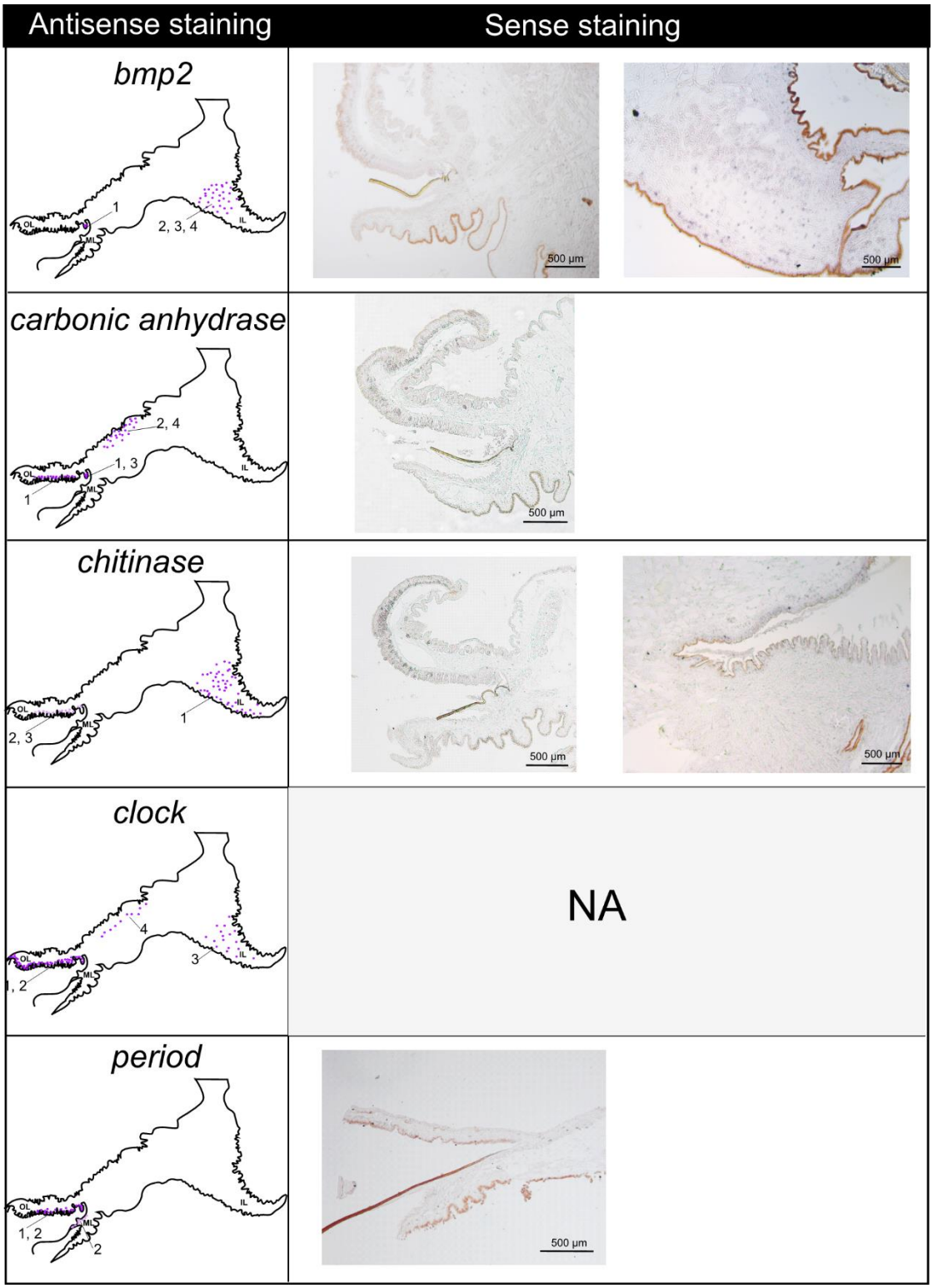

Figure S2: Negative controls of *in situ* hybridisation. Sense probes of *bmp2*, *carbonic anhydrase*, *chitinase* and *period* showed no signal. *Clock* sense probe was not specific.

3. Article n°2:

Clock(s) or no clock(s)? The integration of the rhythmic environment in bivalve's shell

Victoria Louis[1,2], Erwan Peru[1], Charles-Hubert Paulin[2], Pascal Conan[3], Franck Lartaud[1*], Laurence Besseau[2*]

[1] Sorbonne Université, CNRS, Laboratoire d'Ecogéochimie des Environnements Benthiques, LECOB, F-66650, Banyuls-sur-Mer, France

[2] Sorbonne Université, CNRS, Biologie Intégrative des Organismes Marins, BIOM, F-66650, Banyuls-sur-Mer, France

[3] Sorbonne Universités, CNRS, Laboratoire d'Océanographie Microbienne, LOMIC, F-66650, Banyuls sur mer, France

*co-last authors

Key words: Biomineralisation, growth patterns, biological clocks, *Mytilus galloprovincialis*

Abstract

Bivalve shells growth is not homogeneous nor continuous in time, leading to the formation of growth patterns. The growth patterns consist in the alternance of growth lines and increments deposited at regular interval of time. The control of the periodic increment formation is poorly understood. Multiple hypotheses were advanced. It could be a direct control of the environment. However sometimes the environment cannot explain the shell pattern observed and the hypothesis of a control by biological clocks is advanced. In this study both hypotheses were tested *in situ* and in aquaria using gene expressions, behavioural and shell growth pattern measurements. *Mytilus galloprovincialis* was used as model and the environmental variables manipulated in aquaria were the photoperiod and the food availability. Based on molecular and behavioural data, this study showed that the potential biological clock of *M. galloprovincialis* was plastic. Its plasticity might contribute to its invasive success. A large inter-individual variability was observed at the behavioural level. Therefore, the control of the behaviour by biological clocks could not be showed or refuted. The endogenous nature of tidal and daily rhythms were showed based on behavioural measurements. Looking to shell growth patterns, again a large variability was observed. The direct control by the photoperiod or the food availability was not explaining the patterns observed. At the gene expression level, biomineralisation genes did not had similar rhythmicity than core biological clock genes or *xbp1*, which is related to a cell autonomous timekeeping mechanism. The indirect control by the valve activity neither explained growth patterns observed.

Graphical abstract

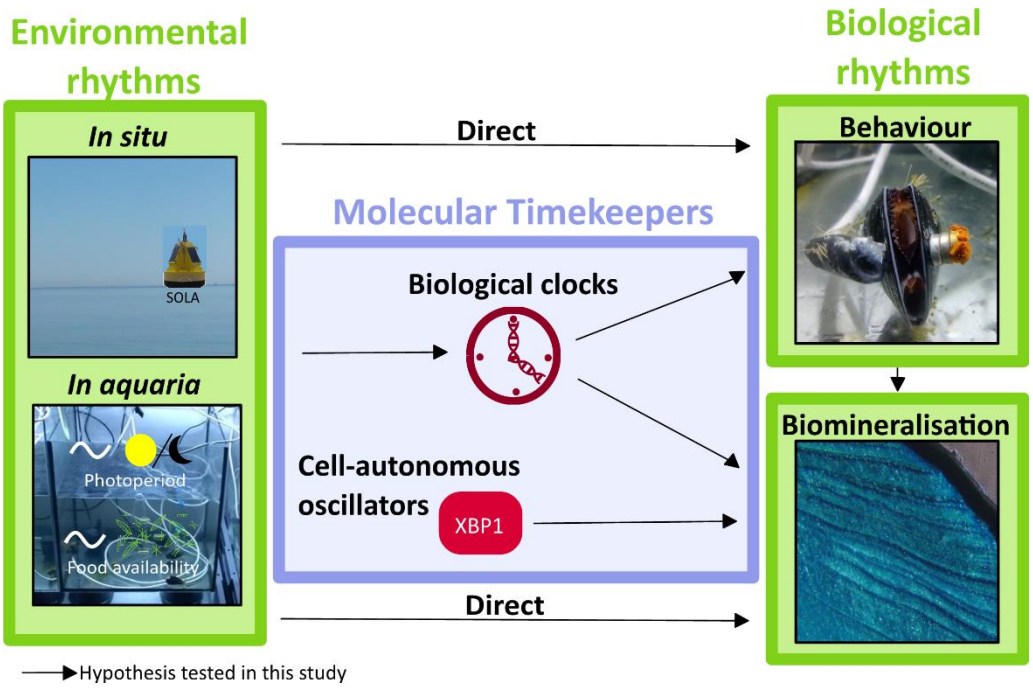

Introduction

Bivalve shells are complex structures made of calcium carbonate and organic compounds (Skinner and Jahren, 2003). Shells are composed of different layers, classically the inner layer is composed of nacre and the external layer, often constituted of prismatic, fibro-prismatic or crossed-lamellar microstructure and covered by an organic rich structure, the periostracum. Shell components are secreted by the mantle into the extrapallial cavity which is filled by a supersaturated extrapallial fluid (EPF) (Marin et al., 2012). The organic matrix, composed of polysaccharides and proteins has a role of stabilisation of the instable nucleus of $CaCO_3$ and participates to the control of the crystal growth and organisation (Giuffre et al., 2013; Checa, 2018). Physical and biological controls of the biomineralisation process were described through self-organisation of the organic matrix, crystal competition and subcellular recognition by the mantle cells (Checa et al., 2016; Checa, 2018). In the last mentioned process, cells may secrete either organic or mineral material depending of the physicochemical properties of the extracellular matrix (Checa et al., 2005; Checa, 2018).

The biomineralisation process by which the shell is secreted is neither homogeneous or continuous in time, leading to the formation of growth patterns (Schöne, 2008). Growth patterns in bivalve shells consist in the alternance of growth lines and increments. Depending of the environment, growth lines are mainly formed on a daily or a tidal basis (Louis et al., 2022). In intertidal areas the origin of growth line is related to an internal pH drop due to valve closure during the aerial phase as the drop leads to a slight decalcification of the shell (Lutz and Rhoads, 1977). At high tide, the bivalve adds calcium carbonate and organic compounds back on the decalcified layer, forming a growth line. This schedule was validated by measurements taken in the EPF of bivalves (Crenshaw and Neff, 1969; Littlewood and Young, 1994). Measurements showed a quick drop of the internal pH followed by an increase of Ca^{2+} concentration when valves were closed. In non-tidal environments, the driver of the biomineralisation process is often less clear and multiple possible factors were advanced such water temperature, food availability and bottom current (Nedoncelle et al., 2015; Andrisoa et al., 2019). However, while reared in stable environmental conditions at laboratory, bivalves are still forming increments at regular interval of time (Richardson et al., 1980; Richardson, 1988). This raised the hypothesis of the involvement of biological clocks in the control of periodic increment formation in shells (Richardson et al., 1980; Schöne, 2008; Louis et al., 2022).

Biological clocks are auto-regulatory transcription and translation feedback loops (TTFL) (Dunlap, 1999). In bivalves, a hypothetical clockwork has been proposed in oysters *Magallana gigas* (Perrigault and Tran, 2017). In this hypothetical TTFL, the complex CLOCK:BMAL activates the transcription of repressor factors by binding to an E-box. Repressors of the transactivation of the complex CLOCK:BMAL are *period, cryptochrome 1* and *2*, *timeless* and *timeout* transcripts. A coupled

feedback loop composed of genes *Rorb* and *Rev-erb* regulates the expression of *Bmal* (Jetten et al., 2001; Perrigault and Tran, 2017). Those genes are considered as core genes of what is called the circadian clock. The clock is set and reset by environmental variables called "*Zeitgebers*" (Aschoff, 1981). One of the most important zeitgebers is the alternance of light and darkness, but other time-givers such tides have been described as crucial, especially in marine environments (Häfker et al., 2023). One hallmark of biological clocks is that it is endogeneous, which means that under constant environmental conditions (*i.e.,* under free-running conditions), the clock is still ticking (Aschoff, 1981). Biological clocks ensure the synchronisation of biological activities as well as the anticipation on environmental variability (Rosbash, 2009). Also, biological clocks can increase the fitness of the organisms by maximising the energy intake and minimising its loss (Paranjpe and Sharma, 2005; Emerson et al., 2008). Cyanobacteria, *Synechococcus elongatus*, has a small genome that can be easily manipulated. Researchers manipulated the rhythmicity of the clock and put strains in competition under alternance of light and dark phase each 12 hours and 15 hours (Ouyang et al., 1998). Strains having biological clocks in phase and in resonance out-competed the others, showing an increased fitness. Biological clocks are synchronizing many physiological and behavioural processes such as the valve activity of bivalves (*i.e.,* the opening and closing cycles of the valves) (Mat et al., 2012; Tran et al., 2016; Perrigault and Tran, 2017).

In bivalves, functional endogenous circadian clocks have been described in oyster, clam and blue mussel, *M. edulis* (Connor and Gracey, 2011; Perrigault and Tran, 2017; Chapman et al., 2020; Perrigault et al., 2020). However, in the marine environment endogenous periodicity of 12.4 hours is also often noticed. Different theories have been developed about clocks oscillating with a circatidal rhythm. First, two circalunidian clocks having a period of 24.8 hours and in antiphase generate the tidal cyclicity. In this case, two acrophases are observed per day and can be uncoupled in constant conditions (Palmer and Williams, 1986; Palmer, 2000). This can be applied to the locomotor activity of the crab *Austrohelice crassa* for example. Second hypothesis, an independent circatidal clock is present (Naylor, 1958). For example, it is proved that the circadian and circatidal clocks of the marine crustacean *Eurydice pulchra* are totally separated (Zhang *et al*., 2013). Third, circatidal and circadian clocks are the same TTFL (Enright, 1976). This is the explanation for the rhythm of activity of the plaice *Pleuronectes platessa*. The hypothesis is that plaice has a circadian clock that can be entertained by tide and become circatidal (Gibson, 1973). Similar observations were done on oysters *M. gigas* (Mat et al., 2012, 2014; Tran et al., 2020). In laboratory, in constant darkness and no tides, all genes adopted a tidal periodicity. Under photoperiod and no tide, all have only the circadian pattern (Tran et al., 2020).

In *M. galloprovincialis*, the hypothesis of clock mediating biomineralisation has already been advanced while looking to shell growth patterns of individuals inhabiting Mediterranean lagunas (Andrisoa et al., 2019) (Chapter 1.1). In this type of environment where tides are almost absent, daily incrementation was observed. In laguna, a direct control of the biomineralisation process might occurred, ensured by many variables showing periodic variations such as photoperiod, water temperature, salinity, water depth and wind speed. This observation led to the question of a direct environmental control or a clock-mediated one on shell growth in Mediterranean mussels.

This study aimed to decipher the relation between the environment and periodic shell growth patterns formation using the Mediterranean mussel, *M. galloprovincialis* as biological model. The question of a direct control of the environment or a control by biological clocks was addressed. In order to respond to this question, the potential biological clock of *M. galloprovincialis* has been first identified by implementing a targeted gene expression analysis on mussels sampled at sea and others reared under controlled conditions in aquaria. Potential core genes were targeted as well as three more genes reputed to be related to biological clocks. Genes of photoreceptors such as *Rhodopsin* showed a role in the entrainment of the biological clock in *Drosophila melanogaster* and are a good candidate to study the entrainment by the photoperiod (Senthilan et al., 2019). The arylakylamine-N-acetyltransferase, AANAT, is an enzyme which is involved in the synthesis pathway of melatonin, the time giving hormone in vertebrates (Klein, 2007). Melatonin exhibits circadian synthesis in clams (Zhu et al., 2022). The melatonin could also have a feedback effect on the biological clock by repressing the synthesis of the proteasome degrading repressive element of the TTFL (Vriend and Reiter, 2014). *HSP70* is known to have variation of expression related to temperatures changes in bivalves (Toyohara et al., 2005; Anestis et al., 2010). The valve behaviour, which is considered as one output of biological clocks in oysters, was characterised under targeted conditions of photoperiod and food availability in *M. galloprovincialis* as well (Perrigault and Tran, 2017). The same experimental design was repeated with another set of mussels, for which the formation of growth patterns has been characterised in the same conditions in aquaria and biomineralisation related genes expression was measured. The gene expression analysis concerned biomineralisation process at different levels: the mineral components transport (*i.e., Plasma membrane calcium ATPase* and *Carbonic anhydrase*), the organic matrix synthesis (*i.e.*, *Chitin synthase*, *Chitinase*, *Tyrosinase* (Engel, 2017; Miglioli et al., 2019)), putative inhibitor of formation of the mineral matrix (*i.e., Perlwapin* and *Nacrein* (Treccani et al., 2006; Song et al., 2019)) and a potential regulator of the process (*i.e., Bmp2* (Miyashita et al., 2008; Zhao et al., 2016)).

Material and Method

Study sites and organisms

Mussels (*Mytilus galloprovincialis*) used in this study were sampled between 1 and 3m depth on the anchor chain of the buoy SOLA. The buoy is an autonomous station monitoring oceanological features of the bay of Banyuls (Mediterranean Sea, SW of France) (Figure 33A). The buoy is located half a nautical mile from the coast. Several samplings took place from November 2019 to December 2021 for a total of five experiments summarised in the table 6.

Table 6: Localisation, inputs and outputs tested in function of the experiment.

		Experiment n°1	Experiment n°2	Experiment n°3	Experiment n°4	Experiment n°5
Localisation	*In situ*	**x**				
	In aquaria		**x**	**x**	**x**	**x**
Input tested	Light		**x**	**x**		**x**
	Food availability				**x**	**x**
Output tested	Gene expression	**x**	**x**		**x**	
	Shell growth patterns		**x**			**x**
	Behaviour			**x**	**x**	**x**

Experiment n°1: In situ e*xperimentation*

Over 36 hours, from the 9th of September 2020 at 12:00 p.m. to the 11th of September at 12:00 a.m., ten mussels were collected at SOLA site every four hours (Experiment n°1) (Table 6). A piece of the posterior region of the mantle was sampled and flash-frozen in liquid nitrogen for molecular analysis. In parallel, physico-chemical measurements were made in the water column by the Banyuls Observation Sea Service (BOSS). Water temperature and salinity were measured using a Sea-bird SBE19-plus CTD probe. Each time, water was sampled using 12 L Niskin bottle. The concentration in chlorophyll *a* and phaeopigments were measured by filtering 300 mL on Whatman GF/F 25 mm filters. Pigments were extracted using 90% acetone and concentrations were measured by fluorimetry using Tuner Design 10-AU fluorometer following the Strickland & Parson (1997) protocol. Tides were retrieved from the SHOM website (SHOM, 2020).

Experimentation under controlled conditions

Aquaria of 36 litres were used, supplied in water by a semi-open system. Water was pumped in the bay of Banyuls and filtered at 200 µm before its storage in a buffer tank. After a second filtration at 5 µm, the water was provided to the aquarium by a drip irrigation and the excess left by overflow. Total renewal was done in approximatively 72 hours in order to break the physico-chemical dynamics of the incoming outside sea water. Temperature and salinity remained stable at 16°C and 38, respectively. Light intensity during the illuminated period was 17±3 µmol m^{-2} s^{-1}.

a. Experiments n°2 and 3: Light manipulation

For this experiment in controlled conditions of light (Experiment n°2) (Table 6), mussels measuring between 50 and 60 mm in total length were selected and their epibionts removed. Before being distributed in the aquariums, mussels were marked using calcein dye at a concentration of 150 mg/L during one hour for further sclerochronological analysis (Moran and Marko, 2005). A total of 450 individuals were distributed into nine aquaria in order to get 50 individuals per aquarium (Supplementary Data B Figure S3A). Mussels were acclimatised during 10 days under alternation of light from 06:00 a.m. to 06:00 p.m. and darkness (L:D 12:12) regime. Food was provided once per photoperiodic cycle, at random hours that were generated using the RAND function of Microsoft Excel. Food consisted in the microalgae *Isochrysis galbana* at an initial concentration of 3000 cells/mL (Maire et al., 2007). After the acclimation period, three conditions of light were experimented each in triplicates: continuous light (L:L), constant darkness (D:D) and L:D 12:12. Aquaria were covered with occulting tissue to be totally hermetic to light. Food supply was stopped 48 hours before sampling. Sampling was done on a period of 28 hours every 4 hours from the 11th of December 2019 at 12:00 p.m. to the 12th of December at 04:00 p.m. The edge of the posterior region of the mantle was sampled on five mussels per condition every four hours and conserved at -80°C for molecular analysis. Shells were kept for sclerochronological analysis.

In a later experiment (Experiment n°3) (Table 6), seven mussels were placed by two to three per aquaria for behaviour measurements through valvometry. After two days of acclimatisation under L:D 12:12 condition, mussels were kept 12 days in total darkness condition, after food (*i.e., I. galbana*) was provided each day at random time, for eight days. Finally, the same mussels were kept under L:D condition with light form 06:00 a.m. to 06:00 p.m. for 13 days.

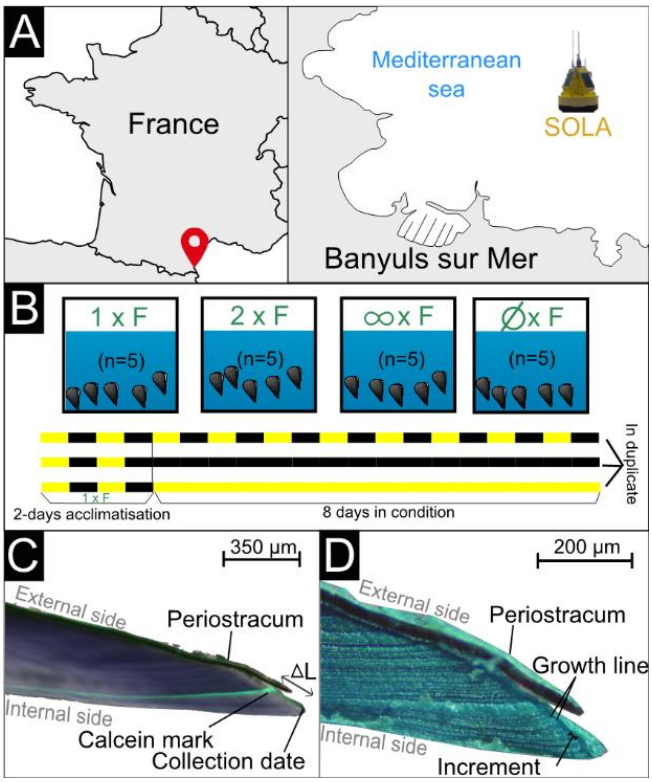

Figure 33: Experimental framework Experimental framework A) Localisation of the study site along the south-east Mediterranean coast of France. At sea, mussels were sampled under the oceanographic buoy SOLA. B) experimental setup for the study of shell growth and behavioural in function of the environment. Experiments were using four aquaria with five mussels for four food availability conditions: fed once a day (1xF), fed twice a day (2xF), fed continuously (∞xF) and never fed (∅xF). At each round of experiment, one condition of was tested (*i.e.*, continuous darkness (D:D), continuous light (L:L) and under the alternation of 12 hours of dark and 12 hours of light (L:D 12:12)). All experiments were duplicated, giving rise to a total of six experiments. They were run over ten days, the two first days were the acclimation phase under L:D 12:12 and 1xF and the following eight in the chosen condition. C) Calcein mark revealed under epifluorescent microscope on a longitudinal cut of shell. The growth during the experiment (ΔL) was measured along the periostracum from the calcein mark to the posterior margin of the shell. D) Mutvei stained longitudinal cut of a shell. The Mutvei etching is revealing the growth pattern (*i.e.*, growth lines and increments) in shell by dissolving calcium carbonate and fixing organic matter.

b. Experiment n°4: Food availability manipulation

For this experiment (Experiment n°4) (Table 6), 160 mussels were distributed into four aquaria on the 25th of November 2021 (Supplementary Data B Figure S3B). The food availability was tested as time-giver using four conditions: fed once a day at 04:00 a.m. (1xF), fed twice a day at 04:00 a.m. and 04:00 p.m. (2xF), fed continuously (∞xF) and not fed (∅xF). Food consisted of a mix of three phytoplanktonic strains (1:1:1); *I. galbana*, *Tetraselmis sp*. and *Rhodomonas salina*. All fed mussels received in total 160 mL of the mixture at a concentration of 4.5x10^{6} cells/mL per 24 hours. Prior to sampling, mussels were acclimatised ten days in total darkness (D:D) and the experimental condition of food availability attributed. Sampling took place over 28 hours and the mantle of five mussels was sampled every four hours.

c. Experiment n°5: Crossed conditions of light and food availability

The experiment n°5 was constituted of a set of six experiments that took place from May 2021 to October 2021 (Figure 33B) (Table 6). For each one, twenty-five mussels were sampled and five were directly sacrificed in order to calculate their condition index (CI). Soft tissues were separated from shell and both were dried in an oven at 65°C for 24 hours and weighted. The ratio between dry soft tissues weight and dry shell weight was calculated in order to get the CI of the organism (Davenport and Chen, 1987; Andrisoa et al., 2019). Difference of CI between mussels at sea at the moment of the experiment and mussels in aquaria was done in order to reduce the effect of seasonality.

Before being distributed in the aquarium, the 20 mussels remaining were marked using calcein dye to measure shell growth through sclerochronological analysis. Among them, 16 mussels were equipped with valvometry sensor (*i.e.*, a magnet and a Hall sensor glued on shell valves) in order to measure their valves aperture in time. Four equipped mussels and one without equipment were placed per aquarium. Two environmental variables (*i.e.*, light; L:L, D:D and L:D 12:12 and food availability; 1xF, 2xF, ∞xF and ∅xF) were tested in a crossed-design experiment and each photoperiodic condition was tested in separated experiment and done twice (Figure 33B). In total, there were eight mussels per experimental condition, four per experiment. Each experiment ran over 10 days in which the two first were acclimation in L:D 12:12 and fed once a day at 04:00 a.m. condition. After 10 days, mussels were sacrificed and soft tissues were removed from shells to calculate their CI. Shells were kept for sclerochronological analysis.

Molecular analysis

a. Total RNA extraction and quantification

The posterior edge of the mantle was sampled for the molecular analysis. RNA was extracted using the Maxwell 16 device using the manufacturer Simply RNA tissue extraction protocol (Promega Corporation, Madison, WI, USA) for samples taken in the experiment n°2. Due to low RNA yield obtained with this technique, TRIzol-chloroform (Invitrogen, Waltham, MA, USA) extraction was done for the other experiments. For this protocol, tissues were ground and homogenised in 500 µL of TRIzol using the FastPrep-24 5G (MP Biomedicals, Irvine, CA, USA). The lysate was centrifuged for 10 minutes at 10 000 rpm and 4°C to collect the supernatant. Then, 100 µL of $CHCl_3$ was added to the supernatant and tubes were mixed well before a centrifugation of 15 minutes at 13 000 rpm at 4°C. The supernatant obtained was kept and 250 µL of isopropanol added. The samples were then vortexed and incubated 10 minutes at room temperature before a centrifugation of 20 minutes at 13 000 rpm and 4°C. The

supernatant was removed and the pellet washed in 50 µL of ethanol 75% followed a centrifugation of 5 minutes at 13 000 rpm at 4°C. This operation was repeated once. Then the pellet was air-dry for 10 minutes at room temperature before being resuspended in 30 µL of water. DNase treatment was applied using the kit DNA-free™ (Ambion; Austin, TX, USA), following the manufacturer protocol.

Concentration and purity were estimated using a NanoDrop spectrophotometer (Nanodrop Technologies, Wilmington, DE, USA) and an Agilent 2100 bioanalyzer (Agilent Technologies, Santa Clara, CA, USA). Gene expression was assessed using the NanoString nCounter™ Gene Expression Assay (NanoString Technologies, Seattle, WA, USA) at the Pôle Technologique CRCT (Toulouse, FR). Twenty-four genes were targeted; ten related to the biomineralisation process, nine related to the biological clock and five housekeeping genes (Supplementary Data A). Probes A and B between 70 to 90 bp long were designed to hybridise to the correspondent targeted mRNA sequence. The set of probes used were designed by IDT (Integrated DNA Technologies, Coralville, IA, USA) (Supplementary Data B Table S5). Probes are constituted of a fluorescent barcode that is read and counted to measure the number of copies and therefore the expression level of the gene.

b. Gene expression rhythm analysis

The number of mRNA counted was normalised following the guidelines of the manufacturer (NanoString Technologies Inc., 2017). Based on the expression of a set of genes, samples considered as outliers were removed using the Spearman correlation coefficient (σ =2.5) and with a PCA test (σ =2.5) as implemented in DiscoRhythm package (Carlucci et al., 2020) running in R (v. 4.1.2) (R Core Team, 2020). Genes expression rhythmicity was assessed using the packages “DiscoRhythm” and “RAIN” (Thaben and Westermark, 2014; Carlucci et al., 2020) in R. In “DiscoRhythm”, cosinor adjustment of the data was used. The package RAIN is complementary as using a non-parametric method that is well suited for biological data as it integrates different peak shapes (Thaben and Westermark, 2014). Tidal range was defined as 12±2 hours and the daily range as 24±4 hours. Multiple testing deviations were applied using Benjamini-Hochberg corrected p-value at 0.05 (Benjamini and Hochberg, 2000).

Valvometry analysis

The behaviour of mussels was recorded using a magnet and a coated Hall element captor glued on each valve of a mussel (Tran et al., 2003). The electric potential difference measured every second was afterward translated into a valve opening amplitude (VOA in %) per hour. The valve opening duration (VOD) was computed by considering valves as open when more than 20% of VOA (Comeau et al., 2018; Bertolini et al., 2021). Actograms were made using the ImageJ plugin ActogramJ (Schmid et

al., 2011). Prior to rhythmic analysis, absence of randomness in the data and absence of stationarity were assessed using an autocorrelation function (ACF) and a partial autocorrelation function (PACF) as implemented in R (Gouthiere *et al.*, 2005; Gouthiere *et al.*, 2005; R Core Team, 2020). Lomb-Scargle periodogram was done on ActogramJ with a threshold p-value at 0.05. Significant peaks were validated using a cosinor model as implemented in the packages "cosinor" and "card" in R (Sachs, 2014; Shah, 2020). The model was statistically validated via a goodness-of-fit test, the normality of the residuals and the homogeneity of their variance (Gouthiere *et al.*, 2005; Cornelissen, 2014). Rhythm was evaluated using an error ellipse test. Percentage of rhythm which is the percentage of cyclic behaviour explained by the model was calculated. In order to assess the presence of imbricated rhythm, residuals were re-injected in a cosinor model and the same tests were done. A cross-validation of significant rhythms was done using the R package "RAIN" (Thaben and Westermark, 2014). Calculations were done at individual and group levels. Rhythmic valve activity was classified according to its period range: daily (24±4 hours), tidal (12±2 hours), bimodal (*i.e.*, both circadian and circatidal) or other.

Sclerochronology analysis

Shells were cut from the umbo to the posterior margin along the maximal growth axis using a Buelher Isomet low-speed saw (Buehler, Lake Bluff, IL, USA). Cut shells were fixed on microscope slides and sliced at 0.5 mm. Samples were grind using sandpapers P120 -P240 -P600 and P1200 and polished using Al_2O_3 powder of 3, 1 and 0.3 µm (Nedoncelle et al., 2013). Calcein mark was observed using an epifluorescent microscope (Olympus BX61, Olympus Corporation, Tokyo, Japan) by exciting the dye at 495 nm (Figure 33C). Then, increments were revealed using a Mutvei solution as described in the chapter 1.1 (Figure 33D) (Schöne et al., 2005). Treated shells were observed using a camera (SONY DF W X700, Sony corporation, Tokyo, Japan) mounted on a microscope (Leitz DIAPLA, Leica Microsystems, Wetzlar, Germany) and reflected light. The software visiolog 6.2 Noesis was used to take pictures. Then increments were counted and measured using the software ImageJ (Rasband, 2020). The number of increments counted were divided by the number of days between two calcein marks to calculate the number of increments formed per day. This rate was classified between daily (1±0.2 increments/day), tidal (2±0.4 increments/day) and other incrementation regime.

Statistical analysis

a. Experiments n°1, 2 and 4

Gene expression variations in time were compared between genes at sea using a ranked Spearman correlation as implemented in R. For better visualisation and groups making, heatmaps were produced using the package Stat v. 4. 1.2 in R.

b. Experiments n°3, 4 and 5

Prior to comparison of measured proxies, conditions of normality and homogeneity were assessed using respectively Shapiro's tests and Levene's tests ("Car" package on R (Fox and Weisberg, 2019)). When respected, the shell growth, valve opening duration (VOD) and ΔCI measured in aquaria under different photoperiodic and food availability conditions were compared using an ANOVA. If conditions of normality were not respected, Kruskal-Wallis rank sum test was used using the package "dunn.test" in R (Dinno, 2017). Behavioural profiles and shell growth patterns were compared using Pearson correlation and simple linear regression as implemented in R. Regression were achieved at the group level and also taking the environmental conditions tested separately. In order to take into consideration average time of each closure period of valves of an individual, the number of valve closures was multiplicated to the valve closure duration (VCD). Valve closure duration is the opposite of the VOD. Smaller was the coefficient, longer was the averaged closure duration.

Results

Gene expression rhythm in the Mediterranean Sea

Putative core biological clock genes and associated genes were successfully described for *M. galloprovincialis* (Supplementary Data A). Most genes were previously described and retrieved based on available mRNA sequences of Mytilidae, notably that of the close-related *M. edulis* (Connor and Gracey, 2011; Chapman et al., 2017; Mat et al., 2020). *Cry2* was retrieved from the oyster *Magallana gigas* (Perrigault and Tran, 2017).

On the 100 samples of mantle analysed in the experiment n°1, ten were considered as outliers based on their gene expression levels for all targeted genes and were removed of further analysis. Among putative core biological clock genes, the positive element *Clock* (RAIN, τ =20h, p=2.3e-4) showed significant daily oscillation of expression (Figure 34) (Supplementary Data B, Table S6). Its expression seemed to decrease after midnight and increased after midday (Supplementary Data B, Figure S5). The second positive element, *Bmal*, did not show expression rhythmicity although its regulator, the gene *Rorb* had a significant daily expression (Cosinor, τ =28 h, p=0.039). Looking to repressor, *Period* expression increased at night and decreased during the day showing a daily expression with a large amplitude (RAIN, τ =24h, p=2e-31). The tidal expression for *Period* was significant although of smaller amplitude (RAIN, τ =12 h, p=0.005). Therefore, this gene showed a bimodal rhythm of expression (Figure 34) (Supplementary Data B, Figure S5). The genes of the two cryptochromes showed tidal expression, similar with water height variations (*Cry1*: Cosinor, τ =14h,

p=0.044 and *Cry2*: Cosinor, τ =13h, p=0.026) (Supplementary Data B, Figure S4 and S5). Looking to the genes related to biological clocks, the photopigment gene *Rhodopsin* showed a bimodal expression (Cosinor, τ =20h, p=0.034 and τ =12h, p=0.023) (Figure 34) (Supplementary Data B, Table S6). *Hsp70* had a daily expression (RAIN, τ =28h, p=0.008) and *Aanat* did not showed rhythmic expression. The expression of the putative cell-autonomous 12 hours clock gene *Xbp1* was not rhythmic.

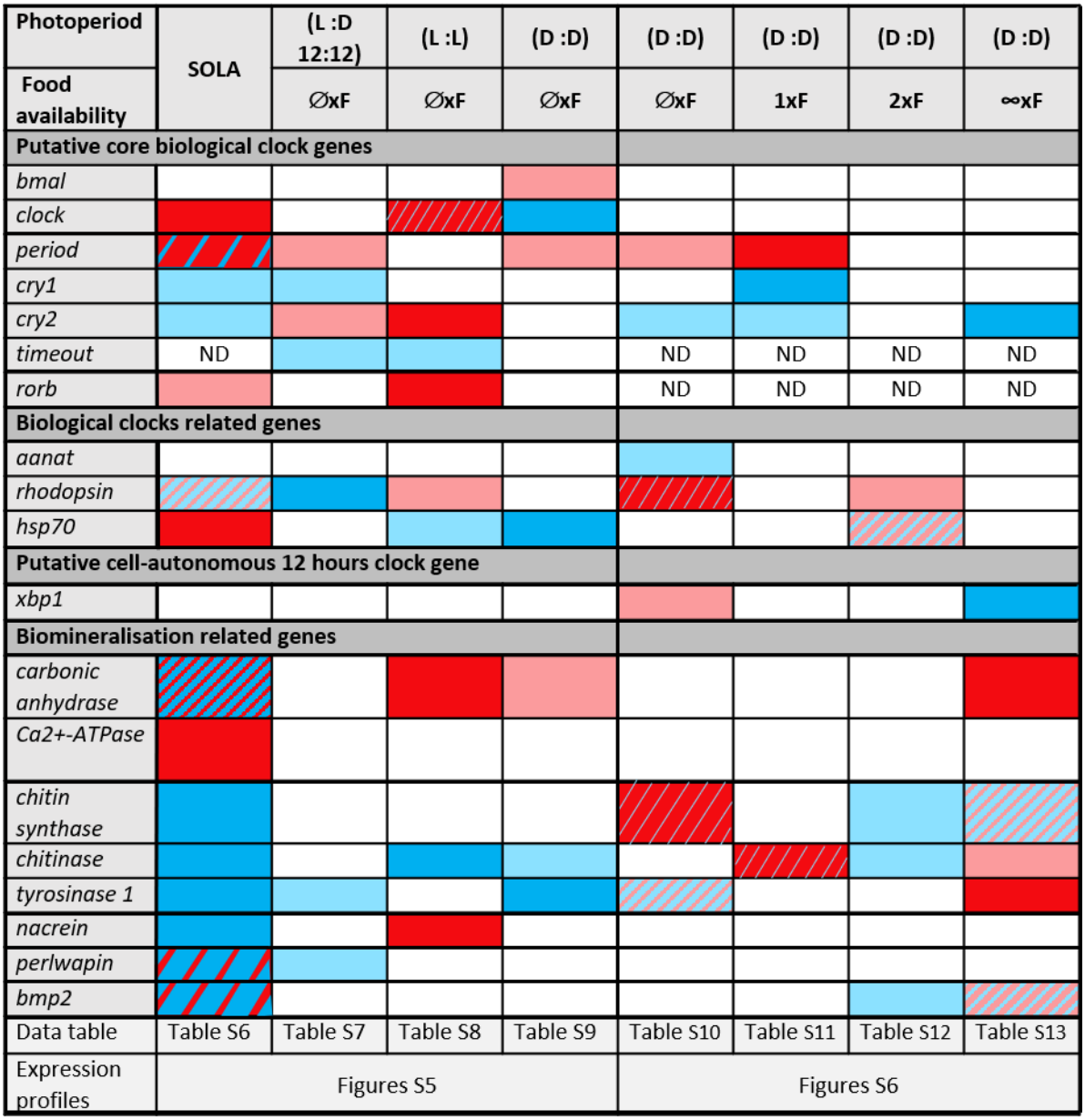

Figure 34: Rhythmicity of expression of biomineralisation and biological clocks related genes. Circatidal rhythmicity is indicated in blue and circadian in red. Two mathematical adjustments (Cosinor and RAIN) were used to test rhythmicity in gene expression. When one adjustment on the two was significant, light blue and light red are used. Bimodal rhythmicity is in mixed colour, the predominant colour corresponds the main rhythm. When no significant rhythmicity was observed, the case is in white. No data are annotated "ND". SOLA corresponds to the experiment at sea. In aquaria, three conditions of light were tested; continuous darkness (D:D), continuous light (L:L) and under the alternation of light (12 hours) and dark (12 hours)(L:D 12:12). Four conditions of food availability were crossed with the photoperiodic conditions: fed once a day (1xF), fed twice a day (2xF), fed continuously (∞xF) and never fed (∅xF).

Among biomineralisation genes, most of them showed tidal expression and similar profiles of expression (Figure 34) (Supplementary Data B, Figure S5). The Spearman analysis grouped five of them (*i.e., Chitinase*, *Tyrosinase*, *Carbonic anhydrase*, *Chitin synthase* and *Perlwapin*) together (Figure 35). All these genes had a peak of expression at low tides (Supplementary Data B, Figure S4 and S5). This was also the case of the chlorophyll *a* concentration which oscillate in antiphase with tides, even if the variations of concentrations were small (*i.e.,* Δ [Chl *a*] = 0.11 mg/m^3) (Supplementary Data B, Figure S4 and S5). *Nacrein* had a tidal expression that was not in phase with the group of genes (Cosinor, τ =11h, p=5.4e-05). Daily oscillation in expression of the calcium transporter *Ca^{2+}ATPase* was observed (RAIN, τ =20h, p=5.5e-04). The regulator *Bmp2* had a bimodal rhythmicity of expression (Figure 34) (Supplementary Data B, Table S6).

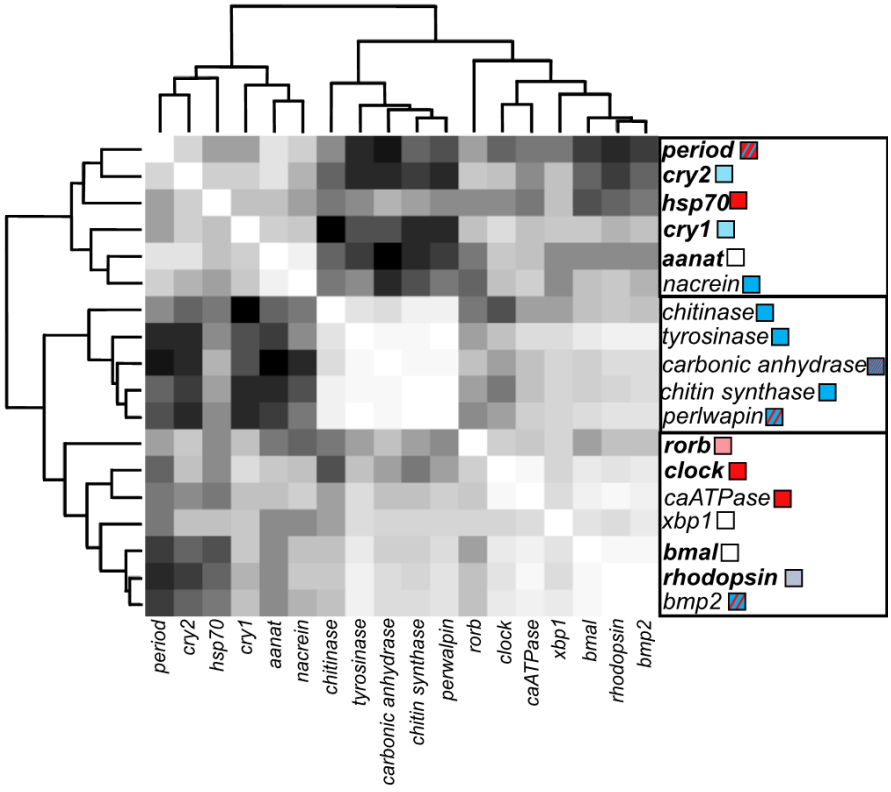

Figure 35: Spearman rank correlation matrix of gene expression in the bay of Banyuls (SOLA). Positive correlations are in white whereas negative are in black. Genes in bold are biological clocks related genes, the others are genes linked to outputs of biological clocks. Coloured squares are representing the periodicity observed. In blue are genes having circatidal expression and in red are genes having circadian expression. Lighter colours represent significant periodicity obtained only on one of the two software used. When both periodicities were present, the width of the stripe represents the p-value of the adjustment (the larger stripe, the lower p-value). White squares represent non-significant p-value.

Spearman analysis showed two other groups than the one composed of tidal expressed genes related to the biomineralisation process. Those were composed of putative core biological clock and biomineralisation related genes (Figure 35). One was formed by the putative negative elements of the auto-regulatory transcription and translation feedback loop (TTFL), *Period*, *Cry2* and the putative light entrainment component *Cry1*. They were grouped with *Nacrein* plus *Hsp70* and *Aanat*. Positive

elements *Bmal* and *Clock* formed another group with *Bmp2* and *Ca2+ATPase* plus *Xbp1*, *Rhodopsin* and *Rorb*.

Gene expression under controlled conditions

a. Light

In the experiment n°2, mussels were reared under three conditions of light: the alternance of 12 hours in dark and 12 hours of light (L:D 12:12), continuous darkness (D:D) and continuous light (L:L). For each photoperiodic regime, 5 mussels were sacrified every four hours over 28 hours (*i.e.,* N=40 per photoperiodic condition). After the removal of the outliers, 37 samples remained in L:D and D:D conditions and 38 in L:L.

Under photoperiodic condition L:D 12:12, most core biological clock genes had a rhythmic expression (Figure 34) (Supplementary Data B, Table S7). Only *Timeout* and *Cry1* had circatidal expressions (*Tim*: Cosinor, τ =10 h, p=0.001 and *Cry1*: Cosinor, τ =10 h, p=0.031) (Figure 34) (Supplementary Data B, Figure S5). The other cryptochrome had a significant daily rythmicity (*Cry2*: RAIN, τ =28 h, p=0.046) and *Period* adopted a unique daily expression rhythmicity (Cosinor, τ =20 h, p=0.044) (Figure 34) (Supplementary Data B, Table S7). The positive elements of the TTFL, *Clock* and *Bmal* did not have rhythmic expression. Under constant conditions of light, the response was different between continuous darkness (D:D) and continuous light (L:L) (Figure 34). Under D:D condition, only *Period* conserved the circadian periodicity previously observed under L:D 12:12 condition (Cosinor, τ =20 h, p=0.029). In D:D, *Clock* exhibited circatidal expression (Cosinor, τ=14 h, p=0.016) and *Bmal* a circadian one (Cosinor, τ =23 h, p=0.019). Under L:L, most rhythmic genes adopted a circadian expression (Figure 34). *Cry2* had a circadian expression (Cosinor, τ =27 h, p=0.045) and *Rorb* (RAIN, τ =24 h, p=0.003) as well. *Clock* kept its circadian expression (RAIN, τ=20 h, p=8.4e-4) and a circatidal component having smaller amplitude (RAIN, τ =16h, p=0.019). *Timeout* kept its circatidal (Cosinor, τ =13h, p=0.013) expression observed under L:D 12:12 condition, with a similar profile (Supplementary Data B, Figure S5). Among genes related to biological clocks, the photopigment *Rhodopsin* (Cosinor, τ =10 h, p=0.016) had tidal patterns in L:D 12:12 and shifted to circadian patterns in L:L (RAIN, τ =28 h, p=0.028). *Aanat* transcripts abundance had no rhythmic variations in the three conditions tested. *Hsp70* had circatidal rythmic expression under constant photoperiodic conditions (D:D; Cosinor, τ =14h, p=0.024, L:L; Cosinor, τ =11h, p=0.016).

Looking to biomineralisation related genes, most had no rhythmic expression when reared in L:D condition apart *Perlwapin* (RAIN, τ =16h, p=0.024) and *Tyrosinase* (RAIN, τ =16h, p=0.026). Both showed circatidal rhythm although they had slightly longer periods than at sea (Figure 34) (Supplementary Data B, Table S7). However, most profiles were similar to those observed at sea (Supplementary Data B, Figure S5). Under D:D condition, *Tyrosinase* (Cosinor, τ =14h, p=0.016) and *Chitinase* (Cosinor, τ =10h, p=0.032) kept their circatidal rhythm of expression observed at sea (Figure 34) (Supplementary Data B, Table S9). *Carbonic anhydrase* showed a circadian expression (RAIN, τ =28h, p=0.038). Under L:L condition, *Chitinase* (Cosinor, τ =14h, p=0.012) kept the same periodicity observed in D:D (Figure 34). In this condition, *Carbonic anhydrase* had a circadian expression (RAIN, τ =24h, p=0.004) and *Nacrein* as well (RAIN, τ =24h, p=4.5e-5) (Supplementary Data B, Table S8).

b. Food availability

In the experiment n°3, the food availability cue was tested using four feeding conditions. Looking to core biological clock genes, when fed once a day (1xF), *Period* showed a daily expression (RAIN, τ =24h, p=9.1e-4) (Supplementary Data B, Table S11) (Supplementary Data B, Figure S6). The two cryptochrome genes showed circatidal expression (*Cry1*: Cosinor, τ =14h, p=0.013 and *Cry2*: Cosinor, τ =12h, p=0.032). No other core biological clock gene showed rythmic expression and their expression profiles were not affected by feeding modalities (Supplementary Data B, Table S11) (Supplementary Data B, Figure S6). In 2xF condition, no core gene had rhythmic expression (Supplementary Data B, Table S12). When mussels were continuously fed (∞xF), *Cry2* showed circatidal expression (Cosinor, τ =14h, p=0.035) (Supplementary Data B, Table S13). When not fed (∅xF), *Period* (Cosinor, τ =21h, p=0.035) and *Cry2* (Cosinor, τ =10h, p=0.002) observed the same periodicity than 1xF condition (Figure 34) (Supplementary Data B, Table S10).

Among genes related to biological clocks, when fed once a day (1xF) none had rhythmic expression. When fed twice a day (2xF), *Rhodopsin* showed circadian expression (RAIN, τ =28h, p=0.049) and *Hsp70* showed bimodal expression (Cosinor, τ =23h, p=0.019 and Cosinor, τ =14h, p=0.038). Under ∅xF, *Rhodopsin* gene had predominantly a circadian expression (RAIN, τ =20h, p=0.010) and *Aanat* a circatidal expression (Cosinor, τ =10h, p=0.028). The expression of the putative cell-autonomous 12 hours clock gene *Xbp1* was circatidal in ∞xF (Cosinor, τ =13h, p=0.019) and circadian in ∅xF (RAIN, τ =28h, p=0.009).

Rhythmicity was lost for most genes of biomineralisation under 1xF and ∅xF conditions (Figure 34). When fed once per day, *Chitinase* gene had a significant daily periodicity of expression (Cosinor, τ

=20h, p=0.004) with a minor circatidal component (RAIN, τ =16h, p=0.013). When in 2xF condition, *Bmp2*, *Chitin synthase* and *Chitinase* had a tidal expression (Figure 34). When in ∞xF condition, contrarily to what has been observed in all the other photoperiodic and food availability conditions, genes had mostly circadian or bimodal rhythm of expression (Figure 34). In this condition, most profile of expression showed a peak of expression at midnight (*i.e*., *Bmp2*, C*hitin synthase*, P*erlwapin* and *Tyrosinase*) (Supplementary Data B, Figure S6). When never fed, *Chitin synthase* had a circadian rhythm of expression (Cosinor, τ =20h, p=0.005), with a minor circatidal component (RAIN, τ =16h, p=0.01). *Tyrosinase* also showed bimodal profile but with smaller amplitudes and at the limits of the ranges of circadian (RAIN, τ =20h, p=0.01) and circatidal (RAIN, τ =16h, p=0.008) definitions.

Valve aperture analysis under controlled conditions

a. Light

The activity of the valves was recorded for a group of mussels (N=7) sampled in the bay of Banlyus and directly put under constant darkness (D:D) and then the alternance of light and dark (L:D 12:12). Under D:D condition, the rhythm had smaller amplitude and was bimodal at the group level (RAIN, τ =12h, p=1.46e-09 and τ = 27h, p=9.35e-10) (Figures 36A-B). Five mussels on seven had no rhythmic behaviour (Figure 36C). Among the two rythmic individuals one showed a circadian behaviour with a period of 26 hours and the other one a circatidal behaviour with a period of 12 hours. Under photoperiodic conditions (L:D 12:12) mussels exhibited a daily activity, being closed during the day and open at night (RAIN, τ =24h, p=3.52e-57) (Figure 36A-B). Looking at the individual level, the majority of mussels (4/6) had a daily behaviour. One other mussel exhibited a circatidal behaviour and another one had no rhythm (Figure 36C). Interestingly, the mussel showing a circatidal behaviour was the same under L:D and D:D conditions.

b. Crossed conditions of light and food availability

The valve activity was tested in a separated set of experiments crossing photoperiodic and food availability conditions. The number of individuals studied varied between conditions because of material failures (*i.e.,* loss of the magnet or sensor glued on the shells) (Figure 37). Valve opening duration (VOD) was not different in between conditions of light (χ^2, n= 64, p>0.05) whereas it was significantly lower when never fed (χ^2, n= 64, p<0.001).

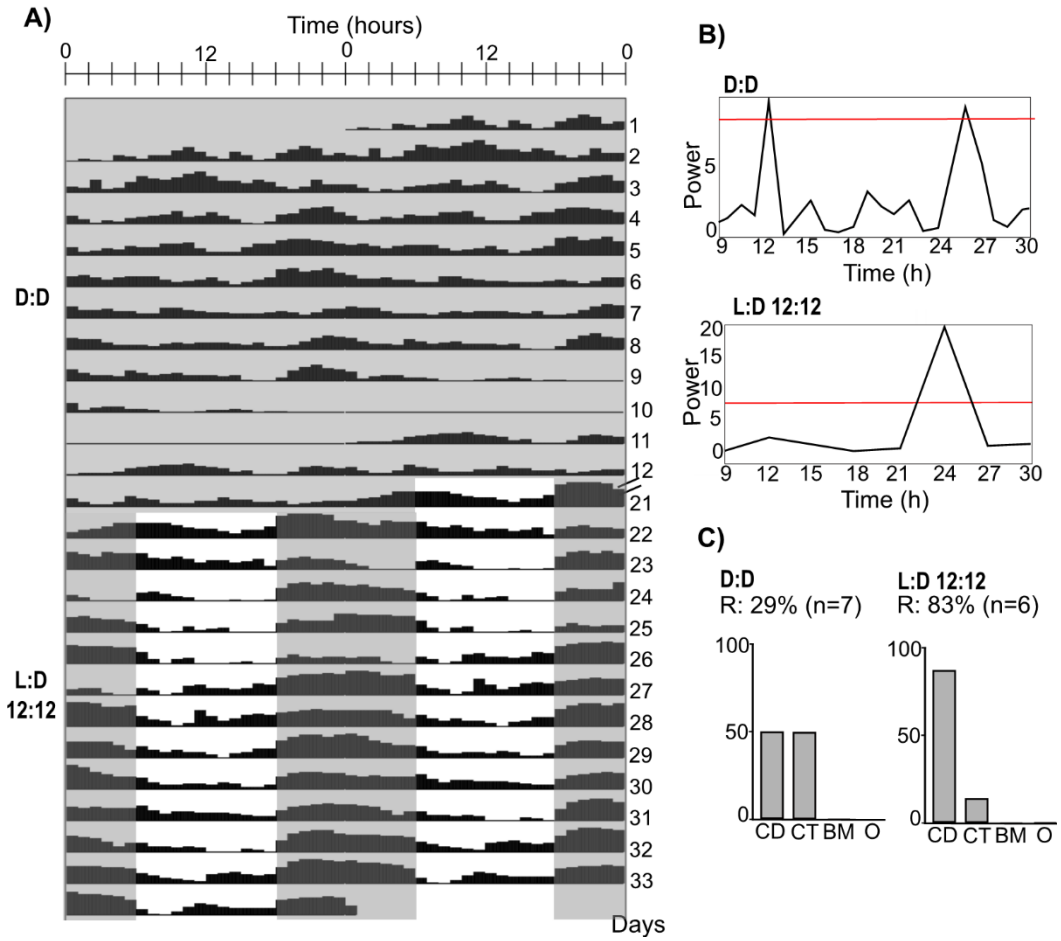

Figure 36: Valve activity of mussels reared under two conditions of light. A) Double plotted actogram of mean valve opening amplitude (VOA) of mussels (N = 7) reared under two photoperiodic conditions. Valve opening amplitude was averaged in percent per hour. Mussels were first put in constant darkness (D:D) for 12 days. Then after 8 days of random feeding in D:D, they were put for 13 days under the alternance of light and dark condition (L:D 12:12) which was an alternance of 12 hours of light and 12 hours of dark. Grey shadings correspond to the darkness phase. B) Lomb-Scargle periodograms established with the mean values of VOA for each photoperiodic condition, peaks above the red line are significant. C) Behavioural rhythmicity expressed at the individual level, rhythmicity was tested and classified for rhythmic individuals (R, in percent) in circadian (CD), circatidal (CT), bimodal (BM) or other (O) periods.

The behaviour recorded was averaged to get a pattern over 24 h per condition (Figure 37). In 2xF condition, significant strong tidal behaviour was observed in each photoperiodic condition at group level (RAIN, τ =12h, $p<0.001$) (Figures 37, A2, B2 and C2). At the individual level, most individuals studied showed rythmic behaviour (*i.e.,* 5 mussels/5 in L:D, 3/4 in D: D and 7/8 in L:L). When under 1xF, mussels showed daily behaviour in all experiments although the period was shorter under L:D condition (L:D; RAIN, τ =20h, $p<0.001$, D:D; RAIN, τ =24h, $p<0.001$ and L:L; RAIN, τ =24h, $p<0.001$). At the individual level most mussels exhibited rhytmic behaviour (*i.e.,* 2 mussels/2 in L:D, 6/7 in D:D and 4/6 in L:L) (Figures 37, A1, A2 and A3). Mussels opened their valves two to three hours after getting the food in D:D and L:L when fed (*i.e.,* 06:00 to 07:00 a.m. and 07:00 to 08:00 p.m.) which was not the case in L:D regime, in which they opened at the time of feeding or a bit before, at 03:00 p.m. When in

1xF condition similar behaviours were observed, the peak of opening at 03:00 p.m was also visible in L:D condition (Figure 37A). Under constant photoperiodic conditions (D:D and L:L) the peak at 07:00 a.m., three hours after feeding, was also present (Figures 37, B1 and C1).

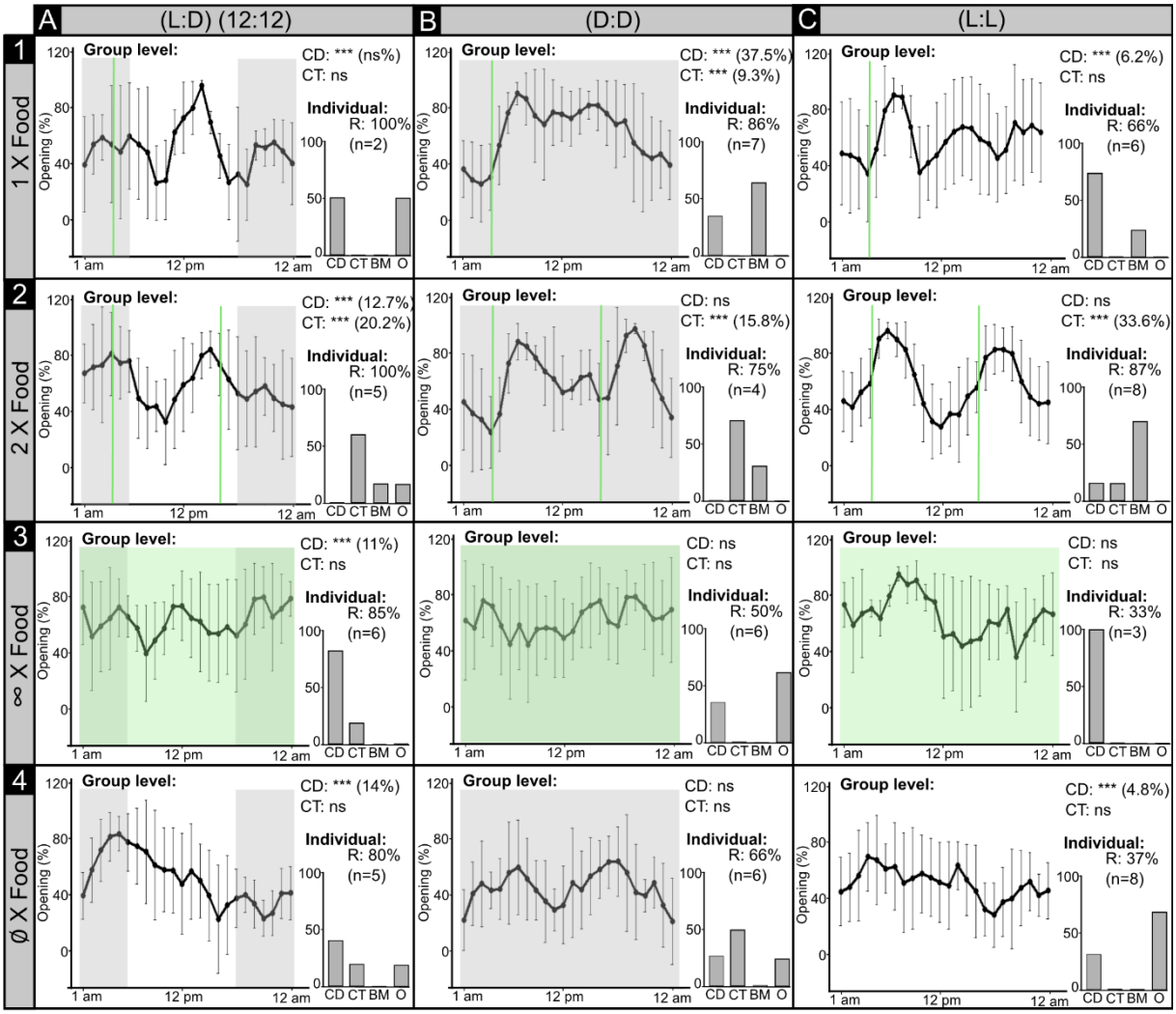

Figure 37: Mean valves opening amplitude (VOA) of mussels under controlled environments during eight days. Grey shading indicates dark phase and light phase is in white. Feeding time is indicated in green. Circadian (CD, 24h+/-4h) rhythmicity and circatidal (CT) (12h+/-2h) one were statistically tested within a group and the percentage of rhythmicity calculated. At the individual level, rhythmicity was tested and classified for rhythmic individuals (R) in circadian (CD), circatidal (CT), bimodal (BM) or other (O) rhythmicities. Significance levels: ns: $p>0.05$; *: $0.05 \geq p \geq 0.01$; **: $0.01 > p \geq 0.001$; ***: $p < 0.001$.

Under constant food condition (∞xF and ∅xF) and L:D condition, the group had a daily behaviour (RAIN, τ =25h, $p<0.001$) and most specimens were rythmic (∞xF: 5/6 and ∅xF: 4/5) (Figures 37, A3 and A4). Under constant photoperiod (D:D and L:L) and constant food availability conditions (∞xF and ∅xF), most mussels did not have rythmic behaviour (*i.e.*, 3 mussels/6, 2/3, 2/6 and 6/8) (Figures 37, B3, B4, C3 and C4).

Shell growth patterns under crossed conditions of light and food availability

Due to failure in the calcein dye revelation or readibility of growth patterns after Mutvei treatment, less than 10 individuals were analysed in the experimental conditions tested. Shell growth rate and condition index were measured in different conditions of photoperiod and feeding in aquaria. No significant difference in CI were observed between conditions (χ^2, n= 116, p>0.05). Shell growth rate of mussels was significantly lower in L:L condition in all feeding regime (χ^2, n= 116, p<0.01), this was also the case when never fed in all photoperiodic conditions (χ^2, n= 116, p<0.01) (Figure 38).

The number of increments formed per day was measured to discriminate daily increments (*i.e.,* 1±0.2 increments/day), tidal ones (*i.e.,* 2±0.4 increments/day) or other types of incrementation in function of the condition tested (Figure 38). As seen with valvometry profiles, when fed twice per day (2xF), mussels tended to adopt a tidal incrementation (*i.e.,* 5 shells/8 under L:D, 7/10 under D:D and 8/9 under L:L) (Figures 38; 2A, 2B,2C). Similar observations could be made on shells from mussels reared under continuous light (L:L) (*i.e*., 8/8 under 1xF, 8/9 under 2xF, 2/4 under ∞xF and 6/9 under ∅xF) (Figures 38; 1C, 2C, 3C, 4C). Under photoperiodic conditions (L:D), the number of increments formed was highly variable, even for mussels fed twice a day (2xF) (Figures 38; 1A, 2A, 3A, 4A) (Supplementary Data B, Table S14). In this condition, many individuals showed other type of incrementation patterns than daily or tidal. When fed once per day in (D:D), no type of incrementation was clearly identified (Figure 38, 1B). Under continuous darkness and constant food availability, mussels tended to form two increments per day when continuously fed (*i.e.*, 6/10 mussels), whereas they shifted to daily or other patterns when never fed (*i.e.*, 3/6 mussels had another incrementation pattern and two had daily incrementation).

Comparison of growth patterns and valve activity under crossed conditions of light and food availability

Behaviour and growth patterns under crossed conditions of photoperiod and food availability were measured on the same individuals, so that putative relationships between proxies could be assessed (Supplementary Data B, Tables S14, S15 and S16). The number of increments formed was positively correlated with growth (Pearson, n= 45, p<0.05) and negatively correlated with the valve closure duration (VCD) (Pearson, n= 45, p<0.05). Regression showed that at the group level, the growth explained 7.3 % of the variation observed (R^2 = 0.07, n= 93, p=0.005) while VCD explained 7.5 % of the variation in the number of increments (R^2 = 0.07, n= 45, p=0.04). Looking to conditions tested individualy, the relationship between growth and increments were conserved only under D:D and ∞xF

conditions (DD: R^2 = 0.24 , n = 31, p = 0.003 ; ∞xF: R^2 = 0.19, n = 20, p= 0.03). At condition level, the VCD only explained the number of increment in ∅xF condition (R^2 = 0.27, n= 12, p=0.04). However the number of increments formed was not explained by the number of closure observed (R^2 = -0.01, n= 45, p>0.05). The coefficient outcompassing the average duration of a closure explained 6.12% of the variability observed in the number of increment formed at group level (R^2 = 0.06, n= 45, p=0.05). This was not the case while looking to separated conditions. When taking behavioural rythmicity and incrementation periodicity, no significant relation was observed.

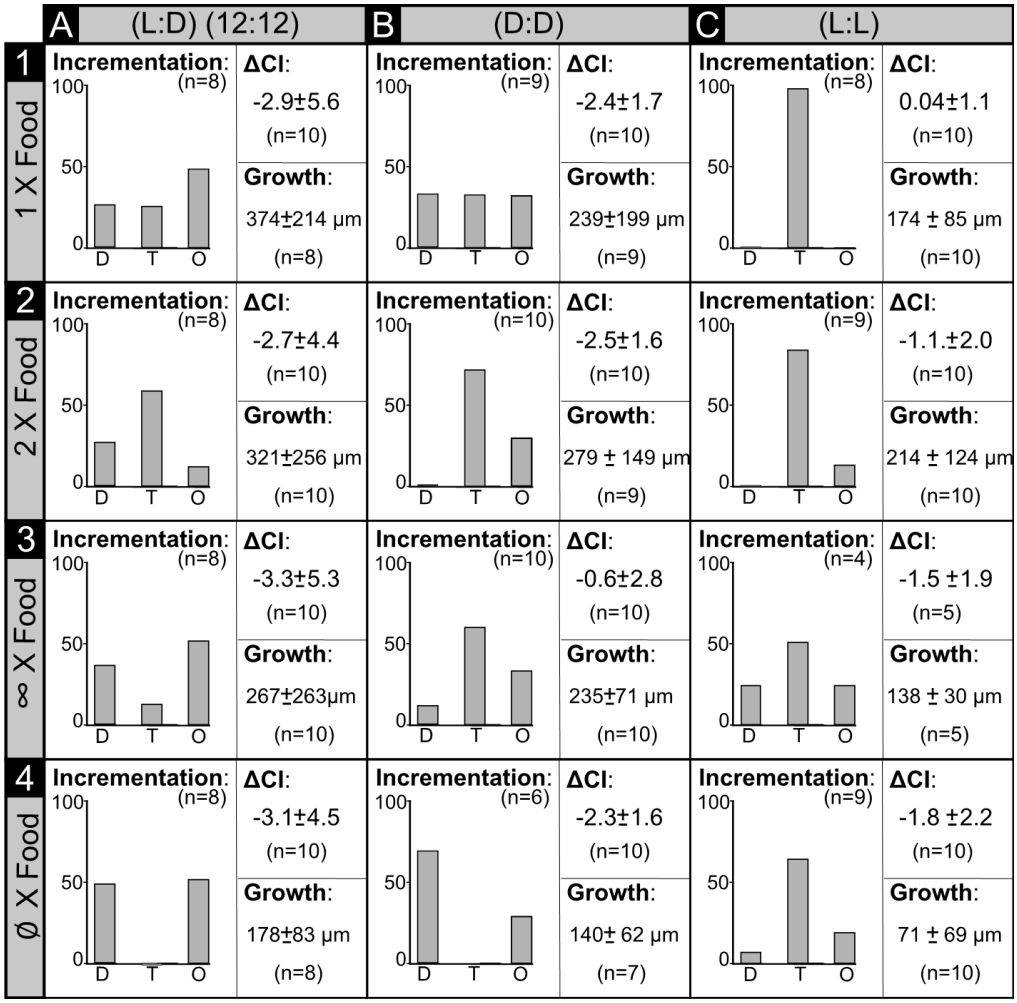

Figure 38: Incrementation, growth and condition index of mussels under controlled environment during ten days. Three photoperiodic conditions were tested; continuous darkness (D:D), continuous light (L:L) and under the alternation of light (12 hours) and dark (12 hours) (L:D 12:12). Four conditions of food availability were crossed with the photoperiodic conditions; fed once a day (1xF), fed twice a day (2xF), fed continuously (∞xF) and never fed (∅xF). Proportion of individuals forming daily (D) (1±0.2 incr./d), tidal (T) (2±0.4 incr./d) or another (O) increments were plotted. The mean difference of condition index (CI) was calculated in function of the CI of mussels at sea at the moment of the experiment.

Discussion

In this study, we aimed to better understand the control of the environment on the shell growth pattern formation. Two main hypotheses were proposed based on literature: i) The direct control by environmental variations and ii) the mediation by biological clocks (Richardson et al., 1980; Schöne, 2008; Louis et al., 2022). Biological clocks are auto-regulatory transcription and translation feedback loops (TTFL) synchronised by environmental variables (Aschoff, 1981; Dunlap, 1999). In bivalves the homologous genes constituting the TTFL were identified in several bivalves but the biological clock of *M. galloprovincialis* was not yet. Biological clocks synchronise many physiological and behavioural processes (Dunlap, 1999). In bivalve the valve activity has been proved to be an output of biological clocks of oysters and clams (Mat et al., 2012, 2016; Perrigault and Tran, 2017; Perrigault et al., 2020). Two other hypotheses were tested in this work: i) the control by a cell autonomous timekeeping mechanism described in mammals and generating 12-hours periodicity (Zhu et al., 2018; Pan et al., 2020) and ii) the indirect control by the valve activity on the control of the growth pattern formation as behavioural output of biological clocks are often subject to the "masking" effect of the environment (Mrosovsky, 1999; Helm et al., 2017).

Mytilus galloprovincialis *biological clock identification*

a. The auto-regulatory transcription and translation feedback loops

The expression of putative core biological clock genes and associated genes variation in time was assessed in the mantle of mussels sampled in the bay of Banyuls. Most potential genes composing the TTFL showed rhythmic expression but on different periods. Looking to potential activators, *Bmal* did not showed rhythmic expression whereas its potential activator *Rorb* and the second positive element, *Clock*, had a daily expression. Looking to repressors, tidal expression was observed for *Cryptochrome 2* and *Period* had a bimodal expression with a daily period having a larger amplitude. *Cryptochrome 1* which is involves in the entrainment by light had a tidal expression. Spearman rank correlation grouped activators together and the repressors in another group. Variability in periodicity observed *in situ* in expression of potential core genes of the biological clock is not an exception and is often observed, even in highly rhythmic environments (Schnytzer et al., 2018; Mat et al., 2020; Tran et al., 2020). In tidal environment, homologues of canonical circadian clock of *M. gigas* showed different periodicities of expression likely entrained by two zeitgebers; the photoperiod and tidal cues (*i.e.*, mechanical vibration and/or water pressure) (Perrigault et al., 2020). Looking to genes related to

biological clocks, mussels from the bay of Banyuls, *Rhodopsin* which is involved in the light transduction (Senthilan et al., 2019) showed a bimodal expression. In oysters, tidal rhythmicity in expression of *Rhodopsin* was related to the valve activity that regulate the light availability (Tran et al., 2020).

Beside observations made on mussels sampled at sea, gene expression was measured under controlled environment to address the endogenous nature of the rhythm. Therefore, experiments in aquarium were achieved under different conditions of light. Under constant photoperiodic conditions, genes showed different profiles. In L:L, *Cry2*, *Timeout* and *Rorb* showed circatidal or circadian rhythmicity in their expressions. *Clock* adopted a bimodal expression with a predominant circadian component. On the contrary under D:D, *Clock, Bmal* and *Period* showed circadian or circatidal expression in the experiment n°2. In oysters, in D:D putative core genes of the TTFL adopted circatidal expression whereas in *M. edulis* a circadian expression was observed demonstrating the endogenous nature of the clock (Chapman et al., 2020; Tran et al., 2020). Also, under L:D 12:12, rhythm of expression in the mantle was different than observed at sea. The potential activators including *Rorb* had no rhythmic expression and the repressors had circatidal or daily expression. Still *Rhodopsin* showed clear circatidal profile of expression. Change in expression in aquarium compared to the natural environment was previously observed in oysters that shifted to only daily expression, likely due to the absence of tidal cue (Tran et al., 2020). When taking the feeding time as time-giver, tidal, daily and bimodal responses were observed. In 2xF, no core gene showed rhythmic profiles of expression. Therefore, in *M. galloprovincialis* the expression profile did not give a clear response about the endogenous nature of the rhythm. Similar observations were made in deep-sea mussels where poor rhythmic expression of identified core biological clock genes were observed likely related to a high inter-individual variability and low expression levels (Mat et al., 2020). The high inter-individual variability observed in *M. galloprovincialis* might mask putative rhythms of expression. In aquaria, less replicates were done per sampling time than at sea *(i.e*., ten at sea and five in aquaria). This could be at the origin of the smaller amplitude of oscillations of genes expression in aquaria in comparison with measurements taken at sea and then to the lower number of rhythmic genes observed.

To summarise *M. galloprovincialis* has homologs of core molecular actors of the TTFL sequences in its genome. Their expressions were rhythmic at sea although they did not have the same periodicity. In aquaria experiments did not give clear response about the endogenous nature of daily and tidal rhythm of gene expression and potential time-givers.

b. Is the valve activity an output of biological clocks?

In many organisms, rhythmic behaviour is controlled by biological clocks (Bartness and Albers, 2000; Bulla et al., 2017). The control by biological clocks of the valval behaviour in bivalve has been demonstrated in *M. gigas* and *C. islandica* (Mat et al., 2012, 2014; Perrigault et al., 2020; Tran et al., 2020). In this study, mussels sampled at sea and placed in D:D condition showed a bimodal behaviour at group level. Five mussels on seven lost their rhythmic valve activity and group rhythmicity observed probably reflected the behaviour of the two rhythmic individuals. The same group placed in L:D 12:12 condition showed a daily behaviour. This behaviour rhythmicity was previously observed *in situ* in subtidal environments (Comeau et al., 2018; Trusevich et al., 2021). However, on the six mussels observed, one had a circatidal behaviour in this study. This situation has been previously observed in the Ria de Arousa where on eight mussels studied, one has tidal valve activity whereas the others had daily activity (Comeau et al., 2018). Authors suggested that this mussel was deeper and did not have access to light variations. It is less likely happening in aquaria although mussels might not have the same access to enlightenment in function of their orientation in the aquarium. Therefore, the photoperiod might have a direct effect of the valve activity of *M. galloprovincialis*.

Food-entrained TTFL has been previously hypothesised in clam *Austrovenus stutchburyi* based on a circatidal food-anticipatory activity (FAA) in constant environmental condition (Williams and Pilditch, 1997). In this study, mussels adopted the tempo of nourishment when fed once (1xF) and twice per day (2xF). Valves opened few hours after the feeding time unless in L:D 12:12 cycles, not showing FAA. Moreover, under constant condition (*i.e.*, ∞xF and ∅xF) most mussels did not have rhythmic behaviour. Looking to crossed conditions of light and food availability, the food seemed to be a stronger driver of valve activity than the light.

However, under constant conditions of photoperiod and food availability, some individuals kept a rhythmicity in their valve activity, characterised by a large range of period (10 to 30 hours). In consequence, periodicity at the group level could be masked as mussels are not synchronised anymore. Asynchronization in behaviour was already described in mussel population inhabiting the Ria of Vigo (Galicia, Spain) and the bay of Sevastopol (Black Sea) (Comeau et al., 2018; Trusevich et al., 2021). Interestingly, similar observations were made on the invasive crab *Carcinus maenas* (Warman and Naylor, 1995). Individuals were placed under free running conditions after entrainment based on circatidal cycles of salinity, temperature and pressure in 120° antiphase. On the 39 individuals tested, 14 were arrhythmic. The others showed a large variability of response, with one to three peaks of activity over 24 hours in function to a response to one, two or all three environmental zeitgebers tested. The authors suggested multiple clocks control influenced by different environmental variables

of the activity of the crab (*i.e.,* salinity, temperature and pressure) (Warman and Naylor, 1995; Naylor, 1996). However, no study has been realised at the molecular level and pattern observed could not be linked to the canonical TTFL.

Regarding gene expression profiles obtained in our experiment and the behaviour observed, in both cases the response was variable. Variability in behavioural response has been pointed out for *M. galloprovincialis* inhabiting the Venice laguna and related to a weak biological clock (Bertolini et al., 2021). Similar observations were made on oysters *M. gigas* based on their behaviour (Mat et al., 2012). A weak circadian oscillator is characterised by i) a large range of entrainment in the synchronised state and subsequently a decreased resynchronisation time to a zeitgeber shift and ii) less stable rhythmicity under constant conditions (Gwinner and Brandstätter, 2001). Both postulates were observed while looking to the behaviour of *M. galloprovincialis* indicating that the biological clock of *M. galloprovincialis* could be qualified of weak. In this study, based on behavioural aspects the endogenous nature of daily and tidal rhythms were observed showing that there are one or two clocks system in *M. galloprovincialis*. However, gene expression analysis gave no clear results.

c. Invasiveness potential and plasticity of the biological clock

Biological clocks could allow organisms to anticipate predictable change in their environment, therefore increasing their fitness (Dodd et al., 2005; Nikhil and Sharma, 2017; Krittika and Yadav, 2019). However, too rigid clock system could be disadvantageous for the organism, therefore balance with plasticity is required (Helm et al., 2017). The ability of *M. galloprovincialis* to develop successfully in several environments suggests its clock might be easily modulated by the environment, so be rather plastic than rigid. Individual-specific response to a common environment suggests different sensitivity and reaction norm within individuals (Helm et al., 2017). Inter-individual variability observed in gene expression is likely linked to genetic and/or epigenetic variations that impact the expression (Helm et al., 2017; Huang et al., 2017; Eirin-Lopez and Putnam, 2019). Pan-genome analysis revealed that the genome of *M. galloprovincialis* is composed of around 20 000 genes subject to absence/presence alongside to a set of 45 000 “core” genes (Gerdol et al., 2020). This was advanced as a possible origin of the resilience and invasiveness of the species. At the expression level, huge variations in genes expression between individuals was also observed looking to fast and slow growing phenotypes in a population (Prieto et al., 2019). Both *C. maenas* and *M. galloprovincialis* showed a large range of periodicity in their behaviour. They have in common their large invasive success, being set up in many environments (Branch and Steffani, 2004; Compton et al., 2010). Plasticity of their clock might be

favouring their invasiveness potential. This hypothesis was already advance for *M. gigas* as this species has a large geographical repartition as well (Mat et al., 2012).

In conclusion, *M. galloprovincialis* putative clock seemed to be plastic and easily modulated by the environment. The weakness of the clock encompasses the time of response to an environmental change and its stability. Therefore, both are complementary. Moreover, consistently with previous genomic and transcriptomic studies, response to the environment looked highly variable between individuals of a same population. The combination of both might lead to a large variability of individual timekeeping response to an environment.

Control of biomineralisation rhythm in Mytilus galloprovincialis

Genes related to biomineralisation exhibit a rhythmic expression, mostly tidal in the case of mussels from the bay of Banyuls. Characterised by a tidal gene expression, there were genes involved in the chitin synthesis and remodelling (*i.e., Chitinase*, *Chitin synthase*, *Tyrosinase*) (Engel, 2017; Miglioli et al., 2019) and Nacrein an inhibitor of the precipitation of $CaCO_3$ (Song et al., 2019). *Perlwapin* and *Bmp2* genes had bimodal expressions with stronger tidal oscillations modulated by daily oscillations. Perlwapin is located between the tablet of nacre and is possibly inhibiting the growth of nacre in the abalone *Haliotis laevigata* (Treccani et al., 2006). In *M. galloprovincialis*, the PERLWAPIN has been identified but its action on calcium carbonate deposition is unknown (Marie et al., 2011; Zhang and Chen, 2012). On the contrary, Bmp2 is known to promote the biomineralisation (Miyashita et al., 2008; Zhao et al., 2016). Together with *Carbonic anhydrase*, all those genes exhibited an expression that oscillated in phase with the chlorophyll *a* concentration and in antiphase with tide. Tidal expression of *Nacrein* at sea has been previously observed in *Pinctada fucata*, related to tidal cues (Miyazaki et al., 2008). In *M. galloprovincialis* as observed in *P. fucata*, *Nacrein* had a peak of expression at low tide. Only *Plasma membrane calcium ATPase* had a circadian expression. This gene is related to calcium ion transport inducing an increase of calcium ions concentration in the extrapallial fluid (Hüning et al., 2013). However, this is not the only calcium transporter supporting the calcification process in bivalves and is less tightly linked to the biomineralisation process genes previously described. As genes directly involved in the biomineralisation process did not show similar profiles and periodicities than potential core biological clock genes, direct control of the biomineralisation by clock genes expressions is less likely than a direct effect of the environment.

This was confirmed by the experiments in aquaria, first the effect of the L:D cycles was tested. It showed that in L:D condition, most genes linked to the biomineralisation process lost the rhythm of expression observed at sea (*i.e.*, *Carbonic anhydrase*, *Plasma membrane calcium ATPase*, *Chitin*

synthase, *Chitinase*, *Nacrein and Bmp2)*. However, profiles of expression were similar than the ones at sea with a lower expression at night. In constant photoperiodic conditions, most genes expression were arrhythmic and rhythmic genes showed circatidal or circadian expression. The relationship with the food availability was never observed when looking to gene expression in function of the food distribution. Profiles of expression showed antiphase pattern with a decrease of the expression when food was given under 1xF and 2xF conditions. Rhythmicity of expression was lost in most conditions except in continuous feeding (∞xF) condition where a peak of expression was observed at midnight for half targeted genes (*i.e.*, *Bmp2*, *Chitin synthase*, *Perlwapin*, *Tyrosinase*). Therefore, our results suggest that the gene expression rhythm observed at sea might be related to another environmental variable than photoperiod or food availability. As observed at sea, genes linked to the biomineralisation process almost never had similar profiles of expression than potential core biological clock genes. Even if tidal range are small in the bay of Banyuls, this environmental variable might be a time-giver for the biomineralisation process as reported in *P. fucata* (Miyazaki et al., 2008). Another possibility is a response to an innate physiological control.

In the recent years, another cell-autonomous 12 hours clock regulation of gene expression was described in mammals (Zhu et al., 2018). XBP1s was suggested as regulator and proved to be independent from the canonical biological clock in mice (Pan et al., 2020). In this study, *Xbp1* showed no rhythmicity of expression in all conditions tested or had circadian and circatidal with small amplitudes respectively in ∅xF and ∞xF. This indicated that based on our data, this timekeeper was not rhythmic in the mantle and therefore not controlling the biomineralisation process.

The observation of the growth patterns of the shell of mussels reared under controlled photoperiod or food availability did not allow to establish a correlation between biomineralisation and environmental rhythmicity. However, some conditions showed stronger effects on incrementation of shells. Most individuals showed tidal incrementation when fed twice per day (2XF) or under constant light (L:L). Those periodicities were not observed at the molecular level. Also, as under constant conditions, increments were still formed indicating a probable internal control of the biomineralisation rhythmicity. As the endogenous control or the direct environmental control did not solely seem to explain the incrementation pattern observed, both might be involved, as suggested by Richardson (1988, 1989). In his work he defined in both *Ruditapes philippinarum* and *M. edulis* two types of growth line, named weak and strong. Strong lines were related to direct environmental control, notably by food availability, and weak lines are the result of an innate control. In both species, a large variability in incrementation periodicity was observed in individuals inhabiting the same environment. High variability in growth patterns were also observed in shells of *M. galloprovincialis* in this study. In studies made by Richardson (1988, 1989), the origin of this variability was linked to the innate control of the

biomineralisation and showed by a great correlation between the growth and the number of increments formed. However, in the present study the linear regression revealed that the number of increments was poorly explained by the growth.

Another hypothesis, which implies an indirect control of the biomineralisation process by biological clocks might occur involving the valve activity of mussels. In this study, we showed a large variability in valve activity, probably related to a plastic biological clock oscillator and showing a large reaction range to an environment. As growth lines are probably formed during the closure of the valves (Lutz and Rhoads, 1977), the number of closures observed was compared to the number of increments. Among our experiments, the number of closures never explained the growth patterns observed. This might be related to the duration of closure as the valves closure duration (VCD) was correlated to the growth line formation. In theory, longer is the closure duration, longer would be the decalcification and then stronger would be the resulting growth line. To test this hypothesis the number of closures was multiplicated to the VCD in order to get a coefficient indicating the average duration of closure. However, no significant relation between this coefficient and the growth line formation was observed. Therefore, the formation of growth lines related to valve activity could not be demonstrated in this study.

In conclusion, alone the direct control by L:D cycles or the food availability could not explain the growth patterns observed. The direct control by biological clocks at the molecular level might not control the biomineralisation regarding both the canonical and the XBP1 timekeeping mechanisms. However, more genes related to the biomineralisation process should be studied with an emphasis on other components in the molecular pathways such transcription factors implicated in the regulation of the secretion of organic compounds. The possibility of an indirect control of biological clocks has been tested using valve activity and growth pattern measurements. The behaviour did not show similar patterns between valve activity and shell incrementation. However, the large variability observed, probably related to genetic variability and a large reaction norm to an environment in this study might mask the control of the biomineralisation process by the environment and/or biological clocks. Similar studies on other bivalves having a more robust clock and testing other environmental variables might help to decipher the control of the growth line formation.

Additional information

Funding

This project has received the financial support from the CNRS through the 80|Prime - MITI interdisciplinary program “TEMPO”, the MITI interdisciplinary program “ARCHIVE” and The Federative Action of the OOB “Rhythms and cycles in the Mediterranean Sea”.

Acknowledgement

We acknowledge the facilities of Biology platform of imaging (BioPIC). We are grateful to the Bio2Mar platform (http://bio2mar.obs-banyuls.fr) for providing access to instrumentation. We acknowledge Michel Groc from Department of Information and Communication Systems and his student Lucas Laveissiere (IMERIR) for the development of the valvometry device. We are thankful to Nancy Trouillard and Pascal Romans at Mutualised Aquariology Service for providing the phytoplankton and the aquariology facilities. We are thankful to captain, Eric Martinez, and crew from the oceanographic boat Néreis II as well as the divers, Jean-Claude Roca and Bruno Hesse (Sea Service from Banyuls Oceanographical Observatory) for the sampling effort at sea. We acknowledge Eric Maria and Paul Labatut (Banyuls Observational Sea Service – BOSS) for sea water sample processing. We are also thankful to Océane Eychenne for processing a part of the sclerological and behavioural data in the framework of her internship.

References

Andrisoa A, Lartaud F, Rodellas V, Neveu I. 2019. Enhanced Growth Rates of the Mediterranean Mussel in a Coastal Lagoon Driven by Groundwater Inflow. *Front. Mar. Sci.* 6:753

Anestis A, Pörtner HO, Michaelidis B. 2010. Anaerobic metabolic patterns related to stress responses in hypoxia exposed mussels *Mytilus galloprovincialis*. *J. Exp. Mar. Bio. Ecol.* 394:123–33

Aschoff J. 1981. Freerunning and Entrained Circadian Rhythms. In *Biological Rhythms*, pp. 81–93. Boston, MA.: Springer US

Bartness TJ, Albers HE. 2000. Activity Patterns and the Biological Clock in Mammals. In *Activity Patterns in Small Mammals*, pp. 23–47. Springer, Berlin, Heidelberg

Benjamini Y, Hochberg Y. 2000. On the Adaptive Control of the False Discovery Rate in Multiple Testing With Independent Statistics: *J. Educ. Behav. Stat.* 25(1):60–83

Bertolini C, Rubinetti S, Umgiesser G, Witbaard R, Bouma TJ, et al. 2021. How to cope in heterogeneous coastal environments: Spatio-temporally endogenous circadian rhythm of valve gaping by mussels. *Sci. Total Environ.* 768:145085

Branch GM, Steffani CN. 2004. Can we predict the effects of alien species? A case-history of the invasion of South Africa by *Mytilus galloprovincialis* (Lamarck). *J. Exp. Mar. Bio. Ecol.* 300:189–215

Bulla M, Oudman T, Bijleveld AI, Piersma T, Kyriacou CP. 2017. Marine biorhythms: Bridging chronobiology and ecology. *Philos. Trans. R. Soc. B Biol. Sci.* 372(1734):

Carlucci M, Krisciunas A, Li H, Gibas P, Koncevicius K, et al. 2020. DiscoRhythm: an easy-to-use web application and R package for discovering rhythmicity. *Bioinformatics*. 36(6):1952–54

Chapman EC, Bonsor BJ, Parsons DR, Rotchell JM. 2020. Influence of light and temperature cycles on the expression of circadian clock genes in the mussel *Mytilus edulis*. *Mar. Environ. Res.* 159:104960

Chapman EC, O'Dell AR, Meligi NM, Parsons DR, Rotchell JM. 2017. Seasonal expression patterns of clock-associated genes in the blue mussel *Mytilus edulis*. *Chronobiol. Int.* 34(9):1300–1314

Checa AG. 2018. Physical and biological determinants of the fabrication of Molluscan shell microstructures. *Front. Mar. Sci.* 5(SEP):353

Checa AG, Macías-Sánchez E, Harper EM, Cartwright JHE. 2016. Organic membranes determine the pattern of the columnar prismatic layer of mollusc shells. *Proc. R. Soc. B Biol. Sci.* 283:20160032

Checa AG, Rodríguez-Navarro AB, Esteban-Delgado FJ. 2005. The nature and formation of calcitic columnar prismatic shell layers in pteriomorphian bivalves. *Biomaterials*. 26(32):6404–14

Comeau LA, Babarro JMF, Longa A, Padin XA. 2018. Valve-gaping behavior of raft-cultivated mussels in the Ría de Arousa, Spain. *Aquac. Reports*. 9:68–73

Compton TJ, Leathwick JR, Inglis GJ. 2010. Thermogeography predicts the potential global range of the invasive European green crab (*Carcinus maenas*). *Divers. Distrib.* 16(2):243–55

Connor KM, Gracey AY. 2011. Circadian cycles are the dominant transcriptional rhythm in the intertidal mussel *Mytilus californianus*. *Pnas*. 108(38):16110–15

Cornelissen G. 2014. Cosinor-based rhythmometry. *Theor. Biol. Med. Model.* 11(1):1–24

Crenshaw MA, Neff JM. 1969. Decalcification at the mantle-shell interface in molluscs. *Integr. Comp. Biol.* 9(3):881–85

Davenport J, Chen X. 1987. A comparison of methods for the assessment of condition in the mussel (*Mytilus edulis* L.). *J. Molluscan Stud.* 53(3):293–97

Dinno A. 2017. dunn.test: Dunn's Test of Multiple Comparisons Using Rank Sums

Dodd AN, Salathia N, Hall A, Kévei E, Tóth R, et al. 2005. Cell biology: Plant circadian clocks increase photosynthesis, growth, survival, and competitive advantage. *Science.* 309(5734):630–33

Dunlap JC. 1999. Molecular bases for circadian clocks. *Cell*. 96(2):271–90

Eirin-Lopez JM, Putnam HM. 2019. Marine Environmental Epigenetics. *Ann. Rev. Mar. Sci.* 11:335–68

Emerson KJ, Bradshaw WE, Holzapfel CM. 2008. Concordance of the circadian clock with the environment is necessary to maximize fitness in natural populations. *Evolution (N. Y).* 62(4):979–83

Engel J. 2017. Chapter 6: Formation of Mollusk Shells. In *A Critical Survey of Biomineralization*, ed. J Engel, pp. 29–40. Springer ed.

Enright JT. 1976. Plasticity in an isopod's clockworks: Shaking shapes form and affects phase and frequency. *J. Comp. Physiol.* 107(1):13–37

Fox J, Weisberg S. 2019. *An R Companion to Applied Regression*. Thousand Oaks (CA): Sage. Third ed.

Gerdol M, Moreira R, Cruz F, Gómez-Garrido J, Vlasova A, et al. 2020. Massive gene presence-absence variation shapes an open pan-genome in the Mediterranean mussel. *Genome Biol.* 21(1):275

Gibson RN. 1973. Tidal and circadian activity rhythms in juvenile plaice, *Pleuronectes platessa*. *Mar. Biol.* 22(4):379–86

Giuffre AJ, Hamm LM, Han N, De Yoreo JJ, Dove PM. 2013. Polysaccharide chemistry regulates kinetics of calcite nucleation through competition of interfacial energies. *Proc. Natl. Acad. Sci. U. S. A.* 110(23):9261–66

Gouthiere L, Claustrat B, Brun J, Mauvieux B. 2005a. Éléments méthodologiques complémentaires dans l'analyse des rythmes: Recherche de périodes, modélisation. Exemples de la Mélatonine plasmatique et de courbes de températures. *Pathol. Biol.* 53(5):285–89

Gouthiere L, Mauvieux B, Davenne D, Waterhouse & J. 2005b. Complementary methodology in the analysis of rhythmic data, using examples from a complex situation, the rhythmicity of temperature in night shift workers. *Biol. Rhythm Res.* 36(3):177–93

Gwinner E, Brandstätter R. 2001. Complex bird clocks. *Philos. Trans. R. Soc. London. Ser. B Biol. Sci.* 356(1415):1801–10

Häfker NS, Andreatta G, Manzotti A, Falciatore A, Raible F, Tessmar-raible K. 2023. Rhythms and Clocks in Marine Organisms. *Ann. Rev. Mar. Sci.* 15:13.1-13.30

Helm B, Visser ME, Schwartz W, Kronfeld-Schor N, Gerkema M, et al. 2017. Two sides of a coin: ecological and chronobiological perspectives of timing in the wild. *Philos. Trans. R. Soc. B Biol. Sci.* 372:20160246

Huang X, Li S, Ni P, Gao Y, Jiang B, et al. 2017. Rapid response to changing environments during biological invasions: DNA methylation perspectives. *Mol. Ecol.* 26(23):6621–33

Hüning AK, Melzner F, Thomsen J, Gutowska MA, Krämer L, et al. 2013. Impacts of seawater

acidification on mantle gene expression patterns of the Baltic Sea blue mussel: implications for shell formation and energy metabolism. *Mar. Biol.* 160(8):1845–61

Jetten AM, Kurebayashi S, Ueda E. 2001. The ROR nuclear orphan receptor subfamily: Critical regulators of multiple biological processes. *Prog. Nucleic Acid Res. Mol. Biol.* 69:205–47

Klein DC. 2007. Arylalkylamine N-Acetyltransferase: "the Timezyme." *J. Biol. Chem.* 282(7):4233–37

Krittika S, Yadav P. 2019. Circadian clocks: an overview on its adaptive significance. *Biol. Rhythm Res.* 51(7):1109–32

Littlewood DTJ, Young RE. 1994. The effect of air-gaping behaviour on extrapallial fluid pH in the tropical oyster *Crassostrea rhizophorae*. *Comp. Biochem. Physiol. -- Part A Physiol.* 107(1):1–6

Louis V, Besseau L, Lartaud F. 2022. Step in Time : Biomineralisation of Bivalve's Shell. *Front. Mar. Sci.* 9:906085

Lutz RA, Rhoads DC. 1977. Anaerobiosis and a Theory of Growth Line Formation. *Science.* 198(4323):1222–27

Maire O, Amouroux JM, Duchêne JC, Grémare A. 2007. Relationship between filtration activity and food availability in the Mediterranean mussel *Mytilus galloprovincialis*. *Mar. Biol.* 152(6):1293–1307

Marie B, Le N, Zanella-Cléon I, Becchi M, Marin F. 2011. Molecular Evolution of Mollusc Shell Proteins : Insights from Proteomic Analysis of the Edible Mussel *Mytilus*. *J. Mol. Evol*. (72):531–46

Marin F, Roy N Le, Marie B. 2012. The formation and mineralization of mollusk. *Front. Biosci.* 4:1099–1125

Mat AM, Charles J, Ciret P, Tran D. 2014. Looking for the clock mechanism responsible for circatidal behavior in the oyster *Crassostrea gigas*. *Mar. Biol.* 161:89–99

Mat AM, Massabuau JC, Ciret P, Tran D. 2012. Evidence for a plastic dual circadian rhythm in the oyster *Crassostrea gigas*. *Chronobiol. Int.* 29(7):857–67

Mat AM, Perrigault M, Massabuau JC, Tran D. 2016. Role and expression of cry1 in the adductor muscle of the oyster *Crassostrea gigas* during daily and tidal valve activity rhythms. *Chronobiol. Int.* 33(8):949–63

Mat AM, Sarrazin J, Markov G V, Apremont V, Dubreuil C, et al. 2020. Biological rhythms in the deep-sea hydrothermal mussel *Bathymodiolus azoricus*. *Nat. Commun.* 11:3454

Miglioli A, Dumollard R, Balbi T, Besnardeau L, Canesi L. 2019. Characterization of the main steps in first shell formation in *Mytilus galloprovincialis*: Possible role of tyrosinase. *Proc. R. Soc. B Biol. Sci.* 286(1916):20192043

Miyashita T, Hanashita T, Toriyama M, Takagi R, Akashika T, Higashikubo N. 2008. Gene cloning and biochemical characterization of the BMP-2 of *Pinctada fucata*. *Biosci. Biotechnol. Biochem.* 72(1):37–47

Miyazaki Y, Usui T, Kajikawa A, Hishiyama H, Matsuzawa N, et al. 2008. Daily oscillation of gene expression associated with nacreous layer formation. *Front. Mater. Sci. China*. 2(2):162–66

Moran AL, Marko PB. 2005. A simple technique for physical marking of larvae of marine bivalves. *J. Shellfish Res.* 24(2):567–71

Mrosovsky N. 1999. Masking: history, definitions, and measurement. *Chronobiol. Int.* 16(4):415–29

NanoString Technologies Inc. 2017. Gene Expression Data Analysis Guidelines

Naylor E. 1958. Tidal and Diurnal Rhythms of Locomotory Activity in *Carcinus Maenas* (L.). *J. Exp. Biol.* 35(3):602–10

Naylor E. 1996. Crab clockwork: The case for interactive circatidal and circadian oscillators controlling rhythmic locomotor activity of *Carcinus maenas*. *Chronobiol. Int.* 13(3):153–61

Nedoncelle K, Lartaud F, de Rafelis M, Boulila S, Le Bris N. 2013. A new method for high-resolution bivalve growth rate studies in hydrothermal environments. *Mar. Biol.* 160(6):1427–39

Nedoncelle K, Lartaud F, Pereira LC, Yücel M, Thurnherr AM, et al. 2015. Bathymodiolus growth dynamics in relation to environmental fluctuations in vent habitats. *Deep. Res. Part I*. 106:183–93

Nikhil KL, Sharma VK. 2017. On the Origin and Implications of Circadian Timekeeping: An Evolutionary Perspective. In *Biological Timekeeping: Clocks, Rhythms and Behaviour*, pp. 81–129. Springer India

Ouyang Y, Andersson CR, Kondo T, Golden SS, Johnson CH. 1998. Resonating circadian clocks enhance fitness in cyanobacteria. *Proc. Natl. Acad. Sci. U. S. A.* 95(15):8660–64

Palmer JD. 2000. The clocks controlling the tide-associated rhythms of intertidal animals. *BioEssays*. 22(1):32–37

Palmer JD, Williams BG. 1986. Comparative studies of tidal rhythms. II. The dual clock control of the locomotor rhythms of two decapod crustaceans. *Mar. Behav. Physiol.* 12(4):269–78

Pan Y, Ballance H, Meng H, Gonzalez N, Kim SM, et al. 2020. *12-h Clock Regulation of Genetic Information Flow by XBP1s*, Vol. 18

Paranjpe DA, Sharma VK. 2005. Evolution of temporal order in living organisms

Perrigault M, Andrade H, Bellec L, Ballantine C, Camus L, Tran D. 2020. Rhythms during the polar night: evidence of clock-gene oscillations in the Arctic scallop *Chlamys islandica*. *Proceedings. Biol. Sci.* 287(1933):20201001

Perrigault M, Tran D. 2017. Identification of the Molecular Clockwork of the Oyster *Crassostrea gigas*. *PLoS One*. 12(1):e0169790

Prieto D, Markaide P, Urrutxurtu I, Navarro E, Artigaud S, et al. 2019. Gill transcriptomic analysis in fast- and slow-growing individuals of *Mytilus galloprovincialis*. *Aquaculture*. 511(June):734242

R Core Team. 2020. R: A Language and Environment for Statistical Computing

Rasband WS. 2020. ImageJ

Richardson CA. 1988. Exogenous and endogenous rhythms of band formation in the shell of the clam *Tapes philippinarum* (Adams et Reeve, 1850). *J. Exp. Mar. Bio. Ecol.* 122(2):105–26

Richardson CA. 1989. An analysis of the microgrowth bands in the shell of the common mussel *Mytilus edulis*. *J. Mar. Biol. Assoc. United Kingdom*. 69(2):477–91

Richardson CA, Crisp DJ, Runham NW. 1980. An endogenous rhythm in shell deposition in *Cerastoderma edule*. *J. Mar. Biol. Assoc. United Kingdom*. 60(4):991–1004

Rosbash M. 2009. The implications of multiple circadian clock origins

Sachs M. 2014. cosinor: Tools for estimating and predicting the cosinor model

Schmid B, Helfrich-Förster C, Yoshii T. 2011. A new ImageJ plugin “ActogramJ” for chronobiological analyses. *J. Biol. Rhythms*. 26:464–67

Schnytzer Y, Simon-Blecher N, Li J, Ben-Asher HW, Salmon-Divon M, et al. 2018. Tidal and diel orchestration of behaviour and gene expression in an intertidal mollusc. *Sci. Rep.* 8(1):1–13

Schöne BR. 2008. The curse of physiology — challenges and opportunities in the interpretation of geochemical data from mollusk shells. *Geo-Marine Lett.* 28:269–85

Schöne BR, Dunca E, Fiebig J, Pfeiffer M. 2005. Mutvei ’ s solution : An ideal agent for resolving microgrowth structures of biogenic carbonates. *Palaeogeogr. Palaeoclimatol. Palaeoecol.* 228:149–66

Senthilan PR, Grebler R, Reinhard N, Rieger D, Helfrich-Förster C. 2019. Role of Rhodopsins as Circadian Photoreceptors in the *Drosophila melanogaster*. *Biology.* 8:6

Shah AS. 2020. card: Cardiovascular and Autonomic Research Design

SHOM. 2020. *Horaires de marées gratuits du SHOM*. https://maree.shom.fr/harbor/BANYULS/hlt/0?date=2020-06-24&utc=standard

Skinner HC., Jahren AH. 2003. Biomineralization. In *Trearise on Geochemistry*, pp. 117–84. Elsevier Ltd.

Song X, Liu Z, Wang L, Song L. 2019. Recent advances of shell matrix proteins and cellular orchestration in marine molluscan shell biomineralization. *Front. Mar. Sci.* 6:41

Strickland JD, Parsons TR. 1997. *A Practical Handbook of Seawater Analysis, 2nd Ed.* Bull. Fish. Res. Bd. Can.

Thaben PF, Westermark PO. 2014. Detecting rhythms in time series with rain. *J. Biol. Rhythms*. 29(6):391–400

Toyohara H, Hosoi M, Hayashi I, Kubota S, Hashimoto H, Yokoyama Y. 2005. Expression of HSP70 in response to heat-shock and its cDNA cloning from Mediterranean blue mussel. *Fish. Sci. 2005 712*. 71(2):327–32

Tran D, Ciret P, Ciutat A, Durrieu G, Massabuau J-C. 2003. Estimation of potential and limits of bivalve closure response to detect contaminants: Application to cadmium. *Environ. Toxicol. Chem.* 22(4):914–20

Tran D, Perrigault M, Ciret P, Payton L. 2020. Bivalve mollusc circadian clock genes can run at tidal frequency. *Proc. R. Soc. B*. 287:20192440

Tran D, Sow M, Camus L, Ciret P, Berge J, Massabuau JC. 2016. In the darkness of the polar night, scallops keep on a steady rhythm. *Sci. Rep.* 6:32435

Treccani L, Mann K, Heinemann F, Fritz M. 2006. Perlwapin, an Abalone Nacre Protein with Three Four-Disulfide Core (Whey Acidic Protein) Domains, Inhibits the Growth of Calcium Carbonate Crystals. *Biophys. J.* 91(7):2601–8

Trusevich V V, Kuz KA, Mishurov VZ, Zhuravsky VY, Vyshkvarkova E V. 2021. Features of Behavioral Responses of the Mediterranean Mussel in Its Natural Habitat of the Black Sea. *Inl. Water Biol.* 14(1):10–19

Vriend J, Reiter RJ. 2014. Melatonin as a proteasome inhibitor. Is there any clinical evidence? *Life Sci.* 115(1–2):8–14

Warman CG, Naylor E. 1995. Evidence for multiple, cue-specific circatidal clocks in the shore crab *Carcinus maenas*. *J. Exp. Mar. Bio. Ecol.* 189(1–2):93–101

Williams BG, Pilditch CA. 1997. The Entrainment of Persistent Tidal Rhythmicity in a Filter-Feeding Bivalve Using Cycles of Food Availability. *J. Biol. Rhythms*. 12(2):173–81

Zhang L, Hastings MH, Green EW, Tauber E, Sladek M, et al. 2013. Dissociation of Circadian and Circatidal Timekeeping in the Marine Crustacean *Eurydice pulchra*. *Curr. Biol.* 23(19):1863–73

Zhang N, Chen Y. 2012. Molecular origin of the sawtooth behavior and the toughness of nacre. *Mater. Sci. Eng. C*. 32(6):1542–47

Zhao M, Shi Y, He M, Huang X, Wang Q. 2016. PfSMAD4 plays a role in biomineralization and can transduce bone morphogenetic protein-2 signals in the pearl oyster *Pinctada fucata*. *BMC Dev. Biol.* 16(1):9

Zhu B, Dacso CC, O'Malley BW. 2018. Unveiling "Musica Universalis" of the Cell: A Brief History of Biological 12-Hour Rhythms. *J. Endocr. Soc.* 2(7):727–52

Zhu Y, Yu Z, Liao K, Zhang L, Ran Z, Xu J. 2022. Melatonin in razor clam *Sinonovacula constricta* : Examination of metabolic pathways , tissue distribution , and daily rhythms. *Aquaculture*. 560:738548

Supplementary Data A- Clock(s) or no clock(s)? The integration of the rhythmic environment in bivalve's shell

Materials and methods

To build the targeted mRNA sequences for *M. galloprovincialis*, a basic alignment search tool (BLAST on Genbank) was used on sequence read archives (accession number SRX1240182) of the targeted species using known sequences of close-related species available on Genbank. Contigs obtained were aligned and collapsed into one sequence using the software BioLign v.2.0.9 (Hall, 2001). The validity of the sequence was assessed by a BLAST on nucleotide and transcript sequences databases in GenBank. Finally, maximum likelihood trees (Nei and Kumar, 2000) were made based on amino acid sequences using the JTT model (Jones et al., 1992) with a gamma distribution as implemented the software Mega X (Kumar et al., 2018). The statistical robustness of relationships was assessed using bootstrap method with 1000 replicates.

In 2020, a partially annotated assembled genome of *M. galloprovincialis* was released (CGA_900618805.1, Gerdol et al., 2020) and sequences were blast on it (*i.e.*, blastx) for cross-validation. When the translated contig was matching with a hypothetical protein in the genome, a research of conserved domain on pfam database was done using the NCBI Conserved Domain Search Service (Yang et al., 2020).

Results

Potential core biological clock genes

Most potential genes of the core set of the biological clock were already identified for *Mytilus edulis* (Chapman et al., 2017, 2020). Looking to positive elements, *Clock* (*i.e.*, *Circadian locomotor output cycles kaput*) gene mRNA sequence built was 409 bp long and matched at 99% with *M. edulis* sequence (KJ671527.1). The translated amino acid sequence had 87% identity with the annotated CLOCK protein (VDI68759.1) on *M. galloprovincialis* genome. Phylogenetic tree showed that the amino acid sequence was similar with identified sequences in close-related bivalves (Figure A). For *Bmal* (*i.e.*, *Aryl hydrocarbon receptor nuclear translocator-like*), the 252 bp sequence built matched at 99% with *M. edulis* sequence (KJ671529.1) and blastx on the annotated genome showed a match with a hypothetical predicted protein (VDI55294.1) at 86%. Conserved domain search on pfam database showed bHLH-Pas (basic helix-loop-helix-Per-ARNT-Sim) domain, which is necessary to bind an E-box and activate the transcription of repressive factors of the feedback loop constituting the biological

clock (Dunlap, 1999). The generated tree based on amino-acid sequences clustered the sequence with close-related species (*i.e.*, *B. azoricus, M. gigas* and *C. islandica*) (Figure B).

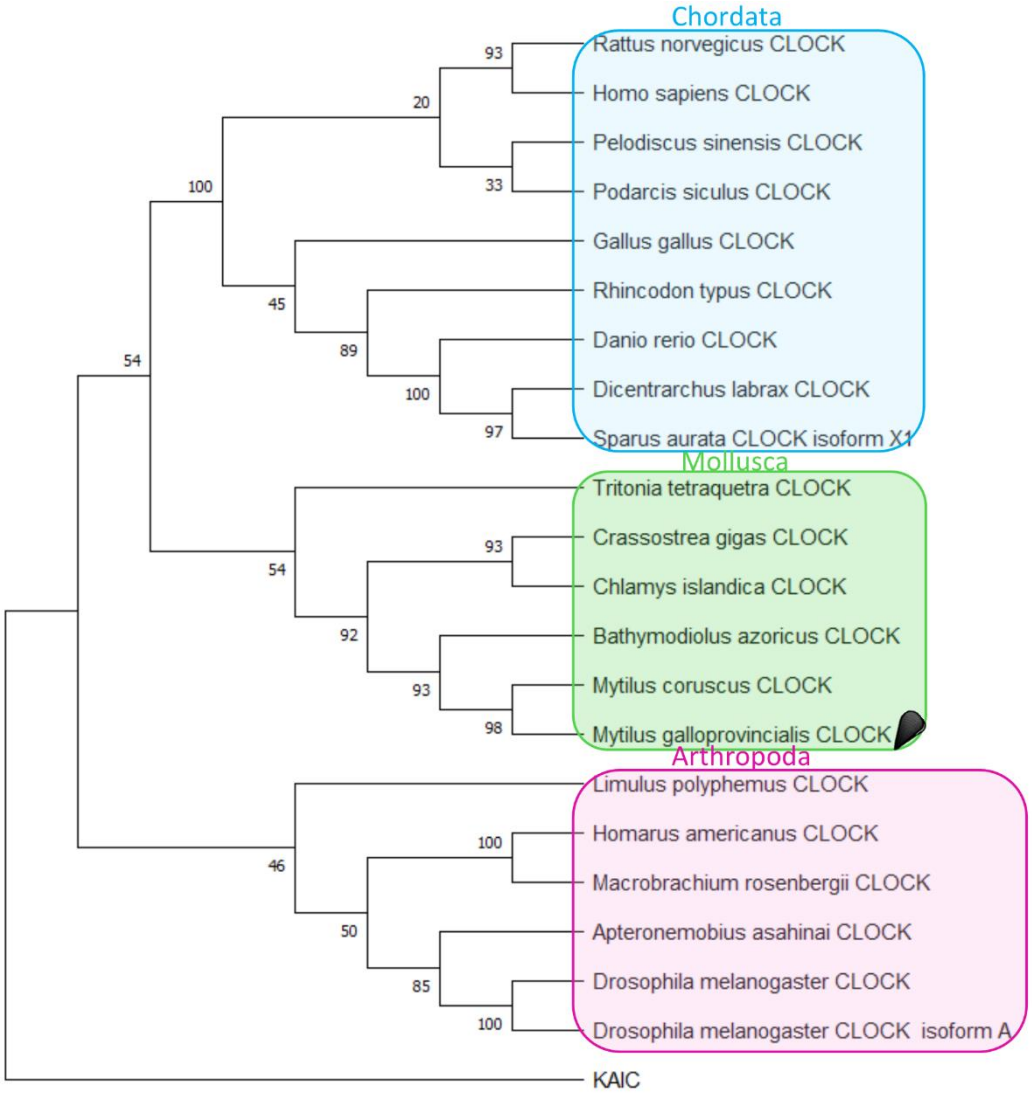

Figure A: Phylogenetic tree based on CLOCK sequences. The tree was generated using the maximum likelihood method and the JTT matrix-based model and the gamma distribution. Percentage of bootstraps were based on 1 000 replicates.

Among negative elements, a 679 bp contig corresponding to *period* mRNA sequence was retrieved from reads alignment, that possess 96% homology with *M. edulis* sequence (MH836580.1) The translated sequence was aligned on the later annotated genome and showed 99% homology with *Period* (VDI70018.1 and VDI70019.1). Phylogeny tree grouped the sequence with Mytilidae PERIOD sequences (Figure C). *Cryptochrome* 1 (*cry*1) contig retrieved was 296 bp long and matched with *M. edulis* at 99% (KJ671528.1). The translated amino acid sequence matched at 99% with the annotated Cryptochrome protein (VDH90443.1). *Cryptochrome 2* (*cry2*) had no sequence described for the *Mytilus* complex, therefore *M. gigas* sequence (KX371074.1) was used to assemble contigs from the sequence read archive. A 643 bp sequence was retrieved and was similar at 75% with the *cry2*

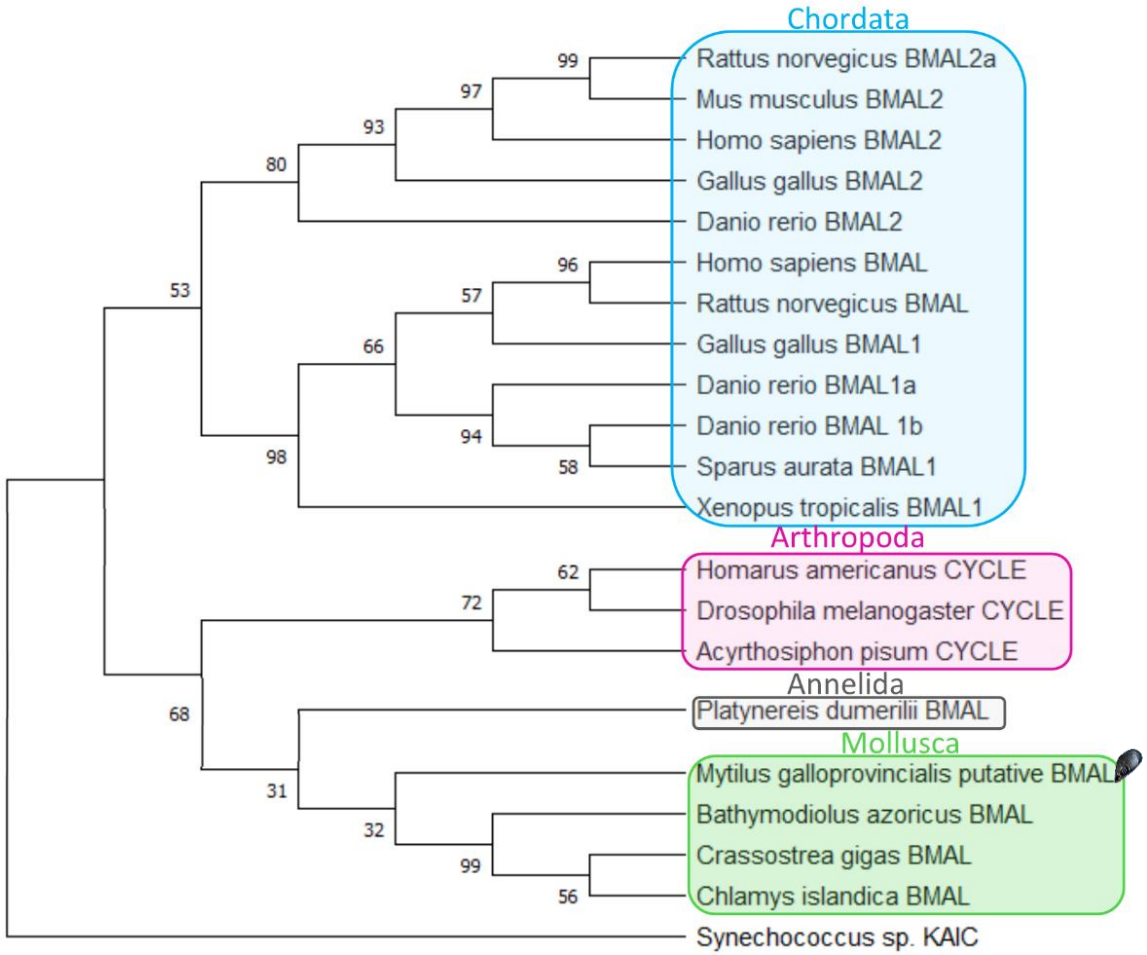

Figure B: Phylogenetic tree based on BMAL sequences. The tree was generated using the maximum likelihood method and the JTT matrix-based model and the gamma distribution. Percentage of bootstraps were based on 1 000 replicates.

sequence of the madeira cockroach, *Rhyparobia maderae*. The translated amino acids sequence matched at 99% with the Cryptochrome protein (VDI01404.1) annotated in *M. galloprovincialis* genome. Phylogeny tree grouped the sequence with close-related bivalves CRY2 (Figure D). *Timeout* assembled mRNA sequence was 851 bp and had 99% homology with *timeout-like* of *M. edulis* (KX576716.1). The amino acid sequence matched with two annotated sequence of the *M. galloprovincialis* genome, the protein Aubergine (VDI77989.1) with 98% of identity and a coverage of 73%, and the protein Timeless (VDI83092.1) with 99% of identity over 65% of the sequence. The first protein, Aubergine, has a role in the development of the germline (Rui et al., 2020). By searching the conserved domain of the sequence, two appeared, the PIWI domain of eukaryote which is related to the germline development and Timeless protein. The match on Timeless annotated protein had only the timeless domain. In insect, it has been suggested that *Timeless* resulted from a gene duplication of *Timeout* (Rubin et al., 2006). In *B. azoricus*, one *Timeless* and two *Timeout* sequences that might be isoforms were identified (Mat et al., 2020).

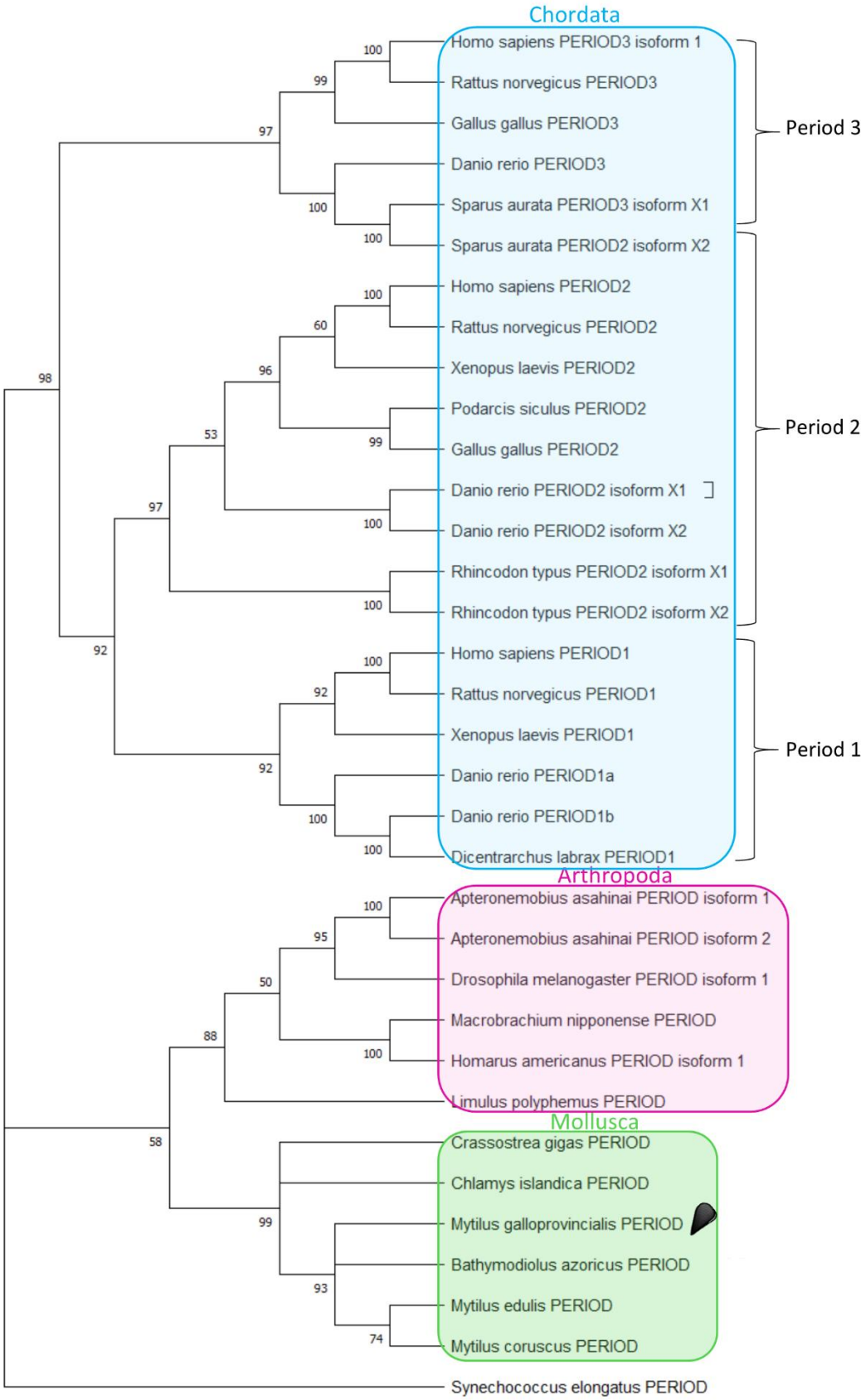

Figure C: Phylogenetic tree based on PERIOD sequences. The tree was generated using the maximum likelihood method and the JTT matrix-based model and the gamma distribution. Percentage of bootstraps were based on 1 000 replicates.

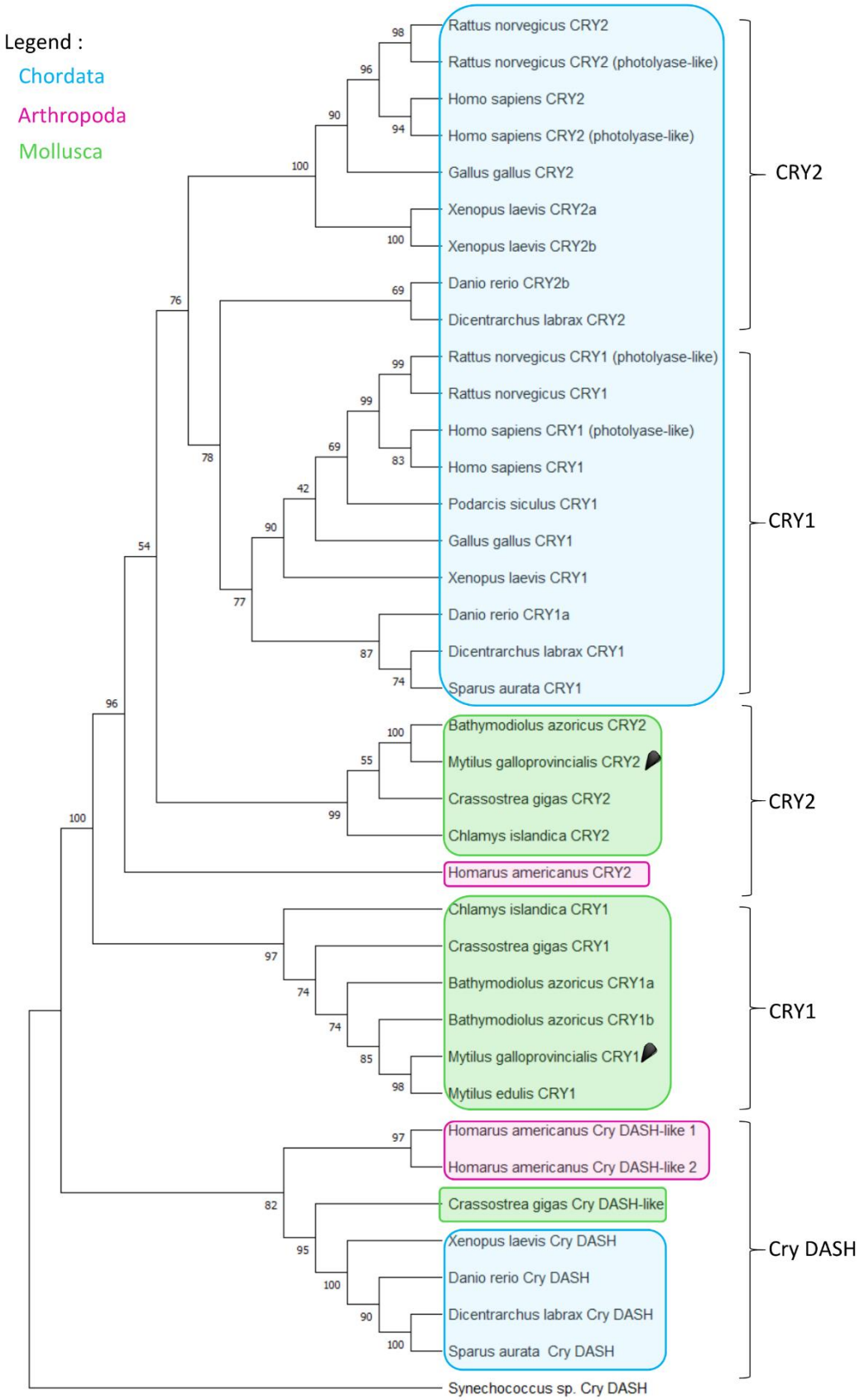

Figure D: Phylogenetic tree based on CRYPTOCHROMES sequences. The tree was generated using the maximum likelihood method and the JTT matrix-based model and the gamma distribution. Percentage of bootstraps were based on 1 000 replicates.

The sequences used in this study matched at 89% with the second isoform of timeout of *B. azoricus*. Phylogenetic tree based on amino-acid sequences grouped the built sequence with TIMEOUT sequences of Mytilidae (Figure E).

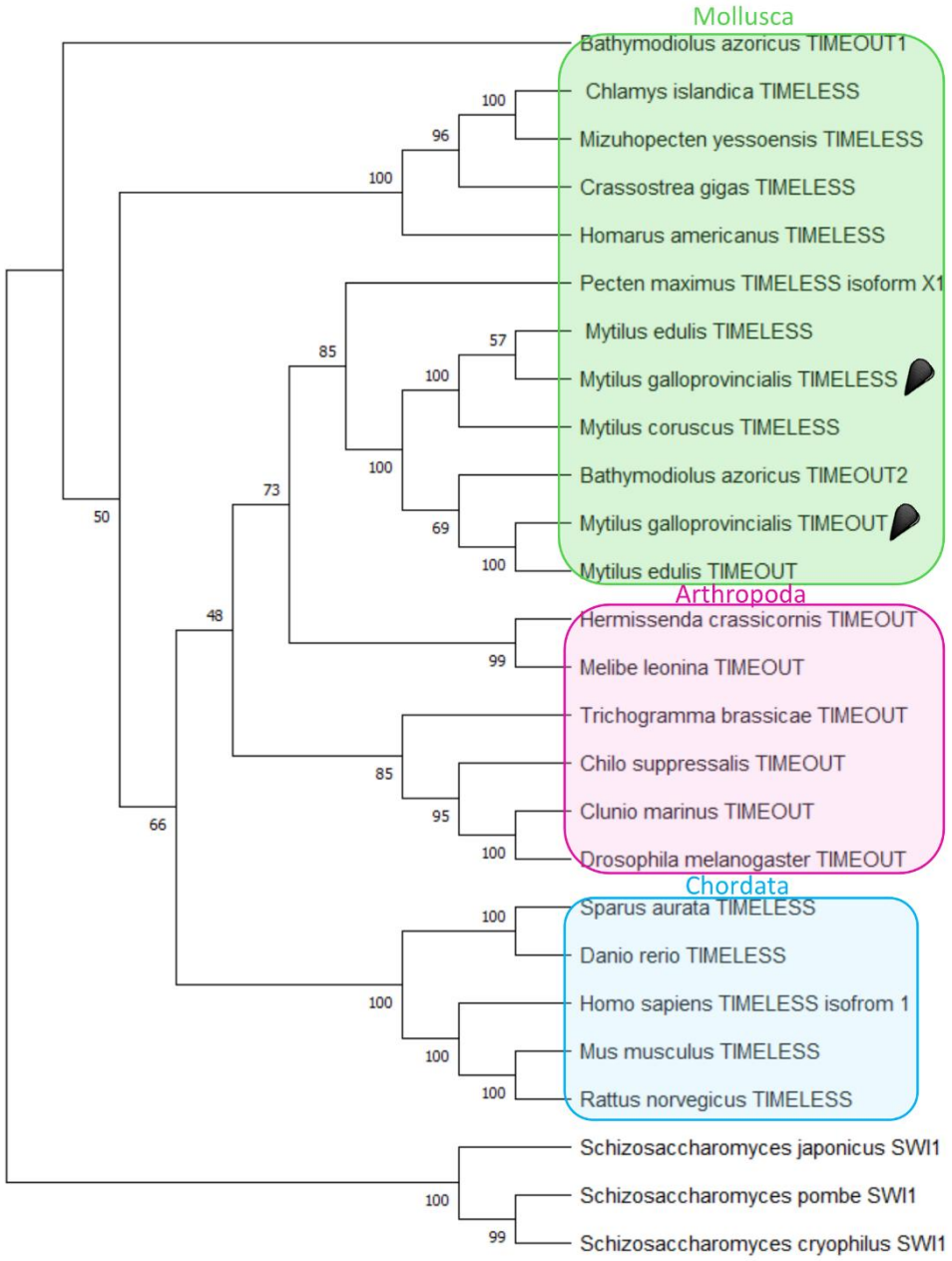

Figure E: Phylogenetic tree based on TIMEOUT and TIMELESS sequences. The tree was generated using the maximum likelihood method and the JTT matrix-based model and the gamma distribution. Percentage of bootstraps were based on 1 000 replicates.

Rorb (*i.e.*, *RAR-related orphan receptor B*) has been recognised to be involved in time keeping mechanisms (Jetten et al., 2001). It has been proved that its alteration disrupts the expression of *Clock*, *Cycle* (*i.e.*, the arthropod ortholog of *Bmal*) and *Tim* in firebrats, *Thermobia domestica* (Kamae et al., 2014). Rhythmic expression of *Rorb* has been previously observed in Mytilids (Connor and Gracey, 2011; Chapman et al., 2020) and has been suggested as likely transcription promotor of *Bmal* in oyster

and be regulated by REV-ERB (Figure 23) (Perrigault and Tran, 2017). No *Rev-erb* sequence was built for *M. galloprovincialis* in this study. *Rorb* sequences built in *M. galloprovincialis was* 469 bp long and matched at 99% with *M. edulis rorb/hr3-like* mRNA but only on 36% of the sequence. Therefore, a blast was done on TSA of *M. galloprovincialis*, and the sequence was identical to a mRNA sequence (GGUW01039936.1), validating the contig. The amino-acid sequence matched with a nuclear receptor from the Subfamily 1 group F member 4 of *M. galloprovincialis* (VDI83019.1). Among the conserved domain of this protein there was the DNA binding domain of Retinoid-related orphan receptor.

Biological clocks related genes

Rhodopsin is a photoreceptor known to have a role in the circadian entrainment of biological clocks notably in the fruit fly, *Drosophila melanogaster* (Senthilan et al., 2019). Rhythmic expression of *Rhodopsin* has been observed in the mantle of the Arctic scallop *C. islandica* (Perrigault et al., 2020). For *rhodopsin*, *M. edulis* mRNA sequence was not published yet and the sequence was built from *rhodopsin* sequence of *Argonauta nodosa* (AY545166.1). A 108 bp contig was constructed but none similar sequence was found in GenBank nucleotide database. To validate it, a blast has been done on transcript sequence archives (TSA) of *M. galloprovincialis* and the sequence matched at 99% over 62% of a sequence (GHIK01098750.1). As a blast of the last sequence on database matched for *rhodopsin* of many molluscs, it was assumed that our sequence was coding for Rhodopsin. Later comparison with the annotated genome validated the sequence with 99% of homology with an annotated *r-Opsin* (VDI13980.1).

In vertebrates Arylalkylamine-N-acetyltransferase, AANAT, is an enzyme involved in the rhythmic production of melatonin which secretion and release are rhythmically controlled by biological clocks (Klein, 2007). Recently, similar observation has been made in labial palps of the razor clam, *Sinonovacula constricta* (Zhu et al., 2022). *Aanat* mRNA sequence was based on *M. edulis* sequence, the 380 bp matched at 99% with *M. edulis* (KX576715.1). Amino acid sequence aligned with a hypothetical protein at 95% but only on 15% of the sequence (VDH95523). Nevertheless, our sequence presented a N-Acyltransferase superfamily conserved domain in which N-acetyltransferase domains are a member. This confirmed that the built sequence is coding for an AANAT.

The last gene targeted was the *HSP70* that is supposed to play a role in the folding and chaperoning shell matrix proteins (Sleight et al., 2020). In bivalve the Hsp70 expression varies in relation with the temperatures (Toyohara et al., 2005; Anestis et al., 2010). The *hsp70* sequence (GenBank accession number AB180908.1, Toyohara et al., 2005) was already described for *M. galloprovincialis*.

Cell-autonomous 12 hours clock gene

In the recent years, another cell-autonomous 12 hours clock regulation of gene expression was described in mammals (Zhu et al., 2018). XBP1s was suggested as regulator and proved to be independent from the canonical biological clock in mice (Pan et al., 2020). This gene was already described in molluscs as part of the signalling pathway IRE1-XBP1 and known to play a role on a large spectrum of biological process (Huang et al., 2018). X-*box binding protein 1* (*Xbp1*) sequence retrieved was 526 bp long and based on the sequence of *M. edulis* (DQ201827.1). It matched at 97% with the sequence of *M. edulis*. The translated sequence matched at 93% on the annotated sequence XBP1 in *M. galloprovincialis* genome (VDI08907.1).

Biomineralisation related genes

Genes involved at different levels of the biomineralisation process were targeted. Shells are made of mineral and organic contents (Skinner and Jahren, 2003). Two genes related to the mineral formation were targeted; *Plasma membrane calcium ATPase* and *Carbonic anhydrase*. Plasma membrane calcium ATPase is known to transport calcium ions, increasing the calcium ions concentration in the extrapallial fluid (EPF) (Hüning et al., 2013). Carbonic anhydrase is an enzyme forming HCO_3^- from CO_2 and H_2O. The HCO_3^- binds with calcium ions to form the mineral part of the shell, the calcium carbonate. Sequence coding for *carbonic anhydrase II* was already available on NCBI (KT818923.1). Concerning *plasma membrane calcium-transporting ATPase* (*ca2$^+$ATPase*) mRNA sequence, reads of *M. galloprovincialis* were collapsed into a contig based on the gastropod *Haliotis rufescens* sequence (XM_048397027.1). The final contig of 247 bp matched at 78% over 74% of the sequence of the gastropod. To validate this sequence, a blast has been done on transcribed-RNA sequences (TSA) of *M. galloprovincialis*. The contig built was identical to a sequence (GHIK01179846.1), validating the contig. The translated sequence matched at 100% over 92% of Ca^{2+} transporting ATPase in the annotated genome of *M. galloprovincialis* (VDI68446.1). However, both proteins have also other functions not directly related to the biomineralisation process and proteins specific to the process were targeted (Le Roy et al., 2014; Pavičić-Hamer et al., 2015).

The organic matrix in shells is composed of several proteins that are recognised to control the shell mineralisation (Marin and Luquet, 2004; Feng et al., 2017). Three of them were implicated in the chitin metabolism which is one major polysaccharide constituting the building frame for nacre tablet formation (Addadi et al., 2006; Engel, 2017). Chitin synthase is involved in the chitin synthesis and Chitinase for the chitin remodelling (Engel, 2017). Tyrosinase has a chitin binding domain and is

recognised to correct the chitin remodelling (Miglioli et al., 2019). C*hitin synthase* (EF535882.1) was already described in NCBI for *M. galloprovincialis*. Again, some targeted genes sequences were described for other Mytilids, facilitating the construction of *M. galloprovincialis* sequences. *Chitinase* contig was constructed from *M. edulis* sequence (MG827131) and was 201 bp long. The nucleotide sequence matched at 100 % with *chitinase-like protein-1* mRNA of *Mytilus chilensis*, validating the contig. The amino-acid sequence was the same than the later-annotated on the genome of *M. galloprovincialis* (VDI28372.1). *Tyrosinase* mRNA sequence has been assembled using the *tyrosinase-like* sequence of *Mytilus coruscus* (KP57802.1) and was 877 bp long. The blast on Genbank nucleotide sequence did not find similar sequence although research on translated sequence matched at 100% over the 69 first amino-acids of the Tyrosinase-like protein of *M. galloprovincialis* (OPL33388.1) from the base pair number 2 to 208 on the nucleotides sequence. Moreover, looking to the reads alignment the coverage between them was insufficient in many places after 280 bp on the contig. Therefore, the contig was trimmed to be 206 bp long.

Two potential inhibitors of the formation of the mineral process were targeted. *Perlwapin* was first the tablets of nacre in the abalone *Haliotis laevigata* (Treccani et al., 2006). It is formed of a succession of WAP (Whey Acidic Protein) domain sequences that may inhibit the growth of nacre. In *M. galloprovincialis*, the PERLWAPIN has been identified (Marie et al., 2011). The WAP domains were conserved but their function in calcium carbonate deposition is unknown. The mRNA sequence of *perlwapin* was already available on NCBI (FL494664.1, Venier et al., 2009). NACREIN has been first identified in the nacreous layer of *Pinctada fucata* and later in the prismatic layer as well (Miyamoto et al., 1996; Miyashita, 2002). The protein is composed of two domains, one acting as a carbonic anhydrase and another that might inhibit the calcium carbonate precipitation (Miyamoto et al., 2005). Daily oscillation of gene expression has been observed in the mantle of *P. fucata* (Miyazaki et al., 2008). A Nacrein-like protein has been identified in the shell of *Mytilus galloprovincialis* and *nacrein* sequence is available in databases (KP670943.1, Gao et al., 2015).

Among other functions, BMP2 is known to regulate the biomineralisation (Miyashita et al., 2008; Zhao et al., 2016). *Bmp2* contig of 176 bp was obtained based on sequence of the clam *Sinonovacula constricta* (MH822126.1). Nucleotide sequence did not match with any sequence on GenBank whereas it was identical to an mRNA sequence in TSA of *M. galloprovincialis* (GHIK01116414.1). The translated amino acid sequence had 100% of identity with *BMP2/4* annotated gene in *M. galloprovincialis* genome (VDI49543.1 and VDI49544.1).

Housekeeping genes

For the housekeeping genes, five were required for the gene expression analysis by NanoString. *α-tubulin* (HM537081.1), *actin* (AF157491.1) and *ef1α* (AB162021.1) mRNA sequences were previously described in *M. galloprovincialis*. The commonly used *18s* and *28s* were not suitable as their expressions were too high in comparison with the targeted genes. Therefore, *Rpl7* and *Hprt1* genes were used. *Rpl7* contig was assembled from *M. gigas rpl7* sequence (AJ557884). It matched with a TSA sequence of *M. galloprovincialis* (GAEN01008711.1), validating the contig. Later analysis on the genome assembly showed a 99% of identity with the annotated protein RPL7e (VDI30485.1). The same was done for *hprt1* based on the known sequence of *M. edulis* (KJ808673.1). The cross-validation on annotated *M. galloprovincialis* genome showed a 100% identity with HPRT sequence (VDI66978.1).

Supplementary Data B- Clock(s) or no clock(s)? The integration of the rhythmic environment in bivalve's shell

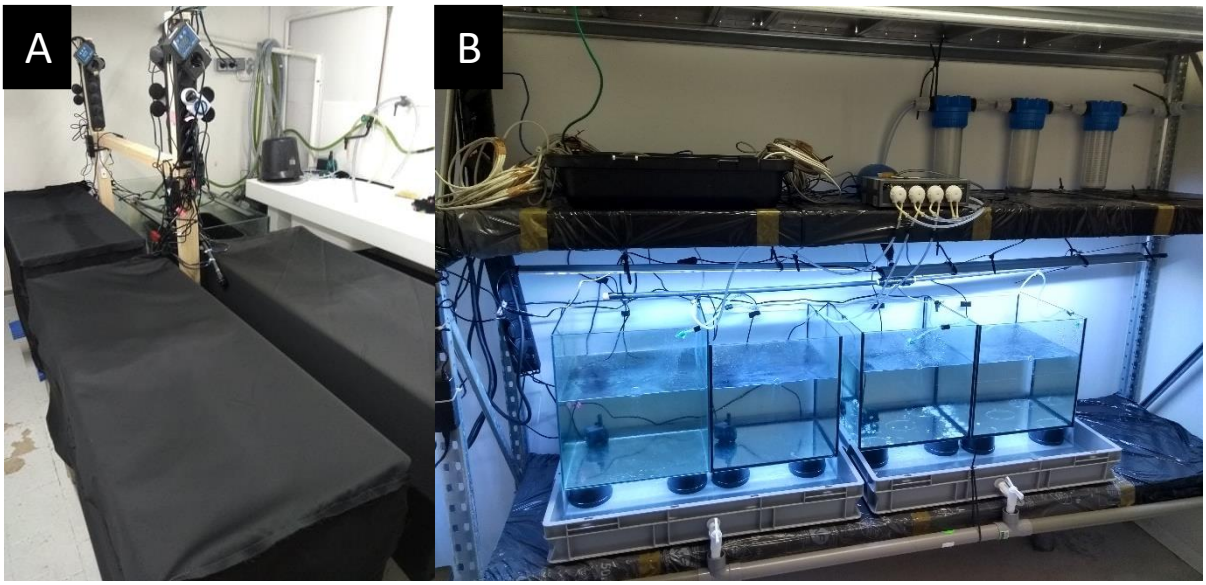

Figure S3: Aquariology structures used in this study. A) Experimental set up for the gene expression analysis under controlled photoperiodic conditions. There were three aquariums in each bigger aquarium. Bigger aquariums were covered with blackout fabrics. B) Structure used to assess the genes expression under different food availability conditions and the behavioral and growth set of experiments. Aquariums were the same as in the structure A. Both systems were semi-open, water was pumped at sea and filtered at 5µm before its storage in a buffer tank. Aquariums were continuously supplied in water by a drip irrigation and the excess left by overflow. The light and water pumps were the same in both structures.

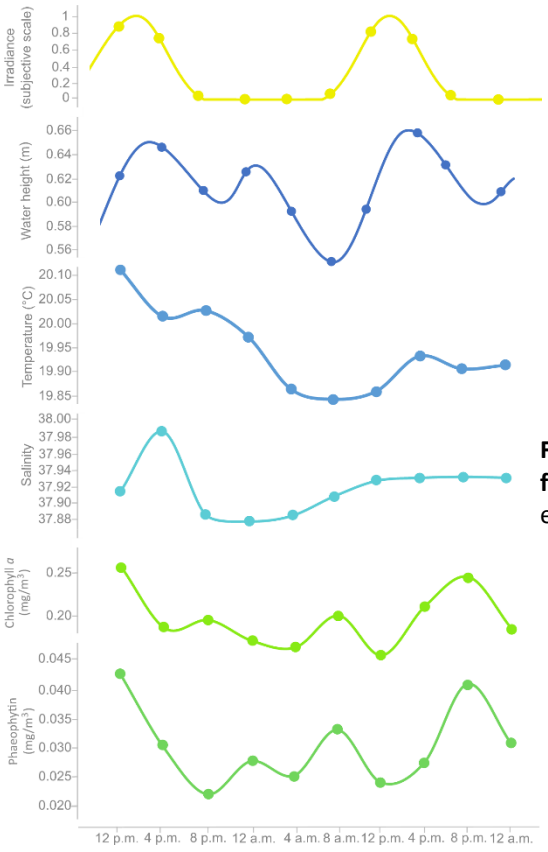

Figure S4: Environmental variables measured at SOLA from the 09/09/20 to the 09/11/20. Measures were taken every four hours during the sampling campaign at sea.

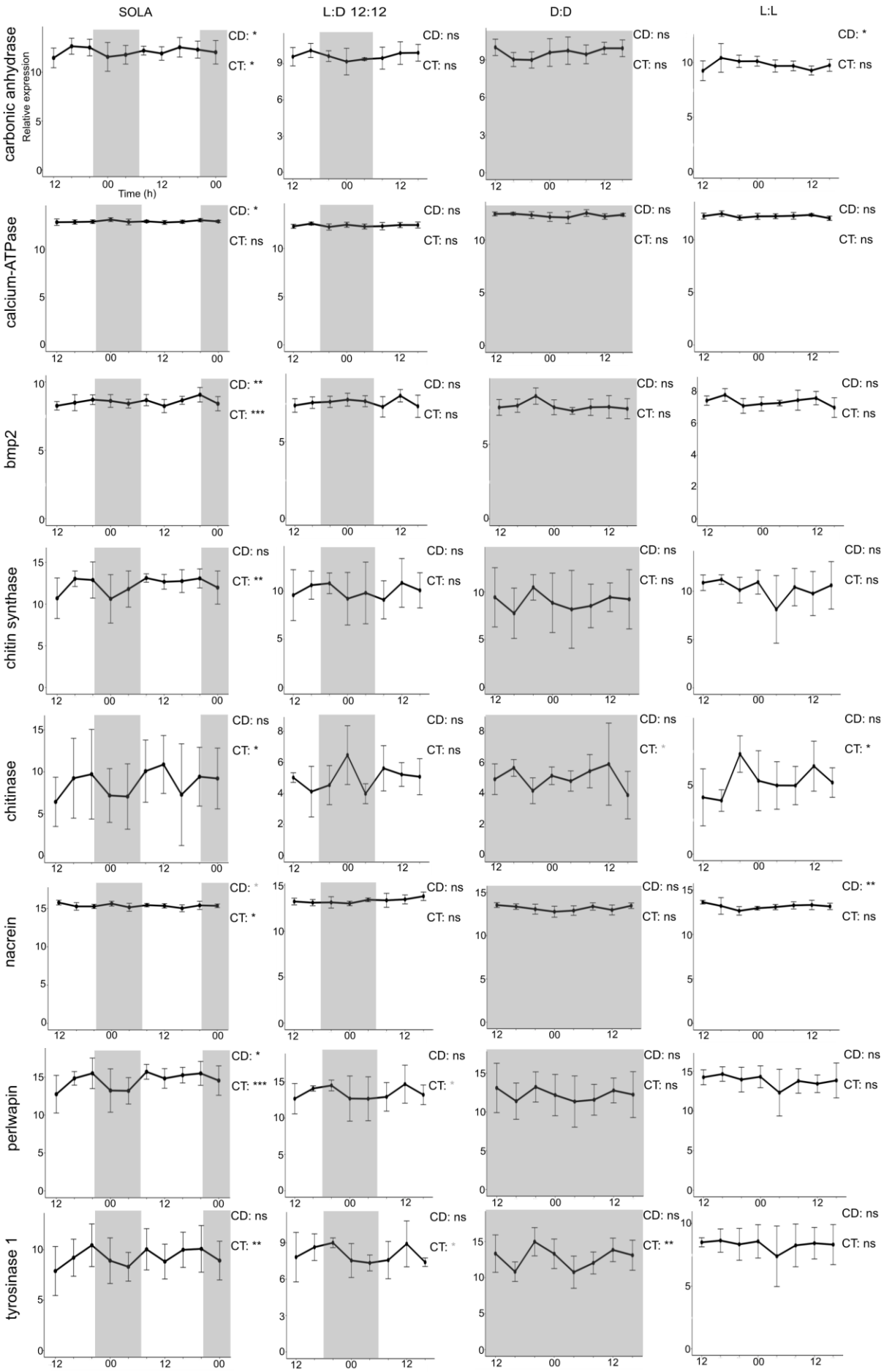
SOLA
L:D 12:12
D:D
L:L
carbonic anhydrase
calcium-ATPase
bmp2
chitin synthase
chitinase
nacrein
perlwapin
tyrosinase 1
Relative expression
Time (h)
CD: * CT: *
CD: ns CT: ns
CD: ns CT: ns
CD: * CT: ns
CD: * CT: ns
CD: ns CT: ns
CD: ns CT: ns
CD: ns CT: ns
CD: ** CT: ***
CD: ns CT: ns
CD: ns CT: ns
CD: ns CT: ns
CD: ns CT: **
CD: ns CT: ns
CD: ns CT: ns
CD: ns CT: ns
CD: ns CT: *
CD: ns CT: ns
CD: ns CT: *
CD: ns CT: *
CD: * CT: *
CD: ns CT: ns
CD: ns CT: ns
CD: ** CT: ns
CD: * CT: ***
CD: ns CT: *
CD: ns CT: ns
CD: ns CT: ns
CD: ns CT: **
CD: ns CT: *
CD: ns CT: **
CD: ns CT: ns
12 00 12 00

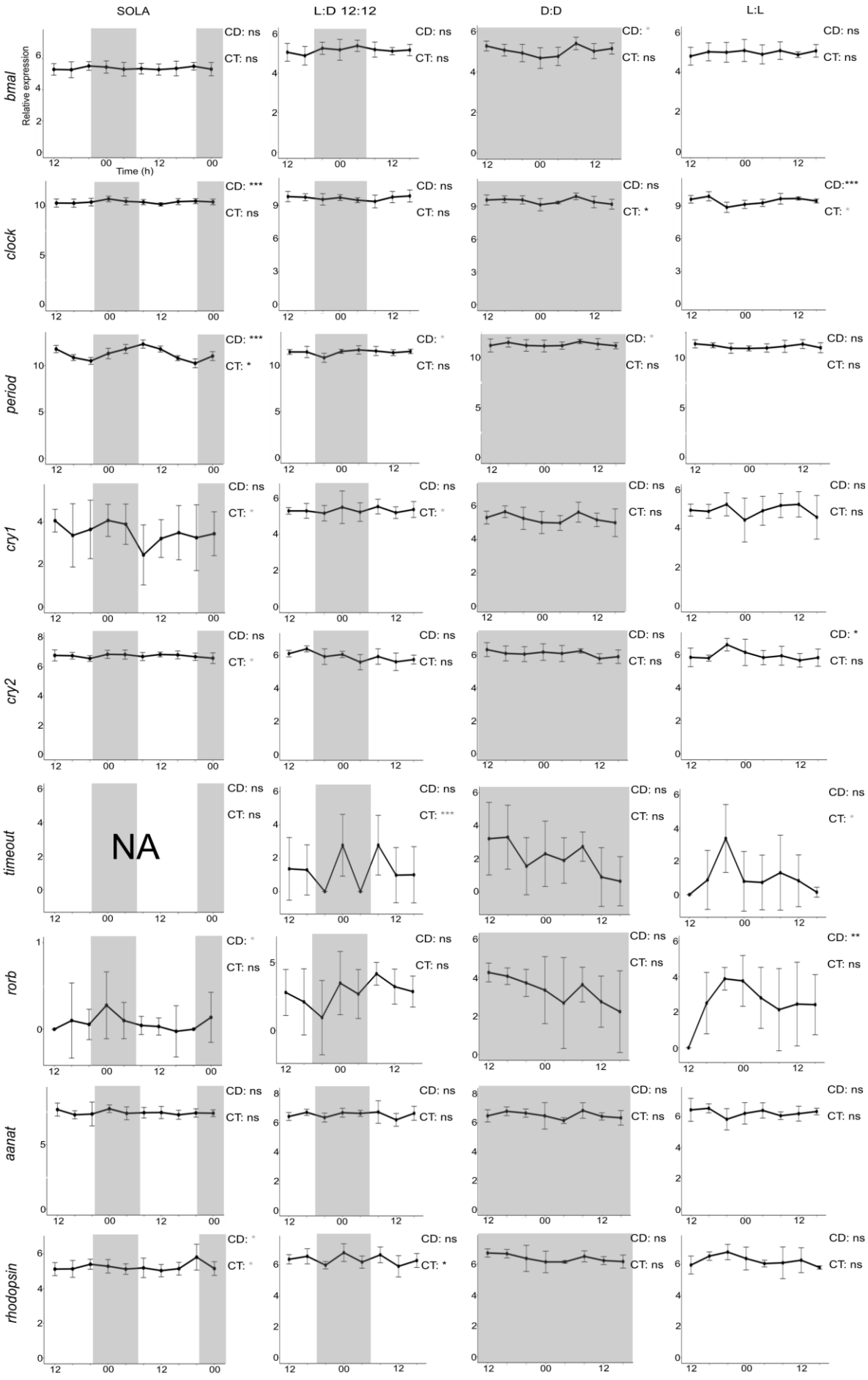
SOLA
L:D 12:12
D:D
L:L
bmal
clock
period
cry1
cry2
timeout
rorb
aanat
rhodopsin
Relative expression
Time (h)
NA
CD: ns
CT: ns
CD: *
CT: *
CD: ***
CT: ***
CD: **
CT: **
12
00

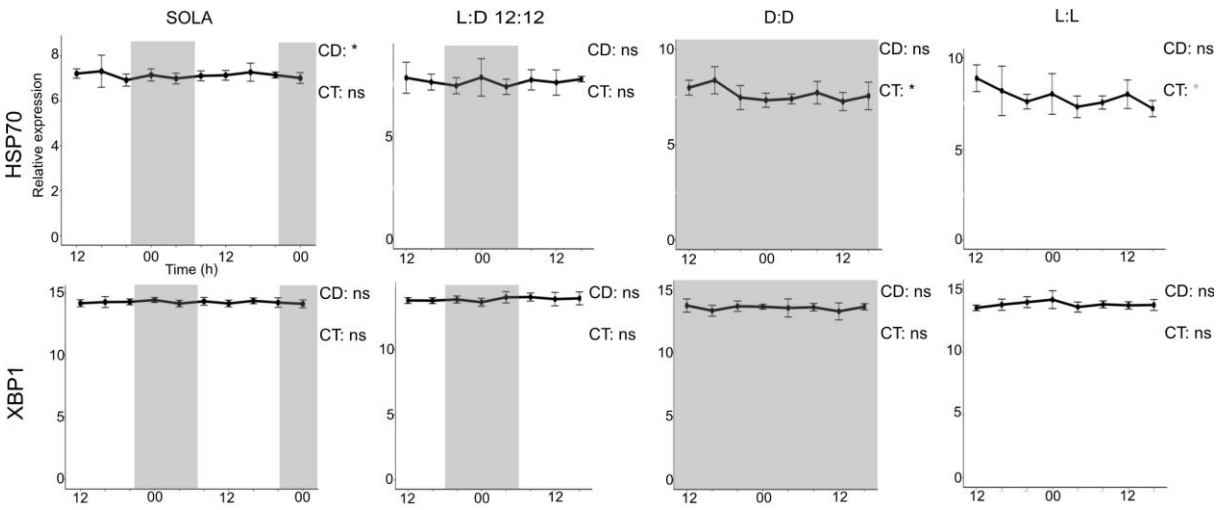

Figure S5: Targeted gene expressions over time at sea (SOLA) and in different conditions of light. Light conditions tested were; photoperiodic condition of an alternance of 12 hours of light (in white) and 12 hours of dark (in grey) (L:D 12:12), continuous darkness (D:D) and continuous enlightenment (L:L). Circadian (CD) and circatidal (CT) rhythmicity of expression were tested. Cosinor adjustment and RAIN analysis were achieved to test rhythmicity of expression. When only one was significant, the significance level is in grey. Significance levels: ns: $p>0.05$; *: $0.05 \geq p \geq 0.01$; **: $0.01 > p \geq 0.001$; ***: $p <0.001$

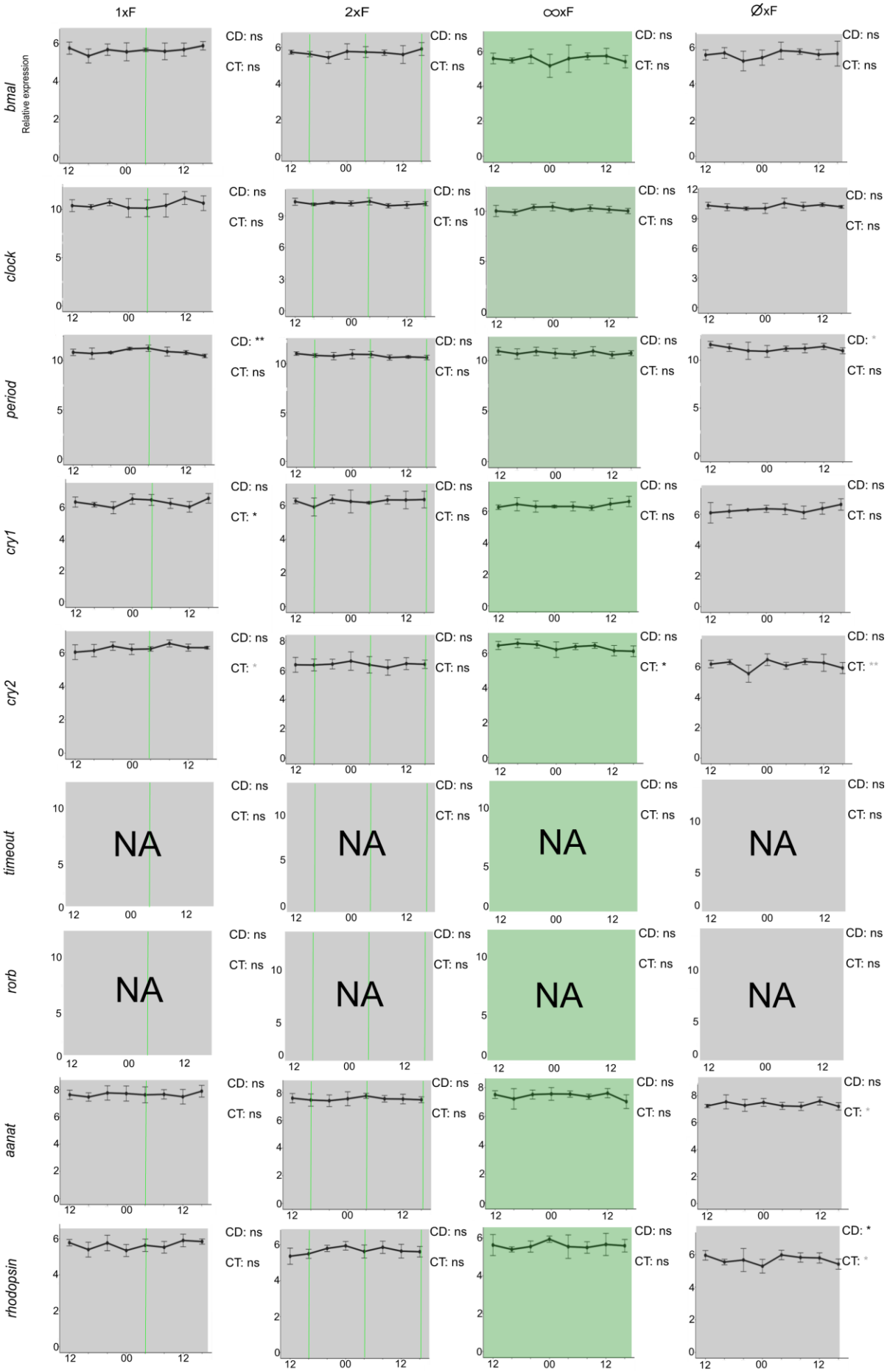
1xF
2xF
∞xF
ØxF
bmal
Relative expression
clock
period
cry1
cry2
timeout
rorb
aanat
rhodopsin
CD: ns
CT: ns
CD: **
CD: *
CT: *
CT: **
NA
12
00

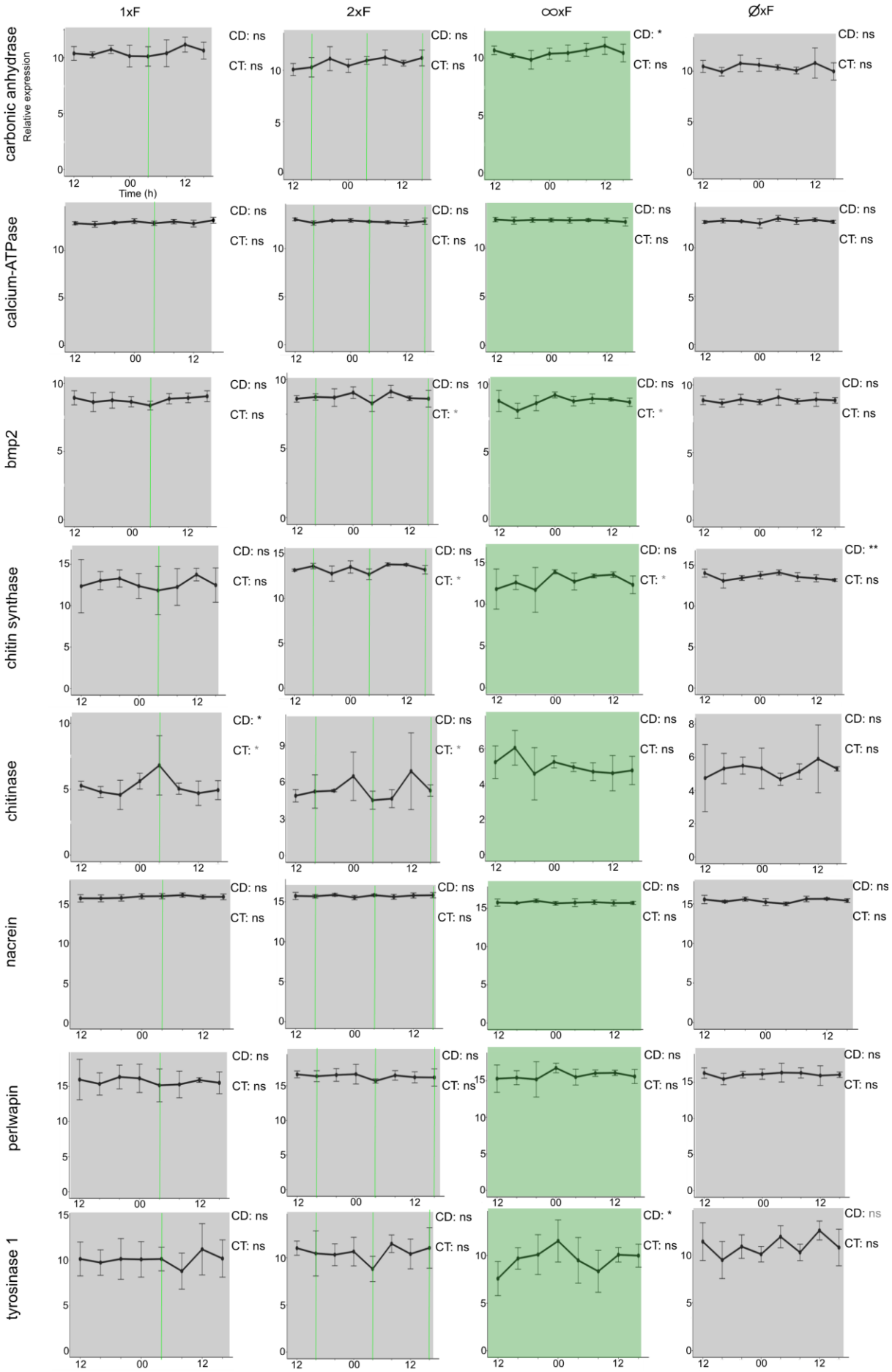
1xF
2xF
∞xF
ØxF
carbonic anhydrase
Relative expression
calcium-ATPase
bmp2
chitin synthase
chitinase
nacrein
perlwapin
tyrosinase 1
Time (h)
12
00
12
CD: ns
CT: ns
CD: *
CT: *
CD: **
CT: **

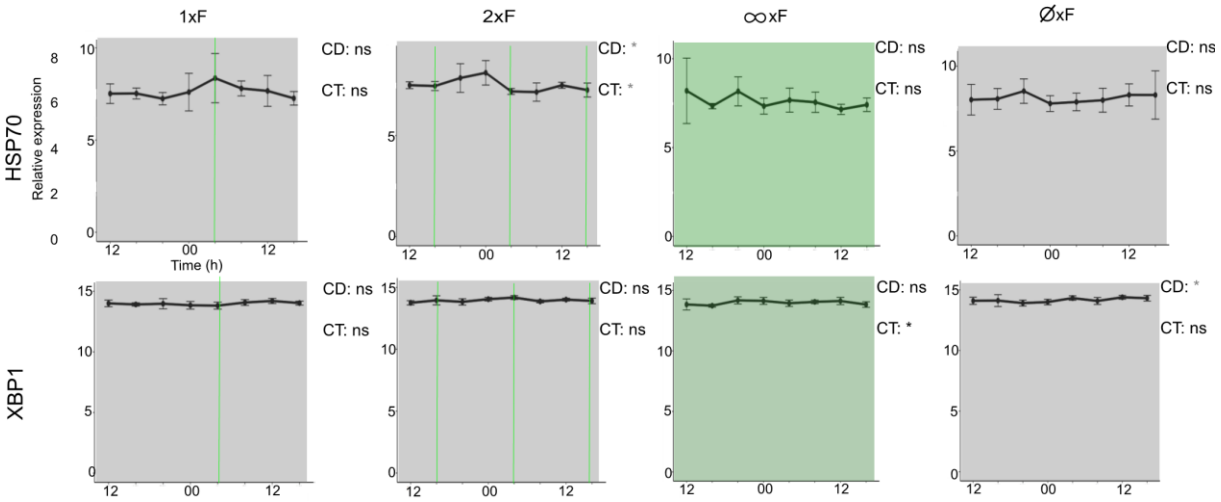

Figure S6: Targeted gene expressions in different conditions of food availability in continuous darkness*. Food availability conditions tested were; fed once a day (1xF), fed twice a day (2xF), fed continuously (∞xF) and never fed (∅xF). Hours of feeding are indicated in green. Circadian (CD) and circatidal (CT) rhythmicity of expression were tested. Cosinor adjustment and RAIN analysis were achieved to test rhythmicity of expression. When only one was significant, the significance level is in grey. Significance levels: ns: p>0.05; *: 0.05 ≥ p ≥ 0.01; **: 0.01 > p ≥ 0.001; ***: p <0.001*

Table S5: Targeted genes and designed set of probes used for the NanoString gene expression assessment.

Gene	Probes
Clock	**Probe A:** CAGACCCCACACTGTGACAGGAAGACATATTAGGCCCTGATGTAACAGAACCTCAAGACCTAAGCGACAGCGTGACCTTGTTTCA **Probe B:** CGAAAGCCATGACCTCCGATCACTCTTGTCATTGTCTCCTAATTTTGATGATCCTGCTCTGTCTGATGAGG
Bmal	**Probe A:** GGATCTGGAGATGGAGGCAAGGGAGGCAACAGAAAAAGGACATCCTCTTCTTTTCTTGGTGTTGAGAAGATGCTC **Probe B:** CGAAAGCCATGACCTCCGATCACTCATTTAGCATGGCCTCTTCAACAATATCTCCAGGACCATCA
Cry1	**Probe A:** AAGTTCGGCATACCAAAACCACAAACTGTGGGTGTGTTTCCTGACTGTAACACAATTCTGCGGGTTAGCAGGAAGGTTAGGGAAC **Probe B:** CGAAAGCCATGACCTCCGATCACTCACCCAGTGTTCCATAACATTGATCTTCCTGTTTACCCTGACCATGAGAAG
Cry2	**Probe A:** GTTATTATTAGATGCTGATTGGAGTGTAAATGCAGGCACGTGGATGTGGTCTGTTGAGATTATTGAGCTTCATCATGACCAGAAG **Probe B:** CGAAAGCCATGACCTCCGATCACTCAGAGGAGATCTGTGGATATCATGGGAGGAAGGCATGAAGGTTTTTGATGA
Rorb	**Probe A:** GCCTTCGAGACGGCATCTCTGCTCAAATGTTACAACAACTGACTCCTGAACAAAGACGCCTATCTTCCAGTTTGATCGGGAAACT **Probe B:** CGAAAGCCATGACCTCCGATCACTCATCAGCGGCTTTTGAAAGCATTAAAGACAATGCCACTTTCCAGTTGGGTG
Period	**Probe A:** ATGTTTAGGGCCACAGTTCTAGCTTCATCTACTACAGGCGAACCTAACTCCTCGCTACATTCCTATTGTTTTC **Probe B:** CGAAAGCCATGACCTCCGATCACTCCACCATCAGGAGTTGGACTAACAGAAACGTCTTCAGTTGGTTCTTCTACG
Tim	**Probe A:** CGATCAGGTTATATGGGCAATACATTGTACAGGACTGGAAGATCTCTTGTCCAATTTGGTTTTACTCCCCTCGATTATGCGGAGT **Probe B:** CGAAAGCCATGACCTCCGATCACTCCCTCCTAATGAAGATAGAGAGCAGAGAACAGACGATGATGCTACAGTCCA
Aanat	**Probe A:** AAGTTCATCTCCATGAAAACAACCTCTGTTTAACTCTGGTGCTTCTGTGTCTTTCGGGTTATATCTATCATTTACTTGACACCCT **Probe B:** CGAAAGCCATGACCTCCGATCACTCTCATCTTTCAGTGTATCTTCATGGTAACGTGTTGCTGACACAAATCCTAT
Rhodopsin	**Probe A:** GGAGGAACCGCCCATACTAATGACCATATCCACACTAAGACTATCATCATCAACAGCCACTTTTTTTCCAAATTTTGCAAGAGCC **Probe B:** CGAAAGCCATGACCTCCGATCACTCTTTGGAATCCTTCAGGGACGTATGCTCCCCACCCAAATATC
Perwalpin	**Probe A:** ATGTCTTTTGCAACTTTTGTCCTTTTTACATCTTTTTCCCTTTTTACCAGCACCGTGTGGACGGCAACTCAGAGATAACGCATAT **Probe B:** CGAAAGCCATGACCTCCGATCACTCGGAGCAATTTTTTTCCTGACTCTTCGGCATCTTTTATTGCAACACTTTTC
Bmp2	**Probe A:** GCTGGGTGAATGTCAAGGGAAACCCATGTTGCATTCTTAGTTTTTACGTGCCTGGAGTTTATGTATTGCCAACGAGTTTGTCTTT **Probe B:** CGAAAGCCATGACCTCCGATCACTCGCACTTCTATTCCATGGTTCTGTTTTGGTGTTTTACGCCATTTTAATACT
Hsp70	**Probe A:** AAAGTACATCTTTGATAGTGTCGCTACGATCGCCGGACAGAATAGCAGCTCAGATAAGGTTGTTATTGTGGAGGATGTTACTACA **Probe B:** CGAAAGCCATGACCTCCGATCACTCTACACCACCTGCAGTTTCAATACCAAGGGACAATGGAGCTACGTCAACTA
Carbonic anhydrase	**Probe A:** TAATCTGTATGTCCCAGTTAAAGGCCCTCCTGATATTTCTGATGCTTTGGCTTCCTTCCTGTGTTCCAGCTACAAACTTAGAAAC **Probe B:** CGAAAGCCATGACCTCCGATCACTCTGTTCAGAACCTTTGTTGTCGTCTGCTCCCCAGTGAAAATGAAACTGTTC
Chitin synthase	**Probe A:** AGCTAGGCCAGCTAGATATGTGCAAATTATTCCAGATCCAAGCTGAATGACATAAAATTGGTTTTGCCTTTCAGCAATTCAACTT **Probe B:** CGAAAGCCATGACCTCCGATCACTCGCAAGTGTCAAAGGCAATGCAAAGGCTGCTTTCTGCATGTGTAATTTACA
Nacrein	**Probe A:** GGCAGTCCAATGGCTGCTAAAAGGTCAACTTCTGTTTCTGACTGGCTGGTCAAGACTTGCATGAGGACCCGCAAATTCCT **Probe B:** CGAAAGCCATGACCTCCGATCACTCCTGGAAAACCTTCCAGTCCAACATCATAAGTAACTCCTTTGCTGGGATCA
Tyrosinase	**Probe A:** CGATTTCTCGTCTCAACAACGTACTCGGGTTTGTTGGCGTTGACCAAAATCTTTCGTTGGGACGCTTGAAGCGCAAGTAGAAAAC **Probe B:** CGAAAGCCATGACCTCCGATCACTCTGTAAACACTGTTTTTACCCTCTCTGGATGAACTGGAGAGCCTACTACTC
Chitinase	**Probe A:** CTTTCCCATGAACCATGCAGGTCATACGCCATTAAGTTGATGAAATCCAGCCAGCAGACCTGCAATATCAAAGTTATAAGCGCGT **Probe B:** CGAAAGCCATGACCTCCGATCACTCCTGTTTCGTCCTTTCTAGGATATAGTGGACTAATGTGACCGGTTTTC
Ca2+ATPase	**Probe A:** GTTGATTCTCCCTTCTTGACATGGTCTGATTCACCTGTTAACGAACTTTCCCTGCCAATGCACTCGATCTTGTCATTTTTTTGCG **Probe B:** CGAAAGCCATGACCTCCGATCACTCTCTTTCCACTTCCTTCCATGACATGGGTACCTGACAGCAAAATAGGACTT
Xbp1	**Probe A:** ACCAGGTTGGCCCAGGCGTTCTTTAAGGTGTTGATTTTCTGTAATTAATGCAAACTGGAGAGAGAAGTGAAGACGATTTAACCCA **Probe B:** CGAAAGCCATGACCTCCGATCACTCTCAAAGGATACTGCAGATCCCGAGGACTCAGACTTTCTCTCAGCCAATGA
α-tubulin	**Probe A:** TGTTCAAGTTGGTGTATGTTGGTCTCTCAATATCCAAGTTACGTCTGCGATTGCTGCATTCCGCTCAACGCTTGAGGAAGTA **Probe B:** CGAAAGCCATGACCTCCGATCACTCGTCAAATCTTAGGGAGGCAGTGATAGGACTGACAATCTGACCAATGAGTC
Actin	**Probe A:** GAGTCGAGTACGATACCAGTGGTACGACCGGAAGCATACAGTGAGAGTACCTGAGGCTGTTAAAGCTGTAGCAACTCTTCCACGA **Probe B:** CGAAAGCCATGACCTCCGATCACTCTAACCTTCGTAGATTGGTACGGTGTGTGTGACACCATCTCCA
Ef1α	**Probe A:** ACTGTTCCAATACCTCCAATTTTGTAAACATCCTGGAGTGGGAGACGGAGCTAGGACGCAAATCACTTGAAGAAGTGAAAGCGAG **Probe B:** CGAAAGCCATGACCTCCGATCACTCTAACAACCATACCTGGTTTGATGATTCCAGTTTCTACTCTACCTACTGGC
Rpl7	**Probe A:** GATGTATGGCTCAGCAATTCTCAGCATGTTGATGGTAGCTTTGCCACGCGATGACGTTCGTCAAGAGTCGCATAATCT **Probe B:** CGAAAGCCATGACCTCCGATCACTCCAATTCTCGTACACTCTTCAAGTTTGGGTAGCCCCATGT
Hprt1	**Probe A:** GCTACTCTCTCCACTCTATCGGCTACAAGACCTGCTGGAACTAAAACTCTCATTTGGAATGATGTGTACTGGGAATAAGACGACG **Probe B:** CGAAAGCCATGACCTCCGATCACTCGCAACAATTGGCTCCTCCTGAGAATCTTGCACTATGTCCAGA

Table S6: Statistics of circadian and circatidal periodicities at sea (SOLA). Bold values are significant. When Cosinor analysis as implemented in Discorhythm and RAIN analysis are both significant, the line is highlight in green. Grey numbers are outputs from RAIN analysis out of the framework of circatidal definition due to the sampling time interval.

	Circadian (24h+/-4h)				Circatidal (12.4h+/2h)			
	Cosinor		RAIN		Cosinor		RAIN	
	Period (h)	p-value	Period (h)	p-value	Period (h)	p-value	Period (h)	p-value
bmal	20	0.243	24	0.681	12	0.324	12	0.836
clock	20	**0.004**	20	**2.3E-4**	10	0.606	16	0.087
period	24	**3E-24**	24	**2E-31**	13	**0.050**	12	**0.005**
cry1	28	0.338	28	0.156	14	**0.044**	16	0.074
cry2	28	0.130	28	0.157	13	**0.026**	12	0.145
timeout	ND	ND	ND	ND	ND	ND	ND	ND
rorb	28	**0.039**	28	1.000	11	0.313	8	1.000
aanat	22	0.505	24	0.338	11	0.061	12	0.148
rhodopsin	20	**0.034**	24	0.068	12	**0.023**	12	0.224
carbonic anhydrase	22	**0.041**	24	**0.025**	12	**0.019**	12	**0.019**
Ca2+-ATPase	20	**0.016**	20	**5.5E-4**	10	0.125	16	0.390
bmp2	21	**0.007**	24	**3.1E-4**	12	**7.4E-3**	12	**5.0E-4**
chitin synthase	20	0.099	24	0.113	13	**0.002**	12	**0.004**
chitinase	20	0.466	28	0.935	14	**0.017**	16	**0.033**
nacrein	20	0.135	20	**0.028**	11	**5.4E-5**	12	**0.015**
perlwapin	20	**0.048**	24	**0.030**	13	**6.5E-4**	12	**3.4E-4**
tyrosinase 1	21	0.113	24	0.182	12	**0.010**	12	**0.004**
hsp70	26	**0.050**	28	**0.008**	13	0.112	16	0.424
xbp1	20	0.269	20	0.779	10	0.263	16	0.150

Table S7: Statistics of circadian and circatidal periodicities in photoperiodic (L:D 12:12) condition in aquarium. Bold values are significant. When Cosinor analysis as implemented in Discorhythm and RAIN analysis are both significant, the line is highlight in green. Grey numbers are outputs from RAIN analysis out of the framework of circatidal definition due to the sampling time interval.

	Circadian				Circatidal			
	Cosinor		RAIN		Cosinor		RAIN	
	Period (h)	p-value	Period (h)	p-value	Period (h)	p-value	Period (h)	p-value
bmal	28	0.359	28	0.559	10	0.195	16	0.839
clock	28	0.339	28	0.319	13	0.276	12	0.497
period	20	**0.044**	24	0.127	14	0.052	16	0.064
cry1	20	0.564	20	0.940	10	**0.031**	8	0.663
cry2	27	0.105	28	**0.046**	14	0.219	16	0.462
timeout	26	0.630	28	1.000	10	**0.001**	8	1.000
rorb	28	0.215	28	0.245	10	0.054	8	0.898
aanat	23	0.217	28	0.795	14	0.353	16	0.184
rhodopsin	20	0.263	20	0.661	10	**0.016**	16	**0.045**
carbonic anhydrase	23	0.091	24	0.166	11	0.867	16	0.829
Ca2+-ATPase	24	0.948	24	0.596	10	0.285	8	0.724
bmp2	20	0.732	28	0.913	14	0.467	16	0.533
chitin synthase	20	0.312	20	0.847	14	0.527	16	0.406
chitinase	20	0.481	28	0.760	14	0.149	12	0.173
nacrein	28	0.206	28	0.332	14	0.523	12	0.899
perlwapin	20	0.115	20	0.617	14	0.286	16	**0.024**
tyrosinase 1	20	0.128	20	0.292	14	0.374	16	**0.026**
hsp70	20	0.933	28	0.927	12	0.338	8	0.819
xbp1	28	0.292	28	0.916	10	0.548	12	0.889

Table S8: Statistics of circadian and circatidal periodicities in constant light (L:L) condition in aquarium. Bold values are significant. When Cosinor analysis as implemented in Discorhythm and RAIN analysis are both significant, the line is highlight in green. Grey numbers are outputs from RAIN analysis out of the framework of circatidal definition due to the sampling time interval.

	Circadian				Circatidal			
	Cosinor		RAIN		Cosinor		RAIN	
	Period (h)	p-value	Period (h)	p-value	Period (h)	p-value	Period (h)	p-value
bmal	22	0.743	24	0.853	12	0.782	8	0.863
clock	22	**6.8E-4**	20	**8.4E-4**	10	0.186	16	**0.019**
period	22	0.063	24	0.122	11	0.401	16	0.827
cry1	20	0.325	24	0.860	14	0.221	16	0.472
cry2	27	**0.045**	28	**0.006**	12	0.105	12	0.443
timeout	28	0.170	24	1.000	13	**0.013**	8	1.000
rorb	23	**0.005**	24	**0.003**	14	0.193	16	0.103
aanat	20	0.655	28	0.924	13	0.082	16	0.129
rhodopsin	28	0.123	28	**0.038**	14	0.140	16	0.234
carbonic anhydrase	27	**0.025**	24	**0.004**	13	0.307	8	0.650
Ca2+-ATPase	20	0.180	20	0.369	10	0.056	16	0.617
bmp2	20	0.051	20	0.122	10	0.103	16	0.175
chitin synthase	28	0.222	24	0.901	10	0.144	8	0.805
chitinase	20	0.113	20	0.492	14	**0.012**	16	**0.004**
nacrein	23	**0.008**	24	**4.5E-5**	12	0.230	16	0.827
perlwapin	28	0.240	28	0.648	10	0.300	8	0.803
tyrosinase 1	24	0.574	24	0.917	10	0.565	16	0.828
hsp70	28	0.243	24	0.198	11	**0.016**	12	0.116
xbp1	23	0.106	24	0.454	14	0.285	16	0.326

Table S9: Statistics of circadian and circatidal periodicities in constant dark (D:D) condition in aquarium. Bold values are significant. When Cosinor analysis as implemented in Discorhythm and RAIN analysis are both significant, the line is highlight in green. Grey numbers are outputs from RAIN analysis out of the framework of circatidal definition due to the sampling time interval.

	Circadian				Circatidal			
	Cosinor		RAIN		Cosinor		RAIN	
	Period (h)	p-value	Period (h)	p-value	Period (h)	p-value	Period (h)	p-value
bmal	23	**0.019**	20	0.140	10	0.268	16	0.381
clock	20	0.051	20	0.577	14	**0.016**	16	**0.023**
period	20	**0.029**	28	0.799	14	0.246	16	0.731
cry1	20	0.145	20	0.886	14	0.083	16	0.277
cry2	20	0.211	20	0.909	10	0.207	16	0.609
timeout	20	0.149	20	0.999	14	0.206	16	0.816
rorb	20	0.487	28	0.918	14	0.396	16	0.823
aanat	20	0.483	28	0.938	14	0.143	16	0.305
rhodopsin	20	0.147	28	0.468	14	0.301	16	0.655
carbonic anhydrase	28	0.130	28	**0.038**	13	0.072	12	0.545
Ca2+-ATPase	20	0.231	28	0.745	14	0.232	16	0.456
bmp2	28	0.207	28	0.187	13	0.142	16	0.068
chitin synthase	20	0.694	20	0.905	14	0.391	16	0.527
chitinase	20	0.172	20	0.617	10	**0.032**	12	0.446
nacrein	28	0.057	28	0.121	14	0.216	16	0.346
perlwapin	20	0.820	28	0.469	13	0.463	16	0.679
tyrosinase 1	20	0.168	20	0.415	14	**0.004**	16	**0.003**
hsp70	20	0.148	28	0.071	14	**0.024**	16	0.051
xbp1	20	0.416	20	0.815	10	0.138	16	0.777

Table S10: Statistics of circadian and circatidal periodicities in no food availability (∅xF) and continuous darkness (D:D) condition in aquarium. Bold values are significant. When Cosinor analysis as implemented in Discorhythm and RAIN analysis are both significant, the line is highlight in green. Grey numbers are outputs from RAIN analysis out of the framework of circatidal definition due to the sampling time interval.

	Circadian				Circatidal			
	Cosinor		RAIN		Cosinor		RAIN	
	Period (h)	p-value	Period (h)	p-value	Period (h)	p-value	Period (h)	p-value
bmal	24	0.241	24	0.343	14	0.257	16	0.346
clock	25	0.112	28	0.117	10	0.659	12	0.760
period	21	**0.035**	24	0.082	11	0.486	16	0.374
cry1	20	0.186	20	0.925	11	0.479	16	0.145
cry2	22	0.200	24	0.410	10	**0.002**	12	0.505
timeout	ND	ND	ND	ND	ND	ND	ND	ND
rorb	ND	ND	ND	ND	ND	ND	ND	ND
aanat	20	0.542	20	0.925	10	**0.028**	12	0.525
rhodopsin	21	**0.019**	20	**0.010**	14	0.663	16	**0.008**
carbonic anhydrase	28	0.808	24	0.675	13	0.095	12	0.364
Ca2+-ATPase	20	0.455	28	0.620	10	0.089	16	0.545
bmp2	28	0.745	20	0.826	10	0.399	8	0.839
chitin synthase	20	**0.005**	24	**0.006**	11	0.201	16	**0.010**
chitinase	20	0.378	20	0.934	14	0.377	16	0.863
nacrein	20	0.109	24	0.098	12	0.067	12	0.099
perlwapin	21	0.335	28	0.947	10	0.405	12	0.857
tyrosinase 1	28	0.146	28	**0.044**	13	0.203	8	**0.026**
hsp70	20	0.378	20	0.897	10	0.547	16	0.578
xbp1	28	0.094	28	**0.009**	11	0.199	12	0.801

Table S11: Statistics of circadian and circatidal periodicities in one feeding time per day (1xF) and continuous darkness (D:D) condition in aquarium. Bold values are significant. When Cosinor analysis as implemented in Discorhythm and RAIN analysis are both significant, the line is highlight in green. Grey numbers are outputs from RAIN analysis out of the framework of circatidal definition due to the sampling time interval.

	Circadian				Circatidal			
	Cosinor		RAIN		Cosinor		RAIN	
	Period (h)	p-value	Period (h)	p-value	Period (h)	p-value	Period (h)	p-value
bmal	28	0.627	28	0.943	10	0.210	16	0.486
clock	20	0.850	28	0.889	10	0.054	16	0.416
period	23	**0.002**	24	**9.1E-4**	11	0.555	16	0.851
cry1	20	0.065	20	0.248	14	**0.013**	16	**0.002**
cry2	28	0.261	28	0.351	12	**0.032**	12	0.079
timeout	ND	ND	ND	ND	ND	ND	ND	ND
rorb	ND	ND	ND	ND	ND	ND	ND	ND
aanat	20	0.494	20	0.812	10	0.375	16	0.793
rhodopsin	28	0.208	28	0.315	10	0.202	8	0.224
carbonic anhydrase	20	0.238	28	0.830	14	0.214	16	0.078
Ca2+-ATPase	20	0.281	28	0.962	10	0.232	16	0.494
bmp2	28	0.170	28	0.422	10	0.401	12	0.777
chitin synthase	20	0.321	24	0.748	14	0.490	16	0.476
chitinase	20	**0.004**	20	**0.042**	14	0.109	16	**0.013**
nacrein	28	0.106	28	0.342	12	0.794	12	0.794
perlwapin	25	0.800	28	0.937	14	0.540	12	0.622
tyrosinase 1	20	0.748	24	0.864	14	0.405	16	0.740
hsp70	23	0.064	20	0.328	14	0.553	16	0.217
xbp1	28	0.160	28	0.534	14	0.443	16	0.329

Table S12: Statistics of circadian and circatidal periodicities in o two feeding time per day (2xF) and continuous darkness (D:D) condition in aquarium. Bold values are significant. When Cosinor analysis as implemented in Discorhythm and RAIN analysis are both significant, the line is highlight in green. Grey numbers are outputs from RAIN analysis out of the framework of circatidal definition due to the sampling time interval.

	Circadian				Circatidal			
	Cosinor		RAIN		Cosinor		RAIN	
	Period (h)	p-value	Period (h)	p-value	Period (h)	p-value	Period (h)	p-value
bmal	28	0.687	28	0.928	14	0.134	16	0.212
clock	20	0.363	20	0.947	14	0.302	16	0.307
period	20	0.300	20	0.761	11	0.320	16	0.219
cry1	28	0.738	28	0.843	10	0.420	16	0.633
cry2	20	0.320	20	0.663	14	0.263	16	0.366
timeout	ND	ND	ND	ND	ND	ND	ND	ND
rorb	ND	ND	ND	ND	ND	ND	ND	ND
aanat	21	0.414	24	0.862	14	0.856	16	0.831
rhodopsin	28	0.088	28	**0.049**	14	0.451	16	0.746
carbonic anhydrase	28	0.556	28	0.919	11	0.136	12	0.423
Ca2+-ATPase	20	0.191	20	0.422	10	0.096	16	0.079
bmp2	28	0.722	24	0.756	10	**0.048**	8	0.409
chitin synthase	20	0.212	20	0.089	10	**0.016**	16	0.124
chitinase	20	0.486	20	0.092	14	0.072	16	**0.033**
nacrein	23	0.554	28	0.848	10	0.156	8	0.855
perlwapin	28	0.809	28	0.834	10	0.303	12	0.833
tyrosinase 1	28	0.572	24	0.944	10	0.191	8	0.867
hsp70	23	**0.019**	28	0.069	14	**0.038**	12	0.151
xbp1	28	0.135	28	0.099	10	0.205	12	0.859

Table S13: Statistics of circadian and circatidal periodicities in continuous food availability (∞xF) and continuous darkness (D:D) condition in aquarium. Bold values are significant. When Cosinor analysis as implemented in Discorhythm and RAIN analysis are both significant, the line is highlight in green. Grey numbers are outputs from RAIN analysis out of the framework of circatidal definition due to the sampling time interval.

	Circadian				Circatidal			
	Cosinor		RAIN		Cosinor		RAIN	
	Period (h)	p-value	Period (h)	p-value	Period (h)	p-value	Period (h)	p-value
bmal	20	0.310	24	0.496	14	0.336	8	0.498
clock	28	0.095	24	0.147	12	0.061	12	0.167
period	28	0.880	20	0.872	11	0.121	12	0.665
cry1	22	0.190	24	0.660	11	0.260	12	0.457
cry2	28	0.439	28	0.583	14	**0.035**	16	**0.016**
timeout	ND	ND	ND	ND	ND	ND	ND	ND
rorb	ND	ND	ND	ND	ND	ND	ND	ND
aanat	25	0.278	24	0.804	12	0.147	8	0.572
rhodopsin	20	0.429	20	0.207	14	0.164	16	0.070
carbonic anhydrase	27	**0.013**	28	**0.004**	12	0.206	12	0.805
Ca2+-ATPase	20	0.695	24	0.868	11	0.554	16	0.758
bmp2	28	0.062	28	**0.006**	13	**0.037**	12	0.214
chitin synthase	28	0.158	28	**0.024**	10	0.067	12	**0.034**
chitinase	28	0.441	28	**0.011**	14	0.299	12	0.866
nacrein	20	0.807	28	0.830	12	0.260	12	0.828
perlwapin	28	0.495	28	0.661	10	0.225	12	0.343
tyrosinase 1	20	**0.017**	20	**0.026**	14	0.266	16	0.172
hsp70	28	0.617	28	0.265	10	0.157	12	0.391
xbp1	28	0.233	24	0.283	13	**0.019**	12	**0.047**

Table S14: Growth patterns and behaviour of mussels reared under photoperiodic (L:D 12:12) condition and different food availability. Two replicates (i.e. V1 and V3) were done in order to get ten replicates per condition tested. The food availability conditions were; fed once a day in the first aquarium (A1), fed twice a day in the second aquarium (A2), fed continuously in the third aquarium (A3) and never fed in the fourth aquarium (A4). Mussel named M5 was not equipped with a valvometry device. The condition index (CI) was calculated based on the ratio between dry soft tissue on dry hard tissue. The growth over the ten days experiment was measured based on the calcein marking and number of increments formed counted. The valve opening duration is the percentage of time where mussels were open (*i.e.*, > 20% of openness). The valve closure duration (VCD) was multiplicated by the number of closures to get a coefficient relative to the mean closure duration per sequence, smaller was the coefficient, longer was the average closure duration.

Mussel	CI	Growth (µm)	Number of incr. per day	Valve opening duration(%)	Valve activity rhythm (h)	Number of closures (total)	VCDx Nber of closures
V1A1M1	15.15	241.40	2.5	ND	ND	11	ND
V1A1M2	19.25	429.63	1.6	ND	ND	6	ND
V1A1M3	20.53	631.85	1.4	ND	ND	ND	ND
V1A1M4	21.48	645.10	1.5	86.4	16	11	1.15
V1A1M5	18.18	499.88	1.7	ND	ND	ND	ND
V3A1M1	6.97	ND	ND	ND	ND	6	ND
V3A1M2	9.33	35.70	0.7	ND	ND	ND	ND
V3A1M3	9.17	264.70	1.2	ND	ND	ND	ND
V3A1M4	12.58	ND	ND	91.6	24	6	1.4
V3A1M5	14.05	243.20	0.9	ND	ND	ND	ND
V1A2M1	19.11	283.03	1.8	ND	ND	ND	ND
V1A2M2	17.54	929.04	1.9	56.7	12	19	2.28
V1A2M3	16.11	340.49	2.1	84.9	12	17	0.89
V1A2M4	21.02	135.86	1.2	79.4	12-27	23	0.95
V1A2M5	18.06	556.00	1.6	ND	ND	ND	ND
V3A2M1	12.88	66.17	0.9	ND	ND	ND	ND
V3A2M2	11.40	126.67	1.3	ND	19	ND	ND
V3A2M3	10.38	352.21	1.9	ND	ND	ND	ND
V3A2M4	12.54	204.04	ND	81.3	12	14	1.34
V3A2M5	9.91	215.41	ND	ND	ND	ND	ND
V1A3M1	18.32	96.48	1	ND	ND	ND	ND
V1A3M2	21.58	258.73	1.5	69.1	27	15	1.99
V1A3M3	16.34	250.13	2.4	84.6	AR	8	1.83
V1A3M4	17.56	940.55	3.7	82.5	23	7	2.33
V1A3M5	19.57	364.45	2.9	ND	ND	ND	ND
V3A3M1	8.86	27.17	ND	ND	ND	ND	ND
V3A3M2	9.62	94.50	1.3	87.5	28	8	1.56
V3A3M3	12.30	275.89	0.8	93.7	11	7	0.31
V3A3M4	10.14	63.80	ND	88.5	23	7	0.83
V3A3M5	9.03	300.06	1	ND	ND	ND	ND
V1A4M1	19.28	277.50	0.7	ND	ND	ND	ND
V1A4M2	19.08	103.73	0.8	39.2	AR	20	3.04
V1A4M3	17.48	ND	ND	70.6	15	20	1.47
V1A4M4	17.27	330.06	1.5	ND	ND	ND	ND
V1A4M5	17.79	135.82	1	ND	ND	ND	ND
V3A4M1	9.05	103.00	0.8	55.2	10	21	2.13
V3A4M2	11.23	146.24	1.4	55.1	23	15	2.99
V3A4M3	11.59	ND	ND	60.5	26	21	1.88
V3A4M4	11.26	190.25	2.5	ND	ND	ND	ND
V3A4M5	10.57	139.07	1.2	ND	ND	ND	ND

Table S15: Growth patterns and behaviour of mussels reared under constant dark (D:D) condition and different food availability. Two replicates (i.e. V2 and V4) were done in order to get ten replicates per condition tested. The food availability conditions were; fed once a day in the first aquarium (A1), fed twice a day in the second aquarium (A2), fed continuously in the third aquarium (A3) and never fed in the fourth aquarium (A4). Mussels named M5 was not equipped with a valvometry device. The condition index (CI) was calculated based on the ratio between dry soft tissue on dry hard tissue. The growth over the ten days experiment was measured based on the calcein marking and number of increments formed counted. The valve opening duration is the percentage of time where mussels were open (i.e. > 20% of openness). Arrhythmic individuals were annotated "AR". The valve closure duration (VCD) was multiplicated by the number of closures to get a coefficient relative to the mean closure duration per sequence, smaller was the coefficient, longer was the average closure duration.

Mussel	CI	Growth (µm)	Number of incr. per day	Valve opening duration(%)	Valve activity rhythm (h)	Number of closures (total)	VCDx Nber of closures
V2A1M1	17.77	95.03	1.3	57.6	25	23	1.84
V2A1M2	16.37	184.46	1	ND	ND	ND	ND
V2A1M3	15.49	728.90	1.7	92.3	AR	12	0.64
V2A1M4	14.90	333.38	1.5	84.6	12-24	13	1.18
V2A1M5	15.49	ND	ND	ND	ND	ND	ND
V4A1M1	16.34	269.22	0.8	88.2	12-24	6	2.23
V4A1M2	13.17	157.83	1	89.5	25	9	1.17
V4A1M3	12.70	134.71	1.4	71.3	12-23	17	1.69
V4A1M4	15.74	130.43	0.7	85.1	12-23	9	1.66
V4A1M5	12.48	120.85	1.3	ND	ND	ND	ND
V2A2M1	18.14	469.41	1.8	84.5	12	17	0.91
V2A2M2	18.43	ND	ND	ND	ND	ND	ND
V2A2M3	14.28	322.52	1.2	ND	ND	ND	ND
V2A2M4	16.74	238.85	1.9	ND	ND	ND	ND
V2A2M5	14.65	549.99	1.4	ND	ND	ND	ND
V4A2M1	13.58	123.14	1.8	76.1	12	14	1.71
V4A2M2	13.80	97.74	1.3	88.3	12-24	9	1.3
V4A2M3	14.25	240.65	2	ND	ND	ND	ND
V4A2M4	11.55	199.69	1.6	85.9	AR	13	1.08
V4A2M5	14.46	271.37	1.5	ND	ND	ND	ND
V2A3M1	22.43	163.31	1.5	81	18	13	1.46
V2A3M2	18.32	340.91	2	68.9	25	12	2.59
V2A3M3	15.63	288.08	1.3	ND	ND	ND	ND
V2A3M4	18.25	320.89	1.5	91.9	AR	6	1.5
V2A3M5	23.00	256.20	1.7	ND	ND	ND	ND
V4A3M1	15.58	214.29	2.1	93.4	AR	8	0.83
V4A3M2	13.05	267.37	2.4	87.1	19	10	1.29
V4A3M3	15.21	202.48	1.8	96.4	AR	7	0.51
V4A3M4	10.37	150.59	1.9	ND	ND	3	ND
V4A3M5	16.50	143.91	0.8	ND	ND	ND	ND
V2A4M1	17.81	165.33	0.7	65.3	12	19	1.91
V2A4M2	18.76	163.19	0.9	ND	ND	ND	ND
V2A4M3	16.04	138.73	0.8	78.3	AR	22	0.99
V2A4M4	17.83	248.82	1.1	65.8	9	23	1.49
V2A4M5	13.53	ND	ND	ND	ND	ND	ND
V4A4M1	15.52	56.04	ND	ND	ND	ND	ND
V4A4M2	13.54	96.33	0.8	34.6	22	21	3.11
V4A4M3	13.45	ND	ND	35.5	AR	7	ND
V4A4M4	12.93	ND	ND	29.1	14	15	4.73
V4A4M5	12.51	111.17	0.6	ND	ND	ND	ND

Table S16: Growth patterns and behaviour of mussels reared under constant light (L:L) condition and different food availability. Two replicates (i.e. V2 and V4) were done in order to get ten replicates per condition tested. The food availability conditions were; fed once a day in the first aquarium (A1), fed twice a day in the second aquarium (A2), fed continuously in the third aquarium (A3) and never fed in the fourth aquarium (A4). Mussel named M5 was not equipped with a valvometry device. The condition index (CI) was calculated based on the ratio between dry soft tissue on dry hard tissue. The growth over the ten days experiment was measured based on the calcein marking and number of increments formed counted. The valve opening duration is the percentage of time where mussels were open (i.e. > 20% of openness). Arrhythmic individuals were annotated "AR". The valve closure duration (VCD) was multiplicated by the number of closures to get a coefficient relative to the mean closure duration per sequence, smaller was the coefficient, longer was the average closure duration.

Mussel	CI	Growth (µm)	Number of incr. per day	Valve opening duration(%)	Valve activity rhythm (h)	Number of closures (total)	VCDx Nber of closures
V6A1M1	10.94	153.83	1.9	95.8	24	7	0.6
V6A1M2	13.21	322.67	ND	95.9	AR	4	0.93
V6A1M3	13.29	297.58	2.2	93	27	10	0.77
V6A1M4	12.90	155.20	2	90.5	AR	8	ND
V6A1M5	12.00	110.68	1.6	ND	ND	ND	ND
V7A1M1	9.05	122.12	ND	44.1	25	18	2.13
V7A1M2	12.06	247.44	1.6	ND	ND	ND	ND
V7A1M3	10.44	93.89	1.7	ND	ND	ND	ND
V7A1M4	10.56	80.56	1.7	66.6	14-24	25	1.34
V7A1M5	11.11	159.98	1.6	ND	ND	ND	ND
V6A2M1	15.37	165.15	2	91.8	12-19	6	1.37
V6A2M2	10.80	90.94	1.8	76.6	12-19	16	1.46
V6A2M3	9.68	159.24	1.4	88.5	12-20	7	1.73
V6A2M4	13.08	306.81	1.9	95.1	21	5	0.98
V6A2M5	13.74	275.73	1.8	ND	ND	ND	ND
V7A2M1	7.11	165.95	1.8	93.5	12	14	0.46
V7A2M2	7.29	218.34	1.7	92.5	12-19	13	0.58
V7A2M3	11.15	87.88	ND	92.1	12-28	10	0.79
V7A2M4	8.19	166.61	2	77.2	AR	19	1.2
V7A2M5	7.44	506.83	1.9	ND	ND	ND	ND
V6A3M1	8.22	148.61	ND	ND	ND	ND	ND
V6A3M2	11.31	167.57	1.5	94.2	AR	9	0.64
V6A3M3	12.39	151.97	2	94.5	23	8	0.69
V6A3M4	12.72	130.39	1.3	93.4	AR	12	0.50
V6A3M5	12.76	89.04	1.1	ND	ND	ND	ND
V7A3M1	ND	ND	ND	ND	ND	ND	ND
V7A3M2	ND	ND	ND	ND	ND	ND	ND
V7A3M3	ND	ND	ND	ND	ND	ND	ND
V7A3M4	ND	ND	ND	ND	ND	ND	ND
V7A3M5	ND	ND	ND	ND	ND	ND	ND
V6A4M1	6.69	11.97	2	63.3	AR	19	1.93
V6A4M2	13.02	25.78	ND	56.2	24	21	2.12
V6A4M3	8.97	11.25	0.8	68.6	18	14	2.24
V6A4M4	9.45	20.18	1.3	94.7	AR	ND	ND
V6A4M5	12.29	65.83	1.6	ND	ND	ND	ND
V7A4M1	9.52	151.69	2	86.8	AR	22	0.6
V7A4M2	10.18	83.20	2.2	67	AR	20	1.63
V7A4M3	9.65	69.90	2	56.4	AR	17	2.56
V7A4M4	7.64	225.51	1.8	74.8	19	12	2.06
V7A4M5	9.90	40.20	1.5	ND	ND	ND	ND

4. Comparison of gene expression quantification: quantitative PCR *vs* NanoString technology

Foreword

The last twenty years a flourishing number of techniques aiming to quantify gene expressions have been developed. Techniques can be subdivided into two categories; the targeted gene approach and the RNA-sequencing (RNAseq) in which all mRNA sequences of a sample are sequenced and numbered. RNAseq are most of the time done via an Illumina technology whereas for the targeted gene approach multiples possibilities exist such as microarrays hybridisation, quantitative polymerase chain reaction (qPCR) and most recently the NanoString technology.

Studies working on biological clocks of bivalves are classically using real-time quantitative polymerase chain reaction (RT-qPCR) to assess the level of expression of targeted genes (Chapman et al., 2017, 2020; Perrigault and Tran, 2017; Perrigault et al., 2020). This is also the case when looking to studies working on the biomineralisation process (Bjärnmark et al., 2016; Li et al., 2017; Mao et al., 2019). This technique is using retro-transcribed mRNA (*i.e.*, cDNA) and a set of primers designed for each targeted gene (Hellemans and Vandesompele, 2011). During the PCR cycling, the hybridisation to the targeted cDNA is producing fluorescence. At each cycle of denaturation-hybridisation-elongation (*i.e.*, CT), the level of fluorescence increases before the saturation of the system. A threshold located in the exponential phase of the fluorescence is set and the CT is measured. For each set of primer designed, a calibration line is drown based on CT of increasing known quantity pooled samples of cDNA. The slope of the equation is used to calculate the amplification efficiency of the set of primers. To calculate the relative expression of the targeted gene, two housekeeping genes (HKG) are at minimum required. HKG are genes recognised as having a constant expression level, they are used to normalised the CT measured of targeted genes. In other term, they are used to compensate the difference of amount of total cDNA in-between samples. The normalisation of the CT into relative expression is using the CT of the house keeping genes and of the targeted gene. One sample is chosen as having a relative expression equal to one and all the other samples will be expressed in relation to this sample.

In the case of the present work, the NanoString technology has been preferred to qPCR to assess the level of expression of genes linked to the biological clock and to the biomineralisation process. This technique relies on a set of probes, designed for each gene, that are coupled to a barcode made of fluorochromes (NanoString Technologies Inc., 2017). After a hybridisation step of the probe

with mRNA, the double stranded products are aligned in a plate. Then, barcodes are read in each well of the plate and the amount of each targeted mRNA strands are counted. The normalisation of the count is also using housekeeping genes plus negative and positives control probes. The negative probes are used as a background threshold, they are designed for engineered RNA sequences which are not present in the biological sample. The positive controls are six synthetic simple strand DNA of croissant concentrations and are used to normalise the machine/well effect. The housekeeping genes are used as in qPCR, to normalise the amount of total material used per sample. The NanoString technology has multiple advantages. First, this method is using directly the mRNA, reducing bias linked to the retrotranscription step (Ozsolak et al., 2009). Also, very little quantity of mRNA is required and all targeted genes are assessed in the same well. Therefore, when a large number of genes are targeted, it is faster to use the NanoString technology.

Multiple studies already compared these two techniques, mostly on samples of mammals. Most of the time the NanoString was proved to be more sensitive than the qPCR (*i.e.*, sensitivity = <1 copy/ cell *versus* 10-200 copies/cells) (Reis et al., 2011; Hyeon et al., 2017; Eastel et al., 2019). But sometimes discrepancies between qPCR and NanoString gene expression appears, mostly in case of low expressed genes (Veldman-Jones et al., 2015; Bergbower et al., 2020).

Based on the literature, rhythmicity of expression of biological clock core gene were expected (Chapman et al., 2020; Perrigault et al., 2020; Tran et al., 2020). But the inter-individual variability (materialised by the standard deviation) was large, masking the expected rhythmicity of expression by lowering the power of statistical test. Therefore, we questioned if this variability was linked to the model used (*Mytilus galloprovincialis*) or the method of mRNA quantification (NanoString technology) as most studies are using qPCR. To respond to this question, expression rhythmicity was evaluated using the two methods with the same set of samples.

Material and Method

Samples of mussel tissues were taken at SOLA, in the bay of Banyuls-sur-Mer (France) in September 2020. Those samples consisted in ten individuals taken every four hours over a period of 36 hours for a total of 100 samples. A piece of the mantle was taken and flash frozen in liquid nitrogen. The extraction was made using TRIzol-chloroform in November 2020. The resulting mRNA extraction has been directly distributed into two tubes that were conserved at -80°C. Extractions for the NanoString has been processed in January 2021 whereas qPCR measurements have been done in May 2022. For the NanoString, twenty-four genes were targeted; nine linked to putative biological clocks, ten related

to the biomineralisation process and five housekeeping genes. The set of probes used were designed by IDT (Integrated DNA Technologies, Coralville, IA, USA) (Table 7).

Table 7: Targeted sequences used for this study in NanoString.

Gene	Target sequences
Clock	GTTCTGTTACATCAGGGCCTAATATGTCTTCCTGTCACAGTGTGGGGTCTGCCTCATCAGACAGAGCAGGATCATCAAAATTAGGAGACAATGACAA
Bmal	GTTGCCTCCCTTGCCTCCATCTCCAGATCCTGATGGTCCTGGAGATATTGTTGAAGAGGCCATGCTAAAT
Period	AGGAGTTGGACTAACAGAAACGTCTTCAGTTGGTTCTTCTACGATGTTTAGGGCCACAGTTCTAGCTTCATCTACTACAGGC
Carbonic anhydrase	CCAAAGCATCAGAAATATCAGGAGGGCCTTTAACTGGGACATACAGATTAGAACAGTTTCATTTTCACTGGGGAGCAGACGACAACAAAGGTTCTGAACA
Chitin synthase	AGGCAGAAGAAGTAGGTGTGTCTTATAGCTTAATGTTCATTCAGCTTGGATCTGGAATAATTTGCACATATCTAGCTGGCCTAGCTTGTAAATTACACATGCAGAAAGCAGCCTTTGCATTGCCTTTGACACTTGCACCACCTCTAACCTTAGTTGTAGTCTTTC

The retro-transcription into cDNA for the qPCR was done using the PrimeScript™ RT Reagent Kit (Takara, Tokyo, Japan) following the manufacturer protocol. Seven genes were targeted, two related to the biomineralisation process, three related to putative biological clocks and two housekeeping genes (Table 8). Efficiencies of designed probes were tested using dilutions of a pool of samples cDNA. Based on CT and the different dilution, a calibration line was draw. Then, the efficiency was calculated using the slope of the line. Amplification efficiency had to be comprised between 90 and 110% to be used for further analysis (Hellemans and Vandesompele, 2011).

Table 8: Primers used for this study in qPCR.

Gene	Primer sequences	Amplicon length (bp)	Efficiency (%)
Clock	F1 5'-AGGACCAGACAAGCCTCCT-3' R1 5'-AGCGTTCTCTATCTGTACCGT-3'	154	154%
Bmal	F1 5'-ACCAGTAGCTTTAGTTTCCAGAA-3' R1 5'-GGCCTGCTGAACCTTGTTG-3'	100	57%
Period	F1 5'-TTTTCACCACCACCCCGTC-3' R1 5'-GGCAACGGTTCTAGCTTCATC-3'	120	89%
Carbonic anhydrase	F1 5'-TGGGGCAAAGCATGTTGGTA-3' R1 5'- CGTTGTCAGAGAACCCAGGT-3'	756	96%
Chitin synthase	F1 5'-AACAAGGGGAGGACAGATGG-3' R1 5'-GTTGGCCAAGGTTGAAGGAG-3'	155	90%

Outliers removal was done prior rhythm analysis using a spearman correlation (σ =2.5) and a PCA test (σ =2.5) as implemented in the R package "DiscoRhythm" (Carlucci et al., 2020). Analysis of

gene expression rhythmicity was done using a cosinor adjustment as implemented in "DiscoRhythm" and using the R package "RAIN" (Thaben and Westermark, 2014). Relative expression obtained by both techniques were transformed in percent in order to be comparable. T-tests were applied on the standard deviations and the means gene expression per sampled time to compare the two techniques.

Results and discussion

On the seven set of probes designed for qPCR analysis, two linked to putative biological clocks (*i.e.*, *clock* and *bmal*) were not efficient enough to be used. Therefore, the gene expression of five genes were assessed using this technique. Before analysing the rhythmicity of genes expressions, outliers were removed. This was done using a Spearman correlation and PCA test based on all calculated genes expression, being 24 genes for the NanoString and only five for the qPCR. In total six outliers on the 100 samples were removed from the NanoString dataset and five in the qPCR one. The sample SOLA2024 was removed in both cases.

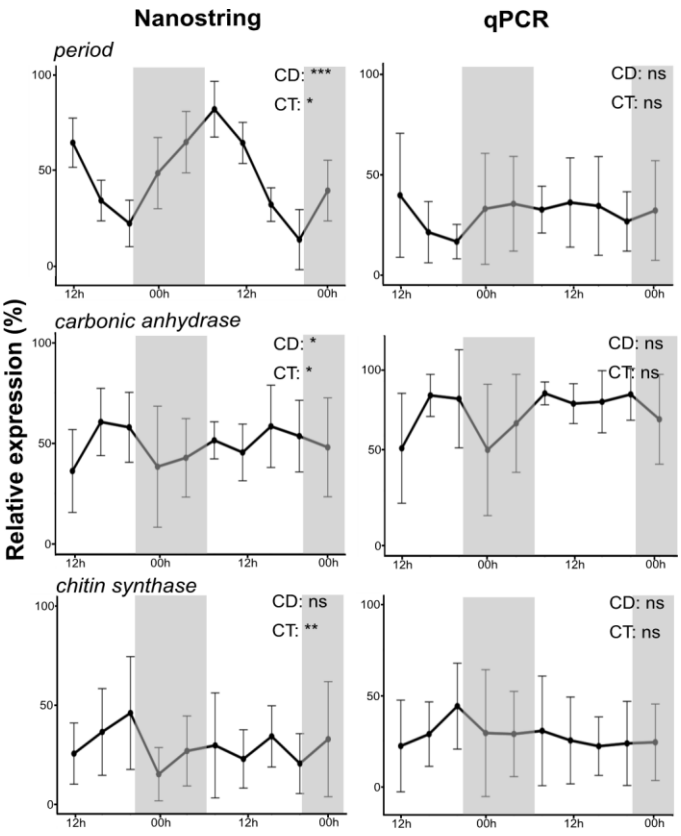

Figure 39: Expression patterns of targeted gene using the NanoString technology and the qPCR. To compare the two techniques, relative expression has been transformed in percent. Grey shaded area are the night and the day period are in white. Gene expressions periodicities were tested for circadian (CD) and circatidal (CT) oscillations. Significance levels: ns: $p>0.05$; *: $0.05 \geq p \geq 0.01$; **: $0.01 > p \geq 0.001$; ***: $p <0.001$

Profiles of expression obtained with the NanoString and the qPCR were transformed in percent in order to be compared. Profiles were similar for *Chitin synthase* and *Carbonic anhydrase*, even if the oscillations looked less strong qPCR (Figure 39). In case of *Period*, the peak of expression that occurred at 8 a.m. was not present. Visual differences between profiles obtained by NanoString and qPCR were reflected in genes expression rhythmic analysis. Significant rhythms were observed for all three targeted genes using the NanoString technology. Using the qPCR, none were significant although the Rain analysis gave a p-value close to 0.05 for the circadian periodicity of expression of *Carbonic anhydrase* (Table 9). The first hypothesis advanced for the difference of rhythmicity of expression was that the standard deviation might be higher in qPCR as it

is known to reduce the power of statistical test (Dahiru, 2008). T-tests showed that the standard deviations of the two techniques were similar (t-test, n=90, p>0.05). The main difference between the two techni ques was the discrimination between sampling points that was significantly higher using NanoString (t-test, n=90, p<0.001). It was already reported that the NanoString was the more sensitive method with a sensitivity at 1 copy/cell versus 10 to 200 for the qPCR (Eastel et al., 2019). This is consistent with the fact that results showed that the NanoString was more precise than the qPCR when treating less expressed genes such *Period*.

Table 9: Gene expression rhythmicity obtained using NanoString and qPCR quantification and DiscoRhythm (DiscoR) and Rain qualification. Bold number are significant.

		Period				*Carbonic anhydrase*				*Chitin synthase*			
		NanoString		qPCR		NanoString		qPCR		NanoString		qPCR	
		DiscoR	Rain	DiscoR	Rain	DiscoR	Rain	DiscoR	Rain	DiscoR	Rain	DiscoR	Rain
CD	τ	**24**	**24**	20	24	**22**	24	20	20	**20**	**24**	28	28
	p	**3E-24**	**7E-29**	0.79	0.07	**0.04**	0.06	0.64	0.05	**0.1**	**0.17**	0.87	0.73
CT	τ	**12**	**12**	9	16	**12**	**12**	9	12	**13**	**12**	14	16
	p	**0.05**	**0.01**	0.34	0.84	**0.02**	**0.03**	0.41	0.28	**2E-03**	**0.01**	0.90	0.59

Abbreviation: CD: circadian; CT: circatidal; τ: period; p: p-value

This study was comporting some pitfalls. First, the number of genes used to compare the two techniques was limited. Secondly, samples were treated later for the qPCR and some degradations might occurred even if they were never defrosted before their retro-transcription. However, this comparative approach of both techniques validated the choice made to use the NanoString technology instead of the RT-qPCR one. It comforted that lack of gene expression rhythmicity observed in the dataset was not linked to the method used. Therefore, the NanoString technology was probably a better option when assessing expression rhythmicity in bivalves.

General discussion, perspectives and conclusion

1. General discussion

Bivalves shells are made of calcium carbonate and organic compounds (Skinner and Jahren, 2003). The biomineralisation by which the shell is secreted is neither homogeneous or continuous in time, leading to the formation of growth patterns (Schöne, 2008). Growth patterns consist in the alternance of growth lines and increments. Depending of the environment daily and tidal incrementation pattern are commonly reported in bivalves (Louis et al., 2022). However, in constant environment growth pattern are still observed in several bivalves (Richardson et al., 1980; Richardson, 1988, 1989). These observations opened the possibility of an implication of biological clock(s). Biological clock(s) are molecular auto-regulatory transcription and translation feedback loops (Dunlap, 1999). One hallmark of biological clocks is that they are endogenous which means that under constant environmental conditions, the clock is still ticking (Aschoff, 1981). This thesis aims to understand how environmental signals, mostly temporal ones, are integrated into the shell of bivalves throughout its growth, so that it become a biological archive. To address this question three hypotheses were tested; i) biomineralisation is an autonomous physiological process which is directly controlled by environmental variations or ii) biomineralisation is a rhythmic process which is under the control of biological clock(s) or iii) both the environment and biological clock(s) are involved through the valve activity.

The environment is not directly controlling the biomineralisation of Mediterranean mussels

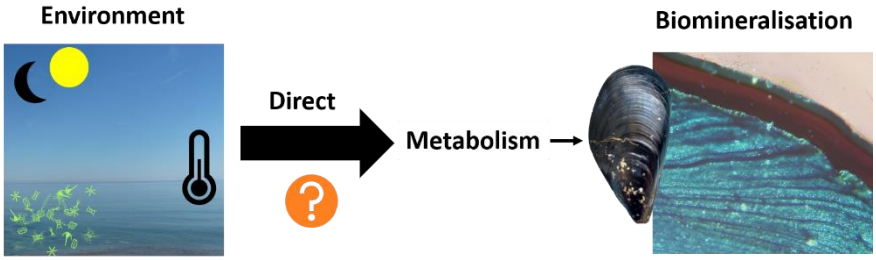

Figure 40: Is the environment controlling directly the biomineralisation process?

The control of biomineralisation occurs at different levels, from the environment to the molecule (Schöne et al., 2003; Rodríguez-Tovar, 2014; Checa, 2018; Song et al., 2019). In chapter 1, we tested the hypothesis of a direct control of the environment on shell biomineralisation. For that purpose, shell growth patterns were studied over one year in three types of environment, two

Mediterranean lagunas and at sea in the bay of Banyuls-sur-Mer. Spatial and temporal differences in incrementation in the biomineralised tissue were observed i) between the types of environment and ii) between the periods of the year. Daily increments (*i.e.*, 1±0.2 increments/day) were observed in shells from the both lagunas, which is consistent with previous studies realised on mussels from the laguna of Salses-Leucate (SL) and also on oysters from Thau laguna, located further north (Langlet et al., 2006; Andrisoa et al., 2019). At sea, tidal increments (*i.e.*, 2±0.4 increments/day) seemed predominant in the growth pattern of the shell. However, an additional incrementation regime following the mixed semidiurnal tidal regime of the region, was observed in the three sites. Shift from regime of incrementation seems to be related to chlorophyll *a* concentration in the water column but the environmental control of the increment formation remains unclear.

Measurements of the dynamic in chlorophyll *a* level at sea, realised during the *in situ* daily experiment in chapter 2 highlight that this parameter, assumed reflecting food conditions, varies with tides. The shells growth patterns observed at this time (*i.e.*, 1.8 to 2.1 increments/day observed in shells), are consistent with the chlorophyll *a* level periodicity observed in the Bay of Banyuls in September 2020. Interestingly, the analysis of expression of genes related to the biomineralisation at this time, exhibits a tidal periodicity, thus a similar profile as shell growth pattern and chlorophyll *a* level, supporting the hypothesis of a direct control of the environment.

However, results are less clear in aquaria. When food is given continuously and when fed twice (2xF) per day, most individuals formed two increments per day. But feeding given once per day do not show a clear pattern in shells. Additionally, the expression of genes related to the biomineralisation in aquaria conditions lost rhythmicity in rhythmic conditions of food availability. This means that (1) food level was insufficient in the aquaria experiment to constitute a direct control on shell biomineralisation and growth pattern formation, or (2) another parameter is primarily driving shell growth, as the quality of food (Fernández-Reiriz et al., 2015) or (3) the environment does not directly control shell growth pattern formation. The first hypothesis is less probable as mussels received phytoplankton in excess (once 20 000 cells/mL when in 1xF, two times 10 000 cells/mL in 2xF) compared to mean levels observed in the bay of Banyuls (~3000 cells/mL ≈ [Chl a] of 1 µg/L). When fed continuously (∞xF) the number of cells present in the aquarium might be lower as the phytoplankton was distributed *via* a drip mechanism. However, if under the threshold of 0.5 µg/L (Maire et al., 2007) no difference would be observed with the condition ∅xF, which was not the case. Therefore, two hypotheses remained, another environmental controller or none direct control by the environment.

In summary, inconsistencies were observed between environmental variations and growth patterns at sea. The variability observed at the gene expression level and in shell incrementation in

aquaria indicates that a direct control of the food availability cannot explain the periodic formation of increments in the shell of *M. galloprovincialis*. The photoperiod neither controlled directly increments formation. Also, when in constant environment, shell growth patterns are still formed. Therefore, a direct control of the environment on biomineralisation is unlikely.

Biological clock(s) are not directly controlling the biomineralisation of Mediterranean mussels

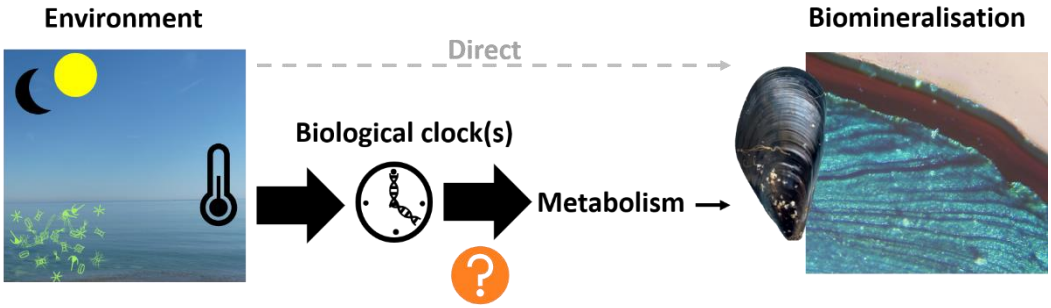

Figure 41: Are the biological clock(s) controlling the biomineralisation process?

The putative biological clock of *M. galloprovincialis* was demonstrated plastic in Chapter 2. This means that its periodicity can be easily modulated by the environment and has a great variability between individuals, giving rise to chronotypes within a population (Helm et al., 2017). At sea, genes of the core of putative biological clock showed: i) tidal expression similarly to water height variations during the sampling period, ii) daily expression likely in relation to L:D cycles, as well as iii) bimodal expression. Similar observations were made in oysters, since potential biological clock core genes adopt a daily, tidal or bimodal activity in their natural environment (Tran et al., 2020b).

In aquaria, the expression of the putative core biological clock genes of *M. galloprovincialis* was variable within the environmental conditions tested, mainly having daily and tidal expressions, which differs from the rhythmicity in expression observed in other bivalves. In aquaria, all core genes expression of oysters placed under L:D follow a daily expression, whereas under D:D they have a circatidal expression (Tran et al., 2020b). *Mytilus edulis* mussels in aquaria showed daily gene expression oscillation both in L:D following L:D cycles and in D:D, showing an endogenous circadian periodicity (Chapman et al., 2020). In *M. galloprovincialis*, neither the photoperiod nor the food availability seem to be time-givers to potential biological clock(s), and under constant environmental conditions, rhythmic expression was only observed for a part of the core genes. Therefore, based on genetic data, endogenous nature of the circadian and circatidal rhythm of *M. galloprovincialis* could

not be clarified. However, behavioural data showed that mussels can adopt a circadian or a circatidal valve activity in free-running condition.

The formation of growth increments under constant environmental condition could however be interpreted as a control by biological clock(s). *In situ* hybridisation made on the posterior edge of the mantle showed that expression of genes related to the biomineralisation and potential core biological clock genes spatially overlap at noon. However, the profiles of expression observed at sea and in aquaria were different between the potential core biological clock genes and genes related to the biomineralisation. In conclusion, biological clocks are likely not driving directly the biomineralisation process.

An additional factor: the role of valve activity on the shell growth pattern formation

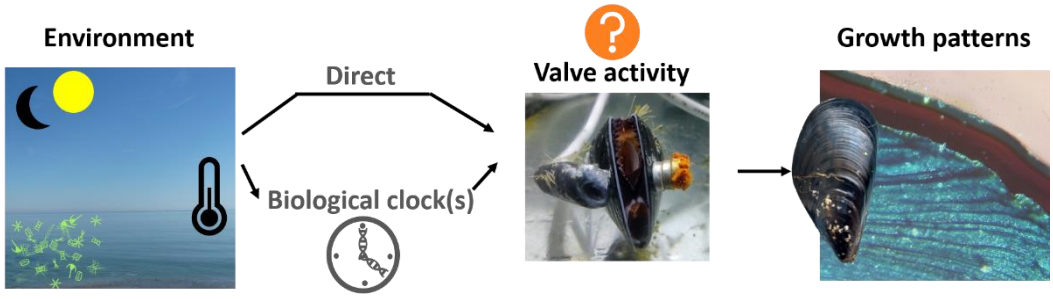

Figure 42: Is valve activity generating shell growth patterns?

Based on *in situ* observations we suggest a possible joint control of both biological clock(s) and environmental cues. Change in incrementation regime observed in this study is not unprecedented for mussels as Richardson et al. (1990) already report variability in the accretionary rhythm of subtidal *M. edulis* shells. Theses authors associated these changes to the possible influence of an innate in addition to exogenous keeping time parameters. In this study, when food availability is limited, putative biological clock(s) appear controlling shell biomineralisation dynamic, leading to the formation of 1 increment per day in laguna and 2 increments per day at sea as biological clock(s) can generate both circadian and circatidal rhythms, depending on the type of environment (Tran et al., 2020b). When food is not restricting, the environment partially controls shell biomineralisation, through an increase in chlorophyll *a* concentration in the water column probably related to the tidal regime of the region. This produces supernumerary increments, which is consistent with the mixed semidiurnal tidal regime that occurs in the region. When the potential clock putatively adopted a circadian endogenous rhythm, an average of ~1.5 increments was observed depending of the month and the tidal coefficients. When the potential clock adopted putatively circatidal endogenous rhythm, sometimes supernumerary

increments can occur, leading to more than 2 increments formed per day when circatidal, showing that the biological clock might not be in phase with chlorophyll *a* level variation. Interestingly, this is the first report of this unconventional rhythm in shell growth although such tidal systems are frequent at sea (Hicks, 2006).

The joint control of shell growth pattern formation might occur through the valve activity of mussels as a prolonged closure was described to be at the origin of growth lines in the shell due to pH drop in the extrapallial fluid (Lutz and Rhoads, 1977). Additionally, the valve periodical activity was proved to be related to biological clocks in other bivalve species such as the oyster *M. gigas* and the clam *C. islandica* (Perrigault et al., 2020; Tran et al., 2020b).

Our aquaria studies have shown that, in *M. galloprovincialis*, the valval activity was primarily responding to the food availability and secondarily to the photoperiod (Chapter 2). Here again, a high inter-individual variability was observed. Under constant environmental conditions, the response of *M. galloprovincialis* was also highly variable and most individuals lost their periodic valve activity. Therefore, the endogenous nature of the valve activity and its control by biological clock(s) is not evidenced. This instability in timekeeping under constant conditions and the wide range of responses to environmental variations suggest a control by a weak biological clock (Gwinner and Brandstätter, 2001). The biological clock of *M. galloprovincialis* has already been qualified of weak based on the observations made in Venice laguna (Bertolini et al., 2021). During summer months, bimodal (*i.e*., circadian and circatidal) valve activity was observed and then shifted to tidal in winter. Variability was related to tidal current strength and the associated food availability.

Given the large range of responses in mussels behaviour, the “masking” effect of the environment on behavioural and physiological output of biological clocks is considered (Mrosovsky, 1999; Helm et al., 2017). This was demonstrated for example in nocturnal spiny mouse (Gutman and Dayan, 2005; Rotics et al., 2010, 2011). Following biological clock control, mice are active at night and rest the day. Under artificial light at night or at full moon, the nocturnal activity of the mice is repressed whereas the core genes of the molecular clock did not change their periodic expression. Therefore, the light at night is masking the control of biological clock on the activity level of mice. Similar masking effect of the environment on clock controlled behaviour was observed on an invertebrate, the drosophila, and in aquatic environment in threespine sticklebacks (*Gasterosteus aculeatus*), both in relation with light (Kempinger et al., 2009; Brochu and Aubin-Horth, 2021). In the case of *M. galloprovincialis*, a control of the valval behaviour by biological clock(s) with a masking effect of the environment (*i.e.*, tidal currents and chlorophyll *a*) is highly probable.

Considering the three environments studied, the concentration in chlorophyll *a* seems to act as a threshold or a switch, inducing a shift in the shell incrementation regimes, as revealed by the behaviour of mussels in the Venice laguna (Bertolini et al., 2021) (Chapter 1). We hypothesised a possible influence of biological clocks running at daily frequency in laguna and at tidal, daily or bimodal at sea depending on the period of the year. In this model, the environmental conditions are forcing factors distorting rhythmic valve opening/closing activity and subsequently the growth pattern formation, joining the concept of masking effect of the environment.

However, the relationship between valve activity and growth patterns could not be confirmed using in aquaria experiments. Under crossed controlled conditions of light and food availability, valve activity and growth pattern have been both characterised for the same individual (Chapter 2). No significant relationship could be established between the number of increments formed and the valve activity (*i.e.*, number of closures, valves closure duration, the combination of both). But in this study, the aquaria conditions might not be optimal as responses observed were highly variable. It is known that discrepancies between field and captive data often occurs while looking to circadian rhythm and related functions (Calisi and Bentley, 2009). Then, *in situ* similar comparisons between behaviour and shell growth patterns are required before rejecting this hypothesis. Further studies are also required to better characterise the link between the valve behaviour and the increment formation in bivalves as this relationship was observed in several bivalves (Rodland et al., 2006; Schwartzmann et al., 2011; Tran et al., 2020a).

2. Perspectives

This PhD thesis aimed to develop a new approach on the temporal control of growth patterns in bivalve shells. I used an innovative study on the formation of periodic growth patterns formation which integrates distinct scientific domains. At the beginning of this PhD thesis, main postulates consisted in either a direct control by the environment or the implication of biological clocks. Through a series of experiments conducted *in vitro*, we suggest a probable indirect effect of biological clocks controlling valve activity, thus modulating growth pattern formation, related to environmental factors acting on the valve behaviour. As a consequence, new questions emerge leading to the design of new experiments. What are the forcing environmental factors on valve activity? In intertidal areas, the alternance between aerial and aquatic phases is a strong forcing factor but in subtidal area it is less clear. What environmental factors can be suggested? Are all individuals of a population sensitive to the same environmental factor? This PhD thesis was a first step to approach this question and open new possibilities to better characterise the temporal control of growth patterns in shells of bivalve. Below, specific questions and experiments are proposed to expand the further investigations on the subject.

Are shell surface growth patterns reliable in *Mytilus galloprovincialis*?

The readability of shell growth patterns in *M. galloprovincialis* can be sometimes challenging as demonstrated by our observations. In this study we showed that the Mutvei etching of shell sections observed under reflected light was the best method compared to cathodoluminescence (CL), laser scanning confocal microscope (LSCM) and semi-thin sections (1 µm) observed with transmitted light microscope. However, the preparation of shell sections (0.5 mm) can be time consuming and proved not always efficient. For pectinid shells, daily growth lines can be counted directly on the surface of the valves (Chauvaud et al., 1998; Thébault et al., 2022). Growth lines are also visible on the surface of mussel shells but to date were never counted and compared to the internal growth structures. Two methods could be used, profilometry and microtomography. Using those methods, the external profile of shell morphology at micrometers scale can be directly computed (preliminary results in Annex 1). The aims of this test would be i) to determine if external patterns are similar to internal patterns in mussels, ii) to improve the readability of shell growth patterns in *M. galloprovincialis*, iii) to limit the error linked to the operator.

Growth lines formation by decalcification in subtidal environment

Growth lines might be related to decalcification occurring when valves are closed due to pH decrease in the extrapallial fluid (EPF) (Crenshaw and Neff, 1969; Lutz and Rhoads, 1977). This has been described in intertidal species (Richardson, 1987; Schöne et al., 2003; Hallmann et al., 2009; Tanaka et al., 2019). When they are emerged, valves are closed for few hours. In subtidal species, complete closures of the valve and the following pH decrease might not be long enough to form growth lines at each closure period. As the relationship between valve activity and growth line formation is not well understood it would be interesting to coupled EPF pH measurement, valvometry and sclerochronology on short period of time and under controlled environments. It would give information about i) if growth line formation is related to valve closure in subtidal bivalves and ii) the time of valve closure and subsequent decalcification time to form a growth line observable.

Organic matrix variations in the EPF

Shells are made of calcium carbonate and organic compounds (Skinner and Jahren, 2003). The organic material is constituting a framework for $CaCO_3$ deposition (Giuffre et al., 2013; Checa, 2018). Organic compounds are a set of proteins, peptides, free amino-acids, lipids, polysaccharides and pigments (Marin et al., 2012). The production of proteins and enzymes involved the shell matrix formation are the result of gene transcription and translation in amino acid chains. In this work, mRNA levels of key constituent of the organic matrix showed tidal oscillations in the mantle at sea. However, it has been shown that rhythmicity in expression poorly correspond to protein levels rhythmicity in some cases (Mauvoisin et al., 2014; Robles et al., 2014; Hurley et al., 2018). For example, studies showed that some proteins exhibited circadian oscillations in quantity although their mRNA levels were stable and the opposite was also observed (Hurley et al., 2018). This could be related to post-transcriptional (*i.e.*, mRNA alternative splicing, deadenylation, degradation, translation (Kojima et al., 2011)) and post-translational regulations (*i.e.*, phosphorylation, acetylation, methylation (Feng and Lazar, 2012)).

Levels in organic material also variate in the extrapallial fluid (EPF) due to biological control of the secretion of organic and mineral material by cells of the mantle. Two hypotheses where advanced in Checa (2018): i) cells secrete indifferently organic and mineral compounds into the EPF or ii) cells of

the mantle recognise the extracellular matrix by its physiochemical properties and secrete in consequence organic or mineral compounds (Checa et al., 2016; Checa, 2018). The second hypothesis is considered as the most probable, in this case cells has to bend closer to the shell surface when it is time to secrete shell components and this "behaviour" could be related to biological clock(s) or direct environmental variable as well.

Therefore, it would be interesting to follow key proteins levels in the EPF and in the mantle of bivalve over time in different environment to assess the effect of the environment on biomineralisation kinetics and if biological clocks have an implication at the protein and/or cellular levels.

From the water to the shell: kinetic of integration of diet compounds in the shell of bivalves.

In this study, sclerochronology using optical observation of shell growth patterns was used. However, sclerochemistry can be used to describe shell growth patterns (*i.e.*, sclerochronochemistry) and reconstruct past and present environments based on well known relationships between physico-chemical environment and shell chemical composition (Moberg and Folke, 1999; Coen et al., 2007; Zuykov and Schindler, 2019). For example the ratio of strontium on calcium ions (Sr/Ca) and of magnesium on calcium (Mg/Ca) in shells are used to reconstruct past water temperature (Richardson et al., 2004) and salinity (Dodd and Crisp, 1982).

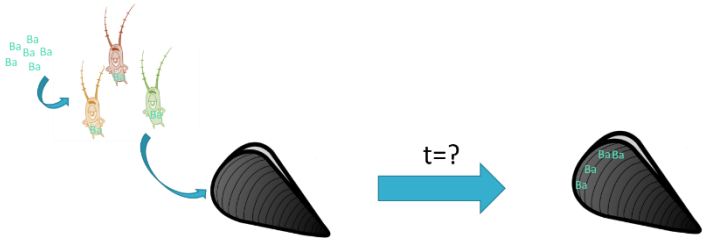

Figure 43: What is the kinetic of integration of barium contained in phytoplankton. t: time between ingestion and incorporation.

In this frame, the ratio of barium on calcium (Ba/Ca) is considered as a promising tool to assess the phytoplankton dynamic (Gillikin et al., 2006; Poulain et al., 2015). Profiles of Ba/Ca ratio in shells are characterised by background values having little variations probably related to salinity variations, interrupted by sharp peaks (Poulain et al., 2015). These peaks are synchronous in a population and often linked to phytoplankton blooms (Gillikin et al., 2008; Doré et al., 2020). However, the factors

controling the Ba/Ca ratio in bivalve shells is still not fully understood and variation observed in shells can not be translated into environmental conditions. To better characterise the relationship between the amount of barium contained in phytoplankton and its incorporation in bivalve shell, in aquaria experiments could be achieved. Mussels could be fed punctually with phytoplankton enriched in barium to measure barium in shells (Figure 43) using Laser Ablation-Inductively Coupled Plasma-Mass Spectrometry (LA-ICP-MS). This experiment would respond to multiple interrogations: i) is a barium portion integrated in shells coming from phytoplankton? and ii) is there a lag between the ingestion of the phytoplankton and the integration of their compounds into the shell?

Is there a central clock running in *M. galloprovincialis*?

The expression of putative core clock gene is widespread in organisms tissues, notably in bivalves (Dibner et al., 2010; Perrigault et al., 2020). Potentially every cell in an organism contains an autonomous canonical biological clock oscillator (Balsalobre et al., 1998; Nagoshi et al., 2004). Those autonomous oscillators respond differently to environmental time givers and control different physiological activities. The architecture of the clock system differs within the living kingdom. In mammals, the hypothalamic suprachiasmatic nucleus (SNC) is the dominant circadian pacemaker giving time to clock oscillators located in other organs (Mohawk et al., 2012). The SNC named the central clock, is primarily synchronised by the L:D cycles (Welsh et al., 2010). However, peripherical clocks can adopt another rhythm in relation to other environmental variables such as the feeding time (Kornmann et al., 2007). In drosophila, it has been shown that the circadian system consists in independent photoreceptive clocks (Giebultowicz et al., 2001; Collins et al., 2006). In the Arctic scallop *C. islandica*, a rhythmic genes expression of putative core biological clock genes was described in the mantle edge, in gills and in the adductor muscle both under L:D and D:D conditions. The authors suggested that peripherical clocks are part of a complex network.

The idea of a central clock is often related to the central nervous system (Mohawk et al., 2012). In mussels the nervous system is composed of three pairs of ganglions (*i.e.*, cerebral, pedal and visceral) joined by connectives (Vitellaro-Zuccarello et al., 1991). To get indications about peripherical and putative central clock in bivalve, *in situ* hybridrisation on series of full mussel body sections could be achieved. Individuals would be sampled at different phases of the photoperiodic cycle. This experiment would determine i) if differences in expression are observed within tissues through time with ii) an emphasis on ganglions and iii) if the expression in pairs of ganglions are synchronised.

Quantity or quality? Food availability as a time-giver for *M. galloprovincialis*.

Bivalve growth is predominantly related to food supply (Gosling, 2004; Sarà et al., 2011). Shell growth is classically correlated to level of chlorophyll *a* in the water column, as we did in this study. However, the level of chlorophyll *a* does not encompass the complete feeding regime of mussels and is not an indicator of the food quality. Mussels are filter-feeders, feeding mostly on microalgae (Bayne et al., 1987), and at a lesser extent on zooplankton (Davenport et al., 2000; Maar et al., 2008), bacteria (Langdon and Newell, 1989), organic detritus (Grant et al., 1997) and dissolved matter (Jørgensen, 1983). Phytoplankton is considered as the main food source of bivalve due to higher absorption efficiency of the organic content (*i.e*., the organic content in faeces in relation to the content in food) (Navarro et al., 1996). Also, the quality of the seston has been shown as the main environmental parameter affecting the absorption efficiency (Babarro et al., 2003). The quality of the seston was defined as the ratio of the particulate organic matter on the total suspended matter (Babarro et al., 2000). The increase in the total particulate matter (TPM) in the water column has been shown to decrease the clearance rate (*i.e*., measurement of the difference of concentration in phytoplankton, organic matter, etc. in a water volume through time in relation to bivalve filtration activity) of *M. galloprovincialis*. Also the size, volume, weight and biochemical content of the phytoplankton has to be taken into consideration as impacting the absorption efficiency (Fernández-Reiriz et al., 2015). Therefore, the species composition of the phytoplankton might be important while looking to shell growth.

Phytoplanktonic assemblages change through the year, the season, the time of the day (Thyssen et al., 2014). In the bay of Villefranche-sur-Mer (Mediterranean Sea, FR), picoeukaryotes were shown to increase in abundance at night, while the nanophytoplankton increased during the day and the microphytoplankton increased in the afternoon. Diel variability of phytoplankton is related to their cell division cycles (Jacquet et al., 2001) and their vertical migration in the water columns (Brunet et al., 2008; Gerbersdorf and Schubert, 2011). Variations were also reported through the year in the bay of Banyuls in picoeukaryote, bacteria and archaea assemblages (Lambert et al., 2019).

Food availability is often considered as the "other" time-giver of biological clocks next to the photoperiod (Stephan, 2002; Van Der Veen et al., 2017). In this study we showed that the expression of most genes related to biological clocks seems to follow the profile of chlorophyll *a* concentration in the bay of Banyuls (Chapter 2). However, under controlled conditions of food availability this pattern was not observed. Mussels were fed in aquaria with a mix of three phytoplanktonic species (*i.e*., *I. galbana*, *Tetraselmis sp*. and *R. salina*) at higher concentrations to what was measured in the bay of Banyuls (Maire et al., 2007). Therefore, the gene expression rhythmicity and the shell growth

associated patterns might not be simply related to the chlorophyll *a* level but also to specific phytoplankton community assemblage or species. In order to test this hypothesis, water phytoplanktonic communities and stomach content of *M. galloprovincialis* could be characterised at infra-daily resolution in the bay of Banyuls. This could be achieved in parallel to gene expression measurements (*i.e.*, biological clock core and related genes and biomineralisation related genes). Results would indicate: i) the variations of phytoplanktonic communities through the day in the bay of Banyuls, ii) change in the stomach content of mussels through the day and iii) if the variations in specific phytoplankton community in the water column drive the biological clock and/or the biomineralisation process in *M. galloprovincialis*.

Oysters as a better biological model to decipher the control by the environment and biological clocks on the biomineralisation process

Currently, oysters *M. gigas* is one of the best studied models in bivalve chronobiology. The core genes of its biological clock are described and its endogenous nature confirmed (Perrigault and Tran, 2017). Also, it has been shown that the core biological clock genes adopt tidal and circadian expression in the field whereas in aquaria circadian expression was observed in L:D and circatidal in D:D condition (Tran et al., 2020b). This showed that the oscillator could be entrained by two different zeitgebers, photoperiod and tides and that the oscillator can adopt both periodicities, being qualified of bimodal. Valval activity has been shown to be under the control of biological clocks in oysters (Mat et al., 2012, 2014, 2016; Tran et al., 2020b).

Growth patterns of oysters have been characterised in both tidal and subtidal environments. Daily shell increments were observed in the Mediterranean laguna of Thau related to the photoperiod and/or biological clocks whereas tidal increments have been seen in intertidal areas submitted to semidiurnal tidal regime as in the Bay of Biscay (Spain) and in the Bay of Veys in Normandy (Langlet et al., 2006; Higuera-Ruiz and Elorza, 2009; Huyghe et al., 2019).

As the potential biological clock of *M. gigas* is better studied and the fact that in function of its environment oysters are forming daily or tidal patterns, it would be a good biological model to test the relationship between biological clocks and the dynamism of the biomineralisation process.

Relationship between valvometry, biological clocks and the shell incrementation using endosymbiotic species

The relationship between the valve activity and the growth line formation is not well understood. It is clear that the shell growth is correlated to the valve opening amplitude notably in *Mytilus* ssp. (Tran et al., 2020a). This relation is mostly related to the feeding activity as the valve aperture in mussels controls the amount of water filtrated (Maire et al., 2007). In the giant clam *Hippopus hippopus* it was shown that valvometry measurements can be used to measure the shell growth rate (Schwartzmann et al., 2011). Interestingly, these authors showed daily incrementation in shells using sclerochronology and in parallel circadian valval behaviour. Valves were open during the day and closed at night. As the thickness of an increment in *H. hippopus* shells was related to the daily opening of the valves, we could hypothesise that the delimitation between increments (*i.e.*, growth lines) were formed at night. Similar hypothesis was made based on freshwater mussels, linking the duration of valve closure to growth breaks (*i.e.*, growth lines) (Rodland et al., 2009).

Hippopus hippopus is a bivalve harbouring photosynthetic symbiont. It has been shown that symbionts are important for the physiology of bivalves, as providing energy and as they might be at the origin of a higher calcification rate in symbiotic species (Beckvar, 1981; Klumpp and Griffiths, 1994; Hawkins and Klumpp, 1995). The photosynthetic activity of the symbiont is related to the light, so the bivalve is supplied in energy at day when valves are open. Light-dependent synthesis of proteins related to the biomineralisation process has been previously described in *Tridacna squamosa* (Ip et al., 2015, 2017, 2018; Boo et al., 2017; Hiong et al., 2017; Cao-Pham et al., 2019; Chew et al., 2019). It would be interesting to do behavioural tracking in relation to shell growth patterns under constant darkness on photosymbiotic bivalves. This would indicate i) if the valve activity observed in L:D is related to biological clocks and ii) if shell growth patterns are related to valval activity.

3. Conclusion

This thesis aimed to understand how environmental signals, mostly temporal ones, are integrated into the shell of a bivalve throughout its growth, so that it becomes a biological archive. In this study, different hypotheses were explored and new ones were formulated. Based on the literature, two hypotheses emerged: i) the rhythmicity of the biomineralisation process is directly controlled by periodic variations in the environment or ii) the process is under the control of biological clock(s). We showed that none of them could solely explain the incrementation patterns observed in the shells of *M. galloprovincialis*. Then, a joint control by both the environment and biological clock(s) *via* the valve behaviour was hypothesised. Based on experiment in aquaria, this hypothesis could not be verified. However, further studies are required to assess the hypothesis of a joint control of the biomineralisation process. This thesis contributes to the knowledge i) in chronobiology by identifying for the first time the molecular constituents of the canonical biological clock of *M. galloprovincialis* and the description of outputs and ii) in sclerochronology by characterising shell growth pattern in Mediterranean organisms at daily and infra-daily resolutions. This thesis is constituting a basis for further investigations as several questions emerged from this work.

Bibliography

Addadi, L., Joester, D., Nudelman, F., and Weiner, S. (2006). Mollusk shell formation: A source of new concepts for understanding biomineralization processes. *Chem. - A Eur. J.* 12, 980–987. doi:10.1002/chem.200500980.

Adema, C. M. (2021). Sticky problems: extraction of nucleic acids from molluscs. *Philos. Trans. R. Soc. B* 376, 20200162. doi:10.1098/RSTB.2020.0162.

Allemand, D., Tambutté, É., Zoccola, D., and Tambutté, S. (2011). "Coral Calcification, Cells to Reefs," in *Coral reefs: An ecosystem in transition* (Dordrecht: Springer), 119–150. doi:10.1007/978-94-007-0114-4_9.

Alves, M. G., and Oliveira, P. F. (2013). Effects of non-steroidal estrogen diethylstilbestrol on pH and ion transport in the mantle epithelium of a bivalve *Anodonta cygnea*. *Ecotoxicol. Environ. Saf.* 97, 230–235. doi:10.1016/j.ecoenv.2013.07.024.

Andrade, H., Massabuau, J.-C., Cochrane, S., Ciret, P., Tran, D., Sow, M., et al. (2016). High Frequency Non-invasive (HFNI) Bio-Sensors As a Potential Tool for Marine Monitoring and Assessments. *Front. Mar. Sci.* 3, 187. doi:10.3389/FMARS.2016.00187.

Andrisoa, A., Lartaud, F., Rodellas, V., and Neveu, I. (2019a). Enhanced Growth Rates of the Mediterranean Mussel in a Coastal Lagoon Driven by Groundwater Inflow. *Front. Mar. Sci.* 6, 753. doi:10.3389/fmars.2019.00753.

Andrisoa, A., Stieglitz, T. C., Rodellas, V., and Raimbault, P. (2019b). Primary production in coastal lagoons supported by groundwater discharge and porewater fluxes inferred from nitrogen and carbon isotope signatures. *Mar. Chem.* 210, 48–60. doi:10.1016/j.marchem.2019.03.003.

Anestis, A., Lazou, A., Pörtner, H. O., and Michaelidis, B. (2007). Behavioral, metabolic, and molecular stress responses of marine bivalve *Mytilus galloprovincialis* during long-term acclimation at increasing ambient temperature. *Am. J. Physiol. - Regul. Integr. Comp. Physiol.* 293, 911–921. doi:10.1152/ajpregu.00124.2007.

Anestis, A., Pörtner, H. O., and Michaelidis, B. (2010). Anaerobic metabolic patterns related to stress responses in hypoxia exposed mussels *Mytilus galloprovincialis*. *J. Exp. Mar. Bio. Ecol.* 394, 123–133. doi:10.1016/J.JEMBE.2010.08.008.

Ansell, A. D. (1968). The rate of growth of the hard clam *Mercenaria mercenaria* (L) throughout the geographical range. *ICES J. Mar. Sci.* 31, 364–409. doi:10.1093/icesjms/31.3.364.

Apte, S., Holland, B. S., Godwin, L. S., and Gardner, J. P. A. (2000). Jumping Ship: A Stepping Stone Event Mediating Transfer of a Non-indigenous Species Via a Potentially Unsuitable Environment. *Biol. Invasions* 2, 75–79. doi:10.1023/A:1010024818644.

Arnaud, P., and Raimbault, R. (1969). The Salses-Leucate pond. Its principal physicochemical characteristics and their variations (in 1955- 1956 and from 1960- 1968). *Rev. Trav. Inst. Pech. Marit.* 33, 335–443.

Aschoff, J. (1981). "Freerunning and Entrained Circadian Rhythms," in *Biological Rhythms* (Boston, MA.: Springer US), 81–93. doi:10.1007/978-1-4615-6552-9_6.

Babarro, J. M. F., Fernández-Reiriz, M. J., and Labarta, U. (2000). Growth of seed mussel (*Mytilus galloprovincialis* LMK): Effects of environmental parameters and seed origin. *J. Shellfish Res.* 19, 187–193.

Babarro, J. M. F., Fernández-Reiriz, M. J., and Labarta, U. (2003). In situ absorption efficiency processes for the cultured mussel *Mytilus galloprovincialis* in Ría de Arousa (north-west Spain). *J. Mar. Biol. Assoc. United Kingdom* 83, 1059–1064. doi:10.1017/S0025315403008270H.

Balbi, T., Fabbri, R., Montagna, M., Camisassi, G., and Canesi, L. (2017). Seasonal variability of different biomarkers in mussels (*Mytilus galloprovincialis*) farmed at different sites of the Gulf of La Spezia, Ligurian sea, Italy. *Mar. Pollut. Bull.* 116, 348–356. doi:10.1016/J.MARPOLBUL.2017.01.035.

Ballesta-Artero, I., Witbaard, R., Carroll, M. L., and van der Meer, J. (2017). Environmental factors regulating gaping activity of the bivalve *Arctica islandica* in Northern Norway. *Mar. Biol.* 164, Article 116. doi:10.1007/s00227-017-3144-7.

Balsalobre, A., Damiola, F., and Schibler, U. (1998). A Serum Shock Induces Circadian Gene Expression in Mammalian Tissue Culture Cells. *Cell* 93, 929–937. doi:10.1016/S0092-8674(00)81199-X.

Banni, M., Negri, A., Mignone, F., Boussetta, H., Viarengo, A., and Dondero, F. (2011). Gene Expression Rhythms in the Mussel *Mytilus galloprovincialis* (Lam.) across an Annual Cycle. *PLoS One* 6, e18904. doi:10.1371/journal.pone.0018904.

Barbin, V. (2000). "Cathodoluminescene of carbonate shells: biochemical vs diagenetic process," in *Cathodoluminescence in Geosciences*, eds. M. Pagel, V. Barbin, P. Blanc, and D. Ohnenstetter (Berlin: Springer), 303–330. doi:10.1007/978-3-662-04086-7.

Barbin, V. (2013). Application of cathodoluminescence microscopy to recent and past biological materials: A decade of progress. *Mineral. Petrol.* 107, 353–362. doi:10.1007/S00710-013-0266-6/FIGURES/2.

Barbin, V., Ramseyer, K., and Elfman, M. (2008). Biological record of added manganese in seawater: A new efficient tool to mark in vivo growth lines in the oyster species *Crassostrea gigas*. *Int. J. Earth Sci.* 97, 193–199. doi:10.1007/S00531-006-0160-0/FIGURES/2.

Barbin, V., and Schvoerer, M. (1997). Cathodoluminescence géosciences. *Comptes Rendus l'Académie des Sci. - Ser. IIA - Earth Planet. Sci.* 325, 157–169. doi:10.1016/S1251-8050(97)88284-5.

Bargione, G., Vasapollo, C., Donato, F., Virgili, M., Petetta, A., and Lucchetti, A. (2020). Age and Growth of Striped Venus Clam *Chamelea gallina* (Linnaeus, 1758) in the Mid-Western Adriatic Sea: A Comparison of Three Laboratory Techniques. *Front. Mar. Sci.* 7, 582703. doi:10.3389/fmars.2020.582703.

Bartness, T. J., and Albers, H. E. (2000). "Activity Patterns and the Biological Clock in Mammals," in *Activity patterns in small mammals* (Springer, Berlin, Heidelberg), 23–47. doi:10.1007/978-3-642-18264-8_3.

Bayne, B. L. (1976). "The biology of mussel larvae," in *Marine Mussels: their Ecology and Physiology*, ed. B. L. Bayne (Cambridge: Cambridge University Press), 81–120.

Bayne, B. L. (2004). Phenotypic Flexibility and Physiological Tradeoffs in the Feeding and Growth of Marine Bivalve Molluscs. *Integr. Comp. Biol.* 44, 425–432. doi:10.1093/ICB/44.6.425.

Bayne, B. L., Hawkins, A. J. S., and Navarro, E. (1987). Feeding and digestion by the mussel *Mytilus edulis* L. (Bivalvia: Mollusca) in mixtures of silt and algal cells at low concentrations. *J. Exp. Mar. Bio. Ecol.* 111, 1–22. doi:10.1016/0022-0981(87)90017-7.

Bec, B., Collos, Y., Souchu, P., Vaquer, A., Lautier, J., Fiandrino, A., et al. (2011). Distribution of picophytoplankton and nanophytoplankton along an anthropogenic eutrophication gradient in French Mediterranean coastal lagoons. *Aquat. Microb. Ecol.* 63, 29–45. doi:10.3354/ame01480.

Beckvar, N. (1981). Cultivation, spawning, and growth of the giant clams *Tridacna gigas*, *T. derasa*, and *T. squamosa* in Palau, Caroline Islands. *Aquaculture* 24, 21–30. doi:10.1016/0044-8486(81)90040-5.

Benjamini, Y., and Hochberg, Y. (2000). On the Adaptive Control of the False Discovery Rate in Multiple

Testing With Independent Statistics: *J. Educ. Behav. Stat.* 25, 60–83. doi:10.3102/10769986025001060.

Bergbower, E. A. S., Pierson, R. N., and Azimzadeh, A. M. (2020). Multi-gene technical assessment of qPCR and NanoString n-Counter analysis platforms in cynomolgus monkey cardiac allograft recipients. *Cell. Immunol.* 347, 104019. doi:10.1016/J.CELLIMM.2019.104019.

Bertolini, C., Rubinetti, S., Umgiesser, G., Witbaard, R., Bouma, T. J., Rubino, A., et al. (2021). How to cope in heterogeneous coastal environments: Spatio-temporally endogenous circadian rhythm of valve gaping by mussels. *Sci. Total Environ.* 768, 145085. doi:10.1016/j.scitotenv.2021.145085.

Besse, J. P., Geffard, O., and Coquery, M. (2012). Relevance and applicability of active biomonitoring in continental waters under the Water Framework Directive. *TrAC Trends Anal. Chem.* 36, 113–127. doi:10.1016/J.TRAC.2012.04.004.

Besseau, L., Benyassi, A., Møller, M., Coon, S. L., Weller, J. L., Boeuf, G., et al. (2006). Melatonin pathway: breaking the 'high-at-night' rule in trout retina. *Exp. Eye Res.* 82, 620–627. doi:10.1016/J.EXER.2005.08.025.

Bingham, C., Arbogast, B., Guillaume, G. C., Lee, J. K., and Halberg, F. (1982). Inferential statistical methods for estimating and comparing cosinor parameters. *Chronobiologia* 9, 397–439.

Bjärnmark, N. A., Yarra, T., Churcher, A. M., Felix, R. C., Clark, M. S., and Power, D. M. (2016). Transcriptomics provides insight into *Mytilus galloprovincialis* (Mollusca: Bivalvia) mantle function and its role in biomineralisation. *Mar. Genomics* 27, 37–45. doi:10.1016/j.margen.2016.03.004.

Boo, M. V., Hiong, K. C., Choo, C. Y. L., Cao-Pham, A. H., Wong, W. P., Chew, S. F., et al. (2017). The inner mantle of the giant clam, *Tridacna squamosa*, expresses a basolateral Na+/K+-ATPase α-subunit, which displays light-dependent gene and protein expression along the shell-facing epithelium. *PLoS One* 12, e0186865. doi:10.1371/journal.pone.0186865.

Boulos, Z., and Terman, M. (1980). Food availability and daily biological rhythms. *Neurosci. Biobehav. Rev.* 4, 119–131. doi:10.1016/0149-7634(80)90010-X.

Brahmi, C., Kopp, C., Domart-Coulon, I., Stolarski, J., and Meibom, A. (2012). Skeletal growth dynamics linked to trace-element composition in the scleractinian coral *Pocillopora damicornis*. *Geochim. Cosmochim. Acta* 99, 146–158. doi:10.1016/j.gca.2012.09.031.

Branch, G. M., and Steffani, C. N. (2004). Can we predict the effects of alien species? A case-history of the invasion of South Africa by *Mytilus galloprovincialis* (Lamarck). *J. Exp. Mar. Bio. Ecol.* 300, 189–215. doi:10.1016/J.JEMBE.2003.12.007.

Brochu, M. P., and Aubin-Horth, N. (2021). Shedding light on the circadian clock of the threespine stickleback. *J. Exp. Biol.* 224, jeb242970. doi:10.1242/JEB.242970/273607/AM/SHEDDING-LIGHT-ON-THE-CIRCADIAN-CLOCK-OF-THE.

Bruland, K. W., Rue, E. L., and Smith, G. J. (2001). Iron and macronutrients in California coastal upwelling regimes: Implications for diatom blooms. *Limnol. Oceanogr.* 46, 1661–1674. doi:10.4319/LO.2001.46.7.1661.

Brunet, C., Casotti, R., and Vantrepotte, V. (2008). Phytoplankton diel and vertical variability in photobiological responses at a coastal station in the Mediterranean Sea. *J. Plankton Res.* 30, 645–654. doi:10.1093/plankt/fbn028.

Bulla, M., Oudman, T., Bijleveld, A. I., Piersma, T., and Kyriacou, C. P. (2017). Marine biorhythms: Bridging chronobiology and ecology. *Philos. Trans. R. Soc. B Biol. Sci.* 372.

doi:10.1098/rstb.2016.0253.

Buschbaum, C., and Saier, B. (2001). Growth of the mussel *Mytilus edulis* L. in the Wadden Sea affected by tidal emergence and barnacle epibionts. *J. Sea Res.* 45, 27–36. doi:10.1016/S1385-1101(00)00061-7.

Busza, A., and Emery, P. (2004). Roles of the two *Drosophila* CRYPTOCHROME structural domains in circadian photoreception. Science. 304, 1503-1506. doi:10.1126/science.1096973.

Butler, P. G., and Schöne, B. R. (2017). New research in the methods and applications of sclerochronology. *Palaeogeogr. Palaeoclimatol. Palaeoecol.* 465, 295–299. doi:10.1016/J.PALAEO.2016.11.013.

Cáceres-Martínez, J., and Figueras, A. (1998a). Long-term survey on wild and cultured mussels (*Mytilus galloprovincialis* Lmk) reproductive cycles in the Ria de Vigo (NW Spain). *Aquaculture* 162, 141–156. doi:10.1016/S0044-8486(98)00210-5.

Cáceres-Martínez, J., and Figueras, A. (1998b). Distribution and abundance of mussel (*Mytilus galloprovincialis* Lmk) larvae and post-larvae in the Ria de Vigo (NW Spain). *J. Exp. Mar. Bio. Ecol.* 229, 277–287. doi:10.1016/S0022-0981(98)00059-8.

Calisi, R. M., and Bentley, G. E. (2009). Lab and field experiments: Are they the same animal? *Horm. Behav.* 56, 1–10. doi:10.1016/J.YHBEH.2009.02.010.

Cao-Pham, A. H., Hiong, K. C., Boo, M. V., Choo, C. Y. L., Wong, W. P., Chew, S. F., et al. (2019). Calcium absorption in the fluted giant clam, *Tridacna squamosa*, may involve a homolog of voltage-gated calcium channel subunit α1 (CACNA1) that has an apical localization and displays light-enhanced protein expression in the ctenidium. *J. Comp. Physiol. B Biochem. Syst. Environ. Physiol.* 189, 693–706. doi:10.1007/s00360-019-01238-4.

Carlucci, M., Krisciunas, A., Li, H., Gibas, P., Koncevicius, K., Petronis, A., et al. (2020). DiscoRhythm: an easy-to-use web application and R package for discovering rhythmicity. *Bioinformatics* 36, 1952–1954. doi:10.1093/BIOINFORMATICS.

Carré, M., Bentaleb, I., Bruguier, O., Ordinola, E., Barrett, N. T., and Fontugne, M. (2006). Calcification rate influence on trace element concentrations in aragonitic bivalve shells: Evidences and mechanisms. *Geochim. Cosmochim. Acta* 70, 4906–4920. doi:10.1016/j.gca.2006.07.019.

Ceccherelli, V., and Rossi, R. (1984). Settlement, growth and production of the mussel *Mytilus galloprovincialis*. *Mar. Ecol. Prog. Ser.* 16, 173–184. doi:10.3354/meps016173.

Chapman, E. C., Bonsor, B. J., Parsons, D. R., and Rotchell, J. M. (2020). Influence of light and temperature cycles on the expression of circadian clock genes in the mussel *Mytilus edulis*. *Mar. Environ. Res.* 159, 104960. doi:10.1016/j.marenvres.2020.104960.

Chapman, E. C., O'Dell, A. R., Meligi, N. M., Parsons, D. R., and Rotchell, J. M. (2017). Seasonal expression patterns of clock-associated genes in the blue mussel *Mytilus edulis*. *Chronobiol. Int.* 34, 1300–1314. doi:10.1080/07420528.2017.1363224.

Chauvaud, L., Thouzeau, G., and Paulet, Y. M. (1998). Effects of environmental factors on the daily growth rate of *Pecten maximus* juveniles in the Bay of Brest (France). *J. Exp. Mar. Bio. Ecol.* 227, 83–111. doi:10.1016/S0022-0981(97)00263-3.

Chaves, I., Pokorny, R., Byrdin, M., Hoang, N., Ritz, T., Brettel, K., et al. (2011). The cryptochromes: Blue light photoreceptors in plants and animals. *Annu. Rev. Plant Biol.* 62, 335–364. doi:10.1146/annurev-arplant-042110-103759.

Checa, A. G. (2018). Physical and biological determinants of the fabrication of Molluscan shell

microstructures. *Front. Mar. Sci.* 5, 353. doi:10.3389/fmars.2018.00353.

Checa, A. G., Esteban-Delgado, F. J., and Rodríguez-Navarro, A. B. (2007). Crystallographic structure of the foliated calcite of bivalves. *J. Struct. Biol.* 157, 393–402. doi:10.1016/j.jsb.2006.09.005.

Checa, A. G., Macías-Sánchez, E., Harper, E. M., and Cartwright, J. H. E. (2016). Organic membranes determine the pattern of the columnar prismatic layer of mollusc shells. *Proc. R. Soc. B Biol. Sci.* 283, 20160032. doi:10.1098/rspb.2016.0032.

Checa, A. G., Okamoto, T., and Ramírez, J. (2006). Organization pattern of nacre in Pteriidae (Bivalvia: Mollusca) explained by crystal competition. *Proc. R. Soc. B Biol. Sci.* 273, 1329–1337. doi:10.1098/rspb.2005.3460.

Checa, A. G., Pina, M., Guez-navarro, B. R., and Harper, M. (2014). Crystalline organization of the fibrous prismatic calcitic layer of the Mediterranean mussel *Mytilus galloprovincialis*. *Biominer. Biomim. Mater.* 26, 495–505. doi:10.1127/0935-1221/2014/0026-2374.

Checa, A. G., Rodríguez-Navarro, A. B., and Esteban-Delgado, F. J. (2005). The nature and formation of calcitic columnar prismatic shell layers in pteriomorphian bivalves. *Biomaterials* 26, 6404–6414. doi:10.1016/j.biomaterials.2005.04.016.

Chew, S. F., Koh, C. Z. Y., Hiong, K. C., Choo, C. Y. L., Wong, W. P., Neo, M. L., et al. (2019). Light-enhanced expression of Carbonic Anhydrase 4-like supports shell formation in the fluted giant clam *Tridacna squamosa*. *Gene* 683, 101–112. doi:10.1016/j.gene.2018.10.023.

Claisse, D., Joanny, M., and Quintin, J. Y. (1992). Le réseau national d'observation de la qualité du milieu marin (RNO). *Analusis* 20, 19–22.

Clark, G. R. (2005). Daily growth lines in some living Pectens (Mollusca: Bivalvia), and some applications in a fossil relative: Time and tide will tell. *Palaeogeogr. Palaeoclimatol. Palaeoecol.* 228, 26–42. doi:10.1016/j.palaeo.2005.03.044.

Clark, M. S. (2020). Molecular mechanisms of biomineralization in marine invertebrates. *J. Exp. Biol.* 223, jeb206961. doi:10.1242/jeb.206961.

Cleveland, W. S. (1979). Robust locally weighted regression and smoothing scatterplots. *J. Am. Stat. Assoc.* 74, 829–836. doi:10.1080/01621459.1979.10481038.

Cocquempot, L., Delacourt, C., Paillet, J., Riou, P., Aucan, J., Castelle, B., et al. (2019). Coastal ocean and nearshore observation: A French case study. *Front. Mar. Sci.* 6, 324. doi:10.3389/fmars.2019.00324.

Coen, L. D., Brumbaugh, R. D., Bushek, D., Grizzle, R., Luckenbach, M. W., Posey, M. H., et al. (2007). Ecosystem services related to oyster restoration. *Mar Ecol Prog Ser* 341, 303–307. doi:10.3354/meps341303.

Coimbra, J., Machado, J., Fernandes, P. L., Ferreira, H. G., and Ferreira, K. G. (1988). Electrophysiology of the Mantle of *Anodonta Cygnea*. *J. Exp. Biol.* 140, 65–88. doi:10.1242/JEB.140.1.65.

Collins, B., Mazzoni, E. O., Stanewsky, R., and Blau, J. (2006). Drosophila CRYPTOCHROME is a circadian transcriptional repressor. *Curr. Biol.* 16, 441–449. doi:10.1016/J.CUB.2006.01.034.

Comeau, L. A., Babarro, J. M. F., Longa, A., and Padin, X. A. (2018). Valve-gaping behavior of raft-cultivated mussels in the Ría de Arousa, Spain. *Aquac. Reports* 9, 68–73. doi:10.1016/J.AQREP.2017.12.005.

Compton, T. J., Leathwick, J. R., and Inglis, G. J. (2010). Thermogeography predicts the potential global range of the invasive European green crab (*Carcinus maenas*). *Divers. Distrib.* 16, 243–255.

doi:10.1111/J.1472-4642.2010.00644.X.

Connor, K. M., and Gracey, A. Y. (2011). Circadian cycles are the dominant transcriptional rhythm in the intertidal mussel *Mytilus californianus*. *Pnas* 108, 16110–16115. doi:10.1073/pnas.1111076108.

Cornelissen, G. (2014). Cosinor-based rhythmometry. *Theor. Biol. Med. Model.* 11, 1–24. doi:10.1186/1742-4682-11-16.

Craeymeersch, J. A., and Jansen, H. M. (2018). "Chapter 14 Bivalve assemblages as hotspots for biodiversity," in *Goods and Services of Marine Bivalves*, 275–294.

Cranford, P. J. (2018). "Chapter 8 Magnitude and extent of water clarification services provided by bivalve suspension feeding," in *Goods and Services of Marine Bivalves*, 119–141.

Crenshaw, A. (1972). The inorganic composition of molluscan extrapallial Fluid. *Biol. Bull.* 143, 506–512. doi:10.2307/1540180.

Crenshaw, M. A., and Neff, J. M. (1969). Decalcification at the mantle-shell interface in molluscs. *Integr. Comp. Biol.* 9, 881–885. doi:10.1093/icb/9.3.881.

Crone, T. J., and Wilcock, W. S. D. (2005). Modeling the effects of tidal loading on mid-ocean ridge hydrothermal systems. *Geochemistry, Geophys. Geosystems* 6, Q07001. doi:10.1029/2004GC000905.

Cubillo, A. M., Peteiro, L. G., Fernández-Reiriz, M. J., and Labarta, U. (2012). Influence of stocking density on growth of mussels (*Mytilus galloprovincialis*) in suspended culture. *Aquaculture* 342–343, 103–111. doi:10.1016/J.AQUACULTURE.2012.02.017.

Cucco, A., and Umgiesser, G. (2006). Modeling the Venice Lagoon residence time. *Ecol. Modell.* 193, 34–51. doi:10.1016/J.ECOLMODEL.2005.07.043.

Cyran, S. A., Buchsbaum, A. M., Reddy, K. L., Lin, M. C., Glossop, N. R. J., Hardin, P. E., et al. (2003). *vrille*, *Pdp1*, and *dClock* form a second feedback loop in the *Drosophila* circadian clock. *Cell* 112, 329–341. doi:10.1016/S0092-8674(03)00074-6.

Dahiru, T. (2008). P-value, a true test of statistical significance? a cautionary note. *Ann. Ibadan Postgrad. Med.* 6, 21–26. doi:10.4314/AIPM.V6I1.64038.

Darlington, T. K., Wager-Smith, K., Ceriani, M. F., Staknis, D., Gekakis, N., Steeves, T. D. L., et al. (1998). Closing the Circadian Loop: CLOCK-Induced Transcription of Its Own Inhibitors per and tim. *New Ser.* 280, 1599–1603.

Dauphin, Y., Cuif, J. P., Doucet, J., Salomé, M., Susini, J., and Williams, C. T. (2003). In situ mapping of growth lines in the calcitic prismatic layers of mollusc shells using X-ray absorption near-edge structure (XANES) spectroscopy at the sulphur K-edge. *Mar. Biol.* 142, 299–304. doi:10.1007/s00227-002-0950-2.

Davenport, J., and Chen, X. (1987). A comparison of methods for the assessment of condition in the mussel (*Mytilus edulis* L.). *J. Molluscan Stud.* 53, 293–297. doi:10.1093/mollus/53.3.293.

Davenport, J., Smith, R. J. J. W., and Packer, M. (2000). Mussels *Mytilus edulis*: significant consumers and destroyers of mesozooplankton. *Mar. Ecol. Prog. Ser.* 198, 131–137. doi:10.3354/meps198131.

de Rafélis, M., Renard, M., Emmanuel, L., and Durlet, C. (2000). Apport de la cathodoluminescence à la connaissance de la spéciation du manganèse dans les carbonates pélagiques. *Comptes Rendus l'Académie des Sci. - Ser. IIA - Earth Planet. Sci.* 330, 391–398. doi:10.1016/S1251-8050(00)00148-

8.

de Winter, N. J., and Claeys, P. (2017). Micro X-ray fluorescence (μXRF) line scanning on Cretaceous rudist bivalves: A new method for reproducible trace element profiles in bivalve calcite. *Sedimentology* 64, 231–251. doi:10.1111/SED.12299.

de Winter, N. J., Goderis, S., Van Malderen, S. J. M., Sinnesael, M., Vansteenberge, S., Snoeck, C., et al. (2020). Subdaily-Scale Chemical Variability in a Torreites Sanchezi Rudist Shell: Implications for Rudist Paleobiology and the Cretaceous Day-Night Cycle. *Paleoceanogr. Paleoclimatology* 35, 1–21. doi:10.1029/2019PA003723.

Derolez, V., Bec, B., Cimiterra, N., Foucault, E., Messiaen, G., Fiandrino, A., et al. (2021). OBSLAG 2020 - volet eutrophisation.Lagunes méditerranéennes (période 2015-2020). Etat DCE de la colonne d'eau et du phytoplancton, tendance et variabilité des indicateurs.

Dibner, C., Schibler, U., and Albrecht, U. (2010). The mammalian circadian timing system: organization and coordination of central and peripheral clocks. *Annu. Rev. Physiol.* 72, 517–549. doi:10.1146/ANNUREV-PHYSIOL-021909-135821.

Dinno, A. (2017). dunn.test: Dunn's Test of Multiple Comparisons Using Rank Sums. Available at: https://cran.r-project.org/package=dunn.test.

Ditty, J. L., Williams, S. B., and Golden, S. S. (2003). A Cyanobacterial Circadian Timing Mechanism. *Annu. Rev. Genet.* 37, 513–543. doi:10.1146/annurev.genet.37.110801.142716.

Dodd, A. N., Salathia, N., Hall, A., Kévei, E., Tóth, R., Nagy, F., et al. (2005). Cell biology: Plant circadian clocks increase photosynthesis, growth, survival, and competitive advantage. *Science.* 309, 630–633. doi:10.1126/SCIENCE.1115581/SUPPL_FILE/DODD.SOM.PDF.

Dodd, J. R. (1965). Environmental control of strontium and magnesium in *Mytilus*. *Geochim. Cosmochim. Acta* 29, 385–398. doi:10.1016/0016-7037(65)90035-9.

Dodd, J. R., and Crisp, E. L. (1982). Non-linear variation with salinity of Sr/Ca and Mg/Ca ratios in water and aragonitic bivalve shells and implications for paleosalinity studies. *Palaeogeogr. Palaeoclimatol. Palaeoecol.* 38, 45–56. doi:10.1016/0031-0182(82)90063-3.

Doré, J., Chaillou, G., Poitevin, P., Lazure, P., Poirier, A., Chauvaud, L., et al. (2020). Assessment of Ba/Ca in *Arctica islandica* shells as a proxy for phytoplankton dynamics in the Northwestern Atlantic Ocean. *Estuar. Coast. Shelf Sci.* 237, 106628. doi:10.1016/J.ECSS.2020.106628.

Dunlap, J. C. (1999). Molecular bases for circadian clocks. *Cell* 96, 271–290. doi:10.1016/s0092-8674(00)80566-8.

Duperron, S. (2010). "The Diversity of Deep-Sea Mussels and Their Bacterial Symbioses," in *The vent and seep biota - Aspect from microbes to ecosystems* (Springer, Dordrecht), 137–167. doi:10.1007/978-90-481-9572-5_6.

Dupraz, C., Reid, R. P., Braissant, O., Decho, A. W., Norman, R. S., and Visscher, P. T. (2009). Processes of carbonate precipitation in modern microbial mats. *Earth-Science Rev.* 96, 141–162. doi:10.1016/j.earscirev.2008.10.005.

Eastel, J. M., Lam, K. W., Lee, N. L., Lok, W. Y., Tsang, A. H. F., Pei, X. M., et al. (2019). Application of NanoString technologies in companion diagnostic development. *Expert Rev. Mol. Diagn.* 19, 591–598. doi:10.1080/14737159.2019.1623672.

Eggermont, M., Cornillie, P., Dierick, M., Adriaens, D., Nevejan, N., Bossier, P., et al. (2020). The blue mussel inside: 3D visualization and description of the vascular-related anatomy of *Mytilus edulis* to unravel hemolymph extraction. *Sci. Rep.* 10, 1–16. doi:10.1038/s41598-020-62933-9.

Eirin-Lopez, J. M., and Putnam, H. M. (2019). Marine Environmental Epigenetics. *Ann. Rev. Mar. Sci.* 11, 335–368. doi:10.1146/ANNUREV-MARINE-010318-095114.

El Ali, A., Barbin, V., Calas, G., Cervelle, B., Ramseyer, K., and Bouroulec, J. (1993). Mn2+-activated luminescence in dolomite, calcite and magnesite: quantitative determination of manganese and site distribution by EPR and CL spectroscopy. *Chem. Geol.* 104, 189–202. doi:10.1016/0009-2541(93)90150-H.

Emerson, K. J., Bradshaw, W. E., and Holzapfel, C. M. (2008). Concordance of the circadian clock with the environment is necessary to maximize fitness in natural populations. *Evolution (N. Y).* 62, 979–983. doi:10.1111/j.1558-5646.2008.00324.x.

Emery, P., and Reppert, S. M. (2004). A Rhythmic Ror. *Neuron* 43, 443–446. doi:10.1016/J.NEURON.2004.08.009.

Emery, P., So, W. V., Kaneko, M., Hall, J. C., and Rosbash, M. (1998). CRY, a *Drosophila* Clock and Light-Regulated Cryptochrome, Is a Major Contributor to Circadian Rhythm Resetting and Photosensitivity. *Cell* 95, 669–679. doi:10.1016/S0092-8674(00)81637-2.

Engel, J. (2017). "Chapter 6: Formation of Mollusk Shells," in *A Critical Survey of Biomineralization*, ed. J. Engel, 29–40. doi:10.1007/978-3-319-47711-4.

Enright, J. T. (1976). Plasticity in an isopod's clockworks: Shaking shapes form and affects phase and frequency. *J. Comp. Physiol.* 107, 13–37. doi:10.1007/BF00663916.

Epstein, S., Buchsbaum, R., Lowenstam, H. A., and Urey, H. C. (1953). Revised carbonate-water isotopic temperature scale. *Geol. Soc. Am. Bull.* 64, 1315–1326. doi:10.1130/0016-7606(1953)64[1315:RCITS]2.0.CO;2.

Escobar, C., Cailotto, C., Angeles-Castellanos, M., Delgado, R. S., and Buijs, R. M. (2009). Peripheral oscillators: The driving force for food-anticipatory activity. *Eur. J. Neurosci.* 30, 1665–1675. doi:10.1111/j.1460-9568.2009.06972.x.

Feng, D., and Lazar, M. A. (2012). Clocks, Metabolism, and the Epigenome. *Mol. Cell* 47, 158–167. doi:10.1016/J.MOLCEL.2012.06.026.

Feng, D., Li, Q., Yu, H., Kong, L., and Du, S. (2017). Identification of conserved proteins from diverse shell matrix proteome in *Crassostrea gigas*: Characterization of genetic bases regulating shell formation. *Sci. Rep.* 7, 1–12. doi:10.1038/srep45754.

Fernández-Reiriz, M. J., Irisarri, J., and Labarta, U. (2015). Feeding behaviour and differential absorption of nutrients in mussel *Mytilus galloprovincialis*: Responses to three microalgae diets. *Aquaculture* 446, 42–47. doi:10.1016/J.AQUACULTURE.2015.04.025.

Fiandrino, A., Serais, O., Caillard, E., Munaron, D., and Cimiterra, N. (2021). Bulletin de la Surveillance de la Qualité du Milieu Marin Littoral 2020. Région Occitanie - Départements des Pyrénées Orientales, de l'Aude, de l'Hérault, du Gard. Languedoc-Roussillon Available at: https://archimer.ifremer.fr/doc/00718/82982/.

Figueroa, F. L., Niell, F. X., Figueiras, F. G., and Villarino, M. L. (1998). Diel migration of phytoplankton and spectral light field in the Ría de Vigo (NW Spain). *Mar. Biol.* 130, 491–499. doi:10.1007/s002270050269.

Filgueira, R., Fernández-Reiriz, M. J., and Labarta, U. (2009). Tasa de aclaramiento del mejillón *Mytilus galloprovincialis*. I. Respuesta a intervalos extremos de clorofila. *Ciencias Mar.* 35, 405–417. doi:10.7773/cm.v35i4.1645.

Filgueira, R., Grant, J., and Petersen, J. K. (2018a). Identifying the optimal depth for mussel suspended

culture in shallow and turbid environments. *J. Sea Res.* 132, 15–23. doi:10.1016/J.SEARES.2017.11.006.

Filgueira, R., Strohmeier, T., and Strand, Ø. (2018b). "Chapter 12 Regulating services of bivalve molluscs in the context of the carbon cycle and implications for ecosystem valuation," in *Goods and Services of Marine Bivalves*, 231–251.

Fox, J., and Weisberg, S. (2019). *An R Companion to Applied Regression*. Third. Thousand Oaks (CA): Sage Available at: https://socialsciences.mcmaster.ca/jfox/Books/Companion/.

Freitas, P. S., Clarke, L. J., Kennedy, H., and Richardson, C. A. (2009). Ion microprobe assessment of the heterogeneity of Mg/Ca, Sr/Ca and Mn/Ca ratios in *Pecten maximus* and *Mytilus edulis* (bivalvia) shell calcite precipitated at constant temperature. *Biogeosciences* 6, 1209–1227. doi:10.5194/bg-6-1209-2009.

Freitas, R., De Marchi, L., Bastos, M., Moreira, A., Velez, C., Chiesa, S., et al. (2017). Effects of seawater acidification and salinity alterations on metabolic, osmoregulation and oxidative stress markers in *Mytilus galloprovincialis*. *Ecol. Indic.* 79, 54–62. doi:10.1016/j.ecolind.2017.04.003.

Galimany, E., Ramón, M., and Durfort, M. (2005). "Desarrollo gonadal del mejillón *Mytilus galloprovincialis* de la bahía de Alfacs (delta del Ebro)," in *X Congreso Nacional de Acuicultura, Abstract Book II*, 616–617.

Gannon, M. E., Pérez-Huerta, A., Aharon, P., and Street, S. C. (2017). A biomineralization study of the Indo-Pacific giant clam *Tridacna gigas*. *Coral Reefs* 36, 503–517. doi:10.1007/s00338-016-1538-5.

Gao, J., Chen, Y., Yang, Y., Liang, J., Xie, J., Liu, J., et al. (2016). The transcription factor Pf-POU3F4 regulates expression of the matrix protein genes *Aspein* and *Prismalin-14* in pearl oyster (*Pinctada fucata*). *FEBS J.* 283, 1962–1978. doi:10.1111/febs.13716.

Gao, P., Liao, Z., Wang, X., Bao, L., Fan, M., Li, X., et al. (2015). Layer-by-Layer Proteomic Analysis of *Mytilus galloprovincialis* Shell. *PLoS One* 10, e0133913. doi:10.1371/journal.pone.0133913.

Gao, Y., Lesven, L., Gillan, D., Sabbe, K., Billon, G., De Galan, S., et al. (2009). Geochemical behavior of trace elements in sub-tidal marine sediments of the Belgian coast. *Mar. Chem.* 117, 88–96. doi:10.1016/J.MARCHEM.2009.05.002.

García-March, J. R., Sanchís Solsona, M. Á., and García-Carrascosa, A. M. (2008). Shell gaping behaviour of *Pinna nobilis* L., 1758: circadian and circalunar rhythms revealed by in situ monitoring. *Mar. Biol.* 153, 689–698. doi:10.1007/s00227-007-0842-6.

Gekakis, N., Saez, L., Delahaye-Brown, A.-M., Myers, M. P., Sehgal, A., Young, M. W., et al. (1995). Isolation of timeless by PER Protein Interaction: Defective Interaction Between timeless Protein and Long-Period Mutant PER^{L}. *Science.* 270 (5237), 811–815.

Gerbersdorf, S. U., and Schubert, H. (2011). Vertical migration of phytoplankton in coastal waters with different UVR transparency. *Environ. Sci. Eur.* 23, 36. doi:10.1186/2190-4715-23-36.

Gerdol, M., Moreira, R., Cruz, F., Gómez-Garrido, J., Vlasova, A., Rosani, U., et al. (2020). Massive gene presence-absence variation shapes an open pan-genome in the Mediterranean mussel. *Genome Biol.* 21, 275. doi:10.1186/s13059-020-02180-3.

Ghenim, L., Allier, C., Obeid, P., Hervé, L., Fortin, J. Y., Balakirev, M., et al. (2021). A new ultradian rhythm in mammalian cell dry mass observed by holography. *Sci. Reports 2021* 11, 1290. doi:10.1038/s41598-020-79661-9.

Gibson, R. N. (1973). Tidal and circadian activity rhythms in juvenile plaice, *Pleuronectes platessa*. *Mar.*

Biol. 22, 379–386. doi:10.1007/BF00391398.

Giebultowicz, J. M., Ivanchenko, M., and Vollintine, T. (2001). "Organization of the insect circadian system: Spatial and developmental expression of clock genes in peripheral tissues of *Drosophila melanogaster*," in *Insect Timing: Circadian Rhythmicity to Seasonality*, eds. D. L. Denlinger, J. M. Giebultowicz, and D. S. Saunders (Elsevier Science B.V.), 31–42. doi:10.1016/B978-044450608-5/50035-0.

Gillikin, D. P., Dehairs, F., Lorrain, A., Steenmans, D., Baeyens, W., and André, L. (2006). Barium uptake into the shells of the common mussel (*Mytilus edulis*) and the potential for estuarine paleo-chemistry reconstruction. *Geochim. Cosmochim. Acta* 70, 395–407. doi:10.1016/J.GCA.2005.09.015.

Gillikin, D. P., Lorrain, A., Paulet, Y. M., André, L., and Dehairs, F. (2008). Synchronous barium peaks in high-resolution profiles of calcite and aragonite marine bivalve shells. *Geo-Marine Lett. 2008 285* 28, 351–358. doi:10.1007/S00367-008-0111-9.

Giuffre, A. J., Hamm, L. M., Han, N., De Yoreo, J. J., and Dove, P. M. (2013). Polysaccharide chemistry regulates kinetics of calcite nucleation through competition of interfacial energies. *Proc. Natl. Acad. Sci. U. S. A.* 110, 9261–9266. doi:10.1073/pnas.1222162110.

Glossop, N. R. J., Houl, J. H., Zheng, H., Ng, F. S., Dudek, S. M., and Hardin, P. E. (2003). VRILLE Feeds Back to Control Circadian Transcription of Clock in the *Drosophila* Circadian Oscillator. *Neuron* 37, 249–261. doi:10.1016/S0896-6273(03)00002-3.

Gnyubkin, V. F. (2010). The circadian rhythms of valve movements in the mussel *Mytilus galloprovincialis*. *Russ. J. Mar. Biol.* 36, 419–428. doi:10.1134/S1063074010060039.

Gobler, C. J., DePasquale, E. L., Griffith, A. W., and Baumann, H. (2014). Hypoxia and Acidification Have Additive and Synergistic Negative Effects on the Growth, Survival, and Metamorphosis of Early Life Stage Bivalves. *PLoS One* 9, e83648. doi:10.1371/JOURNAL.PONE.0083648.

Goldberg, E. D. (1975). The mussel watch — A first step in global marine monitoring. *Mar. Pollut. Bull.* 6, 111. doi:10.1016/0025-326X(75)90271-4.

Gosling, E. (2004). *Bivalve Molluscs: biology, ecology and culture*. , ed. Fishing News Books Oxford and Malden (Massachusetts) doi:10.1002/9780470995532.

Goto, S. G., and Takekata, H. (2015). Circatidal rhythm and the veiled clockwork. *Curr. Opin. Insect Sci.* 7, 92–97. doi:10.1016/J.COIS.2014.12.004.

Gouthiere, L., Claustrat, B., Brun, J., and Mauvieux, B. (2005a). Éléments méthodologiques complémentaires dans l'analyse des rythmes: Recherche de périodes, modélisation. Exemples de la Mélatonine plasmatique et de courbes de températures. *Pathol. Biol.* 53, 285–289. doi:10.1016/j.patbio.2004.12.025.

Gouthiere, L., Mauvieux, B., Davenne, D., and Waterhouse, & J. (2005b). Complementary methodology in the analysis of rhythmic data, using examples from a complex situation, the rhythmicity of temperature in night shift workers. *Biol. Rhythm Res.* 36, 177–193. doi:10.1080/09291010400026298.

Grant, J., Cranford, P., and Emerson, C. (1997). Sediment resuspension rates, organic matter quality and food utilization by sea scallops (*Placopecten magellanicus*) on Georges Bank. *J. Mar. Res.* 55, 965–994. doi:10.1357/0022240973224193.

Gutman, R., and Dayan, T. (2005). Temporal partitioning: An experiment with two species of spiny mice. *Ecology* 86, 164–173. doi:10.1890/03-0369.

Gwinner, E., and Brandstätter, R. (2001). Complex bird clocks. *Philos. Trans. R. Soc. London. Ser. B Biol. Sci.* 356, 1801–1810. doi:10.1098/RSTB.2001.0959.

Häfker, N. S., Andreatta, G., Manzotti, A., Falciatore, A., Raible, F., and Tessmar-raible, K. (2023). Rhythms and Clocks in Marine Organisms. *Ann. Rev. Mar. Sci.* 15, 13.1-13.30.

Hall, T. (2001). Biolign alignment and multiple contig editor. Available at: http://en.bio-soft.net/dna/BioLign.html.

Hallmann, N., Burchell, M., Schöne, B. R., Irvine, G. V., and Maxwell, D. (2009). High-resolution sclerochronological analysis of the bivalve mollusk *Saxidomus gigantea* from Alaska and British Columbia: techniques for revealing environmental archives and archaeological seasonality. *J. Archaeol. Sci.* 36, 2353–2364. doi:10.1016/j.jas.2009.06.018.

Hao, H., Allen, D. L., and Hardin, P. E. (1997). A circadian enhancer mediates PER-dependent mRNA cycling in *Drosophila melanogaster*. *Mol. Cell. Biol.* 17, 3687–3693. doi:10.1128/MCB.17.7.3687.

Hardin, P. E. (1994). Analysis of period mRNA cycling in *Drosophila* head and body tissues indicates that body oscillators behave differently from head oscillators. *Mol. Cell. Biol.* 14, 7211–7218. doi:10.1128/MCB.14.11.7211-7218.1994.

Hardin, P. E., and Panda, S. (2013). Circadian timekeeping and output mechanisms in animals. *Curr. Opin. Neurobiol.* 23, 724–731. doi:10.1016/J.CONB.2013.02.018.

Harris, H. F. (1900). On the rapid conversion of haematoxylin into haematein in staining reactions. *J. Appl. Microsc. Lab. Methods* 3, 777.

Hart, D. R., and Chute, A. S. (2009). Estimating von Bertalanffy growth parameters from growth increment data using a linear mixed-effects model, with an application to the sea scallop *Placopecten magellanicus* . *ICES J. Mar. Sci.* 66, 2165–2175. doi:10.1093/ICESJMS/FSP188.

Hartmann, J. T., Beggel, S., Auerswald, K., and Geist, J. (2016). Determination of the most suitable adhesive for tagging freshwater mussels and its use in an experimental study of filtration behaviour and biological rhythm. *J. Molluscan Stud.* 82, 415–421. doi:10.1093/mollus/eyw003.

Hawkins, A. J. S., and Klumpp, D. W. (1995). Nutrition of the giant clam *Tridacna gigas* (L.). II. Relative contributions of filter-feeding and the ammonium-nitrogen acquired and recycled by symbiotic alga towards total nitrogen requirements for tissue growth and metabolism. *J. Exp. Mar. Bio. Ecol.* 190, 263–290. doi:10.1016/0022-0981(95)00044-r.

Heath, D. D., Rawson, P. D., and Hilbish, T. J. (1995). PCR-based nuclear markers identify alien blue mussel (*Mytilus* spp.) genotypes on the west coast of Canada. *Can. J. Fish. Aquat. Sci.* 52, 2621–2627. doi:10.1139/f95-851.

Hellemans, J., and Vandesompele, J. (2011). qPCR data analysis–unlocking the secret to successful results. *PCR Troubl. Optim. Essent. Guid.*, 139–150.

Helm, B., Visser, M. E., Schwartz, W., Kronfeld-Schor, N., Gerkema, M., Piersma, T., et al. (2017). Two sides of a coin: ecological and chronobiological perspectives of timing in the wild. *Philos. Trans. R. Soc. B Biol. Sci.* 372, 20160246. doi:10.1098/RSTB.2016.0246.

Hervé, P., and Bruslé, J. (1980). L'étang de Salses-Leucate, écologie générale et ichtyofaune. *Vie Milieu* 30, 275–283.

Hervé, P., and Bruslé, J. (1981). L'étang de Canet-Saint-Nazaire (P.O.). Écologie générale et Ichthyofaune. *Vie Milieu* 31, 17–25.

Hicks, S. D. (2006). *Understanding tides*. US Departùent of Commerce, National Oceanic and

Atmospheric Administration, National Ocean Service.

Higuera-Ruiz, R., and Elorza, J. (2009). Biometric, microstructural, and high-resolution trace element studies in *Crassostrea gigas* of Cantabria (Bay of Biscay, Spain): Anthropogenic and seasonal influences. *Estuar. Coast. Shelf Sci.* 82, 201–213. doi:10.1016/J.ECSS.2009.01.001.

Hiong, K. C., Cao-Pham, A. H., Choo, C. Y. L., Boo, M. V., Wong, W. P., Chew, S. F., et al. (2017). Light-dependent expression of a Na + /H + exchanger 3-like transporter in the ctenidium of the giant clam, *Tridacna squamosa* , can be related to increased H + excretion during light-enhanced calcification. *Physiol. Rep.* 5, e13209. doi:10.14814/phy2.13209.

Huang, X., Li, S., Ni, P., Gao, Y., Jiang, B., Zhou, Z., et al. (2017). Rapid response to changing environments during biological invasions: DNA methylation perspectives. *Mol. Ecol.* 26, 6621–6633. doi:10.1111/MEC.14382.

Huang, Y., Sun, J., Wang, L., and Song, L. (2018). The unfolded protein response signaling pathways in molluscs. *Invertebr. Surviv. J.* 15, 183–196.

Hüning, A. K., Melzner, F., Thomsen, J., Gutowska, M. A., Krämer, L., Frickenhaus, S., et al. (2013). Impacts of seawater acidification on mantle gene expression patterns of the Baltic Sea blue mussel: implications for shell formation and energy metabolism. *Mar. Biol.* 160, 1845–1861. doi:10.1007/s00227-012-1930-9.

Hurley, J. M., Jankowski, M. S., De los Santos, H., Crowell, A. M., Fordyce, S. B., Zucker, J. D., et al. (2018). Circadian Proteomic Analysis Uncovers Mechanisms of Post-Transcriptional Regulation in Metabolic Pathways. *Cell Syst.* 7, 613-626.e5. doi:10.1016/J.CELS.2018.10.014.

Huyghe, D., Emmanuel, L., de Rafelis, M., Renard, M., Ropert, M., Labourdette, N., et al. (2020). Oxygen isotope disequilibrium in the juvenile portion of oyster shells biases seawater temperature reconstructions. *Estuar. Coast. Shelf Sci.* 240, 106777. doi:10.1016/j.ecss.2020.106777.

Huyghe, D., Rafelis, M. De, Ropert, M., Mouchi, V., Emmanuel, L., and Renard, M. (2019). New insights into oyster high - resolution hinge growth patterns. *Mar. Biol.* 166, 48. doi:10.1007/s00227-019-3496-2.

Hyeon, J., Cho, S. Y., Hong, M. E., Kang, S. Y., Do, I., Im, Y. H., et al. (2017). NanoString nCounter® approach in breast cancer: A comparative analysis with quantitative real-time polymerase chain reaction, in situ hybridization, and immunohistochemistry. *J. Breast Cancer* 20, 286–296. doi:10.4048/jbc.2017.20.3.286.

Ip, Y. K., Ching, B., Hiong, K. C., Choo, C. Y. L., Boo, M. V., Wong, W. P., et al. (2015). Light induces changes in activities of Na+/K+-ATPase, H+/K+-ATPase and glutamine synthetase in tissues involved directly or indirectly in light-enhanced calcification in the giant clam, *Tridacna squamosa*. *Front. Physiol.* 6, 68. doi:10.3389/fphys.2015.00068.

Ip, Y. K., Hiong, K. C., Lim, L. J. Y., Choo, C. Y. L., Boo, M. V., Wong, W. P., et al. (2018). Molecular characterization, light-dependent expression, and cellular localization of a host vacuolar-type H+-ATPase (VHA) subunit A in the giant clam, *Tridacna squamosa*, indicate the involvement of the host VHA in the uptake of inorganic carbon and. *Gene* 659, 137–148. doi:10.1016/j.gene.2018.03.054.

Ip, Y. K., Koh, C. Z. Y., Hiong, K. C., Choo, C. Y. L., Boo, M. V., Wong, W. P., et al. (2017). Carbonic anhydrase 2-like in the giant clam, *Tridacna squamosa* : characterization, localization, response to light, and possible role in the transport of inorganic carbon from the host to its symbionts. *Physiol. Rep.* 5, e13494. doi:10.14814/phy2.13494.

Ivanina, A. V., Falfushynska, H. I., Beniash, E., Piontkivska, H., and Sokolova, I. M. (2017).

Biomineralization-related specialization of hemocytes and mantle tissues of the Pacific oyster *Crassostrea gigas*. *J. Exp. Biol.* 220, 3209–3221. doi:10.1242/jeb.160861.

Jacquet, S., Partensky, F., Lennon, J. F., and Vaulot, D. (2001). Diel patterns of growth and division in marine picoplankton in culture. *J. Phycol.* 37, 357–369. doi:10.1046/J.1529-8817.2001.037003357.X.

Jansen, H. M., Strand, Ø., van Broekhoven, W., Strohmeier, T., Verdegem, M. C., and Smaal, A. C. (2018). "Chapter 9 Feedbacks from filter feeders: review on the role of mussels in cycling and storage of nutrients in oligo- meso- and eutrophic cultivation areas," in *Goods and Services of Marine Bivalves*, 143–177.

Jetten, A. M., Kurebayashi, S., and Ueda, E. (2001). The ROR nuclear orphan receptor subfamily: Critical regulators of multiple biological processes. *Prog. Nucleic Acid Res. Mol. Biol.* 69, 205–247. doi:10.1016/S0079-6603(01)69048-2.

Jones, D. S. (1980). Annual cycle of shell growth increment formation in two continental shelf bivalves and its paleoecologic significance. *Paleobiology* 3, 331–340. doi:10.1017/S0094837300006837.

Jones, D. T., Taylor, W. R., and Thornton, J. M. (1992). The rapid generation of mutation data matrices from protein sequences. *Bioinformatics* 8, 275–282. doi:10.1093/BIOINFORMATICS/8.3.275.

Jørgensen, C. B. (1983). Patterns of uptake of dissolved amino acids in mussels (*Mytilus edulis*). *Mar. Biol. 1983 732* 73, 177–182. doi:10.1007/BF00406886.

Kamae, Y., Uryu, O., Miki, T., and Tomioka, K. (2014). The Nuclear Receptor Genes HR3 and E75 Are Required for the Circadian Rhythm in a Primitive Insect. *PLoS One* 9, e114899. doi:10.1371/journal.pone.0114899.

Karayücel, S., Çelik, M. Y., Karayücel, I., Öztürk, R., and Eyüboğlu, B. (2015). Effects of stocking density on survival, growth and biochemical composition of cultured mussels (*Mytilus galloprovincialis*, Lamarck 1819) from an offshore submerged longline system. *Aquac. Res.* 46, 1369–1383. doi:10.1111/are.12291.

Karney, G. B., Butler, P. G., Speller, S., Scourse, J. D., Richardson, C. A., Schrder, M., et al. (2012). Characterizing the microstructure of *Arctica islandica* shells using NanoSIMS and EBSD. *Geochemistry, Geophys. Geosystems* 13, Q04002. doi:10.1029/2011GC003961.

Kempinger, L., Dittmann, R., Rieger, D., and Helfrich-Förster, C. (2009). The nocturnal activity of fruit flies exposed to artificial moonlight is partly caused by direct light effects on the activity level that bypass the endogenous clock. *Chronobiol. Int.* 26, 151–166. doi:10.1080/07420520902747124.

Kennish, M. J., and Olsson, R. K. (1975). Effects of thermal discharges on the microstructural growth of *Mercenaria mercenaria*. *Environ. Geol.* 1, 41–64. doi:10.1007/BF02426940.

Killam, D. E., and Clapham, M. E. (2018). Identifying the ticks of bivalve shell clocks: Seasonal growth in relation to temperature and food supply. *Palaios* 33, 228–236. doi:10.2110/palo.2017.072.

Klein, D. C. (2007). Arylalkylamine N-Acetyltransferase: "the Timezyme." *J. Biol. Chem.* 282, 4233–4237. doi:10.1074/JBC.R600036200.

Klumpp, D. W., and Griffiths, C. L. (1994). Contributions of phototrophic and heterotrophic nutrition to the metabolic and growth requirements of four species of giant clam (*Tridacnidae*). *Mar. Ecol. Prog. Ser.* 115, 103–115. doi:10.3354/meps115103.

Kojima, S., Shingle, D. L., and Green, C. B. (2011). Post-transcriptional control of circadian rhythms. *J. Cell Sci.* 124, 311–320. doi:10.1242/JCS.065771.

Komsta, L. (2011). outliers: Tests for Outliers. Available at: https://cran.r-project.org/package=outliers.

Kornmann, B., Schaad, O., Bujard, H., Takahashi, J. S., and Schibler, U. (2007). System-Driven and Oscillator-Dependent Circadian Transcription in Mice with a Conditionally Active Liver Clock. *PLOS Biol.* 5, e34. doi:10.1371/JOURNAL.PBIO.0050034.

Krittika, S., and Yadav, P. (2019). Circadian clocks: an overview on its adaptive significance. *Biol. Rhythm Res.* 51, 1109–1132. doi:10.1080/09291016.2019.1581480.

Kumar, S., Stecher, G., Li, M., Knyaz, C., and Tamura, K. (2018). MEGA X: Molecular Evolutionary Genetics Analysis across Computing Platforms. *Mol. Biol. Evol.* 35, 1547–1549. doi:10.1093/molbev/msy096.

Lambert, S., Tragin, M., Lozano, J. C., Ghiglione, J. F., Vaulot, D., Bouget, F. Y., et al. (2019). Rhythmicity of coastal marine picoeukaryotes, bacteria and archaea despite irregular environmental perturbations. *ISME J.* 13, 388–401. doi:10.1038/s41396-018-0281-z.

Langdon, C., and Newell, R. (1989). Utilization of detritus and bacteria as food sources by two bivalve suspension-feeders, the oyster *Crassostrea virginica* and the mussel *Geukensia demissa*. *Mar. Ecol. Prog. Ser.* 58, 299–310. doi:10.3354/meps058299.

Langlet, D., Alunno-Bruscia, M., Rafélis, M., Renard, M., Roux, M., Schein, E., et al. (2006). Experimental and natural cathodoluminescence in the shell of *Crassostrea gigas* from Thau lagoon (France): Ecological and environmental implications. *Mar. Ecol. Prog. Ser.* 317, 143–156. doi:10.3354/meps317143.

Lartaud, F., Chauvaud, L., Richard, J., Toulot, A., Bollinger, C., Testut, L., et al. (2010a). Experimental growth pattern calibration of Antarctic scallop shells (*Adamussium colbecki*, Smith 1902) to provide a biogenic archive of high-resolution records of environmental and climatic changes. *J. Exp. Mar. Bio. Ecol.* 393, 158–167. doi:10.1016/j.jembe.2010.07.016.

Lartaud, F., de Rafelis, M., Ropert, M., Emmanuel, L., Geairon, P., and Renard, M. (2010b). Mn labelling of living oysters: Artificial and natural cathodoluminescence analyses as a tool for age and growth rate determination of *C. gigas* (Thunberg, 1793) shells. *Aquaculture* 300, 206–217. doi:10.1016/j.aquaculture.2009.12.018.

Le Roy, N., Jackson, D. J., Marie, B., Ramos-Silva, P., and Marin, F. (2014). The evolution of metazoan aα-carbonic anhydrases and their roles in calcium carbonate biomineralization. *Front. Zool.* 11, 1–16. doi:10.1186/s12983-014-0075-8.

Lê, S., Josse, J., and Husson, F. (2008). FactoMineR: An R Package for Multivariate Analysis. *J. Stat. Softw.* 25, 1–18. doi:10.18637/JSS.V025.I01.

Li, S., Liu, Y., Huang, J., Zhan, A., Xie, L., and Zhang, R. (2017). The receptor genes PfBMPR1B and PfBAMBI are involved in regulating shell biomineralization in the pearl oyster *Pinctada fucata*. *Sci. Rep.* 7, 9219. doi:10.1038/s41598-017-10011-y.

Liao, Q., Qin, Y., Zhou, Y., Shi, G., Li, X., Li, J., et al. (2021). Characterization and functional analysis of a chitinase gene: Evidence of *Ch-chit* participates in the regulation of biomineralization in *Crassostrea hongkongensis*. *Aquac. Reports* 21, 100852. doi:10.1016/j.aqrep.2021.100852.

Lin, A. Y. M., Meyers, M. A., and Vecchio, K. S. (2006). Mechanical properties and structure of *Strombus gigas*, *Tridacna gigas*, and *Haliotis rufescens* sea shells: A comparative study. *Mater. Sci. Eng. C* 26, 1380–1389. doi:10.1016/J.MSEC.2005.08.016.

Littlewood, D. T. J., and Young, R. E. (1994). The effect of air-gaping behaviour on extrapallial fluid pH in the tropical oyster *Crassostrea rhizophorae*. *Comp. Biochem. Physiol. -- Part A Physiol.* 107, 1–

6. doi:10.1016/0300-9629(94)90264-X.

Lloyd, D., and Murray, D. B. (2005). Ultradian metronome: Timekeeper for orchestration of cellular coherence. *Trends Biochem. Sci.* 30, 373–377. doi:10.1016/j.tibs.2005.05.005.

Louis, V., Besseau, L., and Lartaud, F. (2022). Step in Time : Biomineralisation of Bivalve's Shell. *Front. Mar. Sci.* 9, 906085. doi:10.3389/fmars.2022.906085.

Lutz, R. A., and Rhoads, D. C. (1977). Anaerobiosis and a Theory of Growth Line Formation. *Science.* 198, 1222–1227. doi:10.1126/science.198.4323.1222.

Maar, M., Nielsen, T. G., and Petersen, J. K. (2008). Depletion of plankton in a raft culture of *Mytilus galloprovincialis* in Ría de Vigo, NW Spain. II. Zooplankton. *Aquat. Biol.* 4, 127–141. doi:10.3354/ab00125.

Machel, H. G., Mason, R. A., Mariano, A. N., and Mucci, A. (1991). "Causes and Emission of Luminescence in Calcite and Dolomite," in *Luminescence Microscopy and Spectroscopy:y: Qualitative and Quantitative Applications*, eds. C. E. Barker, R. C. Burruss, H. G. l Kopp, C. Otto, D. Mache, J. Marshall, et al. (SEPM Society for Sedimentary Geology). doi:10.2110/SCN.91.25.0009.

Mahé, K., Bellamy, E., Lartaud, F., and Rafélis, M. De (2010). Calcein and manganese experiments for marking the shell of the common cockle (*Cerastoderma edule*): tidal rhythm validation of increments formation. *Aquat. Living Resour.* 245, 239–245. doi:https//:doi.org/10.1051/alr/2010025.

Maire, O., Amouroux, J. M., Duchêne, J. C., and Grémare, A. (2007). Relationship between filtration activity and food availability in the Mediterranean mussel *Mytilus galloprovincialis*. *Mar. Biol.* 152, 1293–1307. doi:10.1007/s00227-007-0778-x.

Mao, J., Zhang, W., Wang, X., Song, J., Yin, D., Tian, Y., et al. (2019). Histological and Expression Differences Among Different Mantle Regions of the Yesso Scallop (*Patinopecten yessoensis*) Provide Insights into the Molecular Mechanisms of Biomineralization and Pigmentation. *Mar. Biotechnol.* 21, 683–696. doi:10.1007/s10126-019-09913-x.

Marie, B., Le, N., Zanella-Cléon, I., Becchi, M., and Marin, F. (2011). Molecular Evolution of Mollusc Shell Proteins : Insights from Proteomic Analysis of the Edible Mussel *Mytilus*. *J. Mol. Evol.*, 531–546. doi:10.1007/s00239-011-9451-6.

Marin, F. (2020). Mollusc shellomes: Past, present and future. *J. Struct. Biol.* 212, 107583. doi:10.1016/j.jsb.2020.107583.

Marin, F., and Luquet, G. (2004). Molluscan shell proteins. *Comptes Rendus - Palevol* 3, 469–492. doi:10.1016/j.crpv.2004.07.009.

Marin, F., Luquet, G., Marie, B., and Medakovic, D. (2007). Molluscan Shell Proteins: Primary Structure, Origin, and Evolution. *Curr. Top. Dev. Biol.* 80, 209–276. doi:10.1016/S0070-2153(07)80006-8.

Marin, F., Roy, N. Le, and Marie, B. (2012). The formation and mineralization of mollusk. *Front. Biosci.* 4, 1099–1125. doi:10.2741/S321.

Mat, A. M., Charles, J., Ciret, P., and Tran, D. (2014). Looking for the clock mechanism responsible for circatidal behavior in the oyster *Crassostrea gigas*. *Mar. Biol.* 161, 89–99. doi:10.1007/s00227-013-2317-2.

Mat, A. M., Massabuau, J. C., Ciret, P., and Tran, D. (2012). Evidence for a plastic dual circadian rhythm in the oyster *Crassostrea gigas*. *Chronobiol. Int.* 29, 857–867. doi:10.3109/07420528.2012.699126.

Mat, A. M., Perrigault, M., Massabuau, J. C., and Tran, D. (2016). Role and expression of *cry1* in the adductor muscle of the oyster *Crassostrea gigas* during daily and tidal valve activity rhythms. *Chronobiol. Int.* 33, 949–963. doi:10.1080/07420528.2016.1181645.

Mat, A. M., Sarrazin, J., Markov, G. V, Apremont, V., Dubreuil, C., Eché, C., et al. (2020). Biological rhythms in the deep-sea hydrothermal mussel *Bathymodiolus azoricus*. *Nat. Commun.* 11, 3454. doi:10.1038/s41467-020-17284-4.

Mauvoisin, D., Wang, J., Jouffe, C., Martin, E., Atger, F., Waridel, P., et al. (2014). Circadian clock-dependent and -independent rhythmic proteomes implement distinct diurnal functions in mouse liver. *Proc. Natl. Acad. Sci. U. S. A.* 111, 167–172. doi:10.1073/PNAS.1314066111/SUPPL_FILE/SD03.XLS.

McDonald, J. H., and Koehn, R. K. (1988). The mussels *Mytilus galloprovincialis* and *M. trossulus* on the Pacific coast of North America. *Mar. Biol.* 99, 111–118. doi:10.1007/BF00644984.

McDonald, J. H., Koehn, R. K., Balakirev, E. S., Manchenko, G. P., Pudovkin, A. I., Sergievskii, S. O., et al. (1990). Species identity of the "common mussel" inhabiting the Asiatic coasts of the Pacific Ocean. *Sov. J. Mar. Biol.* 16, 10–18. Available at: https://www.cabdirect.org/cabdirect/abstract/19910189323 [Accessed December 5, 2019].

McDonald, J. H., Seed, R., and Koehn, R. K. (1991). Allozymes and morphometric characters of three species of *Mytilus* in the Northern and Southern Hemispheres. *Mar. Biol.* 111, 323–333. doi:10.1007/BF01319403.

Medvedev, I. P. (2018). Tides in the Black Sea: Observations and Numerical Modelling. *Pure Appl. Geophys.* 175, 1951–1969. doi:10.1007/s00024-018-1878-x.

Météo-France (2020). Les vents régionaux. Available at: https://meteofrance.com/comprendre-la-meteo/le-vent/les-vents-regionaux [Accessed August 26, 2022].

Miglioli, A., Dumollard, R., Balbi, T., Besnardeau, L., and Canesi, L. (2019). Characterization of the main steps in first shell formation in *Mytilus galloprovincialis*: Possible role of tyrosinase. *Proc. R. Soc. B Biol. Sci.* 286, 20192043. doi:10.1098/rspb.2019.2043.

Mirzaei, M. R., and Shau-Hwai, A. T. (2016). Assessing cockle shells (*Anadara granosa*) for reconstruction subdaily environmental parameters: Implication for paleoclimate studies. *Hist. Biol.* 28, 896–906. doi:10.1080/08912963.2015.1052806.

Misogianes, M. J., and Chasteen, N. D. (1979). A chemical and spectral characterization of the extrapallial fluid of *Mytilus edulis*. *Anal. Biochem.* 100, 324–334. doi:10.1016/0003-2697(79)90236-7.

Mistlberger, R. E. (2009). Food-anticipatory circadian rhythms: Concepts and methods. *Eur. J. Neurosci.* 30, 1718–1729. doi:10.1111/j.1460-9568.2009.06965.x.

Miyamoto, H., Miyashita, T., Okushima, M., Nakano, S., Morita, T., and Matsushiro, A. (1996). A carbonic anhydrase from the nacreous layer in oyster pearls. *Proc. Natl. Acad. Sci.* 93, 9657–9660. doi:10.1073/PNAS.93.18.9657.

Miyamoto, H., Miyoshi, F., and Kohno, J. (2005). The Carbonic Anhydrase Domain Protein Nacrein is Expressed in the Epithelial Cells of the Mantle and Acts as a Negative Regulator in Calcification in the Mollusc *Pinctada fucata*. *Zoo. Sc.* 22 (3), 311–315. doi:10.2108/ZSJ.22.311.

Miyashita, T. (2002). Identical carbonic anhydrase contributes to nacreous or prismatic layer formation in *Pinctada fucata* (Mollusca : Bivalvia). *Veliger* 45, 250–255.

Miyashita, T., Hanashita, T., Toriyama, M., Takagi, R., Akashika, T., and Higashikubo, N. (2008). Gene

cloning and biochemical characterization of the BMP-2 of *Pinctada fucata*. *Biosci. Biotechnol. Biochem.* 72, 37–47. doi:10.1271/bbb.70302.

Miyazaki, Y., Usui, T., Kajikawa, A., Hishiyama, H., Matsuzawa, N., Nishida, T., et al. (2008). Daily oscillation of gene expression associated with nacreous layer formation. *Front. Mater. Sci. China* 2, 162–166. doi:10.1007/s11706-008-0027-3.

Moberg, F., and Folke, C. (1999). Ecological goods and services of coral reef ecosystems. *Ecol. Econ.* 29, 215–233. doi:10.1016/S0921-8009(99)00009-9.

Mohawk, J. A., Green, C. B., and Takahashi, J. S. (2012). Central and peripheral circadian clocks in mammals. *Annu. Rev. Neurosci.* 35, 445–462. doi:10.1146/annurev-neuro-060909-153128.

Monaco, C. J., and McQuaid, C. D. (2018). Applicability of Dynamic Energy Budget (DEB) models across steep environmental gradients. *Sci. Rep.* 8, 16384. doi:10.1038/s41598-018-34786-w.

Moran, A. L., and Marko, P. B. (2005). A simple technique for physical marking of larvae of marine bivalves. *J. Shellfish Res.* 24, 567–571. doi:10.2983/0730-8000(2005)24[567:ASTFPM]2.0.CO;2.

Mount, A. S., Wheeler, A. P., Paradkar, R. P., and Snider, D. (2004). Hemocyte-Mediated Shell Mineralization in the Eastern Oyster. *Science.* 304, 297–300.

Mrosovsky, N. (1999). Masking: history, definitions, and measurement. *Chronobiol. Int.* 16, 415–429. doi:10.3109/07420529908998717.

Murdock, D. J. E. (2020). The 'biomineralization toolkit' and the origin of animal skeletons. *Biol. Rev.* 95, 1372–1392. doi:10.1111/brv.12614.

Myers, M. P., Wager-Smith, K., Wesley, C. S., Young, M. W., and Sehgal, A. (1995). Positional cloning and sequence analysis of the *Drosophila* clock gene, *timeless*. *Science* 270, 805–8. doi:10.1126/science.270.5237.805.

Nagai, K., Honjo, T., Go, J., Yamashita, H., and Seok Jin Oh (2006). Detecting the shellfish killer *Heterocapsa circularisquama* (Dinophyceae) by measuring bivalve valve activity with a Hall element sensor. *Aquaculture* 255, 395–401. doi:10.1016/j.aquaculture.2005.12.018.

Nagoshi, E., Saini, C., Bauer, C., Laroche, T., Naef, F., and Schibler, U. (2004). Circadian Gene Expression in Individual Fibroblasts: Cell-Autonomous and Self-Sustained Oscillators Pass Time to Daughter Cells. *Cell* 119, 693–705. doi:10.1016/J.CELL.2004.11.015.

NanoString Technologies Inc. (2017). Gene Expression Data Analysis Guidelines.

Navarro, E., Iglesias, J. I. P., Camacho, A. P., and Labarta, U. (1996). The effect of diets of phytoplankton and suspended bottom material on feeding and absorption of raft mussels (*Mytilus galloprovincialis* Lmk). *J. Exp. Mar. Bio. Ecol.* 198, 175–189. doi:10.1016/0022-0981(95)00210-3.

Naylor, E. (1958). Tidal and Diurnal Rhythms of Locomotory Activity in *Carcinus Maenas* (L.). *J. Exp. Biol.* 35, 602–610. doi:10.1242/jeb.35.3.602.

Naylor, E. (1996). Crab clockwork: The case for interactive circatidal and circadian oscillators controlling rhythmic locomotor activity of *Carcinus maenas*. *Chronobiol. Int.* 13, 153–161. doi:10.3109/07420529609012649.

Nedoncelle, K., Lartaud, F., de Rafelis, M., Boulila, S., and Le Bris, N. (2013). A new method for high-resolution bivalve growth rate studies in hydrothermal environments. *Mar. Biol.* 160, 1427–1439. doi:10.1007/s00227-013-2195-7.

Nedoncelle, K., Lartaud, F., Pereira, L. C., Yücel, M., Thurnherr, A. M., Mullineaux, L., et al. (2015). Bathymodiolus growth dynamics in relation to environmental fluctuations in vent habitats. *Deep.*

Res. Part I 106, 183–193. doi:10.1016/j.dsr.2015.10.003.

Nedoncelle, K., Le Bris, N., de Rafélis, M., Labourdette, N., and Lartaud, F. (2014). Non-equilibrium fractionation of stable carbon isotopes in chemosynthetic mussels. *Chem. Geol.* 387, 35–46. doi:10.1016/J.CHEMGEO.2014.08.002.

Nei, M., and Kumar, S. (2000). *Molecular evolution and phylogenetics*. Oxford University Press

Nelson, W., Tong, Y. L., Lee, J. K., and Halberg, F. (1979). Methods for cosinor-rhythmometry. *Chronobiologia* 6, 305–323.

Nikhil, K. L., and Sharma, V. K. (2017). "On the Origin and Implications of Circadian Timekeeping: An Evolutionary Perspective," in *Biological Timekeeping: Clocks, Rhythms and Behaviour* (Springer India), 81–129. doi:10.1007/978-81-322-3688-7.

Nudelman, F., Chen, H. H., Goldberg, H. A., Weiner, S., and Addadi, L. (2007). Lessons from biomineralization: comparing the growth strategies of mollusc shell prismatic and nacreous layers in *Atrina rigida*. *Faraday Discuss.* 136, 9–25. doi:10.1039/b704418f.

Okada, Y., Yamaura, K., Suzuki, T., Itoh, N., Osada, M., and Takahashi, K. G. (2013). Molecular characterization and expression analysis of chitinase from the Pacific oyster *Crassostrea gigas*. *Comp. Biochem. Physiol. B* 165, 83–89. doi:10.1016/j.cbpb.2013.03.008.

Okaniwa, N., Miyaji, T., Sasaki, T., and Tanabe, K. (2010). Shell growth and reproductive cycle of the Mediterranean mussel *Mytilus galloprovincialis* in Tokyo Bay, Japan: relationship with environmental conditions. *Plankt. Benthos Res.* 5, 214–220. doi:10.3800/pbr.5.214.

Ono, D., Honma, K. I., and Honma, S. (2015). Circadian and ultradian rhythms of clock gene expression in the suprachiasmatic nucleus of freely moving mice. *Sci. Rep.* 5, 12310. doi:10.1038/srep12310.

Ono, R., Koike, N., Inokawa, H., Tsuchiya, Y., Umemura, Y., Yamamoto, T., et al. (2019). Incremental Growth Lines in Mouse Molar Dentin Represent 8-hr Ultradian Rhythm. *Acta Histochem. Cytochem.* 52, 93–99. doi:10.1267/AHC.19017.

Orban, E., Di Lena, G., Nevigato, T., Casini, I., Marzetti, A., and Caproni, R. (2002). Seasonal changes in meat content, condition index and chemical composition of mussels (*Mytilus galloprovincialis*) cultured in two different Italian sites. *Food Chem.* 77, 57–65. doi:10.1016/S0308-8146(01)00322-3.

Otter, L. M., Agbaje, O. B. A., Kilburn, M. R., Lenz, C., Henry, H., Trimby, P., et al. (2019). Insights into architecture, growth dynamics, and biomineralization from pulsed Sr-labelled *Katelysia rhytiphora* shells (Mollusca, Bivalvia). *Biogeosciences* 16, 3439–3455. doi:10.5194/bg-16-3439-2019.

Ouyang, Y., Andersson, C. R., Kondo, T., Golden, S. S., and Johnson, C. H. (1998). Resonating circadian clocks enhance fitness in cyanobacteria. *Proc. Natl. Acad. Sci. U. S. A.* 95, 8660–8664. doi:10.1073/pnas.95.15.8660.

Owen, R., Richardson, C. A., and Kennedy, H. (2002). The influence of shell growth rate on striae deposition in the scallop *Pecten maximus*. *J. Mar. Biol. Assoc. United Kingdom* 82, 621–623. doi:10.1017/S0025315402005969.

Ozsolak, F., Platt, A. R., Jones, D. R., Reifenberger, J. G., Sass, L. E., McInerney, P., et al. (2009). Direct RNA sequencing. *Nature* 461, 814–818. doi:10.1038/NATURE08390.

Paillard, C., and Maes, P. (1995). The brown ring disease in the Malina clam *Ruditapes philippinarum*. *J. invertabrate Pathol.* 65, 91–100. doi:0022-2011/95.

Pairett, A. N., and Serb, J. M. (2013). De Novo Assembly and Characterization of Two Transcriptomes Reveal Multiple Light-Mediated Functions in the Scallop Eye (Bivalvia: Pectinidae). *PLoS One* 8, e69852. doi:10.1371/JOURNAL.PONE.0069852.

Palmer, J. D. (2000). The clocks controlling the tide-associated rhythms of intertidal animals. *BioEssays* 22, 32–37. doi:10.1002/(SICI)1521-1878(200001)22:1<32::AID-BIES7>3.0.CO;2-U.

Palmer, J. D., and Williams, B. G. (1986). Comparative studies of tidal rhythms. II. The dual clock control of the locomotor rhythms of two decapod crustaceans. *Mar. Behav. Physiol.* 12, 269–278. doi:10.1080/10236248609378653.

Pan, Y., Ballance, H., Meng, H., Gonzalez, N., Kim, S. M., Abdurehman, L., et al. (2020). 12-h clock regulation of genetic information flow by XBP1s.Plos Biology. 18(1), e3000580 doi:10.1371/journal.pbio.3000580.

Pannella, G., and MacClintock, C. (1968). Biological and Environmental Rhythms Reflected in Molluscan Shell Growth. *J. Paleontol.* 2, 64–80. doi:10.1017/S0022336000061655.

Paranjpe, D. A., and Sharma, V. K. (2005). Evolution of temporal order in living organisms. *J. Circadian Rhythms* 3, 7. doi:10.1186/1740-3391-3-7.

Partch, C. L., Green, C. B., and Takahashi, J. S. (2014). Molecular architecture of the mammalian circadian clock. *Trends Cell Biol.* 24, 90–99. doi:10.1016/J.TCB.2013.07.002.

Pavičić-Hamer, D., Baričević, A., Gerdol, M., and Hamer, B. (2015). *Mytilus galloprovincialis* carbonic anhydrase II: Activity and cDNA sequence analysis. *Key Eng. Mater.* 672, 137–150. doi:10.4028/www.scientific.net/KEM.672.137.

Payton, L., and Tran, D. (2019). Moonlight cycles synchronize oyster behavior. *Biol. Lett.* 15, doi:20180299. 10.1098/rsbl.2018.0299

Peharda, M., Black, B. A., Purroy, A., and Mihanović, H. (2016). The bivalve *Glycymeris pilosa* as a multidecadal environmental archive for the Adriatic and Mediterranean Seas. *Mar. Environ. Res.* 119, 79–87. doi:10.1016/J.MARENVRES.2016.05.022.

Peharda, M., Schöne, B. R., Black, B. A., and Corrège, T. (2021). Advances of sclerochronology research in the last decade. *Paleoceanogr. Paleoclimatology,Paleoecology* 570, 110371. doi:10.1016/j.palaeo.2021.110371.

Peharda, M., Župan, I., Bavčević, L., Frankić, A., and Klanjšček, T. (2007). Growth and condition index of mussel *Mytilus galloprovincialis* in experimental integrated aquaculture. *Aquac. Res.* 38, 1714–1720. doi:10.1111/j.1365-2109.2007.01840.x.

Pérez-Ruzafa, A., Pérez-Ruzafa, I. M., Newton, A., and Marcos, C. (2019). "Chapter 15: Coastal Lagoons: Environmental Variability, Ecosystem Complexity, and Goods and Services Uniformity," in *Coasts and Estuaries: The Future*, eds. E. Wolanski, J. W. Day, M. Elliot, and R. Ramachandran (Elsevier), 253–276. doi:10.1016/B978-0-12-814003-1.00015-0.

Perrigault, M., Andrade, H., Bellec, L., Ballantine, C., Camus, L., and Tran, D. (2020). Rhythms during the polar night: evidence of clock-gene oscillations in the Arctic scallop *Chlamys islandica*. *Proceedings. Biol. Sci.* 287, 20201001. doi:10.1098/rspb.2020.1001.

Perrigault, M., and Tran, D. (2017). Identification of the Molecular Clockwork of the Oyster *Crassostrea gigas*. *PLoS One* 12, e0169790. doi:10.1371/journal.pone.0169790.

Peterson, C. H. (1985). Patterns of Lagoonal Bivalve Mortality After Heavy Sedimentation and Their Paleoecological Significance. *Paleobiology* 11, 139–153.

Poitevin, P., Chauvaud, L., Pécheyran, C., Lazure, P., Jolivet, A., and Thébault, J. (2020). Does trace element composition of bivalve shells record ultra-high frequency environmental variations? *Mar. Environ. Res.* 158, 104943. doi:10.1016/j.marenvres.2020.104943.

Posa, D., and Tursi, A. (1991). Growth Models of *Mytilus galloprovincialis* Lamarck on the mar grande and on the mar Piccolo of Taranto (Southern Italy). *Stat. Appl* 3, 135–143.

Poulain, C., Gillikin, D. P., Thébault, J., Munaron, J. M., Bohn, M., Robert, R., et al. (2015). An evaluation of Mg/Ca, Sr/Ca, and Ba/Ca ratios as environmental proxies in aragonite bivalve shells. *Chem. Geol.* 396, 42–50. doi:10.1016/J.CHEMGEO.2014.12.019.

Poulain, C., Lorrain, A., Amice, E., Morize, E., and Paulet, Y. (2011). An environmentally induced tidal periodicity of microgrowth increment formation in subtidal populations of the clam *Ruditapes philippinarum*. *J. Exp. Mar. Bio. Ecol.* 397, 58–64. doi:10.1016/j.jembe.2010.11.001.

Price, J. L., Blau, J., Rothenfluh, A., Abodeely, M., Kloss, B., and Young, M. W. (1998). *double-time* is a Novel *Drosophila* Clock Gene that Regulates PERIOD Protein Accumulation. *Cell* 94, 83–95. doi:10.1016/S0092-8674(00)81224-6.

Prieto, D., Markaide, P., Urrutxurtu, I., Navarro, E., Artigaud, S., Fleury, E., et al. (2019). Gill transcriptomic analysis in fast- and slow-growing individuals of *Mytilus galloprovincialis*. *Aquaculture* 511, 734242. doi:10.1016/j.aquaculture.2019.734242.

Prieto, D., Urrutxurtu, I., Navarro, E., Urrutia, M. B., and Ibarrola, I. (2018). *Mytilus galloprovincialis* fast growing phenotypes under different restrictive feeding conditions: Fast feeders and energy savers. *Mar. Environ. Res.* 140, 114–125. doi:10.1016/J.MARENVRES.2018.05.007.

Pulteney, R. (1781). *A General View of the Writing of Linnaeus.* London: Payne and White.

Purroy, A., Milano, S., Schöne, B. R., Thébault, J., and Peharda, M. (2018). Drivers of shell growth of the bivalve, *Callista chione* (L. 1758) – Combined environmental and biological factors. *Mar. Environ. Res.* 134, 138–149. doi:10.1016/J.MARENVRES.2018.01.011.

R Core Team (2020). R: A Language and Environment for Statistical Computing. Available at: https://www.r-project.org/.

Ramírez, S. C., and Cáceres-Martínez, J. (1999). Settlement of the blue mussel *Mytilus galloprovincialis* Lamarck on artificial substrates in bahía de Todos Santos, B.C., México. *J. Shellfish Res.* 18, 33–39.

Ramón, M., Fernández, M., and Galimany, E. (2007). Development of mussel (*Mytilus galloprovincialis*) seed from two different origins in a semi-enclosed Mediterranean Bay (N.E. Spain). *Aquaculture* 264, 148–159. doi:10.1016/J.AQUACULTURE.2006.11.014.

Rasband, W. S. (2020). ImageJ. Available at: https://imagej.nih.gov/ij/.

Réaumur, R.-A. . (1709). De la formation et de l'accroissement des coquilles des animaux tant terrestres qu'aquatiques, soit de mer, soit de rivière. *Hist. Acad. roy, Sci. Mem. Paris*, 364–400.

Reddy, P., Zehring, W. A., Wheeler, D. A., Pirrotta, V., Hadfield, C., Hall, J. C., et al. (1984). Molecular Analysis of the period Locus in *Drosophila melanogaster* and Identification of a Transcript Involved in Biological Rhythms. *Cell* 38, 701-710

Reis, P. P., Waldron, L., Goswami, R. S., Xu, W., Xuan, Y., Perez-Ordonez, B., et al. (2011). mRNA transcript quantification in archival samples using multiplexed, color-coded probes. *BMC Biotechnol.* 11, 46. doi:10.1186/1472-6750-11-46/FIGURES/4.

Rensing, L., and Ruoff, P. (2002). Temperature effect on entrainment, phase shifting, and amplitude of circadian clocks and its molecular bases. *Chronobiol. Int.* 19, 807–864. doi:10.1081/CBI-

120014569.

Richardson, C. A. (1987a). Microgrowth patterns in the shell of the Malaysian cockle *Anadara granosa* (L.) and their use in age determination. *J. Exp. Mar. Bio. Ecol.* 111, 77–98. doi:10.1016/0022-0981(87)90021-9.

Richardson, C. A. (1987b). Tidal bands in the shell of the clam *Tapes philippinarum* (Adams & Reeve, 1850). *Proc. R. Soc. Lond. B.* 230, 367–387. doi:https://doi.org/10.1098/rspb.1987.0025.

Richardson, C. A. (1988). Exogenous and endogenous rhythms of band formation in the shell of the clam *Tapes philippinarum* (Adams et Reeve, 1850). *J. Exp. Mar. Bio. Ecol.* 122, 105–126. doi:10.1016/0022-0981(88)90179-7.

Richardson, C. A. (1989). An analysis of the microgrowth bands in the shell of the common mussel *Mytilus edulis*. *J. Mar. Biol. Assoc. United Kingdom* 69, 477–491. doi:10.1017/S0025315400029544.

Richardson, C. A., Crisp, D. J., and Runham, N. W. (1979). Tidally deposited growth bands in the shell of the common cockle, *Cerastoderma edule*. *Malacologia* 18, 277–290.

Richardson, C. A., Crisp, D. J., and Runham, N. W. (1980). An endogenous rhythm in shell deposition in *Cerastoderma edule*. *J. Mar. Biol. Assoc. United Kingdom* 60, 991–1004. doi:10.1017/S0025315400042041.

Richardson, C. A., Peharda, M., Kennedy, H., Kennedy, P., and Onofri, V. (2004). Age, growth rate and season of recruitment of *Pinna nobilis* (L) in the Croatian Adriatic determined from Mg:Ca and Sr:Ca shell profiles. *J. Exp. Mar. Bio. Ecol.* 299, 1–16. doi:10.1016/J.JEMBE.2003.08.012.

Richardson, C. A., Runham, N. W., and Crisp, D. J. (1981). A histological and ultrastructural study of the cells of the mantle edge of a marine bivalve, *Cerastoderma edule*. *Tissue Cell* 13, 715–730. doi:10.1016/S0040-8166(81)80008-0.

Richardson, C. A., Seed, R., and Naylor, E. (1990). Use of internal growth bands for measuring individual and population growth rates in *Mytilus edulis* from offshore production platforms. *Mar Ecol Prog Ser* 66, 259–265. doi:10.3354/meps066259.

Robles, M. S., Cox, J., and Mann, M. (2014). In-Vivo Quantitative Proteomics Reveals a Key Contribution of Post-Transcriptional Mechanisms to the Circadian Regulation of Liver Metabolism. *PLOS Genet.* 10, e1004047. doi:10.1371/JOURNAL.PGEN.1004047.

Rodellas, V., Cook, P. G., McCallum, J., Andrisoa, A., Meulé, S., and Stieglitz, T. C. (2020). Temporal variations in porewater fluxes to a coastal lagoon driven by wind waves and changes in lagoon water depths. *J. Hydrol.* 581, 124363. doi:10.1016/J.JHYDROL.2019.124363.

Rodellas, V., Stieglitz, T. C., Andrisoa, A., Cook, P. G., Raimbault, P., Tamborski, J. J., et al. (2018). Groundwater-driven nutrient inputs to coastal lagoons: The relevance of lagoon water recirculation as a conveyor of dissolved nutrients. *Sci. Total Environ.* 642, 764–780. doi:10.1016/J.SCITOTENV.2018.06.095.

Rodland, D. L., Schöne, B. R., Baier, S., Zhang, Z., Dreyer, W., and Page, N. A. (2009). Changes in gape frequency, siphon activity and thermal response in the freshwater bivalves *Anodonta cygnea* and *Margaritifera falcata*. *J. Molluscan Stud.* 75, 51–57. doi:10.1093/mollus/eyn038.

Rodland, D. L., Schöne, B. R., Helama, S., Nielsen, J. K., and Baier, S. (2006). A clockwork mollusc : Ultradian rhythms in bivalve activity revealed by digital photography. *J. Exp. Biol. Ecol.* 334, 316–323. doi:10.1016/j.jembe.2006.02.012.

Rodríguez-Tovar, F. J. (2014). Orbital climate cycles in the fossil record: From semidiurnal to million-

year biotic responses. *Annu. Rev. Earth Planet. Sci.* 42, 69–102. doi:10.1146/annurev-earth-120412-145922.

Rosbash, M. (2009). The implications of multiple circadian clock origins. *PLoS Biol.* 7, e1000062. doi:10.1371/journal.pbio.1000062.

Rotics, S., Dayan, T., and Kronfeld-Schor, N. (2011). Effect of artificial night lighting on temporally partitioned spiny mice. *J. Mammal.* 92, 159–168. doi:10.1644/10-MAMM-A-112.1.

Rotics, S., Dayan, T., Levy, O., and Kronfeld-Schor, N. (2010). Light Masking in the Field: An Experiment with Nocturnal and Diurnal Spiny Mice Under Semi-natural Field Conditions. *Chronobiol. Int.* 28, 70–75. doi:10.3109/07420528.2010.525674.

Rubin, E. B., Shemesh, Y., Cohen, M., Elgavish, S., Robertson, H. M., and Bloch, G. (2006). Molecular and phylogenetic analyses reveal mammalian-like clockwork in the honey bee (*Apis mellifera*) and shed new light on the molecular evolution of the circadian clock. *Genome Res.* 16, 1352–1365. doi:10.1101/gr.5094806.

Ruf, T. (2022). lomb: Lomb-Scargle Periodogram. Available at: https://cran.r-project.org/package=lomb.

Rui, X., Qi, L., and Hong, Y. (2020). Expression pattern of Piwi-like gene implies the potential role in germline development in the Pacific oyster *Crassostrea gigas*. *Aquac. Reports* 18, 100486. doi:10.1016/J.AQREP.2020.100486.

Sachs, M. (2014). cosinor: Tools for estimating and predicting the cosinor model.

Salas, C., Bueno-Pérez, J. de D., López-Téllez, J. F., and Checa, A. G. (2022). Form and function of the mantle edge in Protobranchia (Mollusca: Bivalvia). *Zoology* 153, 126027. doi:10.1016/J.ZOOL.2022.126027.

Sarà, G., Kearney, M., and Helmuth, B. (2011). Combining heat-transfer and energy budget models to predict thermal stress in Mediterranean intertidal mussels. *Chem. Ecol.* 27, 135–145. doi:10.1080/02757540.2011.552227.

Scheirer, D. S., Shank, T. M., and Fornari, D. J. (2006). Temperature variations at diffuse and focused flow hydrothermal vent sites along the northern East Pacific Rise. *Geochemistry, Geophys. Geosystems* 7, Q03002. doi:10.1029/2005GC001094.

Schmid, B., Helfrich-Förster, C., and Yoshii, T. (2011). A new ImageJ plugin "ActogramJ" for chronobiological analyses. *J. Biol. Rhythms* 26, 464–467.

Schnytzer, Y., Simon-Blecher, N., Li, J., Ben-Asher, H. W., Salmon-Divon, M., Achituv, Y., et al. (2018). Tidal and diel orchestration of behaviour and gene expression in an intertidal mollusc. *Sci. Rep.* 8, 1–13. doi:10.1038/s41598-018-23167-y.

Schöne, B. R. (2008). The curse of physiology — challenges and opportunities in the interpretation of geochemical data from mollusk shells. *Geo-Marine Lett.* 28, 269–285. doi:10.1007/s00367-008-0114-6.

Schöne, B. R. (2013). *Arctica islandica* (Bivalvia): A unique paleoenvironmental archive of the northern North Atlantic Ocean. *Glob. Planet. Change* 111, 199–225. doi:10.1016/j.gloplacha.2013.09.013.

Schöne, B. R., Dunca, E., Fiebig, J., and Pfeiffer, M. (2005a). Mutvei ' s solution : An ideal agent for resolving microgrowth structures of biogenic carbonates. *Palaeogeogr. Palaeoclimatol. Palaeoecol.* 228, 149–166. doi:10.1016/j.palaeo.2005.03.054.

Schöne, B. R., and Giere, O. (2005). Growth increments and stable isotope variation in shells of the

deep-sea hydrothermal vent bivalve mollusk *Bathymodiolus brevior* from the North Fiji Basin, Pacific Ocean. *Deep. Res. Part I Oceanogr. Res. Pap.* 52, 1896–1910. doi:10.1016/j.dsr.2005.06.003.

Schöne, B. R., and Krause, R. A. (2016). Retrospective environmental biomonitoring – Mussel Watch expanded. *Glob. Planet. Change* 144, 228–251. doi:10.1016/j.gloplacha.2016.08.002.

Schöne, B. R., Lega, J., Flessa, K. W., Goodwin, D. H., and Dettman, D. L. (2002). Reconstructing daily temperatures from growth rates of the intertidal bivalve mollusk *Chione cortezi* (northern Gulf of California, Mexico). *Palaeogeogr. Palaeoclimatol. Palaeoecol.* 184, 131–146. doi:10.1016/S0031-0182(02)00252-3.

Schöne, B. R., Oschmann, W., Rössler, J., Freyre Castro, A. D., Houk, S. D., Kröncke, I., et al. (2003a). North Atlantic Oscillation dynamics recorded in shells of a long-lived bivalve mollusk. *Geology* 31, 1037–1040. doi:10.1130/G20013.1.

Schöne, B. R., Page, N. A., Rodland, D. L., Fiebig, J., Baier, S., Helama, S. O., et al. (2007). ENSO-coupled precipitation records (1959-2004) based on shells of freshwater bivalve mollusks (*Margaritifera falcata*) from British Columbia. *Int. J. Earth Sci.* 96, 525–540. doi:10.1007/s00531-006-0109-3.

Schöne, B. R., Pfeiffer, M., Pohlmann, T., and Siegismund, F. (2005b). A seasonally resolved bottom-water temperature record for the period AD 1866-2002 based on shells of *Arctica islandica* (Mollusca, North Sea). *Int. J. Climatol.* 25, 947–962. doi:10.1002/joc.1174.

Schöne, B. R., Tanabe, K., Dettman, D., and Sato, S. (2003b). Environmental controls on shell growth rates and d 18 O of the shallow-marine bivalve mollusk *Phacosoma japonicum* in Japan. *Mar. Biol.* 142, 473–485. doi:10.1007/s00227-002-0970-y.

Schwartzmann, C., Durrieu, G., Sow, M., Ciret, P., Lazareth, C. E., and Massabuaua, J. C. (2011). In situ giant clam growth rate behavior in relation to temperature: A one-year coupled study of high-frequency noninvasive valvometry and sclerochronology. *Limnol. Oceanogr.* 56, 1940–1951. doi:10.4319/lo.2011.56.5.1940.

Seed, R. (1976). “Ecology,” in *Marine Mussels: their Ecology and Physiology*, ed. B. L. Bayne (Cambridge: Cambridge University Press), 11–65.

Seed, R., and Suchanek, T. H. (1992). “Population and community ecology of Mytilus,” in *The mussel Mytilus: Ecology, physiology, genetics and culture*, ed. E. Gosling, 87–169.

Senthilan, P. R., Grebler, R., Reinhard, N., Rieger, D., and Helfrich-Förster, C. (2019). Role of Rhodopsins as Circadian Photoreceptors in the *Drosophila melanogaster*. *Biology (Basel).* 8, 6. doi:10.3390/BIOLOGY8010006.

Shah, A. S. (2020). card: Cardiovascular and Autonomic Research Design. Available at: https://cran.r-project.org/package=card.

SHOM (2020). Horaires de marées gratuits du SHOM. Available at: https://maree.shom.fr/harbor/BANYULS/hlt/0?date=2020-06-24&utc=standard [Accessed September 13, 2020].

Skinner, H. C. ., and Jahren, A. H. (2003). “Biomineralization,” in *Trearise on Geochemistry* (Elsevier Ltd.), 117–184. doi:10.1016/B0-08-043751-6/08128-7.

Sleight, V. A., Antczak, P., Falciani, F., Clark, M. S., and Cowen, L. (2020). Computationally predicted gene regulatory networks in molluscan biomineralization identify extracellular matrix production and ion transportation pathways. *Bioinformatics* 36, 1326–1332. doi:10.1093/bioinformatics/btz754.

Smaal, A. C., Ferreira, J. G., Grant, J., Petersen, J. K., and Strand, Ø. (2018). *Goods and services of marine bivalves*. doi:10.1007/978-3-319-96776-9.

Smaal, A. C., and Strand, Ø. (2018). "Chapter 16 Introduction to cultural services," in *Goods and Services of Marine Bivalves*, 315–316.

Song, X., Liu, Z., Wang, L., and Song, L. (2019). Recent advances of shell matrix proteins and cellular orchestration in marine molluscan shell biomineralization. *Front. Mar. Sci.* 6, 41. doi:10.3389/fmars.2019.00041.

Souchu, P., Bee, B., Smith, V. H., Laugier, T., Fiandrino, A., Benau, L., et al. (2010). Patterns in nutrient limitation and chlorophyll a along an anthropogenic eutrophication gradient in French Mediterranean coastal lagoons. *Can. J. Fish. Aquat. Sci.* 67, 743–753. doi:10.1139/F10-018/ASSET/IMAGES/F10-018E10H.GIF.

Steinhardt, J., Butler, P. G., Carroll, M. L., and Hartley, J. (2016). The application of long-lived bivalve sclerochronology in environmental baseline monitoring. *Front. Mar. Sci.* 3, 176. doi:10.3389/fmars.2016.00176.

Stemmer, K., Brey, T., and Gutbrod, M. S. (2019). In situ Measurements of pH, CA2+, and Dic Dynamics within the Extrapallial Fluid of the Ocean Quahog *Arctica islandica*. *J. Shellfish Res.* 38, 71–78. doi:10.2983/035.038.0107.

Stephan, F. K. (2002). The "Other" Circadian System: Food as a Zeitgeber. *J. Biol. Rhythms* 17, 284–292. doi:10.1177/074873040201700402.

Strickland, J. D., and Parsons, T. R. (1997). *A practical handbook of seawater analysis, 2nd ed.* Bull. Fish. Res. Bd. Can.

Sun, J., Xu, G., Wang, Z., Li, Q., Cui, Y., Xie, L., et al. (2015). The effect of NF-κB signalling pathway on expression and regulation of nacrein in Pearl Oyster, *Pinctada fucata*. *PLoS One* 10, e0131711. doi:10.1371/journal.pone.0131711.

Sun, X. J., Zhou, L. Q., Tian, J. T., Liu, Z. H., Wu, B., Dong, Y. H., et al. (2016). Transcriptome survey of phototransduction and clock genes in marine bivalves. *Genet. Mol. Res.* 15, gmr15048726. doi:10.4238/gmr15048726.

Tamayo, D., Ibarrola, I., Cigarría, J., and Navarro, E. (2015). The effect of food conditioning on feeding and growth responses to variable rations in fast and slow growing spat of the Manila clam (*Ruditapes philippinarum*). *J. Exp. Mar. Bio. Ecol.* 471, 92–103. doi:10.1016/j.jembe.2015.05.017.

Tamayo, D., Ibarrola, I., Urrutia, M. B., and Navarro, E. (2011). The physiological basis for inter-individual growth variability in the spat of clams (*Ruditapes philippinarum*). *Aquaculture* 321, 113–120. doi:10.1016/J.AQUACULTURE.2011.08.024.

Tan, Y., Merrow, M., and Roenneberg, T. (2004). Photoperiodism in *Neurospora Crassa*. *J. Biol. Rhythms* 19, 135–143. doi:10.1177/0748730404263015.

Tanaka, K., Okaniwa, N., Miyaji, T., Murakami-Sugihara, N., Zhao, L., Tanabe, K., et al. (2019). Microscale magnesium distribution in shell of the Mediterranean mussel *Mytilus galloprovincialis*: An example of multiple factors controlling Mg/Ca in biogenic calcite. *Chem. Geol.* 511, 521–532. doi:10.1016/j.chemgeo.2018.10.025.

Thaben, P. F., and Westermark, P. O. (2014). Detecting rhythms in time series with rain. *J. Biol. Rhythms* 29, 391–400. doi:10.1177/0748730414553029.

Thébault, J., Chauvaud, L., Clavier, J., Fichez, R., and Morize, E. (2006). Evidence of a 2-day periodicity of striae formation in the tropical scallop *Comptopallium radula* using calcein marking. *Mar. Biol.*

149, 257–267. doi:10.1007/s00227-005-0198-8.

Thébault, J., Jolivet, A., Waeles, M., Tabouret, H., Sabarot, S., Pécheyran, C., et al. (2022). Scallop shells as geochemical archives of phytoplankton-related ecological processes in a temperate coastal ecosystem. *Limnol. Oceanogr.* 67, 187–202. doi:10.1002/LNO.11985.

Thyssen, M., Grégori, G. J., Grisoni, J. M., Pedrotti, M. L., Mousseau, L., Artigas, L. F., et al. (2014). Onset of the spring bloom in the northwestern Mediterranean Sea: Influence of environmental pulse events on the in situ hourly-scale dynamics of the phytoplankton community structure. *Front. Microbiol.* 5, 387. doi:10.3389/FMICB.2014.00387.

Tong, H., Hu, J., Ma, W., Zhong, G., Yao, S., and Cao, N. (2002). In situ analysis of the organic framework in the prismatic layer of mollusc shell. *Biomaterials* 23, 2593–2598. doi:10.1016/S0142-9612(01)00397-0.

Toyohara, H., Hosoi, M., Hayashi, I., Kubota, S., Hashimoto, H., and Yokoyama, Y. (2005). Expression of HSP70 in response to heat-shock and its cDNA cloning from Mediterranean blue mussel. *Fish. Sci. 2005 712* 71, 327–332. doi:10.1111/J.1444-2906.2005.00968.X.

Tran, D., Andrade, H., Durier, G., Ciret, P., Leopold, P., Sow, M., et al. (2020a). Growth and behaviour of blue mussels, a re-emerging polar resident, follow a strong annual rhythm shaped by the extreme high Arctic light regime: Mussels' growth and behavior in Arctic. *R. Soc. Open Sci.* 7, 200889. doi:10.1098/rsos.200889.

Tran, D., Ciret, P., Ciutat, A., Durrieu, G., and Massabuau, J.-C. (2003). Estimation of potential and limits of bivalve closure response to detect contaminants: Application to cadmium. *Environ. Toxicol. Chem.* 22, 914–920. doi:10.1002/etc.5620220432.

Tran, D., Nadau, A., Durrieu, G., Ciret, P., Parisot, J. P., and Massabuau, J. C. (2011). Field chronobiology of a molluscan bivalve: How the moon and sun cycles interact to drive oyster activity rhythms. *Chronobiol. Int.* 28, 307–317. doi:10.3109/07420528.2011.565897.

Tran, D., Perrigault, M., Ciret, P., and Payton, L. (2020b). Bivalve mollusc circadian clock genes can run at tidal frequency. *Proc. R. Soc. B* 287, 20192440. doi:http://dx.doi.org/10.1098/rspb.2019.2440.

Tran, D., Sow, M., Camus, L., Ciret, P., Berge, J., and Massabuau, J. C. (2016). In the darkness of the polar night, scallops keep on a steady rhythm. *Sci. Rep.* 6, 32435. doi:10.1038/srep32435.

Treccani, L., Mann, K., Heinemann, F., and Fritz, M. (2006). Perlwapin, an Abalone Nacre Protein with Three Four-Disulfide Core (Whey Acidic Protein) Domains, Inhibits the Growth of Calcium Carbonate Crystals. *Biophys. J.* 91, 2601–2608. doi:10.1529/BIOPHYSJ.106.086108.

Trofimova, T., Alexandroff, S. J., Mette, M. J., Tray, E., Butler, P. G., Campana, S. E., et al. (2020). Fundamental questions and applications of sclerochronology: Community-defined research priorities. *Estuar. Coast. Shelf Sci.* 245, 106977. doi:10.1016/j.ecss.2020.106977.

Trusevich, V. V, Kuz, K. A., Mishurov, V. Z., Zhuravsky, V. Y., and Vyshkvarkova, E. V (2021). Features of Behavioral Responses of the Mediterranean Mussel in Its Natural Habitat of the Black Sea. *Inl. Water Biol.* 14, 10–19. doi:10.1134/S1995082921010132.

Van Der Veen, D. R., Riede, S. J., Heideman, P. D., Hau, M., Van Der Vinne, V., and Hut, R. A. (2017). Flexible clock systems: Adjusting the temporal programme. *Philos. Trans. R. Soc. B Biol. Sci.* 372, 20160254. doi:10.1098/rstb.2016.0254.

Veldman-Jones, M. H., Brant, R., Rooney, C., Geh, C., Emery, H., Harbron, C. G., et al. (2015). Evaluating robustness and sensitivity of the nanostring technologies ncounter platform to enable multiplexed gene expression analysis of clinical samples. *Cancer Res.* 75, 2587–2593.

doi:10.1158/0008-5472.CAN-15-0262.

Venier, P., De Pittà, C., Bernante, F., Varotto, L., De Nardi, B., Bovo, G., et al. (2009). MytiBase: a knowledgebase of mussel (*M. galloprovincialis*) transcribed sequences. *BMC Genomics* 10, 72. doi:10.1186/1471-2164-10-72.

Verrecchia, E. P. (2005). "Multiresolution analysis of shell growth increments to detect variations in natural cycles," in *Image Analysis, Sediments and Paleoenvironments* (Dordrecht: Springer), 273–293. doi:10.1007/1-4020-2122-4_14.

Vitellaro-Zuccarello, L., De Biasi, S., Bernardi, P., and Oggioní, A. (1991). Distribution of serotonin-, gamma-aminobutyric acid- and substance P-like immunoreactivity in the central and peripheral nervous system of *Mytilus galloprovincialis*. *Tissue Cell* 23, 261–270. doi:10.1016/0040-8166(91)90080-D.

von Bertalanffy, L. (1938). A quantitative theory of organic growth. *Hum. Biol.* 10, 181–213.

von Hessling, T. (1859). *Die Perlmuscheln und ihre Perlen naturwissenschaftlich und geschichtlich; mit Berücksichtigung der Perlengewässer Bayerns*. Leipzig: Engelmann.

Vriend, J., and Reiter, R. J. (2014). Melatonin as a proteasome inhibitor. Is there any clinical evidence? *Life Sci.* 115, 8–14. doi:10.1016/J.LFS.2014.08.024.

Vriesman, V. P., Carlson, S., and Hill, T. (2022). Investigating controls of shell growth features in a foundation bivalve species: seasonal trends and decadal changes in the California mussel. *Biogeosciences Discuss.* 19, 329–346. doi:10.5194/bg-2021-219.

Walford, L. A. (1946). A new graphic method of describing the growth of animals. *Biol. Bull.* 90, 141–147. doi:10.2307/1538217.

Wang, X., Wang, M., Jia, Z., Song, X., Wang, L., and Song, L. (2017). A shell-formation related carbonic anhydrase in *Crassostrea gigas* modulates intracellular calcium against CO2 exposure: Implication for impacts of ocean acidification on mollusk calcification. *Aquat. Toxicol.* 189, 216–228. doi:10.1016/J.AQUATOX.2017.06.009.

Warman, C. G., and Naylor, E. (1995). Evidence for multiple, cue-specific circatidal clocks in the shore crab *Carcinus maenas*. *J. Exp. Mar. Bio. Ecol.* 189, 93–101. doi:10.1016/0022-0981(95)00014-I.

Warnes, G. R., Bolker, B., Bonebakker, L., Gentleman , Robert Huber, W., Liaw, A., Lumley, T., et al. (2020). gplots: Various R Programming Tools for Plotting Data. Available at: https://cran.r-project.org/web/packages=gplots/.

Warter, V., Erez, J., and Müller, W. (2018). Environmental and physiological controls on daily trace element incorporation in *Tridacna crocea* from combined laboratory culturing and ultra-high resolution LA-ICP-MS analysis. *Palaeogeogr. Palaeoclimatol. Palaeoecol.* 496, 32–47. doi:10.1016/j.palaeo.2017.12.038.

Warter, V., and Müller, W. (2017). Daily growth and tidal rhythms in Miocene and modern giant clams revealed via ultra-high resolution LA-ICPMS analysis — A novel methodological approach towards improved sclerochemistry. *Palaeogeogr. Palaeoclimatol. Palaeoecol.* 465, 362–375. doi:10.1016/J.PALAEO.2016.03.019.

Weiner, S., and Dove, P. M. (2003). "An overview of biomineralization processes and the problem of the vital effect," in *Biomineralization*, eds. P. M. Dove, J. J. De Yoreo, and S. Weiner (Washington: The mineralogical society of America), 1–24.

Welsh, D. K., Takahashi, J. S., and Kay, S. A. (2010). Suprachiasmatic Nucleus: Cell Autonomy and Network Properties. *Annu. Rev. Physiol.* 72, 551. doi:10.1146/ANNUREV-PHYSIOL-021909-

135919.

Wijsman, J. W. M., Troost, K., Fang, J., and Roncarati, A. (2018). “Chapter 2: Global production of marine bivalves. Trends and challenges,” in *Goods and Services of Marine Bivalves*, 7–26.

Wilbur, K. M., and Saleuddin, A. S. M. (1983). “Shell Formation,” in *The Mollusca: Physiology Part. 1* (New York: Academic Press Inc.), 235–287. doi:10.1016/b978-0-12-751404-8.50014-1.

Wilkins, N. P., Fujino, K., and Gosling, E. M. (1983). The mediterranean mussel *Mytilus galloprovincialis* Lmk. in Japan. *Biol. J. Linn. Soc.* 20, 365–374. doi:10.1111/j.1095-8312.1983.tb01597.x.

Williams, B. G., and Pilditch, C. A. (1997). The entrainment of persistent tidal rhythmicity in a filter-feeding bivalve using cycles of food availability. *J. Biol. Rhythms* 12, 173–81. doi:10.1177/074873049701200208.

Yamaguchi, K., Seto, K., Takayasu, K., and Aizaki, M. (2006). Shell Layers and Structures in the Brackish Water Bivalve, *Corbicula japonica*. *Quat. Res.* 45, 317–331. doi:10.4116/jaqua.45.317.

Yan, H., Liu, C., An, Z., Yang, W., Yang, Y., Huang, P., et al. (2020). Extreme weather events recorded by daily to hourly resolution biogeochemical proxies of marine giant clam shells. *Proc. Natl. Acad. Sci. U. S. A.* 117, 7038–7043. doi:10.1073/pnas.1916784117.

Yang, M., Derbyshire, M. K., Yamashita, R. A., and Marchler-Bauer, A. (2020). NCBI’s Conserved Domain Database and Tools for Protein Domain Analysis. *Curr. Protoc. Bioinforma.* 69, e90. doi:10.1002/CPBI.90.

Ysebaert, T., Walles, B., Haner, J., and Hancock, H. (2018). “Chapter 13 Habitat modification and coastal protection by ecosystem-engineering reef-building bivalves,” in *Goods and Services of Marine Bivalves*, 253–273.

Zeng, H., Hardin, P. E., and Rosbash, M. (1994). Constitutive overexpression of the *Drosophila* period protein inhibits period mRNA cycling. *EMBO J.* 13, 3590–3598. doi:10.1002/J.1460-2075.1994.TB06666.X.

Zhang, L., Hastings, M. H., Green, E. W., Tauber, E., Sladek, M., Webster, S. G., et al. (2013). Dissociation of Circadian and Circatidal Timekeeping in the Marine Crustacean *Eurydice pulchra*. *Curr. Biol.* 23, 1863–1873. doi:10.1016/J.CUB.2013.08.038.

Zhang, N., and Chen, Y. (2012). Molecular origin of the sawtooth behavior and the toughness of nacre. *Mater. Sci. Eng. C* 32, 1542–1547. doi:10.1016/j.msec.2012.04.040.

Zhao, L., Shirai, K., Murakami-Sugihara, N., Higuchi, T., and Tanaka, K. (2019). Mussel periostracum as a high-resolution archive of soft tissue δ13C records in coastal ecosystems. *Geochim. Cosmochim. Acta*. 260, 232-243. doi:10.1016/j.gca.2019.06.038.

Zhao, L., Shirai, K., Tanaka, K., Milano, S., Higuchi, T., Murakami-Sugihara, N., et al. (2020). A review of transgenerational effects of ocean acidification on marine bivalves and their implications for sclerochronology. *Estuar. Coast. Shelf Sci.* 235, 106620. doi:10.1016/j.ecss.2020.106620.

Zhao, M., He, M., Huang, X., and Wang, Q. (2014). A homeodomain transcription factor gene, PfMSX, activates expression of Pif gene in the pearl oyster *Pinctada fucata*. *PLoS One* 9, e103830. doi:10.1371/journal.pone.0103830.

Zhao, M., Shi, Y., He, M., Huang, X., and Wang, Q. (2016). PfSMAD4 plays a role in biomineralization and can transduce bone morphogenetic protein-2 signals in the pearl oyster *Pinctada fucata*. *BMC Dev. Biol.* 16, 9. doi:10.1186/s12861-016-0110-4.

Zheng, X., Cheng, M., Xiang, L., Liang, J., Xie, L., and Zhang, R. (2015). The AP-1 transcription factor

homolog Pf-AP-1 activates transcription of multiple biomineral proteins and potentially participates in *Pinctada fucata* biomineralization. *Sci. Rep.* 5, 14408. doi:10.1038/srep14408.

Zhu, B., Dacso, C. C., and O'Malley, B. W. (2018). Unveiling "Musica Universalis" of the Cell: A Brief History of Biological 12-Hour Rhythms. *J. Endocr. Soc.* 2, 727–752. doi:10.1210/js.2018-00113.

Zhu, Y., Yu, Z., Liao, K., Zhang, L., Ran, Z., and Xu, J. (2022). Melatonin in razor clam Sinonovacula constricta : Examination of metabolic pathways, tissue distribution, and daily rhythms. *Aquaculture* 560, 738548. doi:10.1016/j.aquaculture.2022.738548.

Zordan, M. A., and Sandrelli, F. (2015). Circadian clock dysfunction and psychiatric disease: Could fruit flies have a say? *Front. Neurol.* 6, 80. doi:10.3389/fneur.2015.00080.

Zuykov, M., and Schindler, M. (2019). Sclerochronology-based geochemical studies of bivalve shells: Potential vs reality. *Est. J. Earth Sci.* 68, 37–44. doi:10.3176/earth.2019.05.

Annexes

Annex 1: Profilometry and microtomography of *Mytilus galloprovincialis* shells – ARCHIVE project

1. Profilometry

Élise Rigot[a,b], Denis Tribouillois[a], Christophe Vieu[a,b], Victoria Louis[c,d], Franck Lartaud[d], Laurent Malaquin[a]

[a] LAAS-CNRS, Université de Toulouse, CNRS, F-31400, Toulouse, France

[b] Université de Toulouse, Institut National des Sciences Appliquées - INSA, F-31400, Toulouse, France

[c] Sorbonne Université, CNRS, Biologie Intégrative des Organismes Marins, BIOM, F-66650, Banyuls-sur-Mer, France

[d] Sorbonne Université, CNRS, Laboratoire d'Ecogéochimie des Environnements Benthiques, LECOB, F-66650, Banyuls-sur-Mer, France

Mussels were sampled in the bay of Banyuls-sur-Mer and in Salses-Leucate laguna. Shells were washed using a soft brush and soft tissues were removed. Images were taken using the HIROX HRX-01 3D digital microscope (Tokyo, Japan) (Figures A1.1, A1.2). Longitudinal transect showed an increase of the shell length by steps in both environments. Also, often a big step is followed by a small one (Figures A1.1D, A1.2D). A longitudinal section will be achieved on the two shells imaged to describe shell growth patterns using Mutvei etching and reflected light. Then external pattern observed will be confronted to patterns observed on section to assess the reliability of this technic.

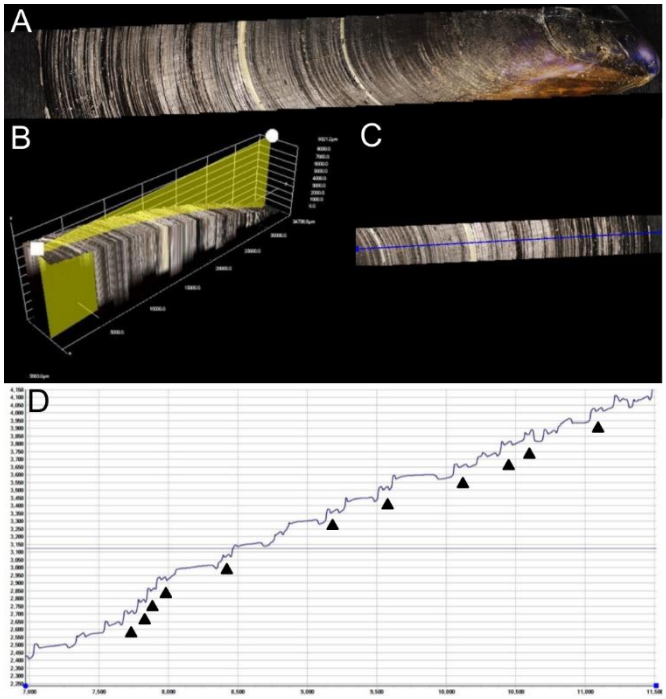

Figure A1.1: 3D profilometry of mussel from Salses-Leucate laguna. A) Surface image B) 3-D reconstitution and the transect studied in yellow C) Transect studied on the shell surface D) Reconstructed profile in x and y. The shell growth show step increase. Arrows indicate alternance of big and small steps.

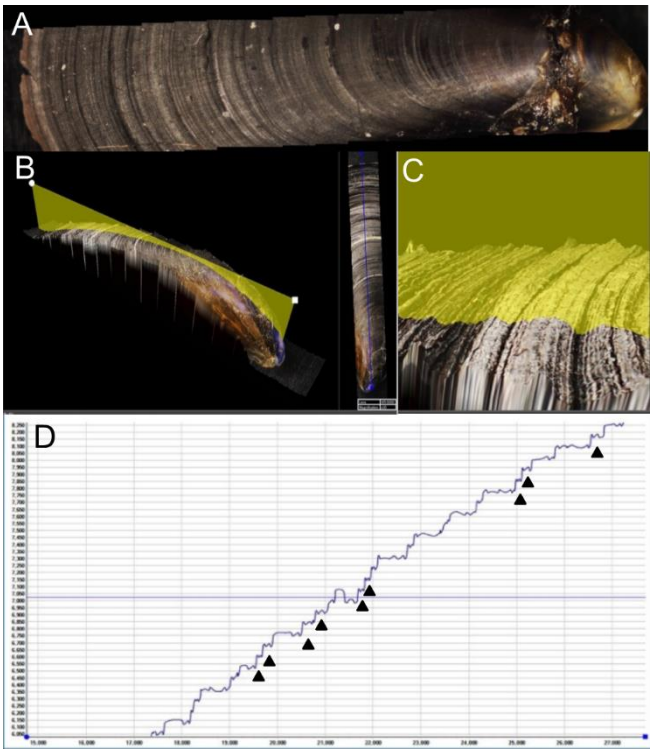

Figure A1.2: 3D profilometry of mussel from the bay of Banyuls-sur-Mer. A) Surface image B) 3-D reconstitution and the transect studied in yellow C) 3-D reconstitution and the transect studied in yellow at higher magnification D) Reconstructed profile in x and y. The shell growth show step increase. Arrows indicate alternance of big and small steps.

2. Microtomography

Samson Bellières[a,b], Clio Dersarkissian[a], Raphaël Martin-Roy[a], Xavier Mata[a], Franck Lartaud[b]

[a] Centre for Anthropobiology and Genomics of Toulouse, UMR5288, CNRS, University Toulouse 3 Paul Sabatier, Toulouse, France

[b] Sorbonne Université, CNRS, Laboratoire d'Ecogéochimie des Environnements Benthiques, LECOB, F-66650, Banyuls-sur-Mer, France

Shells of *Mytilus* ssp. from Banyuls-sur-Mer (FR), Ireland, Mors (DK) and Skagen (DK) were sampled and soft tissues removed. Shells were regrouped by 10 in polyethylene packages for imaging. Imaging in 3D of shells were achieved using a RX EasyTom XL CT Scanner (RX, Chavanod, France) piloted by the software Act64 (RX, Chavanod, France). The technic is using measurement of the absorption, refraction and diffusion of electromagnetic waves by the shell. Parameters used were an intensity of 260 µA and a voltage of 100 kV in source of X-ray, generating a power of 26 W. Per acquisition, 1346 images were taken. Images were treated using the software Avizo v8.1 (Thermofisher Scientific,

Waltham, MA, USA) and Meshmixer (Autodesk Research, San Fransisco, CA, USA). Images were compared to Mutvei etched section of the valve of the same shell.

Analyses showed a difference in resolution between the two methods with 2.5 times less increments observed using microtomography. Growth rate variations tendencies observed were similar in both methods (Figure A1.3). However, it showed that the microtomography had a lower resolution than the Mutvei etching. Therefore, this technic is less suitable for growth pattern characterisation in mussels than the Mutvei etching.

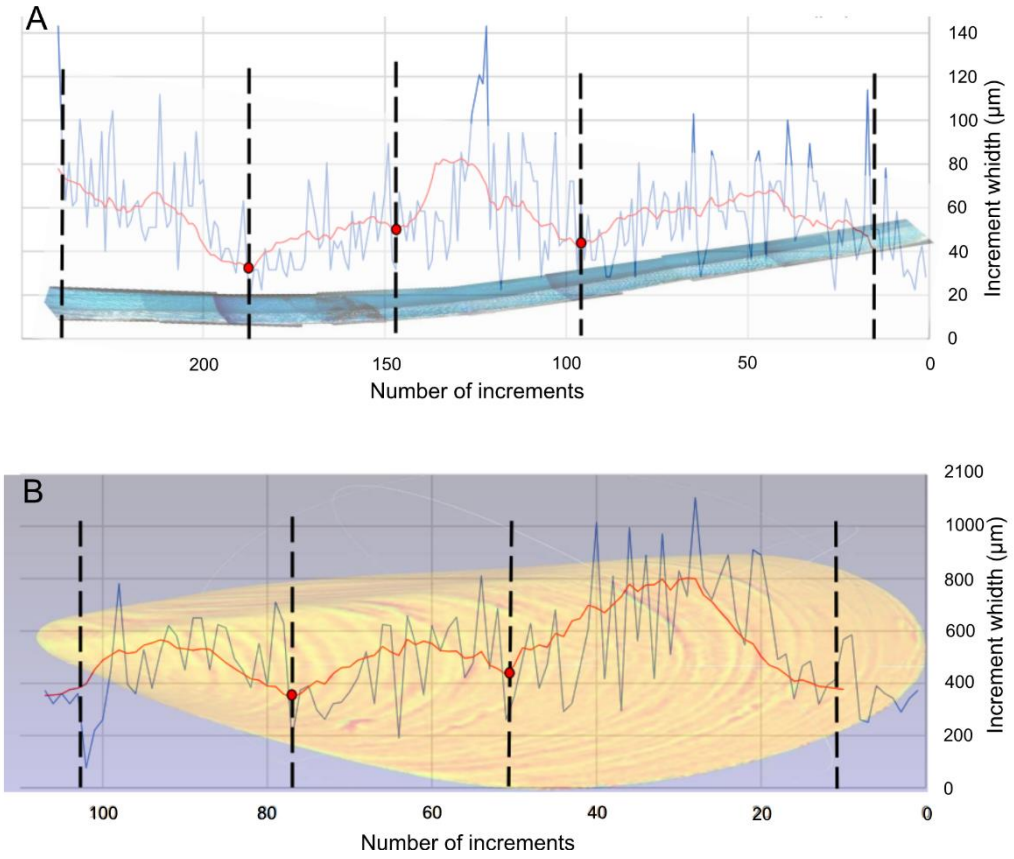

Figure A1.3: Sclerochronological profile of the mussel MOR06R using Mutvei etching and microtomography. A) Longitudinal section etched using Mutvei solution. Increment width measurements are in blue and the moving average in red. Bullet points are growth anomalies. Dash line are delimiting growth phases. B) Microtomography image. Increment width measurements are in blue and the moving average in red. Bullet points are growth anomalies. Dash line are delimiting growth phases. Figure adapted from Master 1 internship report of Samson Bellières.

Article	Order	Family	Organism	Environment	Microstructure	Periodicity growth line	Possible environmental drivers	Not correlated environmental drivers	Periodicity increment width	Timing	Possible environmental drivers	Not correlated environmental drivers
						Growth line			Increment width			
Nedoncelle et al., 2013 Nedoncelle et al., 2015	Mytilida	Mytilidae	*Bathymodiolus thermophilus*	Pacific ocean	Nearly horizontal fibrous prism (Génio 2012)	Lunar /tidal	Thin when 2 tide in the increment, not when 1 tide per lunar day. Lunar effect on hydrothermal fluid (pressure, T°) + bottom current velocities		Circalunar (26+/-4) +Circalunidian(14+/-2)	Thinner for tidal		
Schöne and Giere, 2005	Mytilida	Mytilidae	*Bathymodiolus brevior*	Pacific ocean	Fibrous prismatic calcite (génio 2012)	Daily (tidal?)	Endogeneous physiological parameters ?	Hydrothermal venting activity, food supply by chemosymbionts,temperature, O_2 levels	Circalunar (28) +circalunidian(14)	One on 2 thinner (tidal -> not in the count)		
Richardson , 1989	Mytilida	Mytilidae	*Mytilus edulis*	North Wales	Fibrous prismatic calcite	Tidal and daily	Emmertion-immertion (stronger when emmertion) pattern lost when continuous submertion ->dailyish (endogeneous)	no difference of strength btw ld and dd	/			
Lartaud, unpublished	Mytilida	Mytilidae	*Mytilus galloprovincialis*	SOLA	Fibrous prismatic calcite (Checa,2014)	Tidal						
Andrisoa et al.,2019	Mytilida	Mytilidae	*Mytilus galloprovincialis*	Thau Lagoon	Fibrous prismatic calcite (Checa,2014)	Circadian			Circalunidian(11-13) +3 and 5 days		Spring-neap cycles ->controlling the temperature, salinity, water depth and eventually the nutrient supply	

Article	Order	Family	Organism	Environment	Microstructure	Periodicity growth line	Possible environmental drivers	Not correlated environmental drivers	Periodicity increment width	Timing	Possible environmental drivers	Not correlated environmental drivers
						Growth line			Increment width			
Huyghe et al., 2019	Ostreida	Ostreidae	*Magallana gigas*	Normandy	Foliated and chalky microstructures (Checa, 2018)	Tidal	Circatidal structures result from shell accretion during high tides, and growth cessation at low tides		Circalunar (32) +Circalunidian(~ 15)	Thinner when higher high tide -> growth favored by neap tide than spring tide	Daily temperature, high tide level	Salinity, immersion duration and low tide level
Aguirre velarde et al.,2015	Pectinida	Pectinidae	*Argopecten purpuratus*	Paracas Bay, Peru	Calcite+ Aragonite	Daily						
Thébault et al.,2005	Pectinida	Pectinidae	*Decatopecten radula* (juveniles)	Shallow Tropical (Indo-West Pacific Ocean)	Foliated calcite	2-days	Endogeneoous -> ziegeber = seawater T° (unlikely) or Sea water pressure (these has 2 days variation in Pacific)		/	Decrease with decreasing Chla		
Chauvaud et al., 1998	Pectinida	Pectinidae	P*ecten maximus*	Bay of Brest (Subtidal with freshwater income)	Foliated calcite	Daily					Differences explained by temperature, irradiance and Chla	
Gruffydd, 1981	Pectinida	Pectinidae	*Pecten maximus*	Laboratory reared stock (uk)	Foliated calcite	Daily						
Clark, 2005	Pectinida	Pectinidae	*Pecten maximus*	Aquarium (subtidal species from gulf of california)	Foliated calcite	Daily	Stimulus=illumination more increment than day when increase number of cycles L:D 8:8					

Article	Order	Family	Organism	Environment	Microstructure	Periodicity growth line	Possible environmental drivers	Not correlated environmental drivers	Periodicity increment width	Timing	Possible environmental drivers	Not correlated environmental drivers
						Growth line			Increment width			
Richardson , 1987	Arcida	Arcidae	*Tegillarca granosa*	Penang Island - West Malaysia Mixed semidiurnal tidal cycle Rem: Intertidal and subtidal	Crossed lamellar calcite (richardson,1987)	Tidal	More prononced for intertidal specimen. Difference strongness -> most different during spring tide and almost none at neap tide		/	/	/	/
Mirzaei et al., 2016	Arcida	Arcidae	*Tegillarca granosa*	Penang Island - West Malysia Mixed semidiurnal tidal cycle	Crossed lamellar calcite	Tidal			Constant (no ffp)		Temperature is the major factor (followed by food ->link? " (rainfall effect -> closed valves)	Rainfall, tidal changes rem: no food tested
Hallmann et al., 2009	Venerida	Veneridae	*Saxidomus gigantea*	Alaska,southern British columbia	Aragonite	Daily (british columbia) but following mixed tides	"spring tides showed distinct micro- growth lines near the ventral margin" -> formation increment at high tide and line at low tide		Circalunidian (13-15)	Increments broader during neap tides. Contrary, the nar- rowest at spring tide cycles."	Temperature influence	
Poulin et al., 2011	Venerida	Veneridae	*Ruditapes philippinarum*	South Brittany in France in estuary	Prismatic aragonite	Tidal	Geneticaly drived? Zigebert =salinity (hypothesis)					

Article	Order	Family	Organism	Environment	Microstructure	Periodicity growth line	Possible environmental drivers	Not correlated environmental drivers	Periodicity increment width	Timing	Possible environmental drivers	Not correlated environmental drivers
						Growth line			Increment width			
Pannella and MacClintock, 1968	Venerida	Veneridae	*Mercenaria mercenaria*	Massachusetts	Prismatic aragonite	Daily in winter and tidal in summer (problem of resolution ?)	Genetic factors?	Rem: in tanks:circadian	Circalunar (29) +circalunidian(14)			
Kennish and Olsson 1975	Venerida	Veneridae	*Mercenaria mercenaria*	New Jersay (tidal Bay) subtidal	Prismatic aragonite	Tidal	Rem: very thin line				Temperature	
Schöne et al., 2003	Venerida	Veneridae	*Dosinia japonica*	Tokyo, Japan, intertidal (semi-diurnal tides) and subtidal	Prismatic aragonite? (kobayashi,2006)	Tidal (altern thick and light)	Tide (1 increment +line every high to low tide) line at low tide		Circalunidian (~14+/-0.5)	Incremen largest at spring tide cycle and smallest at neap tide	Temperatures, phyto? Tides	Salinity, precipitations
Schöne et al.,2005	Venerida	Arctidae	*Arctica islandica*	Baltic Sea and North Sea	Homogeneous microstructure +crossed acicular (aragonite) (bielers,2014)	Daily (change with age) -> better younger	Day/night as ziegebert		/	/	Temperature and food availability are the main con-trols	
Gannon et al., 2017	Cardiida	Cardiidae	*Tridacna gigas*	Palm Island, Australia	Cross-lamellar aragonite needles	Daily	Likely link to zooxanthellae		Circalunar (29) +circalunidian(14)	Likely driven by calcification rates controlled by the pho-tosynthetic activity of zooxanthellae		

Article	Order	Family	Organism	Environment	Microstructure	Periodicity growth line	Possible environmental drivers	Not correlated environmental drivers	Periodicity increment width	Timing	Possible environmental drivers	Not correlated environmental drivers
						Growth line			Increment width			
Schwartzmann et al.,2011 Aubert et al., 2009	Cardiida	Cardiidae	*Hippopus hippopus*	New Caledonia Rem: subtidal in a tidal area	Aragonite prismatic (Aubert,2009)	Daily	Rem: symbiotic with zooxantheles		/		Not linear with T° (because thermal limits), T° strengten by food	Salinity
Pannella and MacClintock, 1968	Cardiida	Cardiidae	*Tridacna squamosa*	Museum	Crossed-lamellar aragonite	Daily			Circalunidian(14)		[] of nutrients, influenced by rainfall, and phytoplankton, combined with an increase in solar irradi-ance	
Mahé et al., 2010	Cardiida	Cardiidae	*Cerastoderma edule*	Bay of Somme	Fibrilar composite prismatic (aragonite) (bielers,2014)	Tidal	Classic theory (lutz and rhoads, 1977)					
de Winter et al., 2020	Hippuritida	Hippuritidae	*Torrietes Sanchezi*	Campanian (83.6 ± 0.5 to 72.1 ± 0.2 Ma) at the Samhan formation	Calcite	Daily	Hypoth: light intensity rem: possibely photosynthetic symbiont	Temperatures daily oscillations	Circalunidian +circalunidian		Changes in water depht -> influence of the light availability -> affect metabolisms	
Dunca et al., 2004	Unionida	Margaritiferidae	*Margatifera margatifera*	Sweden	simple aragonite prism (Neotrigonia-like) (bielers,2014)	Daily						

Article	Order	Family	Organism	Environment	microstructure	Periodicity growth line	possible environmental drivers	not correlated environmental drivers	periodicity increment width	Timing	possible environmental drivers	not correlated environmental drivers
						Growth line			Increment width			
Dunca et al., 2004	Unionida	Unionidae	*Unio crassus*	Sweden	simple aragonite prism (Neotrigonia-like) (bielers,2014)	Daily						

Legend

Organism:

Recent Extinct

Environment:

Deep sea Subtidal Intertidal Lagoon and freshwater Other

Microstructure:

Crossed lamellar calcite Fibro-prismatic calcite Foliated calcite Other

Crossed lamellar aragonite Prismatic aragonite

Periodicity growth line:

Daily Tidal Other